


# SCIENTIFIC REPORTS

OPEN

## Electroacupuncture Attenuates Induction of Inflammatory Pain by Regulating Opioid and Adenosine Pathways in Mice

Hsien-Yin Liao<sup>1,2</sup>, Ching-Liang Hsieh<sup>1,3,4,5</sup>, Chun-Ping Huang<sup>5</sup> & Yi-Wen Lin<sup>1,5</sup> 

Although inflammatory pain is a common clinical condition, its mechanisms are still unclear. Electroacupuncture (EA), a well-known method of pain management, may reduce inflammatory pain by regulating neurons, astrocytes, and inflammatory signaling pathways. Injections of complete Freund's adjuvant (CFA), which can initiate cell-mediated inflammatory pain, resulted in significant hyperalgesia, which was subsequently prevented by EA. In CFA-injected mice, a dramatic increase was observed in the expression of the following proteins in the dorsal root ganglion and spinal cord dorsal horn: the astrocytic marker GFAP, S100B, RAGE, pPKC $\epsilon$ , COX-2, pERK, and pNF $\kappa$ B. These effects were reversed by EA. In addition, mechanical hyperalgesia was significantly reduced in the N6-cyclopentyladenosine (CPA) i.p. or i.m. and endomorphin (EM) i.p. groups. Neither EM i.m. nor EM i.p. exhibited any analgesic effect on thermal hyperalgesia. However, both CPA i.m. and CPA i.p. attenuated thermal hyperalgesia in the mouse inflammatory pain model. We showed that CPA reduced COX-2 and pPKC $\epsilon$  expression. However, EM administration did not reduce COX-2 levels. Combined administration of naloxone and rolofylline increased pPKC $\epsilon$  and COX-2 pathways. Taken together, our study results revealed a novel and detailed mechanism of EA-induced analgesia that involves the regulation of the opioid and adenosine pathways.

Inflammatory pain greatly affects the quality of life for countless people worldwide<sup>1</sup>. Despite the numerous side effects of non-steroidal anti-inflammatory drugs, including gastric ulcers, bowel dysfunction caused by morphine, and immune system suppression caused by steroidal drugs, patients spend vast sums of money on these pain medications. Electroacupuncture (EA) is a promising alternative to such drugs and has recently attracted much attention due to increasing evidence of its analgesic effects<sup>2,3</sup>. Previous studies using animal models have demonstrated the therapeutic effects of EA against inflammatory pain via neuronal and non-neuronal pathways, namely suppression of the transient receptor potential cation channel subfamily V member 1 (TRPV1) pathway<sup>4</sup>, generation of anti-nociceptive adenosine on adenosine A1 receptors (A1R) for local acupoints<sup>5-7</sup>, and stimulation of endogenous opioid secretion via the anesthesia pain descending pathway in the central nervous system<sup>8</sup>.

In a previous study, a complete Freund's adjuvant (CFA) injection into the hind paw of a mouse caused local inflammation and resulted in upstream action potentials toward the spine and central nervous system<sup>9</sup>. Another study has demonstrated that limb inflammation triggers spinal inflammatory activity, with increase in IL-1 $\beta$ , IL-6, TNF $\alpha$ , microglia, and astrocytes levels<sup>10</sup>. Other studies have demonstrated the association of inflammatory pain with various channels and kinases, including TRPV1, voltage-gated sodium channels (VGSC) 1.7 and 1.8, protein kinase A (PKA), protein kinase C (PKC), phosphoinositide 3-kinase (PI3K), serine/threonine kinase, mammalian target of rapamycin, extracellular signal regulated kinase (ERK), cAMP response element-binding protein, and the nuclear factor kappa-light-chain-enhancer of activated B cells (pNF $\kappa$ B)<sup>4,11</sup>. However, to date, details of the

<sup>1</sup>College of Chinese Medicine, Graduate Institute of Acupuncture Science, China Medical University, Taichung, 40402, Taiwan. <sup>2</sup>Department of Acupuncture, China Medical University Hospital, Taichung, 40402, Taiwan. <sup>3</sup>College of Chinese Medicine, Graduate Institute of Integrated Medicine, China Medical University, Taichung, 40402, Taiwan. <sup>4</sup>Department of Chinese Medicine, China Medical University Hospital, Taichung, 40402, Taiwan. <sup>5</sup>Research Center for Chinese Medicine & Acupuncture, China Medical University, Taichung, 40402, Taiwan. Correspondence and requests for materials should be addressed to C.-P.H. (email: [agustacagiva@yahoo.com.tw](mailto:agustacagiva@yahoo.com.tw)) or Y.-W.L. (email: [yiwlin@mail.cmu.edu.tw](mailto:yiwlin@mail.cmu.edu.tw))

mechanisms for spinal inflammatory factors, endogenous opioids, and adenosine remain unclear. Further, very few studies have evaluated how EA may function in these mechanisms to reduce inflammatory pain.

In line with existing reviews, we proposed that PKC $\epsilon$  and cyclooxygenase-2 (COX-2) are integral in connecting these pain-related mechanisms. A previous study has indicated that following tissue injury or infection, immune cells secrete inflammatory mediators, such as proinflammatory cytokines, bradykinin, and prostaglandins. These inflammatory mediators act on their respective receptors on peripheral nociceptor neural fibers. The activation of these receptors leads to the generation of secondary messengers, such as Ca<sup>2+</sup> and cAMP, which in turn activate several kinases (e.g., PKC, PKA, PI3K, and ERK). The activation of these kinases causes hypersensitivity and hyperexcitability of nociceptor neurons via the modulation of key transduction molecules, such as TRPV1 and voltage-gated sodium channels<sup>12</sup>. Interestingly, one study has reported that PKA can switch to PKC $\epsilon$  during the transition from early to late phase hyperalgesia<sup>13</sup>.

Researchers also have found that enkephalin activates the presynaptic  $\delta$ -opioid receptor and inhibits nociceptive VGSC 1.7 in the dorsal root ganglion (DRG) through PKC and p38 inhibition<sup>14</sup>. Both PKA and PKC are involved in the modulation of Nav1.8 currents from neonatal neurons<sup>15,16</sup>. However, the relationship among inflammatory mediators, adenosine, and VGSC remains unclear. One study has revealed that the prostaglandin E2 binds to G-proteins, resulting in a subsequent increase in cyclic AMP levels and consequent activation of PKC signaling pathways and purinergic 2X3 (P2X3) receptors; this ultimately causes exaggerated hyperalgesia<sup>17</sup>. Thus, EA intervention reduces inflammatory pain by suppressing P2X3 receptors as well as activating A1R<sup>5</sup>.

COX-2 is an inflammation-related enzyme that transforms arachidonic acid into different types of prostaglandins, including I2 and E2. These proinflammatory mediators cause inflammation and pain. One study that used an arthritis model has reported that COX-2 inhibitors can suppress prostaglandin generation and inflammation<sup>18</sup>. Another study has demonstrated that PKC $\epsilon$  modulates COX-2 generation and plays an important role in an inflammatory pain model<sup>19</sup>. Prophylactic use of non-steroidal anti-inflammatory drugs has been proven to reduce inflammation in ophthalmic and pancreatic diseases and lead to better recovery<sup>20,21</sup>. Further, it is clinically acknowledged that non-steroidal anti-inflammatory drugs can relieve dysmenorrhea and migraines. However, it is unknown whether early use of acupuncture can prevent pain generation in such conditions. Only a few studies have discussed the potential role of acupuncture as a symptomatic treatment to reduce the frequency of headaches<sup>22,23</sup>. Acupuncture, a technique with its origins in Chinese medicine, has been used for over 3000 years across Asia. It has also been recommended by the WHO as an effective analgesic. The present study aimed to identify the role of EA on inflammatory pain in mice and the effects of EA on the regulation of neurons, astrocytes, and other inflammatory signaling pathways.

## Results

**EA significantly reduced mechanical and thermal hyperalgesia in a mouse inflammatory pain model.** As shown in Fig. 1A, no significant difference was observed in mechanical sensitivity under basal conditions among the four groups (Control: 3.14  $\pm$  0.32 g; CFA: 3.08  $\pm$  0.38 g; EA: 3.11  $\pm$  0.29 g; Sham EA: 3.11  $\pm$  0.34 g). In contrast, the pain threshold, also called mechanical hyperalgesia, was significantly lower in the CFA and Sham EA groups on days 1, 2, and 3 after CFA injections (CFA: 1.17  $\pm$  0.19 g, 1.3  $\pm$  0.18 g, and 1.6  $\pm$  0.11 g; Sham EA: 1.23  $\pm$  0.17 g, 1.48  $\pm$  0.10 g, and 1.81  $\pm$  0.09 g, respectively) than in the control group (Control: 3.07  $\pm$  0.25 g, 3.03  $\pm$  0.25 g, and 2.96  $\pm$  0.29 g, respectively). EA significantly prevented the induction of mechanical hyperalgesia (EA: 2.77  $\pm$  0.11 g, 2.86  $\pm$  0.14 g, and 3.16  $\pm$  0.17 g on days 1, 2, and 3, respectively).

As shown in Fig. 1B, no significant difference was observed in withdrawal latencies among the groups prior to CFA injections (Control: 9.74  $\pm$  0.50 s; CFA: 10.88  $\pm$  0.35 s; EA: 10.47  $\pm$  0.32 s; Sham EA: 9.76  $\pm$  0.46 s). However, on days 1, 2, and 3 after CFA injections, withdrawal latencies were shorter in the CFA and Sham EA groups (CFA: 5.07  $\pm$  0.75 s, 5.32  $\pm$  0.56 s, and 6.06  $\pm$  0.48 s; Sham EA: 5.9  $\pm$  0.42 s, 6.07  $\pm$  0.58 s, and 6.46  $\pm$  0.45 s, respectively) than in the control group (Control: 10.41  $\pm$  0.74 s, 9.59  $\pm$  0.45 s, and 10.12  $\pm$  0.76 s, respectively). Interestingly, EA also prevented the induction of thermal hyperalgesia (9.53  $\pm$  0.48 s, 9.51  $\pm$  0.70 s, and 10.06  $\pm$  0.58 s on days 1, 2, and 3, respectively).

**EA reduced non-neuronal and neuronal signaling pathways in the DRG of a mouse inflammatory pain model.** As shown in Fig. 2, the levels of inflammatory biomarkers, namely GFAP (an astrocyte cell marker), S100B, and RAGE, around the DRG were upregulated after CFA injections (163.33%  $\pm$  17.83%, 170.26%  $\pm$  17.75%, and 182.52%  $\pm$  17.34%, respectively); EA attenuated these inflammatory biomarkers (104.04%  $\pm$  8.93%, 1103.14%  $\pm$  14.34%, and 121.11%  $\pm$  8.31%, respectively). Similar results were observed for the levels of inflammatory kinases, namely pPKC $\epsilon$ , pERK, and pNF- $\kappa$ B, within the DRG (CFA group: 144.62  $\pm$  14.66%, 180.44  $\pm$  23.84%, and 182.87  $\pm$  26.34%; EA group: 105.95  $\pm$  11.90%, 102.96  $\pm$  10.97%, and 102.75  $\pm$  11.29%, respectively).

**EA reduced non-neuronal and neuronal signaling pathways in the spinal cord of a mouse inflammatory pain model.** As shown in Fig. 3, levels of inflammatory biomarkers, namely GFAP, S100B, and RAGE, around the spinal cord were upregulated after CFA injections (159.12  $\pm$  7.82%, 167.24  $\pm$  12.07%, and 164.87  $\pm$  15.15%, respectively). Importantly, EA attenuated these inflammatory biomarkers (105.18  $\pm$  4.48%, 104.29  $\pm$  8.21%, 100.31  $\pm$  15.10%, respectively). Similar results were observed for levels of inflammatory kinases, namely pPKC $\epsilon$ , pERK, and pNF- $\kappa$ B, within the spinal cord (CFA group: 183.46  $\pm$  29.12%, 139.15  $\pm$  7.38%, and 185.57  $\pm$  24.20%; EA group: 104.31  $\pm$  14.35%, 99.28  $\pm$  3.38%, and 98.10  $\pm$  16.83%, respectively).

**Opioid and adenosine A1 receptors play a crucial role in EA-induced analgesia in a mouse inflammatory pain model.** Next, to identify the analgesic effects, we used intraperitoneal (i.p.) or intramuscular (i.m.) injections (i.e., acupoint injection) of endomorphin (EM), a  $\mu$ -opioid receptor agonist, or

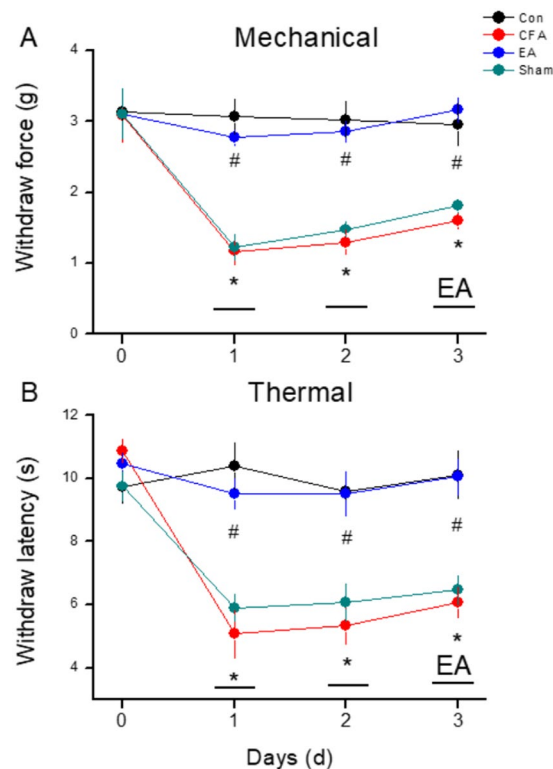


**Figure 1.** (A and B). Changes in the withdraw threshold and latency of mice in the von Frey and radial heat test. The picture shows that analgesic effect of EA can be detected on day 1 and day 2 after treatment. \* $p < 0.05$  means CFA compared with control. # $p < 0.05$  means EA compared with CFA.

N6-cyclopentyladenosine (CPA), an adenosine A1 receptor agonist. Mechanical hyperalgesia persisted in the EM i.m. group (Fig. 4A;  $1.79 \pm 0.09$  g,  $p < 0.05$  compared with day 0;  $n = 8$ ). However, mechanical hyperalgesia was significantly reduced in the CPA i.m., EM i.p., and CPA i.p. groups (Fig. 4A;  $3.48 \pm 0.12$  g,  $2.63 \pm 0.16$ , and  $3.3 \pm 0.16$  g, respectively;  $p > 0.05$  compared with day 0;  $n = 8$ ). Furthermore, thermal hyperalgesia was not affected in the EM i.m. and EM i.p. groups (Fig. 4B;  $4.58 \pm 0.2$  s and  $7.03 \pm 0.51$  s, respectively;  $p < 0.05$  compared with day 0;  $n = 8$ ). However, thermal hyperalgesia was attenuated in the CPA i.m. and CPA i.p. groups (Fig. 4B;  $9.43 \pm 0.72$  s and  $8.87 \pm 0.42$  s, respectively;  $p < 0.05$  compared with day 0;  $n = 8$ ).

**Attenuation of CFA-induced nociceptive pPKC $\epsilon$  and COX-2 levels by EA, endomorphin, and CPA.** As shown in Fig. 5A, pPKC $\epsilon$  levels within the DRG increased in both the CFA ( $1.25 \pm 0.07$ ) and Sham EA ( $1.33 \pm 0.05$ ) groups. This increase was attenuated by EA ( $1.05 \pm 0.08$ ), EM ( $1.04 \pm 0.04$ ), and CPA ( $0.88 \pm 0.03$ ) administration. In addition, COX-2 levels within the DRG increased in both the CFA ( $1.62 \pm 0.13$ ) and Sham EA ( $1.58 \pm 0.13$ ) groups. This increase was attenuated by EA ( $0.98 \pm 0.07$ ) and CPA ( $1.14 \pm 0.03$ ) administration. Interestingly, EM administration induced lower, although insignificant, COX-2 levels ( $1.40 \pm 0.10$ ) than CFA administration. These results are analyzed and plotted in Fig. 5B and C.

**Combined MOR and A1AR antagonists suppressed the anti-inflammatory effects of EA.** As shown in Fig. 6A, based on pPKC $\epsilon$  levels, both naloxone methiodide (Nal) and rolofylline (Rol) failed to completely block the anti-inflammatory effects of EA (EA:  $1.05 \pm 0.12$ , Nal:  $1.31 \pm 0.13$ , and Rol:  $1.49 \pm 0.13$ ). However, combined administration of Nal and Rol significantly increased pPKC $\epsilon$  levels ( $2.09 \pm 0.40$ ) compared with EA. Similar results were found for COX-2 levels (also shown in Fig. 6A). COX-2 levels after EA, Nal+Rol, Nal, and Rol administrations were  $0.90 \pm 0.04$ ,  $1.27 \pm 0.08$ ,  $1.11 \pm 0.09$ , and  $0.99 \pm 0.07$ , respectively. All results were analyzed and plotted (Fig. 6B and C). A schematic diagram (Fig. 7) was prepared, and an inflammatory model was designed to determine the relationships among EA, endogenous opioids, adenosine, and inflammatory mediators. Whether EA could attenuate the CFA-induced inflammatory pain was also analyzed.

## Discussion

Despite growing interest in EA and its widespread use in treating dysmenorrhea and migraines, previous research has only partially indicated the mechanisms by which EA suppresses inflammatory pain; only one relatively complete diagram, reported by Lao *et al.* in 2014<sup>8</sup>, suggests a relationship among endogenous opioids, inflammatory cytokines, and adenosine. Thus, the current study aimed to continue our previous research in the context of EA using serial pain models. A research summary is presented in Fig. 7.

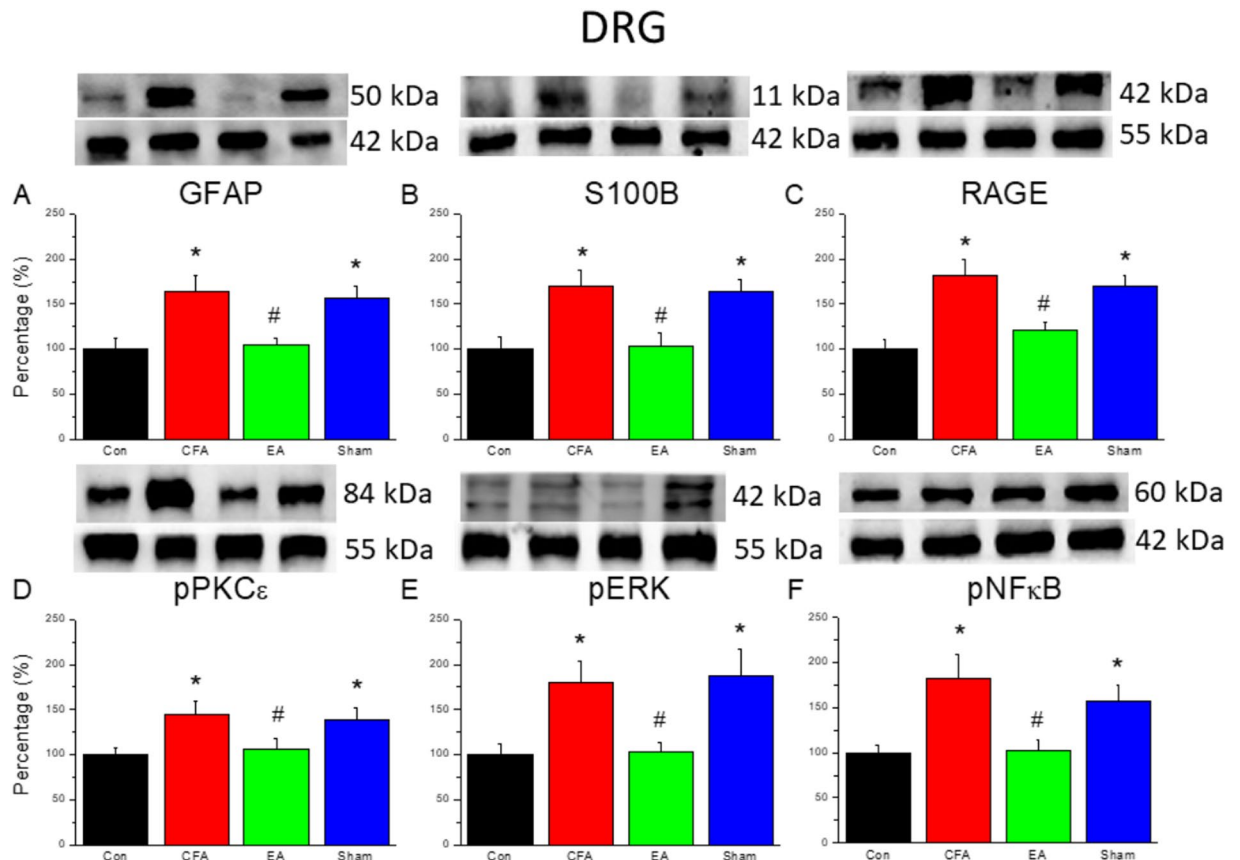


**Figure 2.** (A~F) Expression levels from biomarkers of glia cells and inflammatory kinases in DRG after CFA injection, EA and Sham EA treatment. \* $p < 0.05$  means CFA or Sham EA compared with Control; # $p < 0.05$  means EA compared with CFA. The western blot bands at the top show the cropped target protein. The lower bands are cropped internal controls ( $\beta$ -actin or  $\alpha$ -tubulin).

As shown in Fig. 1, mechanical and thermal hyperalgesia confirmed that CFA injections successfully evoked inflammatory pain. Next, we demonstrated that EA prevented the induction of mechanical and thermal hyperalgesia on days 1, 2, and 3. pPKC $\epsilon$  and COX-2 levels among EA groups also provided indirect evidence that EA attenuated the induction of inflammatory pain, as shown in Fig. 5.

Within the CFA group, we observed an increase in pPKC $\epsilon$ , pERK, and pNF $\kappa$ B levels within the DRG and SCDH on day 3 after CFA injections (Figs 2 and 3). The activation of these kinases increased action potentials toward the central nervous system and subsequently resulted in an increase in GFAP expression. Higher GFAP levels suggested that activated astrocytes secrete S100B to stimulate RAGE expression, thereby activating neurons and microglia. In addition, pPKC $\epsilon$ , pERK, and pNF $\kappa$ B stimulated proinflammatory cytokines in the spinal cord. A previous study using a rat model of monoarthritis demonstrated IL-1, IL-6, and TNF- $\alpha$  activation following an intra-articular CFA injection<sup>10</sup>. In addition, our study demonstrated that COX-2 levels were stimulated in the DRG.

Administration of the adenosine agonist CPA was found to improve animal pain behaviors and downregulate the expression of COX-2 and phosphorylated PKC $\epsilon$  (Fig. 5). However, as shown in Fig. 5, it is unclear why EM administration induced lower, although insignificant, COX-2 levels than CFA administration. One potential explanation is that there was more than one endorphin working in the descending pain suppression pathway at the spinal level. According to a study by Han *et al.* in 2003<sup>24</sup>, four endogenous opioids (namely  $\beta$ -endorphin, enkephalin, endomorphin, and dynorphin) are generated in the central nervous system. During EA,  $\beta$ -endorphin is primarily generated around the periaqueductal gray matter at 2 and 15 Hz, whereas enkephalin and endomorphin are primarily generated around the spinal cord at 2 Hz. Dynorphin is also generated around the spinal cord but at 128 Hz during EA. Therefore, under the 2-Hz EA used in the present study, the endomorphin agonist group could not cover the entire endogenous opioids pathway and thus demonstrated reduced, although insignificant, COX-2 levels compared with those in the CFA group.

## Conclusions

Comparison of the EA and Sham EA groups in this study highlighted the anesthetic specificity of acupoints that non-acupoints lack. Further, by administering the adenosine agonist at a local acupoint and using an i.p. injection of an opioid agonist, we determined the locations at which these drugs affect the pain suppression pathway. Moreover, using an agonist and an antagonist of endogenous opioids and adenosine, we could excite both

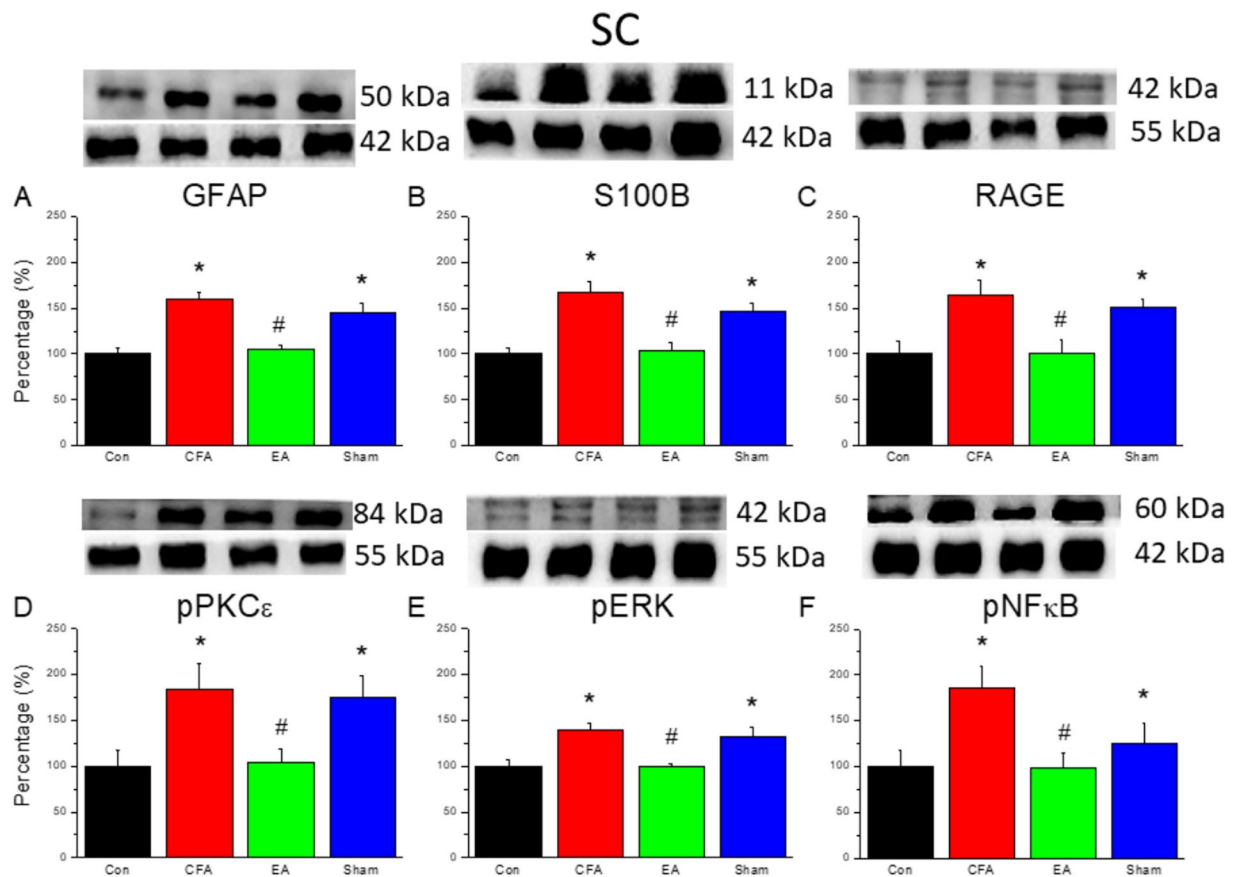


**Figure 3.** (A–F) Expression levels from biomarkers of glia cells and inflammatory kinases in DRG after CFA injection, EA and Sham EA treatment. \* $p < 0.05$  means CFA or Sham EA compared with Control; # $p < 0.05$  means EA compared with CFA. The western blot bands at the top show the cropped target protein. The lower bands are cropped internal controls ( $\beta$ -actin or  $\alpha$ -tubulin).

the adenosine and spinal opioid pathways, demonstrating that EA successfully suppressed inflammatory pain. Blocking the adenosine or opioid pathway alone only partially reduces the anesthetic effects of EA. Furthermore, we demonstrated definitive evidence that EA controls inflammatory factors within the DRG via the two aforementioned pathways, thereby supporting the therapeutic potential of EA treatment for attenuating the induction of inflammatory pain.

## Methods

**Experimental Animals.** All animals were treated according to the guidelines of the National Institutes of Health “Guide for the Care and Use of Laboratory Animals,” and the study protocol was approved by the ethics committee of the China Medical University, Taichung, Taiwan (permit No. 2016-061). C57/B6 mice weighing approximately 22–25 g and aged 8–12 weeks were purchased from the BioLASCO Animal Center (Taipei, Taiwan). Animals were housed in plexiglas cages in a temperature-controlled room ( $25^{\circ}\text{C} \pm 2^{\circ}\text{C}$ ) with a relative humidity of  $60\% \pm 5\%$  and were fed a diet consisting of standard rat chow and water ad libitum.

**Inflammatory Pain Model.** Based on results of our previous studies<sup>4</sup>, it was suggested that a total of 10 mice in each group is the minimum number necessary to perform the experiments. All experiments were performed in our laboratory during daylight hours. First, C57/B6 mice were randomly divided (using simple random sampling) into four groups and then anesthetized with 1% isoflurane for CFA injections and EA treatments. Next, mice were injected with either 20  $\mu\text{l}$  saline (pH 7.4, buffered with 20 mM HEPES) or 0.5 mg/ml CFA (heat-killed *M. tuberculosis* [Sigma, St. Louis, MO]) in the plantar surface of the hind paw to induce intraplantar inflammation. The four groups were as follows: (1) Control group: anesthesia with normal saline injection, (2) CFA group: anesthesia with CFA injection to induce inflammatory pain, (3) EA group: anesthesia with CFA injection and EA manipulation, and (4) Sham EA: anesthesia with CFA injection and Sham EA, to test the potential impact of acupoint and manipulation.

**Electroacupuncture and Sham Electroacupuncture.** EA was conducted in the morning (9:00–10:00 am), immediately after the induction of anesthesia and CFA injections for a total of 15 min, at a frequency of 2 Hz, and at an amplitude of 1 mA. EA procedure was repeated two more times, at 24 and 48 h after CFA injection. The ST36 acupuncture point is located on the tibialis anterior muscle, approximately 1/6 of the distance from the

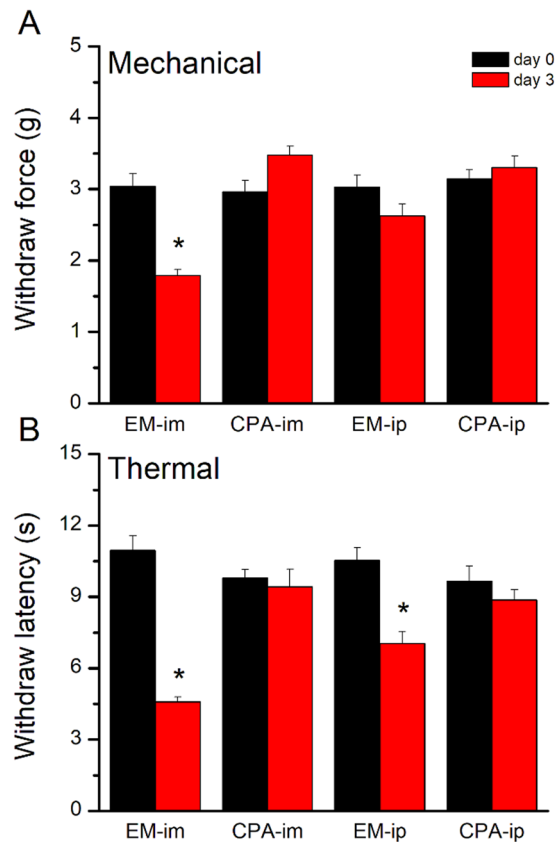


**Figure 4.** Opioid and adenosine A1 receptor agonist administration relieved mechanical and thermal pain. EM-im: endomorphin intramuscularly injection; CPA-im: N6-Cyclopentyladenosine intramuscularly injection. EM-ip: endomorphin intraperitoneally injection; CPA-ip: N6-Cyclopentyladenosine intraperitoneally injection. \* $p < 0.05$  means comparison with day 0.

patella to the lateral malleolus. Disposable needles with a diameter of 0.30 mm and a length of 13 mm (Yu-Kuang Acupuncture Instrument Co., Taiwan) were inserted into the muscle layer at both ST36 acupuncture points to a depth of 2–3 mm. Electrical stimulation was produced by a Trio 300 electrical stimulator (Grand Medical Instrument CO., LTD). A similar protocol was used for the nonacupoint (i.e., the upper lateral gluteal muscle, but not the GB30 acupoint) for the sham control group.

**Opioid or Adenosine A1 Receptor Agonist and Antagonist Administration.** Adult C57BL/6 male mice ( $n = 10$ ), aged 8 to 12 weeks, were used in opioid and adenosine agonist analysis. After inflammation was induced, as described above, the  $\mu$ -opioid agonist EM (Sigma, St. Louis, MO, USA; in 100  $\mu$ l of saline) was administered i.p. or i.m. at a dose of 10 mg/kg, once per day. Alternatively, the adenosine receptor agonist CPA (Sigma, St. Louis, MO, USA; in 10  $\mu$ l of saline) was immediately administered i.p. or i.m. into acupoint ST36 at a dose of 0.1 mg/kg, once per day. Under light isoflurane anesthesia (1%), EM and CPA were given 24 h after CFA injection.

The other group of adult C57BL/6 male mice ( $n = 10$ ), aged 8 to 12 weeks, were used for opioid and adenosine antagonist analysis. The opioid antagonist Nal (Sigma, St. Louis, MO, USA; in 100  $\mu$ l of saline) was injected i.p. at a dose of 10 mg/kg. The adenosine A1 receptor antagonist Rol (Sigma, St. Louis, MO, USA; in 10  $\mu$ l of saline) was injected i.m. at a dose of 3 mg/kg into acupoint ST36. Nal, Rol, and a combination of Nal and Rol were given immediately following CFA injection and were then followed by EA treatments.

**Behavior Test (von Frey test and Hargraves' test).** By using behavior tests at the moment after CFA injection, 24, 48, and 72 hours later, we checked whether there were mechanical and thermal hyperalgesia. All stimuli were administered at room temperature (approximately 25 °C) and applied only when the animals were calm, but not sleeping or grooming. Mechanical sensitivity was measured by testing the force of responses to stimulation with three applications of electronic von Frey filaments (North Coast Medical, Gilroy, CA, USA). Thermal pain was measured with three applications using Hargraves' test IITC analgesiometer (IITC Life Sciences, SERIES8, Model 390 G).

**Tissue sampling and Western blot analysis.** Mice aged 8–12 weeks were sacrificed by use of CO<sub>2</sub> to minimize their suffering. L3-L5 DRG and SCDH were harvested three days later after injection of CFA and then immediately excised to extract proteins. Total proteins were prepared by homogenized DRG and SCDH in lysis buffer containing 50 mM Tris-HCl pH 7.4, 250 mM NaCl, 1% NP-40, 5 mM EDTA, 50 mM NaF, 1 mM Na<sub>3</sub>VO<sub>4</sub>,

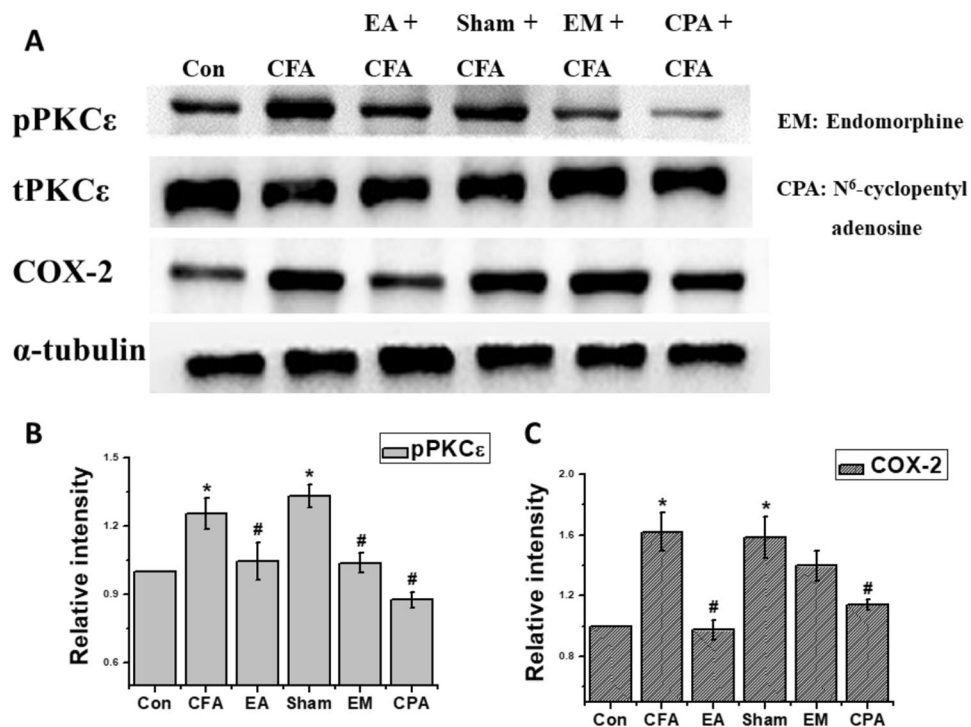


**Figure 5.** Levels of inflammatory kinases under Electroacupuncture, Sham Electroacupuncture and administration of endomorphin and adenosine agonist. \* $p < 0.05$  means CFA or Sham EA compared with Control; # $p < 0.05$  means EA, EM and CPA compared with CFA. The western blot bands at the top show the cropped target protein. The lower bands are cropped internal controls ( $\beta$ -actin or  $\alpha$ -tubulin).

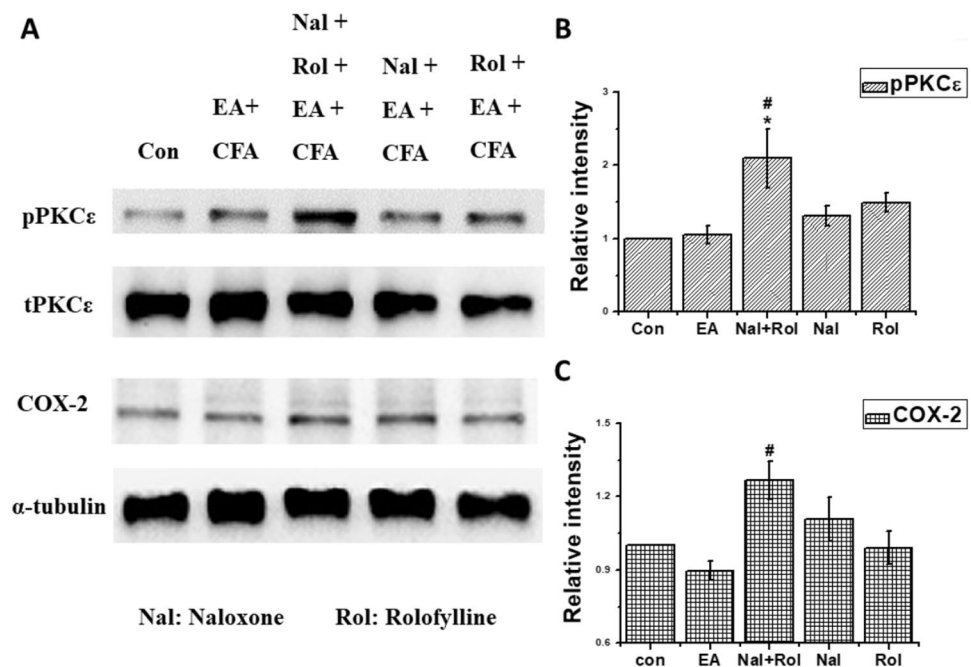


**Figure 6.** levels of Inflammatory kinases under Electroacupuncture, administration of endomorphin antagonist, adenosine antagonist and combination \* $p < 0.05$  means CFA or Sham EA compared with Control; # $p < 0.05$  means EA, EM and CPA compared with CFA. The western blot bands at the top show the cropped target protein. The lower bands are cropped internal controls ( $\beta$ -actin or  $\alpha$ -tubulin).

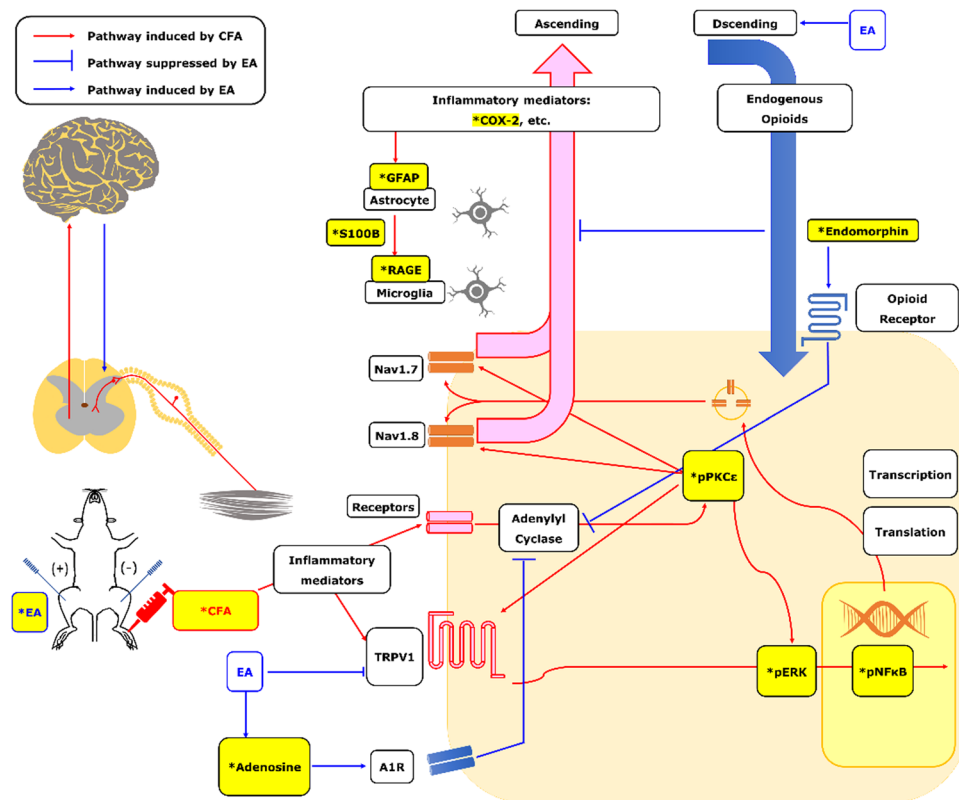


**Figure 7.** Schematic diagram of possible mechanism in EA-mediated analgesia of CFA-induced inflammatory pain. The contents marked in yellow and \* means procedure or factors used in this study. Others are plotted according to previous studies reviewed in introduction.

0.02% NaN<sub>3</sub> and 1× protease inhibitor cocktail (AMRESCO). The extracted proteins (30 µg per sample assessed by BCA protein assay) were subjected to 8% SDS-Tris glycine gel electrophoresis and transferred to a PVDF membrane. The membrane was blocked with 5% nonfat milk in TBS-T buffer (10 mM Tris pH 7.5, 100 mM NaCl, 0.1% Tween 20), incubated with first antibody (anti-GFAP, anti-s100B, anti-RAGE, anti-pPKC $\epsilon$ , anti-pERK, anti-pNF- $\kappa$ B, anti-COX-2) in TBS-T with 1% bovine serum albumin, and incubated for 1 hour at room temperature. Peroxidase-conjugated anti-rabbit antibody (1:5000) was used as a secondary antibody. The bands were visualized by an enhanced chemiluminescent substrate kit (PIERCE) with LAS-3000 Fujifilm (Fuji Photo Film Co. Ltd). Where applicable, the image intensities of specific bands were quantified with NIH ImageJ software (Bethesda, MD, USA). Images were gathered in to figures by using photoimpact 12 without any unnecessary edition.

**Statistical Analysis.** All statistic data were presented as the mean  $\pm$  standard error. A  $P$  value  $< 0.05$  was considered to represent statistical significance. The four groups in this study were: (1) Control group, (2) CFA group, (3) EA group, and (4) Sham EA group ( $n = 10$ /group). Statistical significance between groups was tested using the ANOVA test, followed by a post hoc Tukey's test ( $p < 0.05$  was considered statistically significant). All statistical analyses were carried out using the statistical package SPSS for Windows (Version 21.0, SPSS, Chicago, Illinois, USA).

## References

- Rasu, R. S. *et al.* Cost of pain medication to treat adult patients with nonmalignant chronic pain in the United States. *Journal of managed care & specialty pharmacy* **20**, 921–928 (2014).
- Lin, J. G., Hsieh, C. L. & Lin, Y. W. Analgesic Effect of Electroacupuncture in a Mouse Fibromyalgia Model: Roles of TRPV1, TRPV4, and pERK. *PLoS one* **10**, e0128037 (2015).
- Han, P. *et al.* Inhibition of Spinal Interleukin-33/ST2 Signaling and Downstream ERK and JNK Pathways in Electroacupuncture Analgesia in Formalin Mice. *PLoS one* **10**, e0129576 (2015).
- Lu, K. W., Hsu, C. K., Hsieh, C. L., Yang, J. & Lin, Y. W. Probing the Effects and Mechanisms of Electroacupuncture at Ipsilateral or Contralateral ST36-ST37 Acupoints on CFA-induced Inflammatory Pain. *Scientific reports* **6**, 22123 (2016).
- Ren, W., Tu, W., Jiang, S., Cheng, R. & Du, Y. Electroacupuncture improves neuropathic pain: Adenosine, adenosine 5'-triphosphate disodium and their receptors perhaps change simultaneously. *Neural regeneration research* **7**, 2618–2623 (2012).
- Goldman, N. *et al.* Adenosine A1 receptors mediate local anti-nociceptive effects of acupuncture. *Nature neuroscience* **13**, 883–888 (2010).
- Zylka, M. J. Needling adenosine receptors for pain relief. *Nature neuroscience* **13**, 783–784 (2010).
- Zhang, R., Lao, L., Ren, K. & Berman, B. M. Mechanisms of acupuncture-electroacupuncture on persistent pain. *Anesthesiology* **120**, 482–503 (2014).



9. Huang, C. P. *et al.* Electroacupuncture Reduces Carrageenan- and CFA-Induced Inflammatory Pain Accompanied by Changing the Expression of Nav1.7 and Nav1.8, rather than Nav1.9, in Mice Dorsal Root Ganglia. *Evidence-based complementary and alternative medicine: eCAM* **2013**, 312184 (2013).
10. Shan, S. *et al.* Is functional state of spinal microglia involved in the anti-allodynic and anti-hyperalgesic effects of electroacupuncture in rat model of monoarthritis? *Neurobiology of disease* **26**, 558–568 (2007).
11. Liao, H. Y., Hsieh, C. L., Huang, C. P. & Lin, Y. W. Electroacupuncture Attenuates CFA-induced Inflammatory Pain by suppressing Nav1.8 through S100B, TRPV1, Opioid, and Adenosine Pathways in Mice. *Scientific reports* **7**, 42531 (2017).
12. Ji, R. R., Xu, Z. Z. & Gao, Y. J. Emerging targets in neuroinflammation-driven chronic pain. *Nature reviews. Drug discovery* **13**, 533–548 (2014).
13. Huang, W.-Y., Dai, S.-P., Chang, Y.-C. & Sun, W.-H. Acidosis Mediates the Switching of G(s)-PKA and G(i)-PKC( $\epsilon$ ) Dependence in Prolonged Hyperalgesia Induced by Inflammation. *PLoS one* **10**, e0125022 (2015).
14. Chattopadhyay, M., Mata, M. & Fink, D. J. Continuous delta-opioid receptor activation reduces neuronal voltage-gated sodium channel (Nav1.7) levels through activation of protein kinase C in painful diabetic neuropathy. *The Journal of neuroscience: the official journal of the Society for Neuroscience* **28**, 6652–6658 (2008).
15. Matsumoto, S. *et al.* Effect of 8-bromo-cAMP on the tetrodotoxin-resistant sodium (Nav 1.8) current in small-diameter nodose ganglion neurons. *Neuropharmacology* **52**, 904–924 (2007).
16. Wang, W., Gu, J., Li, Y. Q. & Tao, Y. X. Are voltage-gated sodium channels on the dorsal root ganglion involved in the development of neuropathic pain? *Mol Pain* **7**, 16 (2011).
17. Wang, C., Gu, Y., Li, G. W. & Huang, L. Y. A critical role of the cAMP sensor Epac in switching protein kinase signalling in prostaglandin E2-induced potentiation of P2X3 receptor currents in inflamed rats. *The Journal of physiology* **584**, 191–203 (2007).
18. Pulichino, A. M. *et al.* Prostacyclin antagonism reduces pain and inflammation in rodent models of hyperalgesia and chronic arthritis. *The Journal of pharmacology and experimental therapeutics* **319**, 1043–1050 (2006).
19. Dutra, R. C. *et al.* The antinociceptive effects of the tetracyclic triterpene euphol in inflammatory and neuropathic pain models: The potential role of PKCepsilon. *Neuroscience* **303**, 126–137 (2015).
20. Sajid, M. S., Khawaja, A. H., Sayegh, M., Singh, K. K. & Philipose, Z. Systematic review and meta-analysis on the prophylactic role of non-steroidal anti-inflammatory drugs to prevent post-endoscopic retrograde cholangiopancreatography pancreatitis. *World Journal of Gastrointestinal Endoscopy* **7**, 1341–1349 (2015).
21. O'Brien, T. P. Emerging guidelines for use of NSAID therapy to optimize cataract surgery patient care. *Current medical research and opinion* **21**, 1131–1137 (2005).
22. Linde, K. *et al.* Acupuncture for the prevention of episodic migraine. *The Cochrane database of systematic reviews*, Cd001218, (2016).
23. Lim, S. WHO Standard Acupuncture Point Locations. *Evid Based Complement Alternat Med* **7**, 167–168 (2010).
24. Han, J. S. Acupuncture: neuropeptide release produced by electrical stimulation of different frequencies. *Trends Neurosci* **26**, 17–22 (2003).

## Acknowledgements

This study was supported by CMU under the Aim for Top University Plan of the Ministry of Education, Taiwan, MOST 104-2320-B-039-010, CMU104-S-45. We thank Dr. Yang Jen for his assistance of drawing schematic diagram.

## Author Contributions

C.L.H. and Y.W.L. wrote the manuscript, H.Y.L. and C.P.H. employed the experiments. All authors reviewed the manuscript and agreed for submission.

## Additional Information

**Competing Interests:** The authors declare that they have no competing interests.

**Publisher's note:** Springer Nature remains neutral with regard to jurisdictional claims in published maps and institutional affiliations.



**Open Access** This article is licensed under a Creative Commons Attribution 4.0 International License, which permits use, sharing, adaptation, distribution and reproduction in any medium or format, as long as you give appropriate credit to the original author(s) and the source, provide a link to the Creative Commons license, and indicate if changes were made. The images or other third party material in this article are included in the article's Creative Commons license, unless indicated otherwise in a credit line to the material. If material is not included in the article's Creative Commons license and your intended use is not permitted by statutory regulation or exceeds the permitted use, you will need to obtain permission directly from the copyright holder. To view a copy of this license, visit <http://creativecommons.org/licenses/by/4.0/>.

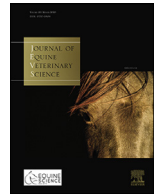
© The Author(s) 2017



ELSEVIER

Contents lists available at ScienceDirect

## Journal of Equine Veterinary Science

journal homepage: [www.j-evs.com](http://www.j-evs.com)

Original Research

## Prevalence, Risk Factors and Diagnosis of Helminths in Thoroughbred Horses Kept at Training Centers in Rio de Janeiro, Brazil

André V. Martins<sup>a,b</sup>, Laís L. Corrêa<sup>a</sup>, Mariana S. Ribeiro<sup>a</sup>, Lucas F. Lobão<sup>a</sup>, Laís V. Dib<sup>a,c</sup>, João P.S. Palmer<sup>a</sup>, Lucas C. de Moura<sup>b</sup>, Fabiana B. Knackfuss<sup>d</sup>, Claudia M.A. Uchôa<sup>a</sup>, Marcelo B. Molento<sup>e</sup>, Alynne da Silva Barbosa<sup>a,c,\*</sup>

<sup>a</sup> Laboratório de Bioagentes Ambientais, Departamento de Microbiologia e Parasitologia, Instituto Biomédico, Universidade Federal Fluminense, Niterói, Rio de Janeiro, Brazil

<sup>b</sup> Laboratório de Parasitologia e Doenças Parasitárias, Faculdade de Medicina Veterinária, Centro Universitário Serra dos Órgãos, Teresópolis, Rio de Janeiro, Brazil

<sup>c</sup> Laboratório de Protozoologia, Instituto Oswaldo Cruz, Fundação Oswaldo Cruz, Rio de Janeiro, Brazil

<sup>d</sup> Zootecnia e Estatística, Escola de Ciências da Saúde, Universidade do Grande Rio, Duque de Caxias, Rio de Janeiro, Brazil

<sup>e</sup> Laboratório de Parasitologia Clínica Veterinária, Departamento de Medicina Veterinária, Universidade Federal do Paraná. Curitiba, Paraná, Brazil

## ARTICLE INFO

## Article history:

Received 12 January 2023

Received in revised form 12 April 2023

Accepted 27 April 2023

Available online 1 May 2023

## Keywords:

Intestinal parasites

strongylids

*Parascaris* spp

## ABSTRACT

The aims of this study were to determine the prevalence of helminths in Thoroughbred horses in Rio de Janeiro; make correlations with risk factors for these infections; and compare the efficiency of three floatation solutions applied in the quantitative Mini-FLOTAC technique. Fecal samples from 520 horses were collected from six training centers between 2019 and 2021. These were subjected to the Mini-FLOTAC technique using three solutions: NaCl (density = 1.200 g/mL), ZnSO<sub>4</sub> (1.350 g/mL) and ZnSO<sub>4</sub> (1.200 g/mL); and also to qualitative techniques. Information on the horses' sex and age of horses was retrieved from the studbook; data on management from a questionnaire. The overall prevalence of intestinal parasites was 71.9%, with significant differences between training centers ( $P \leq .05$ ). On farm C, 87.7% of the samples presented strongylids and 38.7% had *Parascaris* spp., with the highest egg counts per gram of feces (EPG), of 358.33 and 40.41 respectively. Horses less than 3 years of age were about eight times more likely to be parasitized by strongylids and eleven times more likely to have EPG  $\geq 500$ . The NaCl solution used in Mini-FLOTAC enabled recovery of the greatest number of samples with high EPG and reached the highest sensitivity values in the diagnosis when compared to the other solutions. Moreover, in the diagnoses, the levels of agreement between the results from the solutions used in Mini-FLOTAC were substantial. However, in estimating the EPG, full agreement between the results from the solutions used in Mini-FLOTAC was not obtained.

© 2023 Elsevier Inc. All rights reserved.

## 1. Introduction

Brazil is the largest horse-rearing country in Latin America. Its herd is the third largest in the world, comprising around 5.8 million head in around 1.2 million production units [1]. Equid production in Brazil generates profits of about US\$ 7.3 billion per year [2].

*Animal welfare/ethical statement:* This study was approved by the Ethics Committee for Use of Animals of the Fluminense Federal University (CEUA - UFF) on July 4, 2019, under the CEUA number 6742290519.

\* Corresponding author at: Universidade Federal Fluminense, Instituto Biomédico, Prof. Hernani Pires de Mello Street, 101, room 212C, Parasitology, São Domingos, Niterói - Rio de Janeiro, Brazil, Zip Code: 24210-130.

E-mail addresses: [alynnedsb@gmail.com](mailto:alynnedsb@gmail.com), [alynnebarbosa@id.uff.br](mailto:alynnebarbosa@id.uff.br) (A.d.S. Barbosa).

In the state of Rio de Janeiro in 2022, about 93,000 head of horses are registered [3]. Much of this horse rearing is centered on the municipalities of the mountainous region of the state, such as in Petrópolis and Teresópolis, with emphasis on the Thoroughbred breed. In these municipalities, horses are reared and kept in training centers to prepare them for competition in turf events, especially at the Brazilian Jockey Club, located in the city of Rio de Janeiro. These activities have a high financial turnover [4].

Horses are known to become infected with a variety of infectious agents. Among these, helminths can be highlighted and, within this group, strongylid nematodes (family Strongylidae) such as large strongylids (subfamily Strongylinae) due to their high pathogenicity and small strongylids or cyathostomins (subfamily Cyathostominae) due to their high prevalence and their resistance to anthelmintics [5–8]. These parasites, mainly large strongylids,

may cause gastrointestinal alterations ranging from mild to severe, among which diarrhea and abdominal colic's stand out. These are among the main clinical alterations that can lead to the death of these animals [8].

In addition to strongyles, horses can also be infected by the nematode *Parascaris* spp. This parasite inhabits the small intestine, being found parasitizing foals all over the world [9]. Infection with a large number of adult forms of this nematode, particularly in foals, can cause colic associated with enteritis and/or intestinal impaction and obstruction. Clinical signs associated with *Parascaris* spp. include lethargy weight loss and anorexia [10–13].

Nematodes in horses are often controlled through use of anthelmintic drugs, which are administered in accordance with a calendar-based schedule, without making any previous laboratory diagnosis. Such practices may increase the rate of development of resistance in parasites to antiparasite drugs [7]. To combat this problem and reduce the burden of parasites in horses, the American Association of Equine Practitioners (AAEP) recommends that quantitative coproparasitological examinations should be routinely performed. Thus, estimation of the number of eggs per gram of feces (EPG) in horses is a practice that should form part of this monitoring and of the parasite control program [14,15].

Quantitative parasitological techniques have become refined, with improved limits for detection of helminth eggs. Among the laboratory methods used for diagnosing intestinal parasites of horses are those based on egg floatation. Methods in which passive floatation takes place, without the need for centrifugation, stand out because of their simplicity. These include the McMaster technique [16] and the Mini-FLOTAC technique [17]. Over the years, these techniques have been compared and analyzed, and in most of these analyses, Mini-FLOTAC was found to present better accuracy and precision. Mini-FLOTAC is now widely indicated for monitoring parasites and for determining EPG counts in equine feces [18,19].

The prevalence rates of intestinal parasitic infections are unknown in many horse-rearing centers in Brazil because coproparasitological examinations are not performed, including among the racehorses kept at training centers. In this light, the aims of this

study were to determine the prevalence of helminths in Thoroughbred horses that are actively being prepared to compete in turf trials; make correlations with the risk factors inherent to these infections; estimate EPG counts for the most significant associations; and compare the efficiency of different floatation solutions used in the quantitative Mini-FLOTAC coproparasitological technique for helminth monitoring.

## 2. Material and Methods

### 2.1. Sample and Data Collection

Fecal samples were collected between August 2019 and July 2021, from Thoroughbred horses at training centers located in the municipality of Teresópolis, state of Rio de Janeiro. This municipality is located in the mountainous region of the state of Rio de Janeiro, Brazil, occupying an area of 773,338 m<sup>2</sup>. It is the highest municipality in the state, at an altitude of 871 meters above sea level, and therefore is the one with the coldest climate, classified as high-altitude tropical (Cwb), with a short dry season during winter. It has the following geographical coordinates: latitude 22° 24' 44" south; longitude 42° 57' 59" west [20] (Fig. 1).

Six training centers for Thoroughbred horses were included in this study. They are named here using the letters A, B, C, D, E and F, in order to preserve the identity of these centers and their owners. At these training centers, the Thoroughbred horses that are kept under a regimen of intensive husbandry without access to grass and housed in individual masonry stalls. All of the Thoroughbred horses received antiparasitic drugs, containing different active ingredients. Ivermectin and praziquantel were prominent among these and were administered at intervals of 2 to 3 months.

### 2.2. Fecal Sample Collection, Data Retrieval and Sampling

Fecal samples were collected directly from the rectal ampoule of the horses using a palpation glove, or immediately after spontaneous defecation. After each collection, the glove with the fecal material was placed in a sealed container, and these samples were

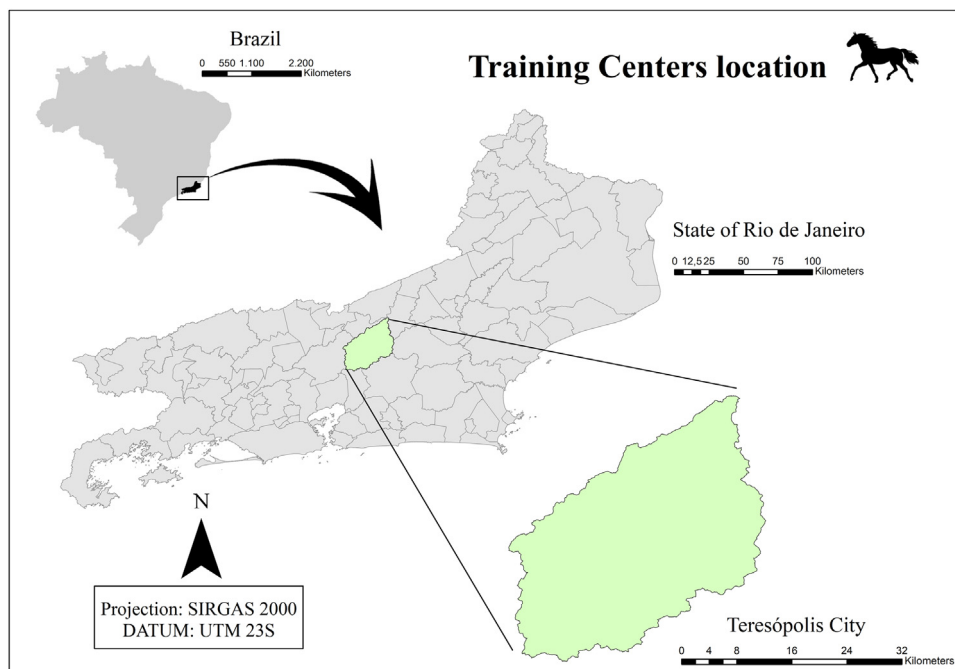


**Fig. 1.** Location of Teresópolis (highlighted in light green), a municipality in the mountainous region of the state of Rio de Janeiro, where the equestrian training centers are sited.

stored in isothermal boxes for transportation of biological samples. The boxes were immediately sent to the laboratory. None of the horses from which fecal samples were obtained had received any anthelmintic treatment over the previous 2 months.

Because of the scarcity of information on the prevalence of intestinal parasite among horses in Rio de Janeiro, the sample calculation was based on previous studies conducted elsewhere in Brazil. The positivity rates were thus considered to range from 50.6% to 96% [21–24]. In this manner, it was estimated that feces samples from 520 horses were needed in order to safely reach a 99% confidence interval.

Among the 520 samples, 84 came from horses at training center A, 126 from B, 49 from C, 73 from D, 82 from E and 106 from F. In addition to fecal samples, information on the sex and age of the horses was obtained from the stud book. Data on animal management were obtained by asking the trainers to answer a questionnaire, seeking the following information: hygiene of the facilities (such as when the stable bedding was changed); anthelmintics provided (and how frequently this was done); whether the doses of the anthelmintics supplied were calculated; and the type of water supplied to the horses.

### 2.3. Parasitological Examination

The samples were subsequently subjected to the Mini-FLOTAC technique using three different flotation solutions, as follows: NaCl flotation solution at a density ( $d$ ) of 1.200 g/mL; ZnSO<sub>4</sub> solution at  $d = 1.200$  g/mL; and ZnSO<sub>4</sub> solution at  $d = 1.350$  g/mL. To perform the technique, the Fill-FLOTAC cup device for herbivores type five [17] was used, containing 5g of feces. At the end of the count, the value obtained was multiplied by five (correction factor). All samples were examined once for each technique and respective solution.

In the laboratory, 45 mL of the flotation solution was added to the Fill-FLOTAC type five container, then 5 g of fecal material was added to the collector. Soon after, the material was homogenized together with the solution. A tip from the kit itself was attached to the device, allowing filling of the two chambers of the Mini-FLOTAC, which subsequently remained at rest for 10 minutes. After this period, the key of the Mini-FLOTAC device was turned and then the reading of each chamber of the Mini-FLOTAC discs was carried out in an optical microscope. To determine the number of eggs per gram of feces, the count of eggs administered in each chamber was performed, which holds a volume of 1 mL each, then 2 mL was counted in each Mini-FLOTAC disc, as the eggs were counted in the two chambers. In order to estimate the amount of helminth eggs counted in 2 mL in relation to the total volume of the material inside each Fill-FLOTAC (total volume of 50 mL = 45 + 5), the result of the count obtained was then multiplied by 25. However, the EPG result is expressed in 1 g of feces, not 5 g, so the value obtained was divided by five. Multiplying by 25 and then dividing by five is the same thing as multiplying the final count by five, and this is the stipulated correction factor.

After the quantitative technique had been used, the qualitative techniques of centrifugation-flotation [25] modified [26], and the spontaneous sedimentation technique [27] were also carried out. Slides produced through using each technique, including the Mini-FLOTAC chambers, were read under an Olympus BX 41 binocular optical microscope (Tokyo, Japan), at magnifications of 100 times and 400 times. The readings on the three Mini-FLOTAC chambers from each horse was made by the same microscopist.

### 2.4. Statistical Analysis of Results

To ascertain the significance of the prevalence of the parasites detected in relation to the training centers and whether these

showed any significant associations with information obtained from the stud book and questionnaire, univariate exploratory analysis was performed using Fisher's exact statistical test at  $P \leq .05$ . Variables that presented statistical significance in the univariate analysis were then included in multivariate analysis. For variables that presented statistical significance in this model, odds ratios were calculated taking into account  $P \leq .05$ , in order to interpret their relevance. After these analyses, the variables that showed statistical relevance were also analyzed using univariate and multivariate tests in relation to the predetermined EPG for each parasite taxon, considering the cutoff for the EPG of 500. The EPG  $\geq 500$  can serve as alert indicating moderate to high infections according to the AAEP [14] as well as by [2,7,22,23,28].

The EPG results obtained using the three different solutions in the quantitative Mini-FLOTAC technique are presented as different quantitative intervals of recovery of helminth eggs, and as the mean, standard deviation and coefficient of variation.

Solutions were analyzed in relation to the frequency of diagnosis of each parasite taxon, among the results obtained from each training center and from two-by-two comparisons. The level of agreement of the diagnoses obtained between the solutions in the Mini-FLOTAC technique, with regard to each helminth taxon detected, was determined by means of Cohen's kappa statistic. This was interpreted following the classification described in [29]. The sensitivity test, that is, the ability of the different flotation solutions applied to the Mini-FLOTAC to detect positive samples, was also evaluated based on two-by-two comparisons.

The results obtained between the three solutions were also evaluated by estimating the medium values of EPG generated in the counts among the eggs of the parasites. Thus, the ANOVA test was applied to verify whether the EPG varied between the solutions applied in the Mini-FLOTAC and in which comparison this variation was defined. For this purpose, the Tukey test was used as post-test, and differences were taken to be significant when  $P \leq .05$ . Regression factors ( $R^2$ ) and their respective  $P$ -values for parasitic EPGs among the techniques and scatterplots were also obtained, to evaluate the linear relationship between the solutions and demonstrate whether there was a linear trend in the results obtained between them.

All analyses were performed using the Statistical Package for the Social Sciences (SPSS) version 25.0, with a significance level of 5%.

## 3. Results

In correlating the results obtained from qualitative copro-parasitological techniques with those from the quantitative Mini-FLOTAC technique, performed three times on each fecal sample collected using solutions of different salts and/or densities, the general prevalence of intestinal parasites was 71.9%. This prevalence showed statistically significant differences between training centers ( $P \leq .05$ ). The training centers with the highest proportions of fecal samples positive for helminths were C (91.8%) and B (85.7%) (Table 1).

The only helminths identified were strongylid nematodes and *Parascaris* spp., and a statistically significant difference in their overall prevalence was also observed among the samples ( $P \leq .05$ ). Strongylid eggs showed higher prevalence in the feces of horses at centers B and C, while *Parascaris* spp. was detected more frequently in feces from horses at centers C (Table 1).

The highest mean EPG counts from strongylids and *Parascaris* spp. were identified in the feces of Thoroughbred horses at training center C. This was seen especially in EPG counts obtained through Mini-FLOTAC performed using sodium chloride solution (Table 1).

The horses included in this study were mostly males, with an average age of 3.7 years, and ages between three and 5 years

**Table 1**

Prevalences, means and standard deviations of egg counts from Mini-FLOTAC using three different floatation solutions (NaCl = 1.200 g/mL, ZnSO<sub>4</sub> = 1.200 g/mL and ZnSO<sub>4</sub> = 1.350 g/mL) to detect helminths in feces from Thoroughbred horses at training centers in Teresópolis, Rio de Janeiro.

Parasites	A (n = 84)	B (n = 126)	C (n = 49)	D (n = 73)	E (n = 82)	F (n = 106)	Total (n = 520)	P Value
Strongyles	54 (64.2%)	106 (84.1%)	43 (87.7%)	43 (58.9%)	36 (43.9%)	65 (61.3%)	347 (66.7%)	.000*
ZnSO <sub>4</sub> 1.200	72.3 ± 239.5	80.0 ± 258.3	231.6 ± 596.7	81.0 ± 271.2	17.9 ± 66.3	55.3 ± 157.2		
ZnSO <sub>4</sub> 1.350	52.4 ± 68.3	57.7 ± 181.1	135.7 ± 341.6	55.3 ± 176.1	12.1 ± 58.4	39.8 ± 114.1		
NaCl 1.200	120.7 ± 421.4	132.9 ± 455.4	358.3 ± 864.1	122.8 ± 395.9	23.3 ± 71.9	117.7 ± 469.1		
<i>Parascaris</i> spp.	17 (20.2%)	32 (26.6%)	19 (38.8%)	23 (31.5%)	21 (25.6%)	7 (6.6%)	119 (22.88%)	.0152*
ZnSO <sub>4</sub> 1.200	27.5 ± 139.4	24.4 ± 131.8	31.2 ± 85.4	31.3 ± 157.2	29.6 ± 158.8	5.8 ± 37.6		
ZnSO <sub>4</sub> 1.350	23.7 ± 145.1	19.6 ± 138.4	30.3 ± 89.0	22.0 ± 108.6	18.7 ± 96.8	3.6 ± 28.4		
NaCl 1.200	32.3 ± 169.2	27.7 ± 158.0	40.4 ± 113.8	31.4 ± 144.4	31.7 ± 151.6	7.4 ± 51.6		
Positive Total (%)	59 (70.2%)	108 (85.7%)	45 (91.8%)	53 (72.6%)	43 (52.4%)	66 (62.2%)	374 (71.9%)	.000*

A, B, C, D, E and F: Thoroughbred horse training centers.

\*  $P \leq .05$  was taken to be significant.

formed the most frequent range. Most of the trainers reported at their centers, the bedding material in the stalls was totally changed once a month or at longer interval (451/520; 86.7%). They administered ivermectin and praziquantel interspersed with other pharmacological agents including moxidectin, pyrantel, abamectin and fenbendazole, based on prior weighing of the animals. In addition, among the horses included in this parasitological survey, the types of water supplied to these animals were almost equally divided between spring water (264/520; 50.8%) and spring water and artesian well water (256/520; 49.2%) (Table 2).

In analyzing the helminth sample, using information obtained from the questionnaires and from the stud book to assess possible associations with helminthic infections, a statistically significant difference ( $P \leq .05$ ) was observed in relation to the specific variables for strongylids and *Parascaris* spp. in the univariate analysis. With regard to strongylids, the statistical difference was observed in the categorization of horses according to age group and the type of anthelmintic provided. With regard to *Parascaris* spp., the statistically significant difference was seen in the interval between administration of anthelmintics and the calculated dose of these anthelmintics (Table 2).

Variables that reached significance in the exploratory univariate analyses were then input to analysis in a logistic regression model. In this, for strongylids, the age group remained statistically significant; while for *Parascaris* spp., anthelmintic supply interval and calculated dose of the anthelmintic remained statistically significant ( $P \leq .05$ ).

It was seen that horses under 3 years of age were about eight times more likely to be parasitized by strongylids than those that were 3 years of age or older. Moreover, regarding the frequency of *Parascaris* spp., supply of anthelmintics with ivermectin and praziquantel at intervals of 2 months and in a whole-paste format, without prior weighing of the animal, were found to constitute protective factors, with OR 0.5775 and OR 0.4664, respectively (Table 2).

Among the 119 samples that were positive for *Parascaris* spp. and 347 for strongylids, 110 and 312 respectively were detected through Mini-FLOTAC, binging together the three floatation solutions. We tried to recover the highest count among the three EPG values identified from each solution and thus to classify them as EPG greater than or equal to 500; or EPG less than 500. In this manner, the risk factors that were statistically significant regarding the prevalence of parasites, previously described in Table 2, were also analyzed quantitatively in terms of their EPG counts. In relation to strongylids, 35 parasitized horses had EPG values greater than or equal to 500 and most of these were younger than 3 years of age, and this age group difference was statistically significant ( $P < .05$ ). Horses less than three years of age were 11 times more likely to present EPG  $\geq 500$ . The risk and protection factors associated with the prevalence of *Parascaris* spp. in Table 2 were not associated with these EPG ranges (Table 3).

The NaCl solution (d = 1.200 g/mL) used in Mini-FLOTAC enabled recovery of the largest number of positive samples. Nonetheless, although positive samples were recovered more frequently through using this solution, it was unable to recover parasite forms from all positive fecal samples, such that some positive samples were only identified through using Mini-FLOTAC with ZnSO<sub>4</sub> solution (d = 1.200 g/mL) and ZnSO<sub>4</sub> (d = 1.350 g/mL). In all comparisons between the techniques, regarding the different solutions used for diagnosing eggs of both *Parascaris* spp. and strongylids, it was observed that the levels of agreement between them were classified as substantial ( $\kappa = 0.61-0.80$ ), and these analyses were statistically significant (Table 4). In addition, the highest sensitivity values were obtained with the diagnosis using the NaCl solution (d = 1.200 g/mL) when compared with ZnSO<sub>4</sub> solution (d = 1.200 g/mL) both in the diagnosis of eggs of *Parascaris* spp. and in strongyles and with the NaCl solution (d = 1.200 g/mL) when compared with ZnSO<sub>4</sub> (d = 1.350 g/mL) in the diagnosis of strongyles eggs (Table 4).

The NaCl solution (d = 1.200 g/mL) used in Mini-FLOTAC was the one that enabled recovery of the highest mean EPG counts for both *Parascaris* spp. and strongylids (Table 3). The coefficients of variation (CV) were high in the EPG counts of nematodes performed with all solutions. In EPG counts on *Parascaris* spp., the highest CV was obtained with the ZnSO<sub>4</sub> solution (d = 1.350 g/mL), followed by the count using the NaCl solution. On the other hand, for EPG counts on strongylids, the highest CV were observed with the NaCl and ZnSO<sub>4</sub> (d = 1.200 g/mL) solutions (Table 5).

Significant variation in the EPG counts on strongylid eggs ( $P \leq .05$ ) was observed. This variation was present in comparisons of mean EPG values between Mini-FLOTAC using NaCl (d = 1.200 g/mL) and Mini-FLOTAC using ZnSO<sub>4</sub> (d = 1.200 g/mL) ( $P < .05$ ) and in comparisons between Mini-FLOTAC using NaCl (d = 1.200 g/mL) and Mini-FLOTAC using ZnSO<sub>4</sub> (d = 1.350 g/mL) ( $P < .05$ ) (Table 5).

The smallest and largest EPG ranges were found through the quantitative Mini-FLOTAC technique using NaCl solution (d = 1.200 g/mL), both for *Parascaris* spp. and for strongylids. For *Parascaris* spp., the technique that showed the second highest frequency of detection of the smallest and largest EPG ranges was Mini-FLOTAC with ZnSO<sub>4</sub> solution (d = 1.350 g/mL) and for strongylids it was Mini-FLOTAC with ZnSO<sub>4</sub> solution (d = 1.200 g/mL) (Table 6).

Positive regression coefficients and increasing linear trends in helminth egg counts were observed through the Mini-FLOTAC technique using the three solutions analyzed. In two-by-two comparisons of the floatation solutions used in Mini-FLOTAC, the level of coefficient of EPG counts for *Parascaris* spp. was higher in relation to the mean, that is,  $R^2$  closer to 1, for ZnSO<sub>4</sub> (d = 1.350 g/mL) vs. NaCl (d = 1.200 g/mL) (Fig. 2C). The other regression analyses on EPG counts for *Parascaris* spp. presented lower  $R^2$  values (Fig. 2A and B).

In an evaluation on scatter plots from strongylid egg counts, there was higher congruence of the points (EPG values) in relation

**Table 2**  
Rates of infection with helminths according to macroscopic variables of feces, stud book data and completed questionnaires answered by horse trainers at different training centers for Thoroughbred horses located in Teresópolis, Rio de Janeiro.

Variables	Strongyles (n = 347)		P Value (Univariate)	P Value (Multivariate)	Odds ratio	Parascaris spp. (n = 119)		P Value (Univariate)	P Value (Multivariate)	Odds ratio	Total (n = 374)
	N° positive	%				N° positive	%				
<b>Gender</b>											
Female (n = 194)	135	69.6	.833			54	27.8	.091			149
Male (n = 326)	212	65				65	19.9				225
<b>Age range</b>											
<3 y o (n = 141)	129	91.5	<.001*	.000*	7.9392* (4.2469–14.841)	37	26.2	.43			129
≥ 3 y.o.(n = 379)	218	41.9				82	21.6				245
<b>Bed change</b>											
Every 15 days (n = 69)	50	72.5	.137			17	24.6	.087			55
30–40 d (n = 451)	297	65.8				102	22.6				319
<b>Anthelmintics provided</b>											
Ivermectin and praziquantel only (n = 226)	137	60.6	.009*	.8647		62	27.4	.441			158
Ivermectin, praziquantel and others (n = 294)	210	71.4				57	19.4				216
<b>Anthelmintic supply interval</b>											
Every 2 months (n = 332)	226	68.1	.191			64	19.3	.021*	.002*	0.5775* (0.3809–0.8754)	239
Every 3 months (n = 188)	121	64.3				55	29.3				135
<b>Calculation of the anthelmintic dose</b>											
Provides the entire tube (n = 214)	123	57.5	.23			33	15.4	.001*	.000*	0.4664* (0.2983–0.7292)	130
Based on animal weight (n = 306)	224	73.2				86	28.1				244
<b>Type of water</b>											
Spring water (n = 264)	171	64.8	.77			56	21.2	.951			185
Spring and artesian well (n = 256)	176	68.7				63	24.6				189

\*  $P \leq .05$ .

**Table 3**

Frequencies of samples and risk factors associated with EPG less than 500 and greater than or equal to 500 in relation to strongylids and *Parascaris* spp., obtained only via the quantitative Mini-FLOTAC technique.

Age range	Strongyles			P Value (Univariate)	Valor de P (Multivariate)	Odds Ratio
	EPG $\geq$ 500 (n = 35)	EPG 5–499 (n = 277)				
< 3 y.o.	30 (85.7%)	94 (33.9%)		<.001	<0.001	11.6809 (4.3888–31.0887)
$\geq$ 3 y.o.	5 (14.9%)	183 (66.06%)				
<b>Parascaris spp.</b>						
	EPG $\geq$ 500 (n = 9)	EPG 5–499 (n = 101)		P Value (Univariate)	Valor de P (Multivariate)	Odds Ratio
<b>Anthelmintic supply interval</b>						
Every 2 mo	6 (66.6%)	53 (52.4%)		.198	NA	NA
Every 3 mo	3 (33.3%)	48 (47.5%)				
<b>Calculation of the anthelmintic dose</b>						
Whole-paste format (n = 214)	3 (33.3%)	28 (27.7%)		.031*	.115	NA
Based on animal weight (n = 306)	6 (66.6%)	73 (72.2%)				

Abbreviation: NA, not assessed.

\*  $P \leq .05$

**Table 4**

Levels of agreement of the results obtained through Mini-FLOTAC using different floatation solutions for detecting helminth eggs in equine feces.

<i>Parascaris</i> spp.					
Mini-FLOTAC NaCl (d = 1.200 g/mL)	Mini-FLOTAC ZnSO4 (d = 1.200 g/mL)		Kappa (IC 95%)	P Value	Sensitivity (IC 95%)
	Positive	Negative			
Positive	66	22	0.78 (0.705–0.857)	0.03*	0.89 (0.798–0.952)
Negative	8	424			
Mini-FLOTAC NaCl (d = 1.200 g/mL)	Mini-FLOTAC ZnSO4 (d = 1.350 g/mL)		Kappa (IC 95%)	P Value	Sensitivity (IC 95%)
	Positive	Negative			
Positive	63	25	0.674 (0.588–0.761)	.04*	0.74 (0.635–0.830)
Negative	22	410			
Mini-FLOTAC ZnSO4 (d = 1.200 g/mL)	Mini-FLOTAC ZnSO4 (d = 1.350 g/mL)		Kappa (IC 95%)	P Value	Sensitivity (IC 95%)
	Positive	Negative			
Positive	66	8	0.8 (0.727–0.872)	.037*	0.77 (0.673–0.859)
Negative	19	427			
<b>Strongyles</b>					
Mini-FLOTAC NaCl (d = 1.200 g/mL)	Mini-FLOTAC ZnSO4 (d = 1.200 g/mL)		Kappa (IC 95%)	P Value	Sensitivity (IC 95%)
	Positive	Negative			
Positive	218	56	0.686 (0.624–0.748)	.032*	0.89 (0.848–0.929)
Negative	26	220			
Mini-FLOTAC NaCl (d = 1.200 g/mL)	Mini-FLOTAC ZnSO4 (d = 1.350 g/mL)		Kappa (IC 95%)	P Value	Sensitivity (IC 95%)
	Positive	Negative			
Positive	197	77	0.622 (0.557–0.688)	.033*	0.89 (0.852–0.936)
Negative	22	224			
Mini-FLOTAC ZnSO4 (d = 1.200 g/mL)	Mini-FLOTAC ZnSO4 (d = 1.350 g/mL)		Kappa (IC 95%)	P Value	Sensitivity (IC 95%)
	Positive	Negative			
Positive	189	55	0.67 (0.606–0.734)	.033*	0.863 (0.810–0.906)
Negative	30	246			

Abbreviation: CI, confidence interval

\*  $P$  value  $\leq$  0.05. Kappa < 0 indicated that there was no agreement; 0 to 0.20, poor agreement; 0.21 to 0.40, reasonable agreement; 0.41 to 0.60, moderate agreement; 0.61 to 0.80, substantial agreement; and 0.81 to 1.00, almost perfect agreement (Landis and Koch, 1987).

**Table 5**

Comparison of mean EPG values, through coefficient of variation and analysis of variance, between the solutions used in Mini-FLOTAC to recover nematode eggs from the feces of Thoroughbred horses kept at training centers in Teresópolis, RJ.

Mini-FLOTAC-Solution	<i>Parascaris</i> spp.	CV(%)	Strongyles	CV(%)
ZnSO4 (d = 1.200 g/mL)	27.51 $\pm$ 139.41	506.8	72.40 $\pm$ 239.55	330.87
ZnSO4 (d = 1.350 g/mL)	23.77 $\pm$ 145.13	610.5	52.52 $\pm$ 168.27	320.39
NaCl (d = 1.200 g/mL)	32.40 $\pm$ 169.20	522.2	120.98 $\pm$ 421.40	348.32
ANOVA (P Value)	0.6511		0.000*	

Abbreviations: SD, standard deviation; CV, coefficient of variation

\*  $P$  value  $\leq$  .05 was taken to be statistically significant.

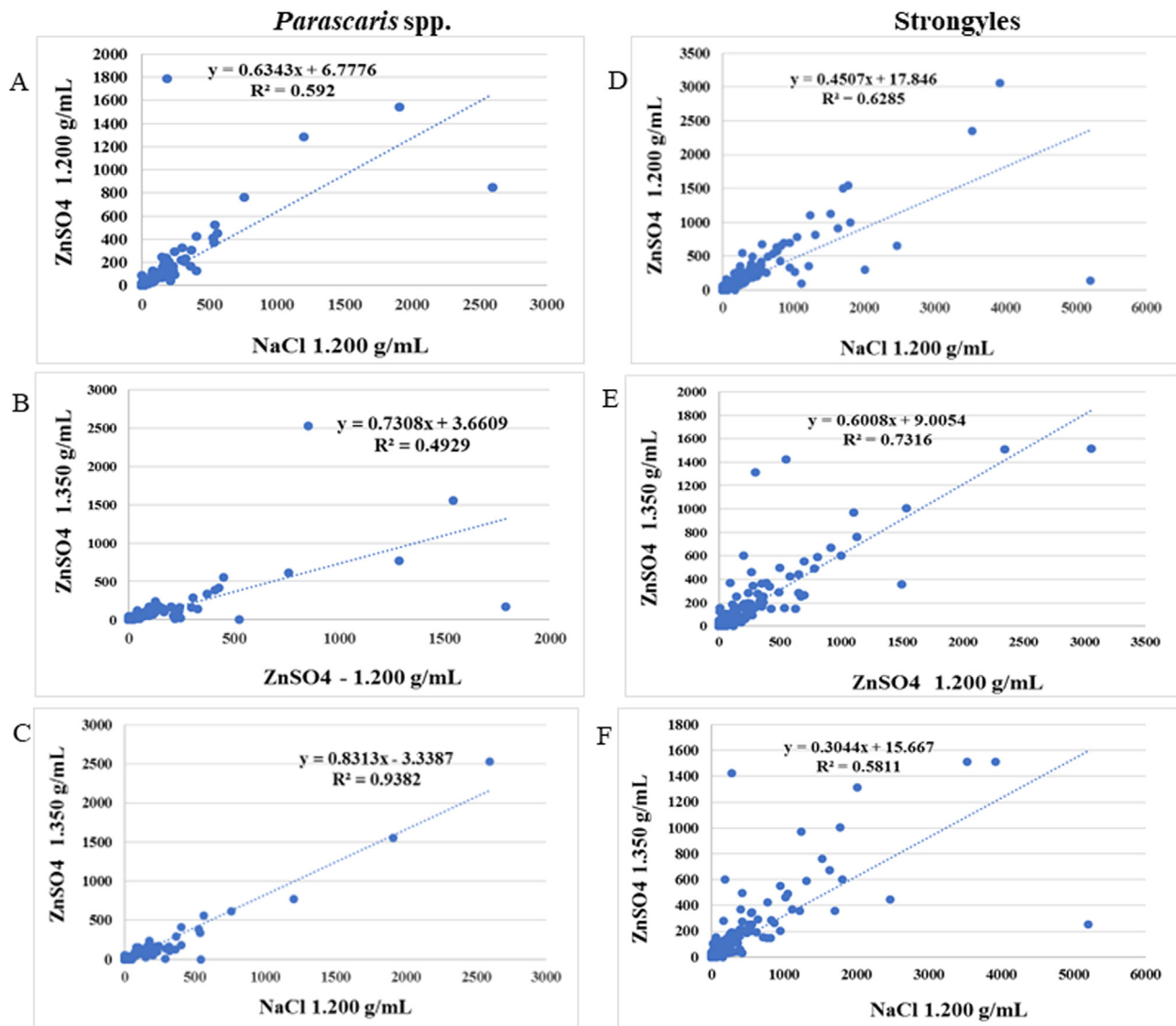
**Table 6**

Absolute frequencies of the numbers of positive samples according to EPG ranges identified through using different solutions in Mini-FLOTAC to recover nematode eggs from the feces of Thoroughbred horses kept at training centers in Teresópolis, Rio de Janeiro.

EPG <i>Parascaris</i> spp.	ZnSO <sub>4</sub> (d = 1.200 g/mL) (n = 74)	ZnSO <sub>4</sub> (d = 1.350 g/mL) (n = 85)	NaCl (d = 1.200 g/mL) (n = 88)
5–499	68	80	80
500–999	3	3	5
1,000–1,790	3	1	1
1,791–2,530	0	1	1
2,595	0	0	1

EPG strongyles	ZnSO <sub>4</sub> (d = 1.200 g/mL) (n = 244)	ZnSO <sub>4</sub> (d = 1.350 g/mL) (n = 219)	NaCl (d = 1.200 g/mL) (n = 274)
5–499	225	207	242
500–1,515	16	12	22
1,516–3,055	3	0	7
3,056–5,204	0	0	2
5,205	0	0	1



**Fig. 2.** Plots of dispersion of helminth egg count and regression factors determined from comparisons of the Mini-FLOTAC technique using solutions of NaCl (d = 1.200 g/mL), ZnSO<sub>4</sub> (d = 1.350 g/mL) and ZnSO<sub>4</sub> (d = 1.200 g/mL), in quantitative parasitic analyses on fecal samples from horses.

to the straight-line plot of the graph and higher R<sup>2</sup> in the Mini-FLOTAC comparison between ZnSO<sub>4</sub> (d = 1.350 g/mL) and ZnSO<sub>4</sub> (d = 1.200 g/mL) (Fig. 2E). The other comparisons between EPG counts, that is, in relation to the NaCl solution (d = 1.200 g/mL), showed lower R<sup>2</sup> and greater dispersion of points (EPG values) in relation to the straight-line plot of the graph (Fig. 2D and 2F).

**4. Discussion**

The overall prevalence of helminths in Thoroughbred horses kept at different training centers located in Teresópolis, Rio de Janeiro, was 71.9% when the results obtained through microscopic coproparasitological techniques were combined. In general, the



helminth frequencies in fecal material from horses reported in the literature have mostly been higher than what was found in the present study. Thus, in parasitological surveys among horses kept on farms located in different states in Brazil, such as São Paulo, Rio Grande do Sul and Minas Gerais, the positivity rates ranged from 89% to 96% [2,21,24]. Frequencies higher than what was identified in the present study were also reported in horse-rearing centers in Mexico, ranging from 91.3% to 100%; Saudi Arabia 86.6%; Germany 77.5%; Ethiopia 78.5% to 94%; and Nepal 84.5% to 84.7% [28,30–37].

The differences in the frequencies found in those parasitological surveys may have been related to the different age of sampled horses, geographical locations of the horse farms, sanitary management, aptitude of the breed of horse for sport, work or leisure; duration of environmental exposure through grazing; number of samples included in the study; and laboratory techniques used for investigating the parasites.

It should be noted that the Thoroughbred horses included in the present study were racehorses with high physical vigor that were fully participating in turf activities, that is, they were taking part in race events at one of the most important racecourses in Brazil. Thus, these animals were being carefully managed. In addition, they were being kept in individual stalls for much of the day without access to grass, such that they were only taken out for training, grooming, washing and participation in trials. These factors may have contributed to lower presence of helminths than in the other studies cited. Even so, the frequency of helminths detected showed significant values for horses kept individually in stables and without grazing. However, the infection rate observed in this study can be explained by the humid tropical climate that favors the development and survival of the infective forms of the parasites, by the direct supply of contaminated hay and grass to the stables, as well as sharing utensils for cleaning and removing feces from the stalls. Although the feces produced are removed daily from the stalls, this biological material is not destined for dunghill, being stored for some time in bags to later be sent to the production of fertilizer on agricultural properties. This management problem may be favoring the contamination of the environment near the stalls.

Generally, the racehorses kept on these training centers are young male adults aged three to 5 years that are at the apex of their athletic body development for racing events. In general, younger horses up to 3 years of age were the ones with the highest chances of becoming parasitized by strongylids. Like in this study, the highest frequency of strongylid infection was observed among horses in the youngest age group, on farms in Pakistan, Ukraine and Hungary [12,38,39]. Host age is known to be an important factor regarding susceptibility to parasite infection, that is, horses under five years of age tend to present higher frequency of infection and parasite burden in relation to these nematodes [12,40].

The higher frequency of strongylid infection in horses under 3 years of age that was observed in the present study may have been due to previous remaining infection that was acquired in the stud farm from which they originated, through grazing on pasture contaminated with infectious larvae. Since Thoroughbred horses arrive at these training centers at about 2 years of age, these findings indicate that younger horses are probably the largest source of strongylid infection and therefore deserve more attention in developing parasite control programs in the original stud farm [39]. This applies especially to horse that have recently been incorporated into training centers, which should go through prior examinations and a quarantine period.

Higher infection rates among younger horses are generally associated with *Parascaris* spp. infections, as observed in Saudi Arabia, Israel, Ethiopia, Nepal, Australia, and Italy [12,13,33–35,41]. Unlike in those studies, the frequency of infection by this nematode in the present study was not associated with the age group of the horses

(<3 years old). However, in the training centers in Rio de Janeiro, this age group is commonly referred to as foals, even though most of them are young adults. Horses up to 2 years of age considered to be foals are the most susceptible to infection by this nematode [42,43].

In relation to *Parascaris* spp., two factors drew attention because they ended up being considered to be protective factors: one that was related to supply of the whole paste containing the anthelmintics without weighing the animal; and the other, to shorter intervals between supplying the drug, as reported by the trainers (every 2 months). The pastes containing commercially available anthelmintics are supplied in a device with a total volume suitable for an adult horse of maximum weight 600 kg, at the recommended dosage of 200 mcg of ivermectin and 1 mg of praziquantel per kg of animal weight. However, male Thoroughbred horses undergoing racing activities reach an average weight of 450 kg [44]. These factors may have made the whole paste, as supplied, sufficient for controlling the nematode, thus leading to low levels of the nematode. Lack of weighing in order to accurately calculate the dose of the drug has already been reported from other horse farms in Brazil [2,21].

These practices of providing horses with whole paste without any prior weighing as part of a strategic treatment scheme, that is, scheduled on a calendar at short intervals, has seemingly led to satisfactory results with regard to controlling *Parascaris* spp. infection. In training center C, which ended up showing the highest frequency of positive samples for *Parascaris* spp. and the highest average egg count of this parasite did not apply these management routines, which ended up generally being considered as protective factors. This may have favored the significant casuistry of the nematode in horses from training center C. It is still worth noting that the excessive use of drugs is known to lead to selection of nematodes that are resistant to the anthelmintics routinely supplied to horses, particularly ivermectin. This situation has already been reported in the literature since 2002 [6,45].

It should be noted that in some training centers in this study, especially in training centers B and C, the prevalence of nematode eggs and their quantification were higher, even though the management conduct reported by the trainers was similar to what was reported from other centers at which parasite prevalence was lower. However, some circumstances may have contributed to the larger number of cases evidenced, such as: in property B there was a greater number of horses stabled, whose production of feces may have intensified environmental contamination, while in property C it can be attributed to the greater interval used for anthelmintic treatments. Even so, cases of anthelmintic resistance must be evaluated to verify the occurrence, even in animals kept in stables such as the Thoroughbreds of the present study. This can be practically done in the field through the egg parasite reappearance test in feces of the horses challenged with specific anthelmintics.

This situation also emphasizes that there is a need to implement selective anthelmintic treatment. In such treatments, the feces from the horses are firstly, subjected to quantitative parasitological techniques to establish the EPG cutoff point that is necessary for treatment to be implemented. This avoids supplying unnecessary anthelmintics and prevents development of resistance to these drugs in future generations of parasites [46]. Unfortunately, in the vast majority of horse farms in Brazil, EPG counts are not performed either for estimating the drug supply or for parasitological monitoring of farms. Suppressive or preventive strategic treatment predominates.

It is important to note that currently in Rio de Janeiro state, most of the Thoroughbred Training Centers are concentrated in the mountainous region of the state, especially in the city of Teresópolis, totaling seven training centers, due to the mild climate and altitude. Of these, only one declined to participate in the study. In

this way, we ended up encompassing most of the city's training centers. In view of the above, the results of the variables were not influenced by the type centers included in the sample panel.

Comparison of the results obtained from the solutions used in the Mini-FLOTAC technique clearly showed that, with the NaCl solution ( $d = 1.200 \text{ g/mL}$ ), it was possible to diagnose a greater number of samples positive for *Parascaris* spp. and strongylids. This fact was also observed through by the higher sensitivity values of this study, that is, the ability to detect positive samples for helminth eggs, which was evidenced mainly from the comparison of the NaCl solution ( $d = 1.200 \text{ g/mL}$ ) with the other solutions. The  $\text{ZnSO}_4$  ( $d = 1.350 \text{ g/mL}$ ) the second best solution for recovering *Parascaris* spp. eggs and  $\text{ZnSO}_4$  ( $d = 1.200 \text{ g/mL}$ ) was the second best for diagnosing strongylids. The greater recovery of strongylid eggs using NaCl solution at the density of  $1.200 \text{ g/mL}$  was concordant with the results from the research group that designed the Mini-FLOTAC device. Those authors showed that this solution was one of the best for recovering eggs of these parasites in equine feces [17,47].

In the fecal analyses of the present parasitological survey, the levels of diagnostic agreement between the solutions applied in Mini-FLOTAC were classified as substantial, but 100% agreement regarding the frequency of samples positive for helminths was not reached. This result was already expected, because the floatation solutions present different sensitivities with regard to recovery of parasite eggs. It is noteworthy that helminth eggs have different densities and thus interact with solutions in different ways. This situation can influence the diagnosis and the EPG estimates [18]. The NaCl and  $\text{ZnSO}_4$  salts were chosen for evaluation in the present study because they are widely used in other traditional coparasitological techniques such as those of Willis and Faust et al [48,49] and are easy to acquire commercially. Thus, these solutions can be routinely applied in making parasitological diagnoses and monitoring EPG estimates in the field among horses in Brazil.

Regarding EPG quantification, it was observed that the highest mean counts were obtained with the NaCl solution for both groups of nematodes. Nevertheless, all the floatation solutions used in Mini-FLOTAC enabled recovery of different EPG count ranges, and this may have influenced the high coefficients of variation obtained. The recovery of all stratified EPG intervals in this study was only obtained through using the NaCl solution ( $d = 1.200 \text{ g/mL}$ ) for strongylids and *Parascaris* spp., followed by  $\text{ZnSO}_4$  solution ( $d = 1.350 \text{ g/mL}$ ) for *Parascaris* spp.. Comparisons with the literature regarding EPG counts according to floatation solutions were impaired, because the articles analyzing Mini-FLOTAC performed on equine feces that we were able to retrieve mainly tended to compare its performance with that of other techniques, especially with the McMaster technique [15,18,50–56] without analyzing the influence of floatation solutions on egg recovery.

The high rate of variation of EPG counts among all solutions that was seen in the present study should be evaluated with caution. This variation seems to be inherent to the disparate quantifications that were observed in feces from some training centers, but especially from some specific horses. These disparities may be related to the inherent management of each farm, the presence of young animals newly incorporated into the herd and the resistance of parasites to the anthelmintics that were routinely provided. These disparities were often more evident in some individuals that ended up presenting higher EPG values, which were mainly seen in the samples from training center C.

In general, the variation in EPG counts was similar between the floatation solutions for *Parascaris* spp., especially between NaCl ( $d = 1.200 \text{ g/mL}$ ) and  $\text{ZnSO}_4$  ( $d = 1.350 \text{ g/mL}$ ). Comparison of EPG counts obtained using these solutions showed that linearity was present in the quantification of eggs from this nematode. This emphasizes that there was a high level of agreement not only regarding the diagnostic frequency but also regarding the similar-

ity in the quantification of eggs. A different situation was seen in relation to EPG counts from strongylids, because comparison of these counts between the floatation solutions used showed that their variation was directly associated with the type of solution used. It was clearly seen that there was a low level of similarity of EPG counts from these nematodes through use of  $\text{ZnSO}_4$  solutions, compared with NaCl. The latter was seen to yield superior recovery, regarding both diagnosis and quantification of eggs.

This was the first coparasitological survey conducted among Thoroughbred horses kept at different training centers in Rio de Janeiro. These horse had high athletic activity and were active in turf trials. Through this survey, the prevalence rates of nematodes diagnosed as strongylids and *Parascaris* spp. could be determined. The estimated EPG counts for these nematodes presented variance, even though the horses were subjected to similar management routines. The factors associated with infections could be characterized, and the main factors found were the age group less than 3 years for strongylids. For *Parascaris* spp., use of an excess quantity of the drug, through administration of whole paste at short intervals of time was characterized as a protective factor. However, this conduct was seen as quite worrying because, within a short period of time, it can worsen the resistance of nematodes to the anthelmintic drugs supplied to the animals.

In order to prevent parasites from causing damage to the health of horses and worsening the problem of resistance to anthelmintic drugs, it is essential to recommend that coparasitological diagnoses with estimation of EPG counts should be undertaken at these training centers. In this manner, parasitological monitoring of the herd can be performed and, consequently, parasite control measures based on selective treatment can be implemented. This would avoid excessive supply of drugs to the animals. In this regard, Mini-FLOTAC using NaCl solution proved to be the method most indicated for diagnosing and estimating EPG counts of *Parascaris* spp. and strongylids. However, further studies on this topic need to be conducted in order to evaluate the accuracy and precision of different floatation solutions.

## Acknowledgments

The authors would like to thank the equine training centers in the municipality of Teresópolis for allowing us to collect fecal samples from their animals. We also gratefully acknowledge the Rio de Janeiro Research Support Foundation (FAPERJ) for providing funding under Grant no. E-26/010.002748/2019, the Office of the Vice Dean of Research, Graduate Studies and Innovation (PROPMI) of Fluminense Federal University (UFF) for granting financial aid through its FOPESQ 2022 Program.

## Declaration of Competing Interest

The authors declare that they have no known competing financial interests or personal relationships that could have appeared to influence the work reported in this paper.

## References

- [1] IBGE - Instituto Brasileiro de Geografia e Estatística. Rebanho de equinos, 2021. Available at: <https://www.ibge.gov.br/explica/producao-agropecuaria/equinos/br>. Accessed November 01, 2022.
- [2] Rosa HFM, Garcia AM, Daher DO, Lima IG, Félix MB, Capellari LA, et al. Factors associated with the prevalence of helminths in Mangalarga Machador horses in southern of Minas Gerais, Brazil. *Pesqui Vet Bras* 2018;38(6):1097–104 English. doi:10.1590/1678-5150-PVB-5177.
- [3] SIAPEC - Sistema de Integração Agropecuária. Available at: <https://siapec3.agricultura.rj.gov.br/siapec3/login.wsp> Accessed November 12, 2022.
- [4] Brasil. Revisão do Estudo Complexo do Agronegócio do Cavalo - Ministério da 462 Agricultura, Pecuária e Abastecimento, 2016
- [5] Matthews JB. Anthelmintic resistance in equine nematodes. *Int J Parasitol Drugs Drug Resist* 2014;25(3):310–15 4. doi:10.1016/j.ijpddr.2014.10.003.

- [6] Kaplan RM. Drug resistance in nematodes of veterinary importance: a status report. *Trends Parasitol* 2004;20(10):477–81. doi:10.1016/j.pt.2004.08.001.
- [7] Flanagan KL, Morton JM, Sandeman RM. Prevalence of infestation with gastrointestinal nematodes in Pony Club horses in Victoria. *Aust Vet J* 2013;91(6):241–5. doi:10.1111/avj.12052.
- [8] Villa-Mancera A, Aldeco-Pérez M, Molina-Mendoza P, Hernández-Guzmán K, Figueroa-Castillo JA, Reynoso-Palomar A. Prevalence and risk factors of gastrointestinal nematode infestation of horses, donkeys and mules in tropical, dry and temperate regions in Mexico. *Parasitol Int* 2021;81:102265. doi:10.1016/j.parint.2020.102265.
- [9] Nielsen MK. Evidence-based considerations for control of *Parascaris* spp. infections in horses. *Equine Vet Educ* 2016;28:224–31. doi:10.1111/eve.12536.
- [10] Clayton HM. Ascariids: recent advances. *Vet Clin North Am Equine Pract* 1986;2(2):313–28.
- [11] Jabbar A, Littlewood DT, Mohandas N, Briscoe AG, Foster PG, Müller F, von Samson-Himmelstjerna G, Jex AR, Gasser RB. The mitochondrial genome of *Parascaris univalens*-implications for a "forgotten" parasite. *Parasit Vectors*. 2014;7(428):1–8. doi:10.1186/1756-3305-7-428.
- [12] Saeed MA, Beveridge I, Abbas G, Beasley A, Bauquier J, Wilkes E, et al. Systematic review of gastrointestinal nematodes of horses from Australia. *Parasite Vector* 2019;12(1):1–16. doi:10.1186/s13071-019-3445-4.
- [13] Scala A, Tamponi C, Sanna G, Predieri G, Meloni L, Knoll S, et al. *Parascaris* spp. eggs in horses of Italy: a large-scale epidemiological analysis of the egg excretion and conditioning factors. *Parasite Vector* 2021;14(1):1–8. doi:10.1186/s13071-021-04747-w.
- [14] Nielsen MK, Mittel L, Grice A, Erskine M, Grave E, Vaala W, et al. AAEP Parasite Control Guidelines, Lexington, KY: American Association of Equine Practitioners; 2019. Available at: [www.aaep.org](http://www.aaep.org) Accessed October, 05 2022.
- [15] Went HA, Scare JA, Steuer AE, Nielsen MK. Effects of homogenizing methods on accuracy and precision of equine strongylid egg counts. *Vet Parasitol* 2018;261:91–5. doi:10.1016/j.vetpar.2018.09.001.
- [16] Gordon HMCL, Whitlock HV. A new technique for counting nematode eggs in sheep faeces. *J Scient Res* 1939;12(1):50–2.
- [17] Cringoli G, Maurelli MP, Leveck B, Bosco A, Vercruyse J, Utzinger J, et al. The Mini – FLOTAC technique for the diagnosis of helminth and protozoan infections in humans and animals. *Nat Protoc* 2017;12(9):1723–32. doi:10.1038/nprot.2017.067.
- [18] Dias de Castro LL, Abrahão CLH, Buzatti A, Molento MB, Bastianetto E, Rodrigues DS, et al. Comparison of McMaster and Mini-FLOTAC fecal egg counting techniques in cattle and horses. *Vet Parasitol Reg Stud Rep* 2017;10:132–5. doi:10.1016/j.vprsr.2017.10.003.
- [19] Ghafar A, Abbas G, King J, Jacobson C, Hughes KJ, El-Hage C, et al. Comparative studies on faecal egg counting techniques used for the detection of gastrointestinal parasites of equines: A systematic review. *Curr Res Parasitol Vector Borne Dis* 2021;9(1):100046. doi:10.1016/j.crvbd.2021.100046.
- [20] Cidade-Brasil, 2020. Município de Teresópolis. Available at: <https://www.cidade-brasil.491.com.br/municipio-teresopolis.html>. Accessed November 12, 2022.
- [21] Martins IVF, Verocai GG, Correia TR, Melo MPSR, Pereira MJS, Scott FB, et al. Survey on control and management practices of equine helminthes infection. *Pesqui Vet Bras* 2009;29(3):253–7. doi:10.1590/S0100-736X2009000300011.
- [22] Pereira JR, Vianna SS. Gastrointestinal parasitic worms in equines in the Paraíba Valley, State of São Paulo, Brazil. *Vet Parasitol* 2006;140(3–4):289–95. doi:10.1016/j.vetpar.2006.03.036.
- [23] Moraes CBR, Santiago JM, de Lima MM, Lucena JEC. Parasite prevalence among equidae in the backland of the State of Pernambuco, Brazil. *Semin Cienc Agrar* 2017;38(6):3629–38. doi:10.5433/1679-0359.2017v38n6p3629.
- [24] Lignon JS, Martins NS, Cardoso TAEM, Leão MS, Pellegrini TG, Camassola JLT, et al. Frequency of gastrointestinal parasites in Creole horses from the Southern Rio Grande do Sul. *Arq Bras Med Vet Zootec* 2020;72(3):1067–8. doi:10.1590/1678-4162-11305.
- [25] Sheather AL. The detection of intestinal protozoa and mange parasites by a flotation technic. *J Comp Pathol* 1923;36:266–75. doi:10.1016/S0368-1742(23)80052-2.
- [26] Huber F, Bomfim TC, Gomes RS. Comparação da eficiência da técnica de sedimentação pelo formaldeído-éter e da técnica de centrífugo-flutuação modificada na detecção de cistos de *Giardia* sp. e oocistos de *Cryptosporidium* sp. em amostras fecais de bezerros. *Rev Bras Parasitol Vet* 2003;12(2):135–7.
- [27] Lutz AO. *Schistosomum mansoni* e a schistosomatose segundo observações feitas no Brasil. *Mem Inst Oswaldo Cruz* 1919;11(1):121–55.
- [28] Valdéz-Cruz MP, Hernández-Gil M, Galindo-Rodríguez L, Alonso-Díaz MA. Gastrointestinal nematode burden in working equids from humid tropical areas of central Veracruz, Mexico, and its relationship with body condition and haematological values. *Trop Anim Health Prod* 2013;45(2):603–7. doi:10.1007/s11250-012-0265-3.
- [29] Landis JR, Koch GG. The measurement of observer agreement for categorical data. *Biometrics* 1977;33(1):159–74. doi:10.2307/2529310.
- [30] Güiris AD, Rojas HN, Berovides AV, Sosa PJ, Pérez EM, Cruz AE, et al. Biodiversity and distribution of helminths and protozoa in naturally infected horses from the biosphere reserve La Sierra Madre de Chiapas, México. *Vet Parasitol* 2010;24(170):268–77. doi:10.1016/j.vetpar.2010.02.016.
- [31] Al Anazi AD, Alyousif MS. Prevalence of non-strongyle gastrointestinal parasites of horses in Riyadh region of Saudi Arabia. *Saudi J Biol Sci* 2011;18(3):299–303. doi:10.1016/j.sjbs.2011.02.001.
- [32] Rehbein S, Visser M, Winter R. Prevalence, intensity and seasonality of gastrointestinal parasites in abattoir horses in Germany. *Parasitol Res* 2013;112(1):407–13. doi:10.1007/s00436-012-3150-0.
- [33] Mezgebu T, Tafess K, Tamiru F. Prevalence of gastrointestinal parasites of horses and donkeys in and around Gondar town, Ethiopia. *Open J Vet Med* 2013;3:267–72. doi:10.4236/ojvm.2013.36043.
- [34] Chemeda R, Mekonnen N, Muktar Y, Terfa W. Study on prevalence of internal parasites of horses in anda round Ambo town, Central Ethiopia. *Am-Eurasian J Agric Environ Sci* 2016;16(6):1051–7. doi:10.5829/idosi.aejaes.2016.16.6.10366.
- [35] Oli N, Subedi JR. Prevalence of gastro-intestinal parasites of horse (*Equus caballus linnaeus*, 1758) in seven village development committee of rukum district, nepal. *J Inst Sci Technol* 2018;22(2):69–75. doi:10.3126/jist.v22i2.19596.
- [36] Mathewos M, Girma D, Fesseha H, Yirgalem M, Eshetu E. Prevalence of gastrointestinal helminthiasis in horses and donkeys of Hawassa district, Southern Ethiopia. *Vet Med Int* 2021;7(2021):6686688. doi:10.1155/2021/6686688.
- [37] Devkota RD, Subedi JR, Wagley K. Prevalence of gastrointestinal parasites in equines of Mustang District. Nepal. *Biodivers J* 2021;22(9):3958–63. doi:10.13057/biodiv/d220943.
- [38] Kuzmina TA, Dzeverin I, Kharchenko VA. Strongylids in domestic horses: Influence of horse age, breed and deworming programs on the strongyle parasite community. *Vet Parasitol* 2016;227:56–63. doi:10.1016/j.vetpar.2016.07.024.
- [39] Joó K, Trúzi RL, Kálmán CZ, Ács V, Jakab S, Bába A, et al. Evaluation of risk factors affecting strongylid egg shedding on Hungarian horse farms. *Vet Parasitol: Reg Stud Rep* 2022;27:100663. doi:10.1016/j.vprsr.2021.100663.
- [40] Shite A, Admassu B, Abere A. Large strongyle parasites in equine: a review. *Adv Biol Res* 2015;9(4):247–52. doi:10.5829/idosi.abr.2015.9.9559.
- [41] Levy ST, Kaminiski-Perez Y, Mandel HH, Sutton GA, Markovics A, Steinman A. Prevalence and risk factor analysis of equine infestation with gastrointestinal. *Parasites in Israel*. *Isr J Vet Med* 2015;70:32–40.
- [42] Barriga OO. *Veterinary parasitology*. Columbus, OH: Ed Greyden Press; 1995.
- [43] Aromaa M, Hautala K, Oksanen A, Sukura A, Näreaho A. Parasite infections and their risk factors in foals and young horses in Finland. *Vet Parasitol Reg Stud Reports* 2018;12:35–8. doi:10.1016/j.vprsr.2018.01.006.
- [44] Takahashi Y, Takahashi T. Seasonal fluctuations in body weight during growth of Thoroughbred racehorses during their athletic career. *BMC Vet Res* 2017;13(1):257. doi:10.1186/s12917-017-1184-3.
- [45] Boersma JH, Eysker M, Nas JW. Apparent resistance of *Parascaris equorum* to macrocyclic lactones. *Vet Rec* 2002;150(9):279–81. doi:10.1136/vr.150.9.279.
- [46] Schneider S, Pfister K, Becher AM, Scheuerle MC. Strongyle infections and parasitic control strategies in German horses - a risk assessment. *BMC Vet Res* 2014;10:262. doi:10.1186/s12917-014-0262-z.
- [47] Cringoli G, Rinaldi L, Maurelli MP, Utzinger J. FLOTAC: new multivalent techniques for qualitative and quantitative coproscopic diagnosis of parasites in animals and humans. *Nat Protoc* 2010;5(3):503–15. doi:10.1038/nprot.2009.235.
- [48] Willis HH. A simple levitation method for the detection of hookworm ova. *Med J Aust* 1921;8:375–6. doi:10.5694/j.1326-5377.1921.tb60654.x.
- [49] Faust EC, D'Antoni JS, Odom V, Miller MJ, Peres C, Sawitz W, et al. A critical study of clinical laboratory technicians for the diagnosis of protozoan cyst and helminth eggs in feces I. preliminary communication. *Am J Trop Med* 1938;18(2):169–83. doi:10.4269/ajtmh.1938.s1-18.169.
- [50] Noel ML, Scare JA, Bellaw JL, Nielsen MK. Accuracy and precision of Mini-FLOTAC and McMaster techniques for determining equine strongyle egg counts. *J Equine Vet Sci* 2017;48:182–7. doi:10.1016/j.jevs.2016.09.006.
- [51] Paras KL, George MM, Vidyashankar AN, Kaplan RM. Comparison of fecal egg counting methods in four livestock species. *Vet Parasitol* 2018;257:21–7. doi:10.1016/j.vetpar.2018.05.015.
- [52] Scare JA, Slusarewicz P, Noel ML, Wielgus KM, Nielsen MK. Evaluation of accuracy and precision of a smartphone based automated parasite egg counting system in comparison to the McMaster and Mini-FLOTAC methods. *Vet Parasitol* 2017;247:85–92. doi:10.1016/j.vetpar.2017.10.005.7.
- [53] Britt A, Kaplan R, Paras K, Turner K, Abrams A, Duberstein K. A comparison of McMasters versus Mini-FLOTAC techniques in quantifying small strongyles in equine fecal egg assessments. *J Equine Vet Sci* 2017;52:92–7. doi:10.1016/j.jevs.2017.03.143.
- [54] Bosco A, Maurelli MP, Ianniello D, Morgoglione ME, Amadesi A, Coles GC, et al. The recovery of added nematode eggs from horse and sheep faeces by three methods. *BMC Vet Res* 2018;14(1):1–6. doi:10.1186/s12917-017-1326-7.
- [55] Nápravniková J, Petrýl M, Stupka R, Vadlejch J. Reliability of three common fecal egg counting techniques for detecting strongylid and ascarid infections in horses. *Vet Parasitol* 2019;272:53–7. doi:10.1016/j.vetpar.2019.07.001.
- [56] Capello BP, Arce AA, Barbieri FA, Alvarez FDR, Lozina LA. Estudio comparativo entre las técnicas de McMaster modificada INTA y Mini Flotac para el conteo de huevos de nematodos en materia fecal de equinos. *Rev Divulgación Técnica Agropecuaria. Agroindustrial y Ambiental*. Facultad de Ciencias Agrarias. 2020;7:17–24.



# Reproductive seasonality of hair rams under tropical conditions: an alternative for non-seasonal lamb production?

Arnaldo de Sá Geraldo<sup>1</sup> · Pedro Henrique Nicolau Pinto<sup>1</sup> · Ana Beatriz da Silva Carvalho<sup>1</sup> ·  
Marta Maria Campos Pereira da Costa<sup>1</sup> · Juliana Dantas Rodrigues Santos<sup>1</sup> · Augusto Ryonosuke Taira<sup>1</sup> ·  
Isabel Oliveira Cosentino<sup>1</sup> · Bruna Ramalho Rigaud de Figueiredo<sup>1</sup> · Mário Felipe Alvarez Balaro<sup>1</sup> ·  
Rodolfo Ungerfeld<sup>2</sup> · Felipe Zandonadi Brandão<sup>1</sup>

Received: 9 July 2023 / Accepted: 27 November 2023  
© The Author(s), under exclusive licence to Springer Nature B.V. 2023

## Abstract

Reproductive seasonality limits the periods of breeding on the year and, therefore, productive output. However, some breeds appear as probably non-seasonal. The aim of the study was to characterize the seasonal pattern of Santa Inês rams, including an ultrasound characterization of the reproductive tract, testosterone concentrations, and semen characteristics. Fifteen Santa Inês rams remained in a grazing system with concentrate supplementation, and measurements of the reproductive tract and ultrasound evaluation (biometrics and pixel intensity) of the testicles and accessory sex glands were monthly recorded. Computerized seminal evaluations were also performed monthly, and serum testosterone concentration was measured every 15 days. Body weight and condition remained stable throughout the year. In general, reproductive traits varied along the year and reached maximum values during autumn and minimum in spring. Despite that, as fresh semen remained with enough quality to breed all along the year, seasonality does not appear as a limiting factor to breed along the year. Therefore, Santa Inês rams can be used for all-year-round breeding or for crossbreeding when rams from other breeds decrease their fertilizing ability.

**Keywords** Breeding period · Seasonality · Photoperiod · Hair sheep

## Introduction

Most small ruminants are classified as short-day seasonal polyestrous animals, which implies that their reproductive activity increases when the day time length decreases (summer to autumn). The intensity of the changes in photoperiod along the year is greater at higher latitudes, therefore making more pronounced the reproductive changes in sheep throughout the year (Fraser and Lincoln, 1980). However, as domestication has reduced the environmental influences on seasonality, currently, there are other factors influencing the length and intensity of reproductive activity in livestock

during the photoperiod season (Lincoln et al., 1990). However, in many regions of the world, the sheep industry is limited by the seasonality of its products (Chemineau et al. 2007) as lambs can be only delivered to the market according to the seasonal period of births. The spermatogenic process limits the reproductive ability in males to breed, so there is a lack between male and female seasonal patterns. In general, males increase their reproductive activity 2 or 3 months before the onset of the female breeding season. (Ungerfeld et al., 2020).

Several reproductive biotechnologies including hormonal treatments have been explored to overcome the seasonal barrier to induce estrus and ovulation in the ewe and to stimulate the ram reproductive activity (Amiridis and Cseh, 2012; Espírito-Santo et al. 2021). However, new consumers demand hormone-free products (Scaramuzi and Martin, 2008), so the interest in the development of natural strategies to modify or even switch seasonal reproduction is increasing (Martin and Kadokawa, 2006). This implies a deeper knowledge of the physiological mechanisms involved in the

✉ Felipe Zandonadi Brandão  
fzbrandao@id.uff.br

<sup>1</sup> Faculdade de Veterinária, Universidade Federal Fluminense, Niterói, RJ, Brazil

<sup>2</sup> Departamento de Biociencias Veterinarias, Facultad de Veterinaria, Universidad de La República, Ruta 8 Km 18, 13000 Montevideo, Uruguay

regulation of the reproductive pattern, especially in understand how breeds and their evolution are related to their seasonal pattern. In this sense, searching for less or non-seasonal biotypes breeds is an alternative to mitigate the seasonal lamb production. From this perspective, hair sheep breeds are considered non-seasonal or light seasonal breeds (Balara et al. 2014), although there are scarce systematic studies in the ram focused on the breeding activity and changes of the reproductive tract throughout the year. Moreover, seasonality can be affecting in different intensities on some traits, disturbing the effectiveness of rams for breeding purposes. Although in some studies the hair sheep breeds are considered as non-seasonal (Cerna et al., 2000; Arroyo et al., 2007), the reproductive development of Saint Croix male lambs differs according to the birth season (Sánchez-Dávila et al. 2019).

In this context, Santa Inês is a hair sheep breed locally originated in Brazil, adapted to tropical climate (Rocha et al 2004), which presents maternal ability, prolificacy, early puberty (Silva et al., 2011), and resistance to parasitic infections (Amarante et al., 2004). Moreover, this breed is adapted to tropical conditions. Therefore, the aim of this study was to characterize the seasonal pattern of Santa Inês rams, including an ultrasound characterization of the reproductive tract, testosterone levels, and semen traits.

## Materials and methods

This study was approved by the Ethics Committee for Use of Animals (CEUA no. 5526080119) of Universidade Federal Fluminense, following the guidelines of the “Brazilian Society of Science in Laboratory Animal” and the “Animal Research: Report of In vivo Experiences” (ARRIVE).

### Location and animals

The study was performed at the Unidade de Pesquisa Experimental em Caprinos e Ovinos (UNIPECO) in Cachoeiras de Macacu (22°27' SL), Rio de Janeiro, Brazil, from June 2019 to May 2020. Fifteen Santa Inês rams of  $1.2 \pm 0.2$  years old at the beginning of the study, weighing  $49.3 \pm 1.8$  kg and with a body condition score of  $2.7 \pm 0.4$  (1–5 scale) (Suiter, 1994), were used. At the onset of the study, none of the animals had a clinical disorder and were approved in a breeding soundness exam. Animals included had at least 75% progressive motile sperm (subjective evaluation) and 90% of cells with normal morphology, in agreement with the recommendations of the Brazilian College of Animal Reproduction (CBRA, 2013). Rams were allocated in pens with grass (*Brachiaria decumbens*) during the day and sheltered at night when they were fed chopped grass (*Pennisetum purpureum*; 2.0 kg DM/day/ram) and 500 g concentrate each

(18% crude protein). Water and mineral salt (Salminas, Sal Minas, Minas Gerais Brazil) were provided ad libitum.

### Biometric variables

Epididymis and testicles' depth, width, and height were monthly determined using a caliper (Levolpe, São Paulo, Brazil). The testicular and the epididymis volume were estimated as  $(4 \cdot \pi \cdot \text{testicular or epididymis height} \cdot \text{length} \cdot \text{width})/3$ , and a gonadosomatic index expressed as percentage (testicular volume/body weight) was calculated. Scrotal circumference was determined using flexible measuring tape (WalMur, Porto Alegre, Brazil).

### Ultrasound evaluation

Ultrasound evaluations of the reproductive tract were monthly performed by the same operator using a portable transrectal B-mode ultrasonography equipment (Sonoscape S6, SonoScape, Shenzhen, China), with a 7.5 MHz linear transducer. Accessory sex glands were scanned through transrectal ultrasound according to Espírito-Santo et al. (2021). The areas of the bulbourethral and vesicular glands (BUG-A and VG-A, respectively) and the prostatic gland diameter (PG-D) were measured.

A pixel evaluation from the images produced during ultrasonography was performed according to Espírito-Santo et al. (2021). For that, one spot in the center of accessory sex glands was selected ( $w = 250$ ;  $h = 80$ ). The pixel intensity ranged from 0 to 255, where 0 was assigned to a black pixel (anechoic) and 255 to a white pixel (hyperechoic). ImageJ software was used to calculate the average number of pixels or their echogenicity. This variable was determined for the vesicular gland, prostate, and bulbourethral gland echogenicity. Mean data was calculated in each variable and used for the analysis.

### Testosterone measurement

Blood samples were collected every 15 days for testosterone assessment. Blood was collected by jugular venipuncture, using vacuum tubes without anticoagulant or preservative (Vacutainer, BD, Juiz de Fora, Brazil). Samples were immediately centrifuged at 1500 g for 15 min. Serum was removed and stored in 1.5 mL microtubes and refrigerated ( $-20^\circ\text{C}$ ) until analysis. Serum testosterone was determined by solid-phase radioimmunoassay, using commercial kits (Beckman Coulter, Immunotech, Prague, Czech Republic) following the manufacturer's instructions. The sensitivity was 0.05 ng/mL, and the intra-assay coefficient of variation was 10%. All data were found to be within the minimum and maximum points of the curve.

## Semen collection and assessment

Semen was monthly collected for 12 months — except March, due to technical problems — by electro-ejaculator (2–5 V) following the method described by Ungerfeld et al. (2022). The rams were mechanically restrained in a sheep crush, and the prepuce was shaved, and its inner part washed with saline solution. The rectum was emptied of feces, and the electro-ejaculator's (TK800, TK Reprodução Animal, Minas Gerais, Brazil) probe was lubricated with carboxymethyl cellulose and then inserted. Series of 10 electrical pulses were applied, beginning with 2 V and increasing by 1 V every ten pulses until a maximum of 5 V. Each pulse lasted 3–5 s, with resting periods of 2 s. The process was manually controlled. After the semen collection, the volume was measured using graduated micropipettes, and sperm concentration was determined using a Neubauer chamber (1:800 dilution). Vigor (velocity of the sperm cell to cross a visual section under the microscope) was assessed using a subjective 1–5 scale (being, 1 minimum speed and 5 maximum speed) by observing one drop of diluted semen with a coverslip at 400× magnification. The functional integrity of the sperm membrane was evaluated with the hypo-osmotic swelling test (HOST) according to Ramu and Jeyendran (2013).

An aliquot of 10 µL was diluted in 990 µL of saline solution at 37 °C (1:100 dilution) for computer-assisted semen analysis (CASA) using the SCA system (Sperm Class Analyzer – SCA, Microscopic Automatic Diagnostic Systems, Barcelona, Spain). Five fields from each sample were randomly selected and evaluated. Software settings were adjusted to ram spermatozoa. Sperm kinetics variables included the percentage of motile sperm (MS); sperm with progressive motility (SPM); fast, medium, and slow sperm; the average path velocity (VAP); and curvilinear velocity (VCL). CASA analyses were not performed in September due to technical problems the equipment. Observing one drop of diluted semen with a coverslip (400× magnification), and using a subjective 1–5 scale (being, 1 minimum speed and 5 maximum speed) vigor (velocity of the sperm cell to cross a visual section under the microscope), was assessed.

## Statistical analysis

Data were analyzed with a mixed model, including time (month) as the main fact, considering it as a repeated measure. All data were analyzed with the SAS on Demand for Academics. Post hoc comparisons were performed with the pdiff tool of SAS. Data are presented as LS mean ± SEM. Differences were considered significant when  $P \leq 0.05$  and as tendencies when  $0.1 \leq P < 0.05$ .

## Results

Overall, the reproductive traits varied along the year, with greater development at autumn and worst at spring. In all the figures, the upper panel presents the daylight hours to make it easy to relate it with the different variables.

### Biometric variables and testosterone concentrations

During the experimental period, body weight and body condition did not change significantly (body weight, Fig. 1B). Testicular volume and the scrotal circumference changed along the year ( $P < 0.0001$  and  $P = 0.02$  respectively). Testicular volume increased during winter and showed a significant drop in February. Scrotal circumference increased during the months of July to December, and then it stabilized (Fig. 1C). The relative amount of testes volume (gonadosomatic index) varied along the year ( $P < 0.0001$ ), showed an important drop in February, and remained low until the end of the study (Fig. 1D). Testosterone concentrations varied throughout the year ( $P < 0.0001$ ) and showed higher values from February to April (Fig. 1E).

Epididymis volume varied along the year ( $P < 0.0001$ ), with a significant drop in February, and ended the experimental period at its lowest levels (Fig. 2B). The prostatic gland diameter varied throughout the year ( $P < 0.0001$ ), with lower values from June to August, and a significant increase in March (Fig. 2C). Its pixel intensity also varied throughout the year ( $P < 0.0001$ ), with greater values from November to April (Fig. 2C). The bulbourethral gland area and its' pixel intensity varied with time ( $P = 0.001$  and  $P < 0.0001$  respectively) and increased from February to March (Fig. 2D). The vesicular gland area increased during the experiment, and its' pixel intensity tended to vary throughout the year ( $P = 0.09$ ) (Fig. 2E).

### Spermatic variables

Semen volume varied along the year ( $P = 0.02$ ), with stable values in most months, with a significant increase in February (Fig. 3B). Sperm concentration did not change significantly throughout the year (Fig. 3B). The total number of ejaculated sperm did not change significantly over the year. The total number of sperm with functional membrane ejaculated increased ( $P = 0.04$ ) from January to April (Fig. 3C). The percentage of motile sperm tended to vary along the year ( $P = 0.057$ ). The percentage of sperm with progressive motility showed a punctual decrease in May (Fig. 3D). The total number of motile sperm ejaculated did not vary significantly along the year. The total number of progressive motile sperm ejaculated had a significant peak in April

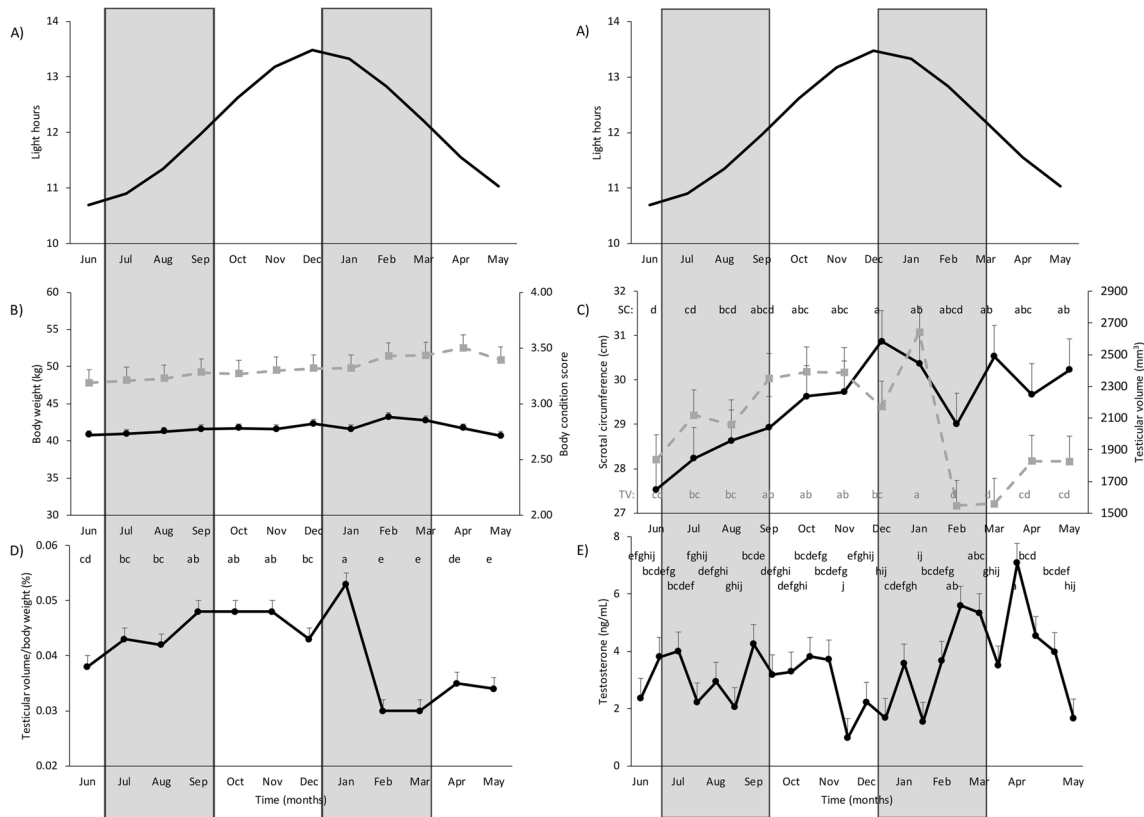


**Fig. 1** Seasonal variation in **A** light hours, **B** body weight (solid line) and body condition score (dotted line), **C** scrotal circumference (solid line) and testicular volume (dotted line), **D** testicular volume-to-body

weight ratio, **E** serum testosterone concentrations in Santa Inês rams located at 22°27' SL. Gray bars indicate winter and summer. Different letters in the same line indicate significant differences ( $P < 0.05$ )

and a decrease in May (Fig. 3E). Vigor varied along the year ( $P = 0.01$ ) and had lower values in July and October to December. The percentage of sperm with integral membrane tended to vary along the year ( $P = 0.06$ ) (Fig. 3F).

The percentage of fast, medium, and slow sperm varied along the year ( $P = 0.001$ ,  $P = 0.004$ , and  $P < 0.0001$ , respectively). While the percentage of fast sperm showed a significant drop from April to May, the percentage of medium and slow sperm increased during that period (Fig. 4B). Sperm velocity variables, VCL and VAP, also varied along the year ( $P < 0.0001$  for both variables). Both had minimum values in November, January, and May (Fig. 4C).

## Discussion

Santa Inês rams have seasonal changes but considering that motile sperm, vigor, and sperm concentration are the main markers used in breeding soundness exams (CBRA, 2013); it appears that these rams are probably able to impregnate ewes at any moment of the year. In this sense, the breed can be characterized as a light seasonal

breed in which ewes are cycling at any moment of the year (Balara et al., 2014), expanding now the knowledge to rams. For example, despite there being variations, the percentage of motile sperm remained above 80% throughout the whole year. This year-long suitability for reproduction was also observed in Pelibuey and Zulu rams in similar latitudes (Aguirre et al., 2007; Ngcobo et al., 2020), with the advantage that Santa Inês sheep are well adapted to local conditions, including low-fat meat and good maternal traits (Paim et al. 2013). Therefore, this breed provides an opportunity for terminal crossbreeding with meat-producing breeds whose rams may be more seasonal (Pool et al., 2020), enhancing production efficiency. However, it should be noted that the success of males is related not only to semen quality but also to the display of a libido enough strong to search for estrous ewes and mate them effectively, a factor that should be studied to have a whole view of the breed. In any case, according to the results of this study, at least fresh semen appears as usable throughout the year, remaining also to determine its' cryoresistance to produce semen from superior breeders all along the year.

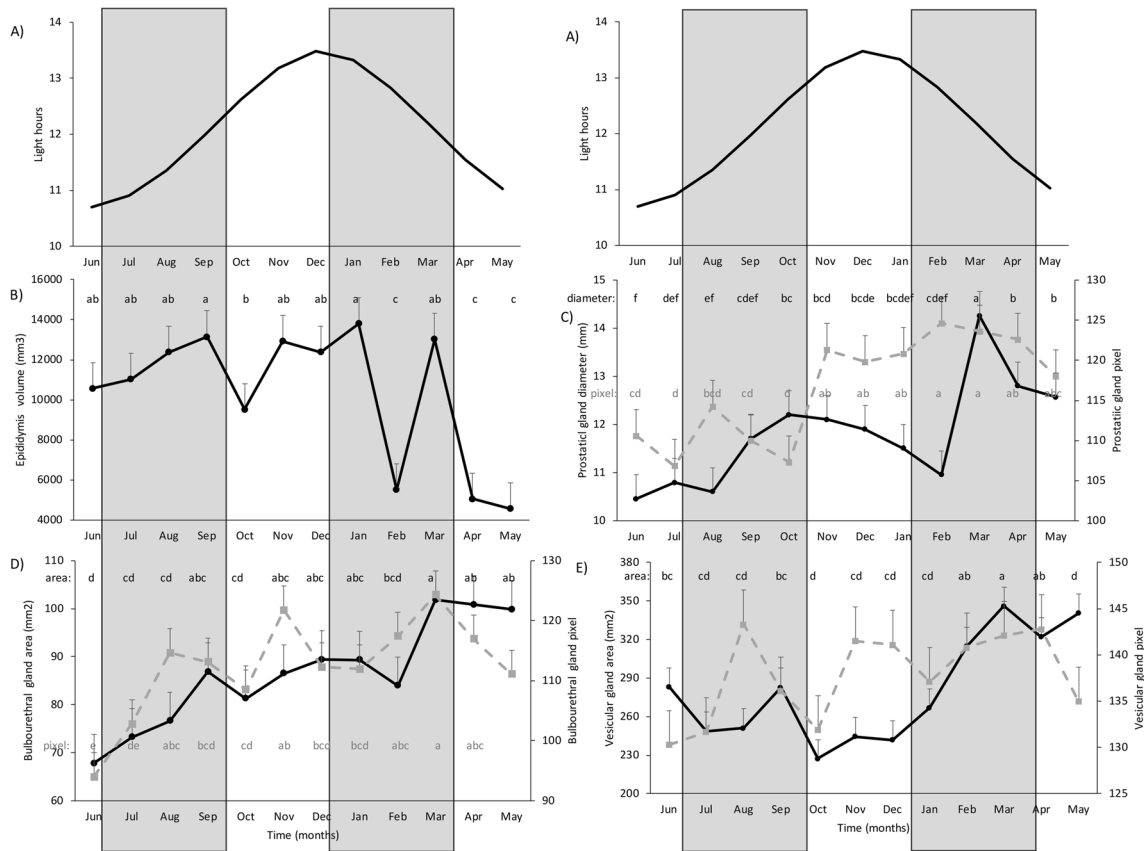


**Fig. 2** Seasonal variation in **A** light hours, **B** epididymis volume, **C** prostatic gland diameter (solid line) and echogenicity (dotted line), **D** bulbourethral gland area (solid line) and echogenicity (dotted line), **E** vesicular gland area (solid line) and echogenicity (dotted line) in

Santa Inês rams located at 22°27' SL. Gray bars indicate winter and summer. Different letters in the same line indicate significant differences ( $P < 0.05$ )

It is important to point out that body weight and body condition had only slight non-significant changes along the year, so the fluctuations reported in most reproductive traits were independent of changes in the general status of the animals and, therefore, dependent on other environmental signals. The changes reported on the testicular volume-to-body weight relationship reinforce this concept, indicating changes in testicular size not associated with changes in rams body weight. However, the annual increase in this trait was delayed from the absolute value of testicular volume and more closely associated with the period in which testosterone concentrations increased. Therefore, it is suggested that the recovery of testicular functionality was delayed in relation to testicular size. In concordance, the period with greater relative testicular size was related with also the greater number of sperm ejaculated and the increase in the size of the accessory glands. Indicating that testicular size is an easy and non-costly trait very practical to evaluate potential performance. However, it should be considered as a dynamic trait with more predictable results if it is evaluated

over time. In this sense, although being able to breed along the year, Santa Inês rams have important variations in their reproductive status, being able therefore to be categorized as a seasonal breed.

As was mentioned, there were not important variations in the metabolic status as body weight and body condition remained stable throughout the year. In general, in small ruminants, it is assumed that photoperiod is the main influence on seasonality (Lincoln and Short, 1980; Bronson, 1990). A reduction in the length of time that light is perceived by the animal leads to a longer period of melatonin secretion, associated with an increase in the production of steroid hormones, such as testosterone (Bhattacharya et al., 2019). Unfortunately, it was not possible to evaluate semen during March, apparently a crucial month in the middle of the negative photoperiod phase, so those data remain to be assessed. However, according to the general trend, it is expected to collect semen with high-quality characteristics, also consistent with what may be expected during that period of the year.



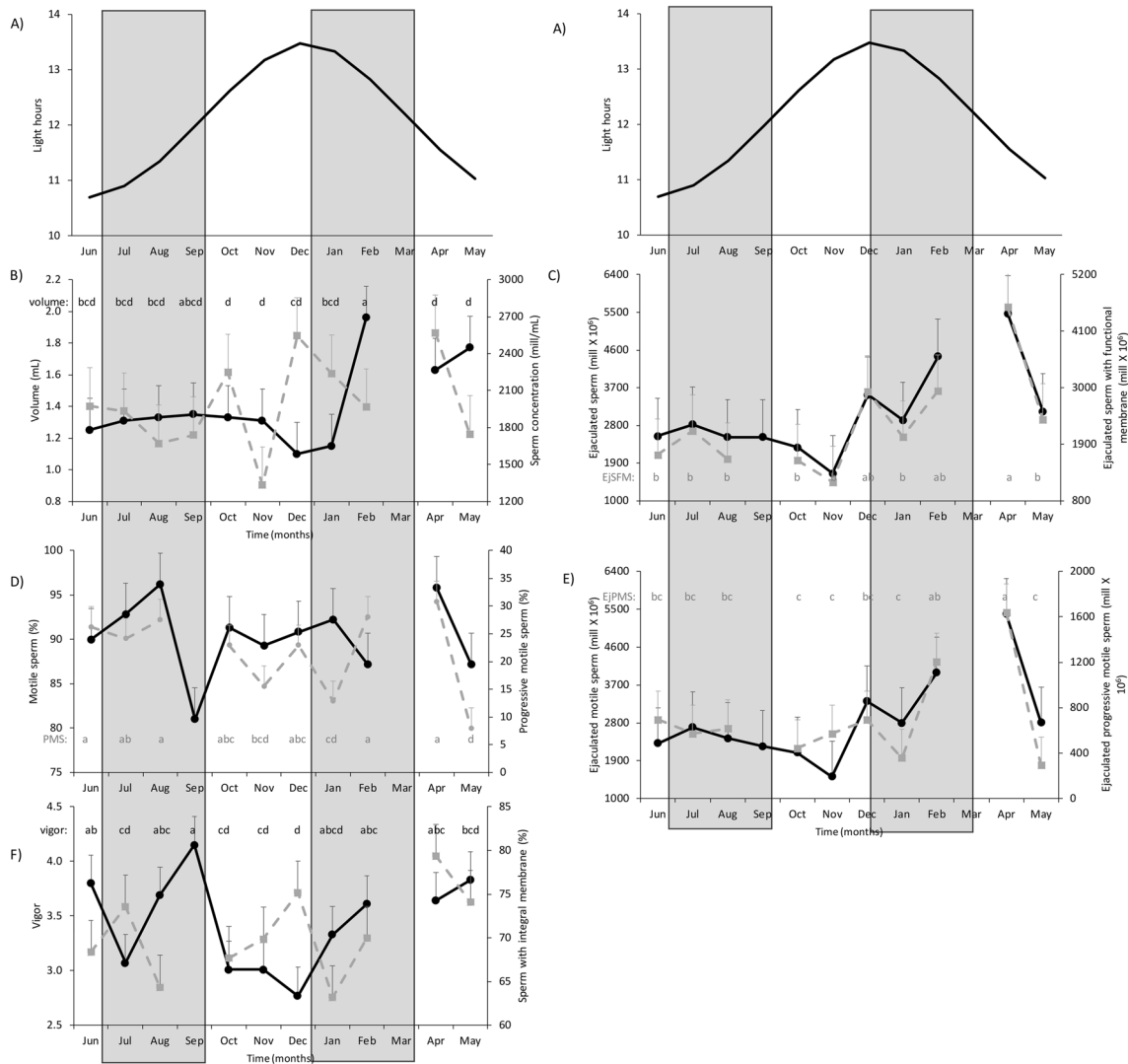


**Fig. 3** Seasonal variation in **A** light hours, **B** semen volume (solid line) and sperm concentration (dotted line), **C** ejaculated sperm (solid line) and ejaculated sperm with a functional membrane (dotted line), **D** total motile sperm (solid line) and sperm with progressive motility (dotted line), **E** ejaculated motile sperm (solid line) and ejaculated

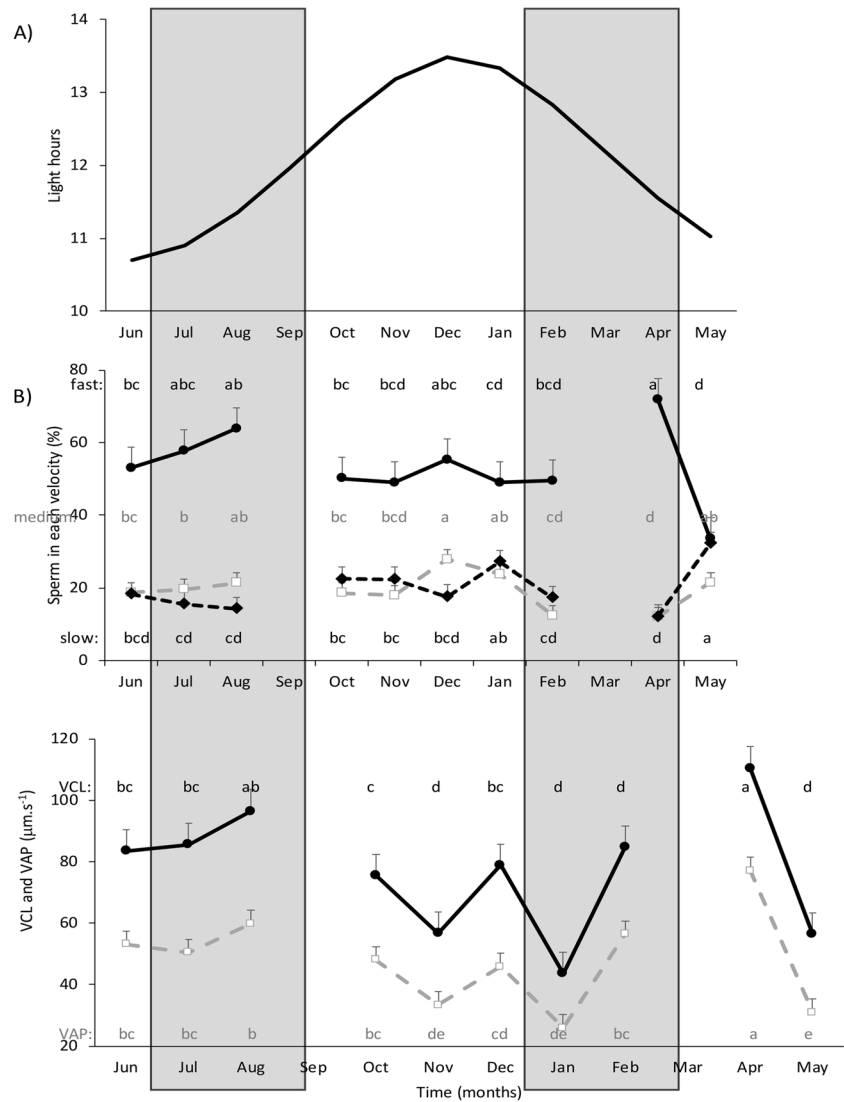
progressive motile sperm (dotted line), **F** vigor (solid line) and sperm with a functional membrane (dotted line) in Santa Inês rams located at 22°27' SL. Gray columns indicate winter and summer. Different letters in the same line indicate significant differences ( $P < 0.05$ )

In our study, rams received similar amounts of food of stable quality throughout the year, which in concordance, allowed them to maintain their body condition. However, in typical tropical systems, food availability and quality vary along the year, with higher availability of forage in summer (Feitosa et al., 2021), which may also impact testosterone production (Martin et al., 1994; Selvaraju et al., 2012). In our study, testosterone concentration remained during the year in values similar to those reported in summer in this breed (Espírito Santo et al., 2021), which may be related to the breed per se or to the high body condition of these rams. This may be an interesting characteristic of the breed, as there are more strong seasonal breeds in which rams are unresponsive to nutritional “flushing”

stimulation, but rams from less seasonal breeds are more responsive to nutritional stimulus (Hötzel et al., 2003). If so, this would allow managing the reproductive status of the rams according to breeding periods independent of the moment of the year.

In conclusion, Santa Inês rams raise at 22° south latitude do not have slight reproductive changes throughout seasons the year. However, there are seasonal variations with traits reaching greater values in autumn and lower in spring. However, these oscillations appear as non-limiting Santa Inês rams’ ability to impregnate ewes all along the year. Therefore, this breed can be used for all-year-round breeding or for crossbreeding when rams from other breeds decrease their fertilizing ability.

**Fig. 4** Seasonal variation in **A** light hours; **B** sperm in each velocity, fast (solid line), medium (gray dotted line), and slow (black dotted line); **C** curvilinear velocity (VCL, solid line) and average path velocity (VAP, dotted line) in Santa Inês rams located at 22°27' SL. Gray columns indicate winter and summer. Different letters in the same line indicate significant differences ( $P < 0.05$ )



**Author contribution** A.S.G. and P.H.N.P., data interpretation and first draft production; A.B.S.C., M.M.C.P., J.D.R.S., A.R.T., I.O.C., B.R.R., and M.F.A.B., contributed with data collection and animal handling. R.U. and F.Z.B. participated in the conception of the study, developed the hypothesis, study design, data collection, and draft production. R.U. also performed statistical analysis. In addition, all authors revised and approved the final version of the manuscript.

**Funding** This work was supported by Universidade Federal Fluminense and FAPERJ (E-26/010.002238/2019). MFAB, BRR, and FZB are fellows of the CNPq and PHNP, ABSC, and JDRS of FAPERJ.

**Data availability** The data that support our findings are available upon reasonable request.

## Declarations

**Ethics approval** This study was approved by the Ethics Committee for Use of Animals (CEUA no. 5526080119) of Universidade Federal Fluminense, following the guidelines of the “Brazilian Society of Science

in Laboratory Animal” and the “Animal Research: Report of In vivo Experiences” (ARRIVE).

**Conflict of interest** The authors declare no competing interests.

## References

- Aguirre, V., Orihuela, A., Vázquez, R., 2007. Effect of semen collection frequency on seasonal variation in sexual behaviour, testosterone, testicular size and semen characteristics of tropical hair rams (*Ovis aries*). *Tropical Animal Health and Production*, 39, 271–277. <https://doi.org/10.1007/s11250-007-9010-8>
- Amarante, A.F.T., Bricarello, P.A., Rocha, R.A., Gennari, S.M., 2004. Resistance of Santa Inês, Suffolk and Ile de France sheep to naturally acquired gastrointestinal nematode infections. *Veterinary Parasitology*, 120, 91–106. <https://doi.org/10.1016/j.vetpar.2003.12.004>

- Amiridis, G.S, Cseh, S., 2012. Assisted reproductive technologies in the reproductive management of small ruminants. *Animal Reproduction Science*, 130, 152–161. <https://doi.org/10.1016/j.anireprosci.2012.01.009>
- Arroyo, L. J., Gallegos-Sánchez, J., Villa-Godoy, A., Berruecos, J. M., Perera, G., Valencia, J., 2007. Reproductive activity of Pelibuey and Suffolk ewes at 19 north latitude. *Animal Reproduction Science*, 102, 24–30. <https://doi.org/10.1016/j.anireprosci.2006.09.025>
- Balaro, M.F.A., Fonseca, J.F., Oba, E., Cardoso, E.C., Brandão, F.Z., 2014. Is the Santa Inês sheep a typical non-seasonal breeder in the Brazilian Southeast? *Tropical Animal Health and Production*, 46, 1533–1537. <https://doi.org/10.1007/s11250-014-0672-8>
- Bhattacharya, K., Sengupta, P., Dutta, S., 2019. Role of melatonin in male reproduction. *Asian Pacific Journal of Reproduction*, 8, 211.
- Bronson F.H., 1990. *Mammalian reproductive biology*, (The University of Chicago Press, Chicago)
- CBRA, 2013. *Manual para exame andrológico e avaliação de sêmen animal*. (Colégio Brasileiro de Reprodução Animal: Belo Horizonte, MG, Brazil)
- Cerna, C., Porras, A., Valencia, M.J., Perera, G., Zarco, L., 2000. Effect of an inverse subtropical (19° 13' N) photoperiod on ovarian activity, melatonin and prolactin secretion in Pelibuey ewes. *Animal Reproduction Science*, 60/61, 511–525. [https://doi.org/10.1016/s0378-4320\(00\)00127-5](https://doi.org/10.1016/s0378-4320(00)00127-5)
- Chemineau, P., Malpaux, B., Brillard, J.P., Fostier, A., 2007. Seasonality of reproduction and production in farm fishes, birds and mammals, *Animal*, 1, 419–423. <https://doi.org/10.1017/S1751731107691873>
- Espírito-Santo, C.G., Balaro, M.F.A., Santos, J.D.R., Correia, L.F.L., Souza, C.V., Taira, A.R., Costa, M.M.C.P., Carvalho, A.B.S., Ungerfeld, R., Brandão, F.Z., 2021. Semen quality, testosterone values, and testicular and accessory gland parameters in rams receiving sustained stimulation with low doses of buserelin. *Animal Production Science*, 62, 152–162. <https://doi.org/10.1071/AN20679>
- Feitosa, O.S., Leite, R.C., Alexandrino, E., Pires, T.J.S., Oliveira, L.B.T., Neto, J.J.P., Santos, A.C. 2021. Forage performance and cattle production as a function of the seasonality of a Brazilian tropical region. *Acta Scientiarum Animal Science*, 44, 2-11. <https://doi.org/10.4025/actascianimsci.v44i1.53779>
- Fraser, H.M., Lincoln, G.A., 1980. Effects of chronic treatment with an LHRH agonist on the secretion of LH, FSH and testosterone in the ram. *Biology of Reproduction*, 22, 269–276. <https://doi.org/10.1095/biolreprod22.2.269>
- Hötzel, M.J., Walkden-Brown, W.W., Fisher, J.S., Martin, G.B., 2003. Determinants of the annual pattern of reproduction in mature male Merino and Suffolk sheep: responses to a nutritional stimulus in the breeding and non-breeding seasons. *Reproduction and Fertility and Development*, 15, 1-9. <https://doi.org/10.1071/rd02024>
- Lincoln, G.A., Lincoln, C.E., McNeilly, A.S., 1990. Seasonal cycles in the blood plasma concentration of FSH, inhibin and testosterone, and testicular size in rams of wild, feral and domesticated breeds of sheep. *Journal Reproduction and Fertility*, 88, 623–633. <https://doi.org/10.1530/jrf.0.0880623>
- Lincoln G.A, Short R.V., 1980. Seasonal breeding: Nature's contraceptive. *Recent Progress Hormone Research*, 36, 1–52. <https://doi.org/10.1016/B978-0-12-571136-4.50007-3>
- Martin, G.B., Tjondronegor, S., Blackberry, M.A., 1994. Effects of nutrition on testicular size and the concentrations of gonadotrophins, testosterone and inhibin in plasma of mature male sheep. *Journal of Reproduction and Fertility*, 101, 121–128. <https://doi.org/10.1530/jrf.0.1010121>
- Martin G.B., Kadokawa H., 2006. 'Clean, green and ethical' animal production. Case study: Reproductive efficiency in small ruminants. *Journal of Reproduction and Development*, 52, 145–152. <https://doi.org/10.1262/jrd.17086-2>
- Ngcobo, J.N., Nephawe, K.A., Maqhashu, A., Nedanbale, T.L., 2020. Seasonal Variations in Semen Parameters of Zulu Rams Preserved at 10°C for 72 H During Breeding and NonBreeding Season. *American Journal of Animal and Veterinary Sciences*, 15, 226-239. <https://doi.org/10.3844/ajavsp.2020.226.239>
- Paim, T.P., Silva, A.F., Martins, R.F.S., Borges, B.O., Lima, P.M.T., Cardoso, C.C., Esteves, G.I.F., Louvandini, H., McManus, C.M., 2013. Performance, survivability and carcass traits of crossbred lambs from five paternal breeds with local hair breed Santa Inês ewes. *Small Ruminant Research*, 112, 28–34. <http://dx.doi.org/https://doi.org/10.1016/j.smallrumres.2012.12.024>
- Pool, K.R., Rickard, J.P., Pini, T., Graaf, S.P., 2020. Exogenous melatonin advances the ram breeding season and increases testicular function. *Scientific Reports*, 10, 9711. <https://doi.org/10.1038/s41598-020-66594-6>
- Ramu S., Jeyendran R.S., 2013. The hypo-osmotic swelling test for evaluation of sperm membrane integrity. *Methods in Molecular Biology*, 927, 21-25. [https://doi.org/10.1007/978-1-62703-038-0\\_3](https://doi.org/10.1007/978-1-62703-038-0_3)
- Rocha, R.A., Amarante, A.F.T., Bricarello, P.A., 2004. Influence of reproduction status on susceptibility of Santa Inês and Ile de France ewes to nematode parasitism. *Small Ruminant Research*, 55, 65-75. <https://doi.org/10.1016/j.smallrumres.2003.12.004>
- Sánchez-Dávila F., Ungerfeld, R., Bosque-González A.S.D., Bernal-Barragán H., 2019. Seasonality in Saint Croix male lamb reproductive development in northern Mexico. *Reproduction in Domestic Animals*, 54, 391-400. <https://doi.org/10.1111/rda.13372>
- Scaramuzzi, R.J., Martin G.B., 2008. The Importance of Interactions Among Nutrition, Seasonality and Socio-sexual Factors in the Development of Hormone-free Methods for Controlling Fertility. *Reproduction in Domestic Animals*, 43, 129-136. <https://doi.org/10.1111/j.1439-0531.2008.01152.x>
- Selvajaru, S., Sivasubramani, T., Raghavendra, B.S., Raju, P., Rao, S.B.N., Sineshkumar, D., Ravindra, J.P., 2012. Effect of dietary energy on seminal plasma insulin-like growth factor-I (IGF-I), serum IGF-I and testosterone levels, semen quality and fertility in adult rams. *Theriogenology*, 78, 646-655. <https://doi.org/10.1016/j.theriogenology.2012.03.010>

- Silva B.D.M., Castro E.A., Souza C.J.H., Paiva S.R., Sartori R., Franco M.M., Azevedo, H.C., Silva, T.A.S.N., Vieira, A.M.C., Neves, J.P., Melo, E.O., 2011. A new polymorphism in the Growth and Differentiation Factor 9 (GDF9) gene is associated with increased ovulation rate and prolificacy in homozygous sheep. *Animal Genetics*, 42), 89–92. <https://doi.org/10.1111/j.1365-2052.2010.02078.x>
- Suiter J. 1994. Body condition scoring in sheep and goats. *Farmnote*, 69. <https://www.agric.wa.gov.au/>. Accessed 01/11/2022
- Ungerfeld, R., Villagrán, M., Gil-Laureiro, J., Sestelo, A., Beracochea, F., Fumagalli, F., Bielli, A., 2020. Adult and yearling pampas deer stags (*Ozotoceros bezoarticus*) display mild reproductive seasonal patterns with maximum values in autumn. *Animal Reproduction*, 17, e20200021.
- Ungerfeld, R., Fernandes, D.A.M., Balaro, M.F.A., Taira, A.R., Espírito-Santo, C.G., Santos, J.D.R., Costa, M.M.C.P., Carvalho, A.B.S., Rodrigues, A.L.R., Brandão, F.Z., 2022. Administration of butorphanol with ketamine/xylazine sedation reduces the negative responses to electroejaculation in rams. *Theriogenology*, 191, 96-101. <https://doi.org/10.1016/j.theriogenology.2022.08.008>

**Publisher's Note** Springer Nature remains neutral with regard to jurisdictional claims in published maps and institutional affiliations.

Springer Nature or its licensor (e.g. a society or other partner) holds exclusive rights to this article under a publishing agreement with the author(s) or other rightsholder(s); author self-archiving of the accepted manuscript version of this article is solely governed by the terms of such publishing agreement and applicable law.

# FACTORS INVOLVED IN THE EJECTION OF MILK\*

FORDYCE ELY

*Kentucky Agricultural Experiment Station*

AND

W. E. PETERSEN

*Minnesota Agricultural Experiment Station*

Cows which habitually "let down" or "hold up" their milk are common in all herds. Several theories have been advanced in an effort to explain the physiological processes involved, but each has been found at fault in some regard. In reviewing the literature dealing with the factors involved in the ejection of milk we find that the majority of investigators have failed to differentiate between the processes involved in the synthesis or the secretion of milk within the gland, and the act of ejecting the milk from the alveoli and the small ductules. This has caused some confusion in the interpretation of experimental results.

## LITERATURE REVIEW

Routh (21) and Ribbert (20) offered evidence at an early date that the nervous system does not exercise a direct control over the combined acts of secretion and ejection. McKenzie (16) and McCandlish (15) injected numerous drugs, several of which might be classed as nerve stimulants, and failed to produce a marked effect on the rate of secretion or ejection of milk. Both, however, noted that pituitrin produced a marked galactagogic effect.

McKenzie (16), working with cats, noted some galactagogic effect from injecting extracts of corpus luteum and pineal body, and report some inhibitory effects of placental extracts on milk secretion. In these reports, however, no differentiation was noted between "secretion" and "ejection." Cannon and Bright (1) concluded that the autonomic nervous system was essential to lactation, from their work with a sympathectomized dog. They describe the effect as a belated one which caused the mother to be indifferent to her young and the gathering of a viscous, creamy material in the glands.

Hammond (7) and Macy *et al.* (13) accept Gaines (3) view that milk secretion in the sense of formation of the milk constituents is one thing and the ejection of the milk from the gland after it is formed is quite another.

Ingelbrecht (11), working with ten lactating rats, sectioned their spinal cords between the last thoracic and first lumbar vertebrae, thus incapacitating the six posterior glands and permitting the anterior six to remain intact. Nursing young died when permitted access only to the posterior six glands,

Received for publication October 28, 1940.

\* The investigation reported in this paper is in connection with a project of the Kentucky Agricultural Experiment Station and is published by permission of the Director.

but when two of the anterior glands were offered, all glands functioned normally, due probably to a stimulus which was transmitted in some manner to the denervated glands. Selye *et al.* (24) also found that nursing caused continued gland function in adjacent glands which were not nursed.

Gaines and Sanmann (4) Petersen, Palmer and Eckles (19), and Swett *et al.* (28) have recovered as much as 100 per cent of the milk from excised glands which they would have expected to obtain from a normal milking of the same glands. Their investigations have also demonstrated the existence of residual milk, or milk which cannot be removed from the glands under normal milking conditions.

Zietzschmann (32) takes the view that the involuntary excitation of the muscles of the teat provokes the retaining of milk in the gland, while most investigators are of the opinion that there is ample argument for the opposite view in nursing Cetacea where the act of suckling is incompatible with the under-water life of these animals. The ducts of their mammary glands are enlarged into reservoirs from which the milk is ejected into the mouths of the young. Circumstantial evidence has gradually accumulated which indicates the presence of a somewhat similar musculature within the bovine mammary gland, these muscles surrounding the small ducts and alveoli, and that the act of milk ejection consists in the contraction of these muscles. Gaines (3) found that the ejection of milk in a goat was coincident with a high intra-gland pressure and that low-pressure latent periods occurred between high-pressure periods. This pressure as related to the rate of milk ejection was further demonstrated by Tgetgel (29) who explains the sudden swelling of the glands from an internal pressure, as the milk is ejected before being withdrawn. Hammond (7), after reviewing the literature, offers an entirely different explanation for the occurrence of this pressure. He believes, "It is due to erection in the udder and nipples, which is caused reflexly by stimulation of the nipple by the act of sucking or milking."

Gielsing and Robbins (5) point out that the preparations of the anterior lobe of the pituitary body exert their characteristic effects slowly, require repeated administration and affect more particularly the structural elements of the body; for example, the growth of the mammary gland, the persistence of secretion and other time-consuming functions. The posterior lobe, however, is much more abundantly supplied with nerves and its extracts "Elicit an immediate pharmacodynamic response" on isolated tissue preparations (*e.g.* the uterus) or in the intact animal.

Oliver and Schafer (17) noted the sudden increase in blood pressure following intravenous injection of extracts of the posterior lobe. Ott and Scott (18), Gaines (3), McKenzie (16), Schafer (22), Hammond (6), Hill and Simpson (9 and 10), Simpson and Hill (25 and 26), Turner and Slaughter (31), Maxwell and Rothera (14) injected pituitrin intravenously using various species including the human. They agree to a stimulating

effect although all except Gaines fail to differentiate between secretion and ejection. Two of these (3) and (25) report a lessening in effect when the administrations were continued for a period of time. Several (6 and 25) are of the opinion, however, that the response to pituitrin injection is caused by a direct action of the principle on the secreting tissues of the gland, and that it is not due to the contraction of smooth musculature around the secreting cells, a precedent for which has been mentioned with suckling Cetacea. Turner and Slaughter (31) are "Inclined to the theory that pituitrin is not a galactagogue but rather acts on the mechanism normally effective during the milking process. We are inclined to believe that contractile elements in the walls of the alveoli and ducts furnish the *vis a tergo* observed."

Kamn *et al.* (12) accomplished a fairly complete separation of the oxytocic and the pressor principle from pituitrin. The name "Pitocin" was chosen to designate a solution containing the oxytocic principle, alpha-hypophamine, which is "comparatively free" from pressor activity. This product is otherwise referred to as oxytocin or obstetrical pituitrin because its action is specific for smooth muscle and it is used by the medical profession to stimulate uterine contractions. Kamn's "Pitressin" designates a solution of the pressor principle, beta-hypophamine, which is "comparatively free" from the oxytocic principle and this "surgical pituitrin" is frequently used to reduce surgical shock. Stehle (27) has more recently devised other methods for effecting a separation of these two principles. It is quite possible that the existence of these two fractions in pituitrin may account for the differences in the observed effects on the mammary gland when injected intravenously.

#### EXPERIMENTAL

According to Turner (30) and Espe (2) each half of the bovine mammary gland derives its nerve supply from three sources: (1) the ilio-hypogastric nerve, (2) the ilio-inguinal nerve and, (3) the posterior inguinal nerve. The first carries only afferent fibers from the gland periphery while the second and third carry both afferent and efferent fibers between the interior of the gland and central nervous systems. It was believed, therefore, that if an operation could impair the functioning of (2) and (3) nerve supplies to half the udder, practically all motor or efferent impulses would be removed and the intact half of the udder could be used as a check.

Three Jersey cows were selected from the Kentucky Agricultural Experiment Station herd on which to experiment, to determine more exactly the relationship which exists between the nervous mechanism and the ejection of milk. The first two cows, E 124 and E 237, were chosen because they were due to freshen January 2nd and 4th, respectively, and it was possible to treat them together experimentally. On November 17th, 1936, while both

cows were dry, the left half of the udder of each was denervated to the extent of removing about two inches of the sympathetic trunk nerve, which is made up of the ilio-inguinal and the posterior inguinal nerves, at a point just below the left inguinal ring. Each cow received as a general anesthetic, one ounce of chloral hydrate and, after being placed on the operating table, 1 per cent procaine was used as a local anesthetic. The incision was made at a point above the secreting tissue about midway between the left front and rear teats. This nerve trunk is located between the external pudic artery and vein which descend together through the left inguinal ring. No infection occurred in either case and within eight or ten days the wounds were well healed. These cows freshened normally early in January, 1937, and were subjected to experimental milkings which were designed to measure the effect of the denervation on the rate of ejection of milk from the glands. A mechanical milker\* was especially designed which directed the milk from each half of the udder into a separate container, and which hung on a Chatillon milk balance suspended on opposite sides of the cow. Thus both halves of the udder of each cow were subjected to a uniform vacuum at the same time and the yield of milk was observed and recorded at fifteen-second intervals.

In September, 1938, another cow, E 307, was operated on in exactly the same manner. She calved normally on October 20th and for a period of three and one half months was experimentally milked using the same special equipment.

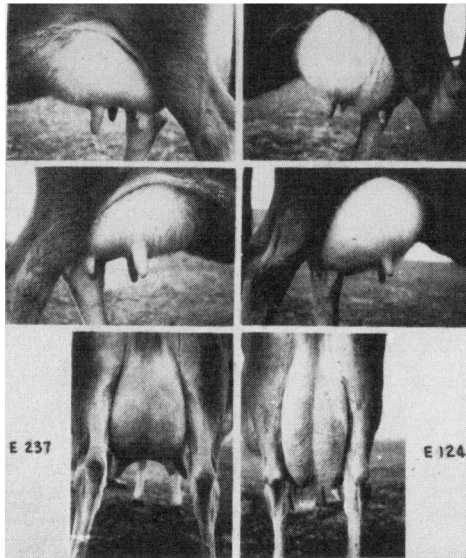
#### RESULTS

The photograph shows views of the udders of the first two cows, E 124 and E 237, taken soon after they freshened. The development of the left half of these udders seems not to be affected by the denervating operation. Figures 1 and 2 show the rate of ejection of milk (6 A. M. and 5 P. M.) each line representing an average of 13 milkings. In each figure the solid line represents the right or intact half of the udder while the broken line shows the response from the left or denervated half. It is quite apparent that the denervated half of the gland seemed as able to eject the milk as the intact half. Figure 3 shows the response measured in exactly the same manner for the third cow, E 307, and each line represents an average of twenty-eight normal milkings. No significance is given to the fact that in each individual milking the left half of 307's udder yielded more than the right or intact half. Such a difference was not noted in the other cows and is probably an individual characteristic of the normal udder of the experimental subject. These data indicate that the motor or efferent nerve supply to the bovine udder has little to do with determining the rate of ejection of milk under normal conditions. E 307 was then subjected to a series of experiments to determine the effect of the efferent nerve supply to the glands under various abnormal conditions such as fright and intravenous hormone injections.

\* Courtesy of Mr. L. Dinesen, Perfection Milker Corp.



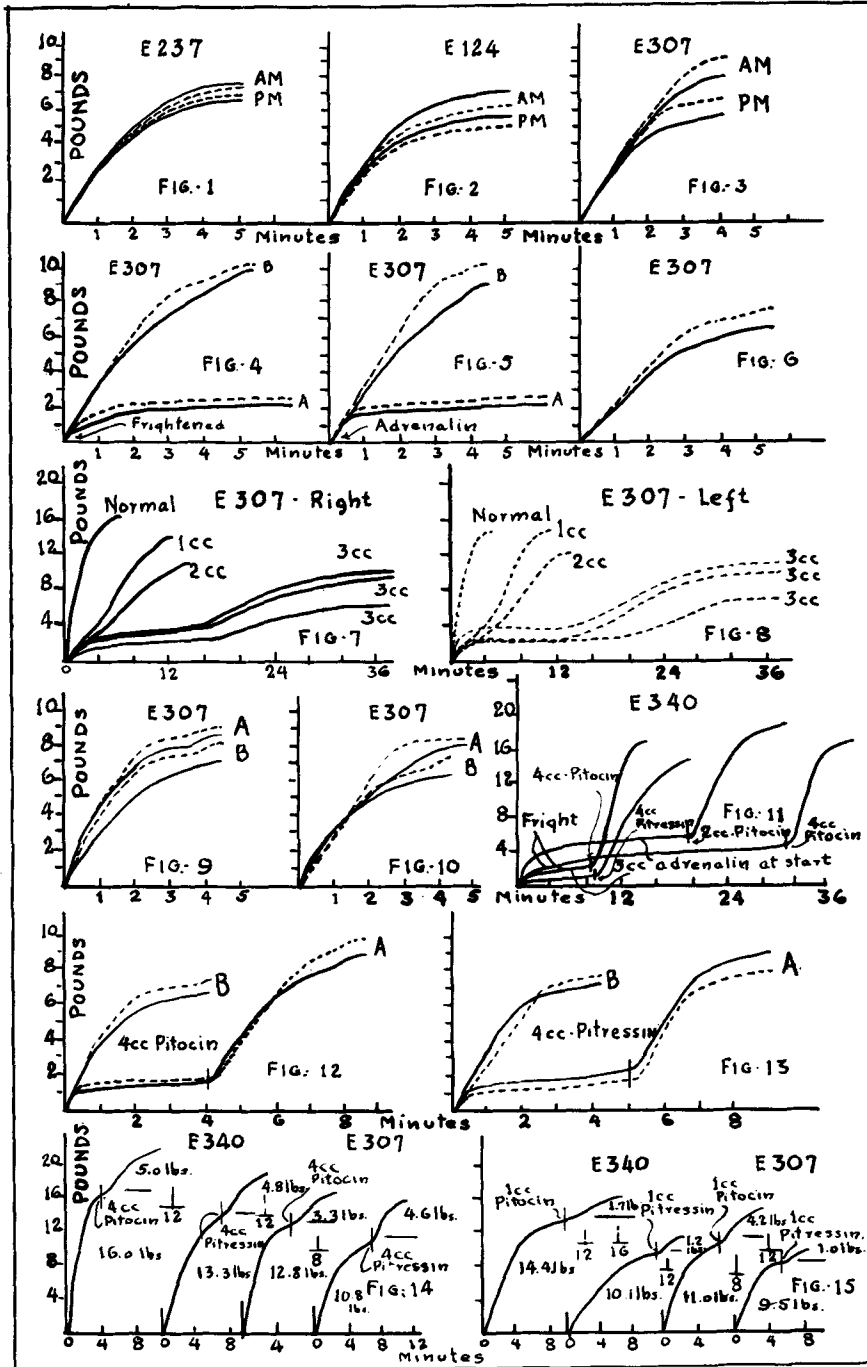
*The effect of fright on the ejection of milk:* Physiologists agree that animals can exist in an apparently normal state following gross sympathectomy but are unable to adapt themselves to a changing environment. It was thought that there might be a difference in the response of the two halves of the udder as measured by the rate of ejection of milk if the cow was severely frightened. Accordingly, E 307 was systematically frightened as the mechanical milker was attached. Frightening at first consisted in placing a cat on the cow's back and exploding paper bags every ten seconds for two minutes. Later the cat was dispensed with as unnecessary.



Photograph shows three views of the udders of E 237 and E 124 taken soon after freshening.

The result is shown in figure 4. Both halves of the udder responded alike in A. The milk was promptly drained from the cistern, followed by practically a complete cessation of ejection. In this instance 11.0 pounds of milk was removed from the entire udder by hand milking thirty minutes later, although the gland was still relatively hard, but considerably more relaxed than at the time of frightening. The subsequent milking yielded 19.8 pounds, or 3 to 5 pounds above normal. Figure 4 is typical of similar responses in repeated experiments. These experiments with fright indicate that the effect of denervation is not reflected by a different response as measured by the rate of ejection of milk.

*The effect of intravenous adrenalin injections on the rate of ejection of milk:* Physiologists agree that adrenalin is ejected into the blood from the medulla of the suprarenals in especially large quantities at a time of emo-



tional stress. It is also believed that musculature served by sympathetic nerves shows an especial response to the action of adrenalin. The sympathetics had been removed from the left half of the udder of E 307, and so it was decided to substitute for the fright an injection of 4 cc. of adrenalin solution (1 to 1000 Parke, Davis and Company) and note the result on the rate of milk ejection. This was repeated a number of times and a typical result is shown in figure 5 in A. The similarity to A in figure 4 is apparent. An hour after this particular milking 7.3 pounds of milk were removed by hand after considerable effort. The subsequent milking B was 19.1 pounds and above normal as was the case following fright.

In order to be assured that the response was due to the effect of the intravenous injection of adrenalin and not due to a degree of fright occasioned by the act of consummating an intrajugular injection, the experiment was repeated using 4 cc. of physiological saline instead of the adrenalin solution. Figure 6 shows that the saline failed to cause the response which was typical of adrenalin or fright. Undoubtedly some pain and excitement is caused by the act of making the injection, but sight and sound stimuli (exploding bags, etc.) seem to have a much more pronounced effect as measured by the rate of milk ejection.

Four cubic centimeters of the adrenalin solution seemed to be a serious shock to this cow, E 307. She always took her feed readily when it was placed before her prior to milking. Following adrenalin injections, she stood still, trembled slightly and refused to touch her feed and her udder became hard. Later experiments revealed that 4 cc. doses seemed to have a still more marked effect. In one instance E 307 threw herself three times in the stanchion, and due to such violent struggles, it was impossible to keep the milker attached. It was, therefore, considered advisable to limit the adrenalin injections to a maximum of 3 cc. to cows of her size (1000 lbs.).

*The effect of intravenous injections of different quantities of adrenalin on the rate of ejection of milk:* It was thought advisable to determine the effect of quantitative intrajugular injections of the adrenalin solution. E 307 was again used as the experimental subject because at the same time it would be possible to again measure the effect of denervation on the rate of response. Two to four days were allowed to lapse between experimental injections in order to permit the cow to resume her normal milking rate.

Figures 7 and 8 indicate that as the amount of adrenalin solution injected intravenously at the beginning of milking is increased, more time is required for its effect to diminish and permit the milk to be ejected. Figure 7 shows the response in the right or intact half of the udder, and figure 8 shows the same milkings for the left half of the udder which had been denervated. The similarity is quite apparent. Sixteen to twenty minutes elapsed before a relatively small amount of milk was ejected at a slow rate following the injection of 3 cc. of the adrenalin solution. The responses were less marked

when smaller amounts of adrenalin were injected. In each instance as the amount injected was reduced the response in terms of rate of ejection of milk more closely approached normal. Very similar results were noted when the series of injections was repeated on the Jersey cow E 194, a large-uddered fresh cow of known quiet disposition.

*The effect of intravenous injections of posterior pituitary lobe fractions on the rate of ejection of milk:* Due to the fact that pharmacodynamic responses, attributed to intravenous injections of posterior lobe fractions, were as pronounced in their effects as with similar adrenalin injections, it was decided to measure their effect on the rate of ejection of milk. Data were obtained in exactly the same manner as described for the adrenalin injections. E 307 was again used as an experimental subject. Repeated experiments with other cows also gave similar results.

Figure 9 shows the effect of an intravenous injection of 4 cc. of Pitocin (oxytocin 1:100) at the start of milking. The relationship between milking A, experimental, and B, the subsequent milking, is very typical of the many times this experiment was repeated. Again both halves of the udder responded in the same manner and the total yield following injection was from 2 to 5 pounds above normal, and the subsequent milking B was correspondingly less. Figure 10 shows the effect of an intrajugular injection of the same amount (4 cc.) of Pitressin (pressor fraction 1:100). The response in this case was the same as with Pitocin. The fact must be borne in mind, however, that Kamn *et al.* (12) do not claim that these two active fractions of pituitrin are completely separated in the Pitocin and Pitressin. There probably exists as much as twenty per cent Pitocin in the Pitressin and vice versa. When 4 cc. of either Pitocin or Pitressin was intravenously injected at the start of milking the result was a more complete drainage of the gland. This result seems directly opposed to the effect of fright or adrenalin solution when injected in a like manner.

It was decided, therefore, to determine the effect of delayed injections of posterior lobe fractions, following fright or adrenalin injections, at the start of the milking act. The results, using Jersey cows E 340 and E 307, are shown in figures 11, 12 and 13. These figures indicate that following fright, cessation of ejection is typical, but that within 30 seconds after the intrajugular injection of 4 cc. of either Pitocin or Pitressin, the ejection of milk is resumed in a very positive manner, and resulted in each instance in a total milk yield which was above normal, A. The subsequent milking B was always below normal in amount.

Jersey cow E 340 was used in a series of similar experiments, figure 11. These and experiments with other cows produced similar results when measured in terms of the rate of ejection of milk. There exists every indication that when 4 cc. of either of the posterior pituitary lobe fractions is intravenously injected, the result will be a prompt resumption of rapid milk

ejection. The length of time which is permitted to pass following the initial frightening or adrenalin injections seems not to affect the response to the delayed injections of the posterior lobe fractions.

When smaller quantities of Pitocin and Pitressin were used, following a standard intrajugular injection of 3 cc. adrenalin solution, the response was much more pronounced using Pitocin than Pitressin. Such data would seem to indicate that the response in the case of Pitressin, as measured by the rate of ejection of milk, might be due to the presence of Pitocin contained therein.

*The effect of intravenous injections of Pitocin and Pitressin after a normal complete milking:* Following a normal milking of two Jersey cows, E 340 and E 307, 4 cc. of Pitocin was injected intravenously and 4 days later the experiment was repeated, using Pitressin in place of Pitocin. The results are shown in figures 14 and 15.

A very marked response to 4 cc. of each of the posterior lobe fractions was noted. The yield of milk was slightly in excess of the expected normal yield. When the experiment was repeated using only 1 cc. of each fraction a greater response was noted in favor of the Pitocin. Apparently these "Super Strippings" consisted of milk which was literally squeezed from the alveoli and small ductules due to the presence in the blood of the oxytocic fraction of the product of the posterior lobe of the pituitary. The responses shown in figures 14 and 15 are typical of those obtained in other experiments using other cows.

The composition of the "Super Strippings" as compared with the normal complete milking is of interest. The following table shows only slight differences in specific gravity (lact. corrected to 60° F.), protein (N × 6.38) and lactose, when compared on a fat free basis. Great differences were apparent, however, in the per cent of fat.

	Cow E 332		Cow E 307	
	Normal	Pitocin Super Strippings	Normal	Pitocin Super Strippings
Milk lbs. ....	10.9	3.2	8.8	3.6
Specific Gravity .....	1.0338	1.0207	1.0347	1.0215
Lactose % .....	4.95	4.44	5.83	4.08
Protein % .....	4.52	3.87	4.17	3.75
Fat % .....	3.8	17.0	4.0	17.0

The percentage of fat in the "Pitocin super strippings" seemed to reflect the completeness of the normal milking. One cow, E 340, was subjected to this experiment on numerous occasions. Often she became excited and failed to let down her milk normally. Consequently her "normal" milking on one occasion amounted to only 7.6 pounds and tested as low as 1.9 per cent fat, while her super strippings which followed the injection of 2 cc. of Pitocin were equal in amount and contained 10 per cent fat.

On other occasions other Jersey cows were milked normally followed by two minutes of hand stripping preceding the intravenous injection of 2 cc. of Pitocin. Super strippings so obtained usually ranged from 14 to 24 per cent fat and the subsequent milking was always proportionately lower in fat.

#### A SUGGESTED THEORY BASED ON THESE FINDINGS

The delicate balance between the product of the suprarenal medulla, adrenalin, and the oxytocic principle of the posterior lobe of the pituitary body, in the blood of the cow at the time of the milking act, seems to be responsible for the rate of ejection of milk. The resection of the sympathetic nerves to the gland seem to play no important part as is shown in these experiments. The palpation of the teat, which so quickly increases intra-glandular pressure, can cause an impulse to reach the central nervous system through the afferent or sensory fibers of the ilio-hypogastric nerve which remained intact in these experiments. This teat palpation, however, is only one source of sensory impulses which reach the central nervous system, and this seems to be the initial step in a series of events which result in a high intra-glandular pressure.

There are many other sources of afferent stimuli which presumably might cause similar effects which occur regularly in a well-managed dairy. Rattling milk buckets, washing udders, the placing of feed before the cows, muzzling calves, etc., all occur regularly and are associated with the milking act or the relieving of the pressure within the gland. Any one or all of these, conceivably can cause afferent impulses to reach the central nervous system which, in turn, stimulates the posterior lobe to secrete the oxytocin into the blood, and it is this which is believed to be largely responsible for the increase in intra-glandular pressure, which literally squeezes the milk from the alveoli and smaller ductules. On the other hand, a variety of afferent impulses may reach the central nervous system of quite a different sort. Fright, caused by any unusual event, could in a similar manner, reflexly stimulate the natural production of adrenalin by the medulla of the suprarenals. Thus, under the influence of emotional stress, an extra quantity of adrenalin is ejected into the blood.

Evidence as to the very existence of the musculature surrounding the alveoli and small ductules is only circumstantial, but nevertheless quite convincing. The same may be said for the existence of a larger quantity of oxytocin in the blood at the moment the gland reaches its high point in pressure. These constitute special problem assignments which would throw still more light on this problem.

It would seem, therefore, that the positive act of "letting down" milk may be best explained as a conditioned reflex, and directly due to a high intra-glandular pressure caused by the presence of active oxytocin in the blood, which is responsible for the contraction of the alveoli and small

ductule musculature. On the other hand, the failure to "let down" milk is similarly due to the presence of adrenalin in the blood, which prevents the muscular contractions which are responsible for the high intra-glandular pressure.

#### SUMMARY AND CONCLUSIONS

Data are presented describing a series of experiments using Jersey cows, subjecting them to fright stimuli and intrajugular injections of adrenalin (In sol. 1:1000), Pitocin (oxytocic principle of the posterior pituitary lobe 1:100) and Pitressin (pressor principle of the posterior pituitary lobe 1:100). The left half of the udder of three of these cows had been denervated, and the response of this half of the gland was compared with the right or intact half measured in terms of the rate of ejection of milk. These data seem to justify the following conclusions.

1. Denervating the gland during the dry period resulted in no effect on the rate of ejection of milk during a subsequent lactation. There was also no change in the appearance of the two halves of the udders following the operation. This is additional evidence that the act of milk ejection is not under the direct control of the central nervous system.

2. Fright and intrajugular injections of adrenalin resulted in cessation of ejection of milk. The amount of adrenalin injected seems to determine the length of time that must elapse before natural ejection is possible. Presumably this length of time would also be proportional to the degree of fright, but this is difficult to measure.

3. Other symptoms of adrenalin shock were: a hard udder, refusal of feed, trembling and other signs of a severe nervous shock.

4. Intravenous injections of 4 cc. of either Pitocin or Pitressin caused the gland to be more completely drained than would be the case with a normal complete milking. This was also the case when the injection of these posterior pituitary lobe fractions followed fright or adrenalin injections, or at the end of a normal complete milking.

5. A smaller quantity of Pitocin showed greater potency in inducing prompt resumption of rapid ejection than was the case with Pitressin. These data support the belief that the effect of Pitressin may be due to incomplete separation of these two pituitrin fractions.

6. The extra or residual milk removed from the udder, following the injection of Pitocin, varied from normal composition of milk chiefly in per cent of fat. As one would expect, the more complete the normal milking the higher the per cent of fat in the "super strippings." The per cent of fat in these strippings ranged from 7.6 per cent to 24.0 per cent in a series of experiments.

7. A new theory is advanced which explains the "holding up" and "letting down" of milk, based on the results of these experiments.

## REFERENCES

- (1) CANNON, W. B. AND BRIGHT, E. M. A belated effect of sympathectomy on lactation. *Am. J. Physiol.*, **97**: 319-321. 1931.
- (2) ESPE, D. L. Secretion of milk. Collegiate Press Inc., Ames, Iowa, pp. 29-40 and Chapter VI, pp. 115-154. 1938.
- (3) GAINES, W. L. A contribution to the physiology of lactation. *Am. J. Physiol.*, **38**: No. 2, 285-312. 1915.
- (4) GAINES, W. L. AND SANMANN, F. P. The quantity of milk present in the udder of the cow at milking time. *Am. J. Physiol.*, **80**: 691-701. 1927.
- (5) GIELING, E. M. D. AND ROBBINS, L. I. The posterior lobe of the pituitary gland of the whale; and pituitrin and its fractions pitressin and pitocin. The pituitary gland, p. 437. Williams and Wilkins, Baltimore. 1938.
- (6) HAMMOND, J. The effect of pituitary extract on the secretion of milk. *Quart. J. Exp. Physiol.*, **6**: No. 4, 311-338. 1913.
- (7) HAMMOND, J. The physiology of milk and butterfat secretion. *Vet. Record N-S*, **16**: 519-535. 1936.
- (8) HAMMOND, J. AND HAWK, J. C. Studies in milk secretion. II. The relation of the glands of internal secretion to milk production. *J. Agr. Sci.*, **8**: No. 2, 147-153. 1917.
- (9) HILL, R. L. AND SIMPSON, S. The effect of pituitary extract on the secretion of milk in the cow. *Proc. Soc. Exp. Biol. Med.*, **11**: 82-85. 1914.
- (10) HILL, R. L. AND SIMPSON, S. The effect of pituitary extract on milk secretion in the goat. *Quart. J. Exp. Physiol.*, **8**: 103-111. 1914.
- (11) INGELBRECHT, P. L'influence du systeme nerveux central sur la mamelle lactante chez le rat blanc. *Compt. Rend. Soc. de Biol.* **120**: 1369-1371. 1935.
- (12) KAMN, O., ALDRICH, T. B., GROTE, I. W., ROWE, L. W. AND BUGBEE, E. P. The active principle of the posterior lobe of the pituitary gland. 3 parts. *J. Am. Chem. Soc.*, **50**: 573-601. 1928.
- (13) MACY, I. G., HUNCHER, H. A., DONELSON, EVA, AND NIMS, BETTY. Human milk flow. *Am. J. Diseases of Children*, **39**: 1186-1204. 1930.
- (14) MAXWELL, A. L. I. AND ROTHERA, A. C. H. The action of pituitrin on the secretion of milk. *J. Physiol.*, **49**: No. 6, 483-491. 1915.
- (15) MCCANDLISH, A. C. The possibility of increasing milk and butterfat production by the administration of drugs. *J. DAIRY SC.*, **1**: 6. 1918.
- (16) MCKENZIE, K. An experimental investigation of the mechanism of milk secretion, with special reference to the action of animal extracts. *J. Exp. Physiol.*, **4**: 305-330. 1911.
- (17) OLIVER, G. AND SCHAFER, E. A. On the physiological action of extracts of the pituitary body and certain other glandular organs. *J. Physiol.*, **18**: 277-279. 1895.
- (18) OTT, ISAAC AND SCOTT, J. C. The action of infundibulin upon the mammary secretion. *Proc. Soc. Exp. Biol. Med.*, **8**: 48-49. 1910.
- (19) PETERSEN, W. E., PALMER, L. S. AND ECKLES, C. H. The synthesis and secretion of milk fat. I. The time of milk and fat secretion. *Am. J. Physiol.*, **90**: 573. 1929.
- (20) RIBBERT, HUGO. Über Transplantation von Ovarium, Hoden und Mamma. *Arch. Enwick, Mechanik der Organismen*, **7**: 688-704. 1898.
- (21) ROUTH, A. Parturition during paraplegia, with cases. *Trans. Obstet. Soc. London*, **34**: 191. 1897.
- (22) SCHAFER, E. A. On the effect of pituitary and corpus luteum extracts on the mammary gland in the human subject. *Quart. J. Exp. Physiol.*, **6**: 17-19. 1913.



- (23) SCHAFER, E. A. Note on preceding paper by Simpson and Hill. "The mode of action in pituitary extract on the mammary gland." *Quart. J. Exp. Physiol.*, **8**: 379. 1915.
- (24) SELYE, H., COLLIP, J. B. AND THOMSON, D. L. Nervous and hormonal factors in lactation. *Endocrinology*, **18**: 237-248. 1934.
- (25) SIMPSON, S. AND HILL, R. L. The effect of repeated injections of pituitrin on milk secretion. *Am. J. Physiol.*, **36**: 347-351. 1915.
- (26) SIMPSON, S. AND HILL, R. L. The mode of action of pituitary extract on the mammary gland. *Quart. J. Exp. Physiol.*, **8**: 377-378. 1915.
- (27) STEHLE, R. L. A new method for separating pressor and oxytocic substances from the posterior lobe of the pituitary gland. *J. Biol. Chem.*, **102**: 573-590. 1933.
- (28) SWETT, W. W., MILLER, F. L. AND GRAVES, R. R. Quantity of milk obtained from amputated cows udders. *J. Agr. Res.*, **45**: 385-400. 1932.
- (29) TGETGEL, B. Untersuchungen über den Sekretions-druck und über das Einschieszen der Milch im Euter des Rindes. *Schweiz. Arch. f. Tierh.*, **68**: No. 6, 335-348 and No. 7, 369-387. 1926.
- (30) TURNER, C. W. The comparative anatomy of the mammary glands. Univ. of Mo. Cooperative Store, Columbia, Mo. Chap. 6, pp. 70-73. 1939.
- (31) TURNER, C. W. AND SLAUGHTER, I. S. The physiological effect of pituitary extract (posterior lobe) on the lactating mammary gland. *J. DAIRY SC.*, **13**: 8-24. 1930.
- (32) ZIETZSCHMANN, O. Etude sur les vaches qui "retiennent" leur lait. *Le Lait II*: 229. 1922.

# Is *Candida auris* the first multidrug-resistant fungal zoonosis emerging from climate change?

Victor Garcia-Bustos<sup>1,2,3</sup>

**AUTHOR AFFILIATIONS** See affiliation list on p. 3.

**ABSTRACT** The emergence and evolutionary path of *Candida auris* poses an intriguing scientific enigma. Its isolation from a pet dog's oral cavity in Kansas, reported by White et al. (T. C. White, B. D. Esquivel, E. M. Rouse Salcido, A. M. Schweiker, et al., mBio 15:e03080-23, 2024, <https://doi.org/10.1128/mbio.03080-23>), carries significant implications. This discovery intensifies concerns about its hypothetical capacity for zoonotic transmission, particularly considering the dog's extensive human contact and the absence of secondary animal/human cases in both animals and humans. The findings challenge established notions of *C. auris* transmissibility and underscore the need for further investigation into the transmission dynamics, especially zooanthropotic pathways. It raises concerns about its adaptability in different hosts and environments, highlighting potential role of environmental and animal reservoirs in its dissemination. Critical points include the evolving thermal tolerance and the genetic divergence in the isolate. This case exemplifies the necessity for an integrated One Health approach, combining human, animal, and environmental health perspectives, to unravel the complexities of *C. auris*'s emergence and behavior.

**KEYWORDS** *Candida auris*, zoonosis, dog, animal, thermal resistance, climate change

*Candida auris* is an emerging fungal pathogen distinguished by its unprecedented multidrug resistance, environmental survivability, and high transmissibility. Its evolutionary trajectory presents a significant and intriguing scientific enigma. Whole-genome sequencing has identified five genetically distinct clades that appeared nearly simultaneously and independently across three continents (1, 2). Population genomics dates the most recent common ancestor of each clade to within the last 360 years. Notably, the clusters causing outbreaks in clades I, III, and IV are thought to have emerged 36 to 38 years ago, suggesting a recent divergence and the acquisition of virulence from a non-pathogenic environmental ancestor (3). This unusual pattern of emergence challenges traditional epidemiological models and indicates that a founder effect may have played a crucial role in the global spread and independent evolutionary paths of *C. auris*, predating its recognition in clinical environments.

Climate change and animal colonization are hypothesized to play roles in the evolutionary dynamics of *C. auris* (4, 5). The 2019 study by Casadevall et al. indicated that *C. auris* possesses greater thermal tolerance than its marine relatives, such as *C. haemulonii*. Furthermore, an important saline tolerance has also been reported in several studies, demonstrating enhanced resistance to salinity compared to other *Candida* species, such as *C. albicans* (6, 7). This enhanced halotolerance and thermal adaptability suggest its origin in saline ecosystems like wetlands and its subsequent evolution into a pathogen or colonizer in endothermic species, potentially aiding its global dissemination (4). The isolation of *C. auris* from environmental sources in the Andaman Islands in 2021 and Colombian estuaries in 2022 confirmed its presence in marine habitats (6, 8). Additionally, its detection in public swimming pools in the Netherlands in 2018 (9), and

**Editor** J. Andrew Alspaugh, Duke University Hospital, Durham, North Carolina, USA

Address correspondence to Victor Garcia-Bustos, [victorgarciabustos@gmail.com](mailto:victorgarciabustos@gmail.com).

The author declares no conflict of interest.

The views expressed in this article do not necessarily reflect the views of the journal or of ASM.

See the original article at <https://doi.org/10.1128/mbio.03080-23>.

**Published** 13 March 2024

Copyright © 2024 Garcia-Bustos. This is an open-access article distributed under the terms of the [Creative Commons Attribution 4.0 International license](https://creativecommons.org/licenses/by/4.0/).

hospital and municipal wastewaters in Nevada and Florida in 2022 (10, 11), demonstrates its adaptability to various aquatic environments. A strain from the Andaman Islands, characterized by reduced drug resistance and thermal tolerance (6), appears more closely related to the ancestral marine forms of the fungus, providing insights into its evolution from an environmental organism to a human pathogen. However, animals might play a crucial role in its dissemination.

Initial evidence of *C. auris* in animal hosts emerged from retrospective *in silico* analyses using culture-independent metabarcoding techniques (12). *Candida auris* sequences were identified in the ear canal of a Spanish dog with otitis externa and on the skin of two newt species in Cambridgeshire, UK. Subsequent findings extended beyond metabarcoding evidence; live *C. auris* was isolated from two stray dogs with otitis externa in India (13) and from the oral cavity of a pet dog in Kansas as documented in the interesting study by White et al. (14).

These findings raise critical questions about the hypothetical zoonotic potential of *C. auris*, particularly in the context of climate change. Transmission routes remain to be elucidated, with no documented interspecies spread in the cases from the US and India. The case in Kansas is particularly noteworthy due to the pet dog's frequent human interaction, contrasting with the established transmissibility of *C. auris* among humans in clinical settings. This instance was the first documented occurrence in Kansas, in an area without previous reports of the pathogen. Notably, despite *C. auris*'s known transmission capability and surface survivability, there were no secondary cases in other dogs at the shelter, including the dog's littermate, even with regular oral contact among dogs and humans (14). This pattern was also seen in the Indian stray dogs (13).

The absence of screening for *C. auris* in the shelter environment, caregivers, and current owners represents a significant oversight, given the relevance of the finding. However, this contact tracing was performed in the Indian animal intensive care unit, but no colonization in healthcare workers or surfaces was observed. It is yet to be elucidated whether the transmissibility of *C. auris* is altered in colonization of non-human hosts with higher basal temperatures. However, as in humans, the unifocal colonization and the low fungal burden in described cases might also be implicated, especially considering the spontaneous clearance in the Kansas dog.

Moreover, these findings suggest a plausible scenario of zoonothonotic transmission, where humans previously infected or colonized with *C. auris* could transfer the pathogen to their pets. However, this has not been yet demonstrated. This mode of transmission could establish animals as reservoirs for the fungus, potentially leading to persistent colonization and an expanded host range. Such dynamics might contribute to the acquisition of increased drug resistance or even recurrent candidemia episodes, as previously documented (15).

The ability of *C. auris* to thrive in hosts with basal temperatures exceeding 38°C underscores its ongoing thermal tolerance, a point notably emphasized by White et al. This evolving thermoresistance prompts questions about the role of heat shock proteins and related pathways in enhancing this capacity and its correlation with its virulence, including the potential for increased pathogenicity in these isolates (16). Additionally, the discovery of over 90 single-nucleotide polymorphisms differentiating the clade IV *C. auris* isolate from a Kansas dog from other clade IV strains indicates substantial evolutionary divergence. This genetic diversity warrants functional exploration, as it could influence the pathogen's characteristics, including virulence, drug resistance, and host range. There is also a notable mention of genetically distinct clade I *C. auris* strains in two Indian dogs. One strain is more closely related to the azole-susceptible Pakistan clade I reference strain, while the other shows a closer relationship to Indian-resistant clinical strains. This variation further exemplifies this pathogen's genetic complexity and adaptability of this pathogen across different hosts and environments.

These animal isolations underscore that contemporary clinical isolates, including those in animals, have surpassed the thermal barrier traditionally limiting colonization or infection in endothermal hosts. Consequently, we could speculate that a wide

range of hosts, including birds with higher basal temperatures and extensive migration patterns involving human contact, could potentially serve as reservoirs for fungal spread. The recent live isolation from dogs adds to the growing body of evidence about *C. auris*'s evolutionary history. Birds have been proposed as possible intermediate hosts in the historical global dissemination of *C. auris* ancestors (4), potentially explaining the founder effect that led to the independent evolution of different clades across continents over the last four centuries. However, the evolutionary leap to bird hosts might be too great for more primitive strains of the fungus (5). Environmental strains are anticipated to be less thermotolerant and drug resistant but more halotolerant compared to the more thermotolerant and multidrug-resistant clinical strains found in animals, such as the amphotericin B-resistant strain isolated from the Kansas dog. An intermediate evolutionary lineage of *C. auris* strains may have historically existed or could still coexist in nature in marine migratory hosts like marine mammals. These hosts, characterized by lower basal temperatures and migration patterns linked to marine ecosystems, could represent a critical evolutionary bridge between environmental and clinical strains.

White et al.'s findings highlight the necessity for a collaborative multifaceted approach, focusing on elucidating transmission dynamics, especially potential zoonotic and zooanthroponotic pathways, and investigating environmental and animal reservoirs. Extensive genomic studies comparing animal, human, and less thermal-tolerant environmental isolates are vital for understanding diversity, evolutionary history, resistance, and virulence. An interdisciplinary One Health approach integrating human, animal, and environmental health perspectives is essential for a comprehensive understanding and management of *C. auris*.

#### AUTHOR AFFILIATIONS

<sup>1</sup>Severe Infection Research Group, Health Research Institute La Fe, Valencia, Spain

<sup>2</sup>Instituto Universitario de Sanidad Animal y Seguridad Alimentaria (IUSA), Universidad de Las Palmas de Gran Canaria, Arucas, Spain

<sup>3</sup>Department of Internal Medicine and Infectious Diseases, University and Polytechnic Hospital La Fe, Valencia, Spain

#### AUTHOR ORCIDs

Victor Garcia-Bustos  <http://orcid.org/0000-0002-1785-258X>

#### AUTHOR CONTRIBUTIONS

Victor Garcia-Bustos, Conceptualization, Investigation, Writing – original draft, Writing – review and editing

#### REFERENCES

1. Rhodes J, Fisher MC. 2019. Global epidemiology of emerging *Candida auris*. *Curr Opin Microbiol* 52:84–89. <https://doi.org/10.1016/j.mib.2019.05.008>
2. Spruijtenburg B, Badali H, Abastabar M, Mirhendi H, Khodavaisy S, Sharifisooraki J, Taghizadeh Armaki M, de Groot T, Meis JF. 2022. Confirmation of fifth *Candida auris* clade by whole genome sequencing. *Emerg Microbes Infect* 11:2405–2411. <https://doi.org/10.1080/22221751.2022.2125349>
3. Chow NA, Muñoz JF, Gade L, Berkow EL, Li X, Welsh RM, Forsberg K, Lockhart SR, Adam R, Alanio A, Alastruey-Izquierdo A, Althawadi S, Araúz AB, Ben-Ami R, Bharat A, Calvo B, Desnos-Ollivier M, Escandón P, Gardam D, Gunturu R, Heath CH, Kurzai O, Martin R, Litvintseva AP, Cuomo CA. 2020. Tracing the evolutionary history and global expansion of *Candida auris* using population genomic analyses. *mBio* 11:e03364-19. <https://doi.org/10.1128/mBio.03364-19>
4. Casadevall A, Kontoyiannis DP, Robert V. 2019. On the emergence of *Candida auris*: climate change, azoles, swamps, and birds. *mBio* 10:e01397-19. <https://doi.org/10.1128/mBio.01397-19>
5. Garcia-Bustos V, Cabañero-Navalon MD, Ruiz-Gaitán A, Salavert M, Tormo-Mas MÁ, Pemán J. 2023. Climate change, animals, and *Candida auris*: insights into the ecological niche of a new species from a one health approach. *Clin Microbiol Infect* 29:858–862. <https://doi.org/10.1016/j.cmi.2023.03.016>
6. Arora P, Singh P, Wang Y, Yadav A, Pawar K, Singh A, Padmavati G, Xu J, Chowdhary A. 2021. Environmental isolation of *Candida auris* from the coastal wetlands of Andaman Islands. *mBio* 12:e03181-20. <https://doi.org/10.1128/mBio.03181-20>
7. Heaney H, Laing J, Paterson L, Walker AW, Gow NAR, Johnson EM, MacCallum DM, Brown AJP. 2020. The environmental stress sensitivities of pathogenic *Candida* species, including *Candida auris*, and implications for their spread in the hospital setting. *Med Mycol* 58:744–755. <https://doi.org/10.1093/mmy/myz127>
8. Escandón P. 2022. Novel environmental niches for *Candida auris*: isolation from a coastal habitat in Colombia. *J Fungi (Basel)* 8:748. <https://doi.org/10.3390/jof8070748>

9. Ekowati Y, Ferrero G, Kennedy MD, de Roda Husman AM, Schets FM. 2018. Potential transmission pathways of clinically relevant fungi in indoor swimming pool facilities. *Int J Hyg Environ Health* 221:1107–1115. <https://doi.org/10.1016/j.ijheh.2018.07.013>
10. Rossi A, Chavez J, Iverson T, Hergert J, Oakeson K, LaCross N, Njoku C, Gorzalski A, Gerrity D. 2023. *Candida auris* discovery through community wastewater surveillance during healthcare outbreak. *Emerg Infect Dis* 29:422–425. <https://doi.org/10.3201/eid2902.221523>
11. Babler K, Sharkey M, Arenas S, Amirali A, Beaver C, Comerford S, Goodman K, Grills G, Holung M, Kobetz E, Laine J, Lamar W, Mason C, Pronty D, Reding B, Schürer S, Schaefer Solle N, Stevenson M, Vidović D, Solo-Gabriele H, Shukla B. 2023. Detection of the clinically persistent, pathogenic yeast spp. *Candida auris* from hospital and municipal wastewater in Miami-Dade County, Florida. *Sci Total Environ* 898:165459. <https://doi.org/10.1016/j.scitotenv.2023.165459>
12. Irinyi L, Roper M, Malik R, Meyer W. 2022. Finding a needle in a haystack - *in silico* search for environmental traces of *Candida auris*. *Jpn J Infect Dis* 75:490–495. <https://doi.org/10.7883/yoken.JJID.2022.068>
13. Yadav A, Wang Y, Jain K, Panwar VAR, Kaur H, Kasana V, Xu J, Chowdhary A. 2023. *Candida auris* in dog ears. *J Fungi (Basel)* 9:720. <https://doi.org/10.3390/jof9070720>
14. White TC, Esquivel BD, Rouse Salcido EM, Schweiker AM, Dos Santos AR, Gade L, Petro E, KuKanich B, KuKanich KS. 2024. *Candida auris* detected in the oral cavity of a dog in Kansas. *mBio* 15:e0308023. <https://doi.org/10.1128/mbio.03080-23>
15. Biagi MJ, Wiederhold NP, Gibas C, Wickes BL, Lozano V, Bleasdale SC, Danziger L. 2019. Development of high-level echinocandin resistance in a patient with recurrent *Candida auris* candidemia secondary to chronic candiduria. *Open Forum Infect Dis* 6:ofz262. <https://doi.org/10.1093/ofid/ofz262>
16. Gong Y, Li T, Yu C, Sun S. 2017. *Candida albicans* heat shock proteins and Hsps-associated signaling pathways as potential antifungal targets. *Front Cell Infect Microbiol* 7:520. <https://doi.org/10.3389/fcimb.2017.00520>

# Three-Dimensional Printed Models of the Heart Represent an Opportunity for Inclusive Learning

Kieran Borgeat ■ Andrew I.U. Shearn ■ Jessie Rose Payne ■ Melanie Hezzell ■ Giovanni Biglino

## ABSTRACT

Three-dimensional (3D) printed models of anatomic structures offer an alternative to studying manufactured, “idealized” models or cadaveric specimens. The utility of 3D printed models of the heart for clinical veterinary students learning echocardiographic anatomy is unreported. This study aimed to assess the feasibility and utility of 3D printed models of the canine heart as a supplementary teaching aid in final-year vet students. We hypothesized that using 3D printed cardiac models would improve test scores and feedback when compared with a control group. Students ( $n = 31$ ) were randomized to use either a video guide to echocardiographic anatomy alongside 3D printed models (3DMs) or video only (VO). Prior to a self-directed learning session, students answered eight extended matching questions as a baseline knowledge assessment. They then undertook the learning session and provided feedback (Likert scores and free text). Students repeated the test within 1 to 3 days. Changes in test scores and feedback were compared between 3DM and VO groups, and between track and non-track rotation students. The 3DM group had increased test scores in the non-track subgroup. Track students' test scores in the VO group increased, but not in the 3DM group. Students in the 3DM group had a higher completion rate, and more left free-text feedback. Feedback from 3DM was almost universally positive, and students believed more strongly that these should be used for future veterinary anatomy teaching. In conclusion, these pilot data suggest that 3D printed canine cardiac models are feasible to produce and represent an inclusive learning opportunity, promoting student engagement.

**Key words:** 3D printing, rapid prototyping, echocardiography

## INTRODUCTION

Contextualizing a knowledge of anatomy with clinical imaging techniques is essential for final-year veterinary students, as this will allow them to interpret images obtained during case investigations and facilitate decision making for the benefit of the patient. A particular challenge may be encountered when students must incorporate a three-dimensional (3D) visual map of a complex structure, often learned using cadavers in the early years of veterinary school, into two-dimensional (2D) clinical imaging techniques. One example of this is when final-year students are called upon to interpret echocardiographic images: a greyscale, 2D representation of a complex, moving structure. A common way for students to be introduced to echocardiographic anatomy is by being verbally guided through an echocardiogram as it is being performed by a veterinary cardiologist. This may not be the best method to help many students understand the anatomical structures that are being imaged, and using 3D models has been shown to improve medical students' understanding of spatial anatomy.<sup>1</sup>

Models of anatomic structures have been used in teaching and learning for many years, initially made from resin and plaster, then more recently using plastics. 3D printing is a technique for building physical models using a layer-by-layer technique, which is built around a computer-generated 3D image of a structure (the source data). In veterinary and medical patients, source data are often derived from numerous 2D slices of anatomic structures, such as those obtained from a computed tomography (CT) or magnetic resonance imaging study. In this way, 3D printed anatomic models can be manufactured that reflect particular species- or breed-specific anatomy and therefore provide an authentic representation from which students can learn.<sup>1</sup> Anatomic models of diseased organs can also be printed, which may help

further in undergraduate education, specialist post-graduate training,<sup>2</sup> and surgical planning.<sup>3,4</sup>

In human medicine, using 3D printed models has been shown to complement the curriculum of body-wide anatomy education,<sup>5</sup> and 3D printed cardiac models were reported to improve undergraduate student test scores compared with the use of cadaver-derived material<sup>6</sup> or traditional small group seminars.<sup>7</sup> In addition, using 3D printed models of the heart has been shown to improve engagement and communication between members of the public and clinicians.<sup>8</sup> However, using a 3D printed model compared with using traditional models of the heart did not improve test scores or student satisfaction in another study.<sup>9</sup> Similarly, using a 3D computer model (not printed) of hepatobiliary anatomy did not show test-performance benefit over use of an instructional textbook, but student satisfaction scores were higher with the 3D onscreen model.<sup>10</sup>

In veterinary undergraduate students, 3D printed models from clinical imaging data sets have shown academic and student satisfaction benefits in addition to standard teaching methods.<sup>11-14</sup> In addition, 3D printed models have the added benefit of not involving the handling of animal tissues, which may present a biohazard and limit the opportunities for study outside of a specific, controlled environment.<sup>14</sup>

Currently, no data evaluating the use of 3D printed cardiac models in teaching veterinary anatomy have been published. Our overall project aim was to evaluate the fitness of 3D printed models of the heart as a learning tool for veterinary cardiac anatomy in a clinical context. We hypothesized that using 3D models in addition to a video guide to echocardiographic anatomy would result in higher test scores and more positive student feedback after a self-directed learning exercise for final-year veterinary students.

## MATERIALS AND METHODS

### Source Data and Modeling

Raw data from a CT scan<sup>a</sup> of an 8-year-old male neutered lurcher (weighing 26 kg) was used to generate the 3D computer models. Images had been obtained during investigation of a cardiac arrhythmia, but no primary heart disease was identified on echocardiography, and the results of the CT scan were reported to be normal by the attending radiologist. Intravascular contrast was used to delineate cardiac structures and the great vessels.

Images (DICOM format) were imported into Materialise Mimics<sup>b</sup> v21.0 and segmented to remove non-cardiac structures, as previously described by Schievano et al.<sup>15</sup> Computer models were then imported into 3-Matic post processing software (Materialise) and reviewed by a veterinary cardiologist (author KB). They were cut in four standard echocardiographic image planes as follows: right parasternal long-axis 4-chamber view; right parasternal long-axis 5-chamber view; right parasternal short-axis view at the level of the papillary muscles; and right parasternal short-axis view at the level of the left atrium and aortic root. This produced four pairs of computer models, each representing the heart bisected at an angle to represent a standard clinical echocardiographic image view.

### 3D Printing

The finalized computer models were exported life size from 3-Matic as STL files, a format suitable for import into the 3D printer-specific software Preform.<sup>c</sup> Models were printed on a Form 2 3D printer (Formlabs) using white V4 resin (FLGPWH04, Formlabs). Once printed, the models were washed in isopropanol in a Form Wash station (Formlabs), then cured using a Form Cure (Formlabs), both according to the instructions of the manufacturer.

Supports, which had been previously built around the model to support the printing, were removed manually. Paper was cut into an appropriate shape and used as a substitute material for heart valves. These were attached using superglue in an anatomically accurate position where required within each model (Figure 1).

### Experimental Design

The study design was approved by the University of Bristol CREATE Ethics Approval Process. Final year veterinary students were eligible for participation if they provided signed consent after reading a participant information sheet. Students were recruited in one of two ways: first, those undertaking an elective 1-week rotation in cardiology (known as a track rotation) were invited to participate during their scheduled week; second, students not choosing to undertake the track rotation were invited by email to participate (these students were working elsewhere in clinics or on-site study). All students had completed a previous core cardiology rotation of 2 days' duration, in addition to clinical lectures on the subject (anatomy—including cadaver specimens—and physiology in year 1, pharmacology and clinical cardiology including basics of imaging anatomy in year 3). The students undertaking the track rotation received teaching around clinical cases, including discussion of echocardiographic anatomy, during the study. This was not the case for non-track students who were undertaking non-cardiology rotations during this time.

Enrolled students were assigned a unique identification number and then randomized to one of two groups using a random number generator through Siri for iPhone 7. The control group was assigned a self-directed learning exercise using an online video, in which a veterinary cardiologist (KB) guided them through canine echocardiographic anatomy (see Appendix 1,

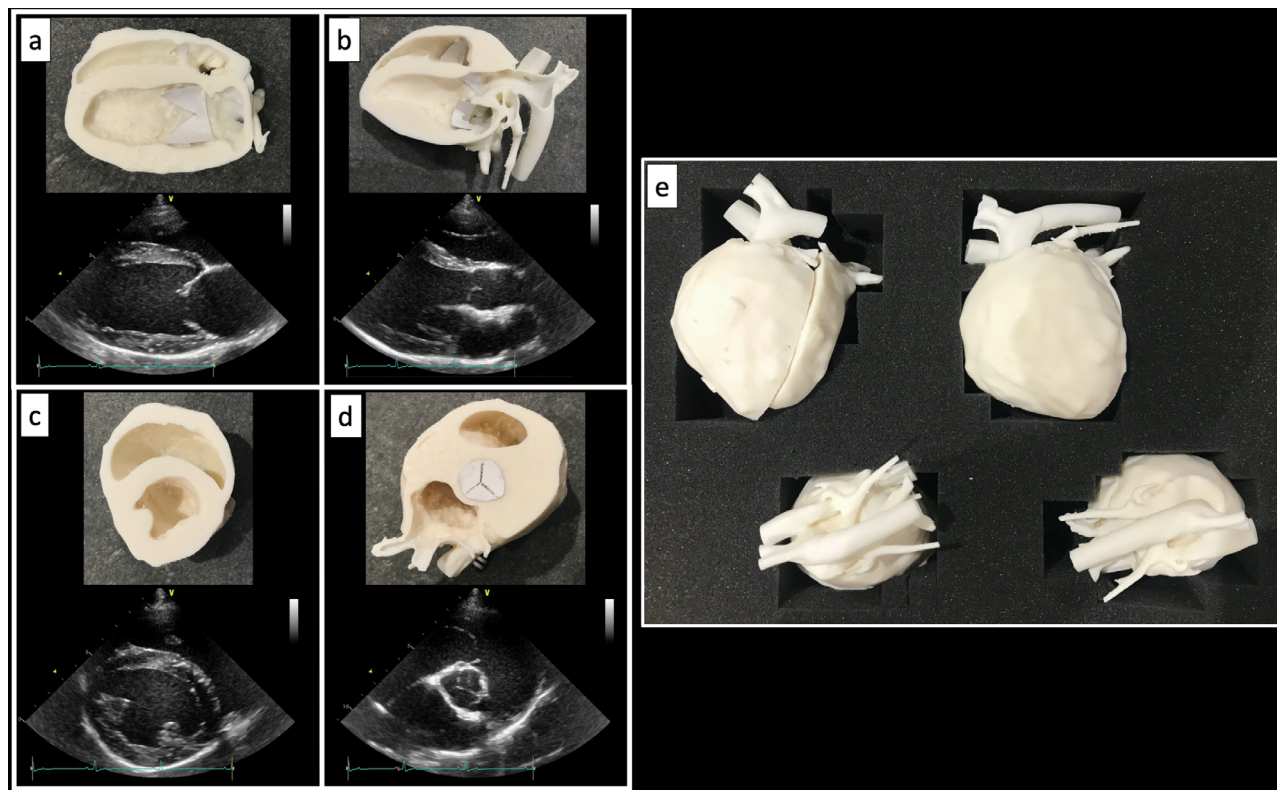


**Figure 1:** Photographs of 3D models in cut-section (a–d) and in position as whole hearts as displayed to students upon opening the storage case (e)

Note: Models were designed to represent the four most important echocardiographic views: (a) right parasternal long-axis 4-chamber; (b) right parasternal long-axis 5-chamber; (c) right parasternal short-axis at the papillary muscles, and (d) right parasternal short-axis at the aortic root.

available at <https://doi.org/10.3138/jvme-2020-0141>). The test group was assigned the same exercise but was allowed to use the 3D printed models alongside the video to consider the relationships between the 2D video images and 3D anatomic structures. It was clearly stated that there was no time limit for the learning exercise and that the video could be rewatched if so desired. Students underwent pre- and post-intervention testing of their anatomic knowledge using an online quiz<sup>d</sup> and were asked to provide feedback on the learning experience after they had completed the exercise (Figure 2). Unique identification numbers were used throughout to anonymize data.

The test was designed to be a simple and rapid assessment of the student's ability to recognize a cardiac chamber or blood vessel on echocardiographic video loops. Questions were of the extended matching question (EMQ) type; the same answer options were available for each question so as not to provide a leading set of answers or limit the student's options for their response. Each question had a set of 15 possible answers, including 14 anatomic structures and one option for "I don't know." Only one answer was correct, and others were marked as incorrect. Eight different but standard echocardiographic views were used to formulate questions (Table 1), with one video showing an abnormality and two showing a left-sided view (not featured in the video).

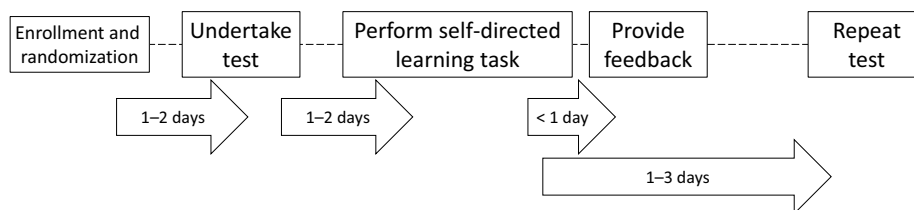


**Figure 2:** Timeline of tasks for students enrolling in the study  
 Note: Each student was involved for no more than one 5-day week.

**Table 1:** Echocardiographic views used as test material, with anatomic structure indicated for each

Question no.	Echocardiographic view	Structure indicated
1	Right parasternal short-axis view at the papillary muscles	Right ventricle
2	Right parasternal long-axis 4-chamber view (mitral valve)	Left ventricle
3	Left apical 4-chamber view (left ventricular inflow)	Pulmonary vein
4	Right parasternal short-axis view optimized for the pulmonary artery	Pulmonary artery
5	Right parasternal long-axis 5-chamber view (aortic valve)	Aorta
6	Right parasternal short-axis view optimized for the left atrium and aortic root (normal left atrial size)	Left atrium
7	Left apical 4-chamber view (left ventricular inflow)	Right atrium
8	Right parasternal short-axis view optimized for the left atrium and aortic root (dilated left atrium)	Left atrium

Note: Views for questions 3 and 7 were not shown during the video tutorial.

The feedback form was divided into two sections: first, a series of statements evaluating various aspects of the learning experience using a 5-point Likert scale (ranging from 1 = *strongly disagree* to 5 = *strongly agree*), followed by a free-text box for participants to input additional information (see Appendix 2, available at <https://doi.org/10.3138/jvme-2020-0141>).

**Analysis**

Test scores before and after intervention were compared between the groups 3D models and video (3DM) versus video only (VO), and between track and non-track rotation groups, using a Wilcoxon signed-rank test. Feedback was compared between 3DM and VO groups, including a review of free-text statements. Statistical significance was set at  $p < .05$ . Because of small sample sizes, a trend toward statistical significance was defined as  $p < .1$ .

**RESULTS**

**Participants**

Out of a year group of 143 students, 31 (22%) volunteered to participate in the study. Failure to complete one or more elements of the study occurred in 5/16 cases (31%) of the VO group (Figure 3) but none of the 3DM group.

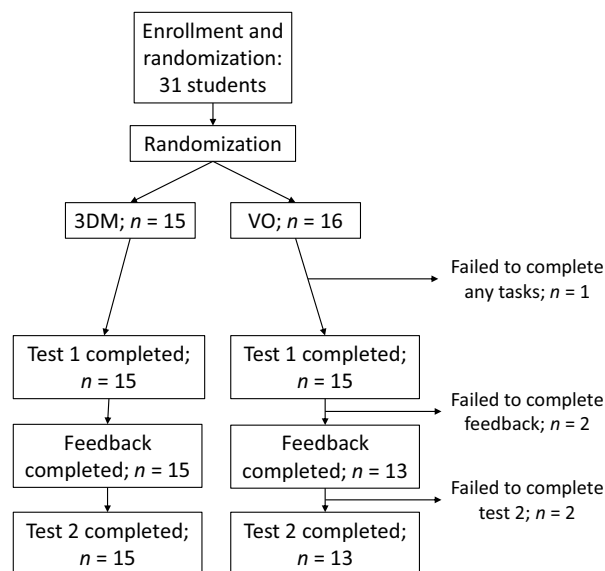


**Figure 3:** Flowchart to show dropout rate of students at various stages  
 3DM = 3D printed model; VO = video only  
 Notes: One of the VO group did not undertake any tasks after providing consent. Two further students failed to complete feedback (but did complete test 2), and a different two students failed to complete test 2 (but did give feedback). This left 13 students in the VO group for analysis. None of the 3DM group of students withdrew from the study and all completed all required tasks.



### Test Scores

The VO group for analysis of test scores ( $n = 13$ ) comprised 6 non-track and 7 track students. The 3DM group ( $n = 15$ ) was composed of 7 non-track and 8 track students. Median test scores were not different between 3DM and VO groups (5/8 pre-intervention, 6/8 post-intervention for both). However, when the demographics were broken down, non-track and track students appear to have benefited from different learning materials (Figure 4). In the VO group, no significant difference was identified in test scores before and after the intervention for non-track students ( $p = .5$ ). In contrast, test scores improved significantly in track students between test 1 and test 2 ( $p = .016$ ). In the 3D models group, non-track students' test scores increased between the first and second test (statistical trend:  $p = .062$ ), but track students' test scores did not ( $p = .75$ ).

### Feedback Scores

Feedback was generally positive about both types of learning resources. Results are summarized in Table 2. All students in both groups enjoyed using the learning materials. In the 3DM group,

all students agreed that their knowledge had improved after the learning session, whereas two students in the VO group had mixed feelings. Most students in the VO group listed negative or mixed feelings about there being sufficient time to use the learning materials, whereas the majority of 3DM students gave positive responses. However, both groups expressed some concerns about the time allowed for the learning exercise, despite no time limit being set.

While most members of both groups felt positively that 3D models should be used more in teaching anatomy when looking in detail at the breakdown of *strongly agree* to *partially agree* statements, the 3DM group has a greater proportion of strongly positive statements in response (Figure 5).

### Free-Text Feedback

Free-text comments were made by 8/13 (62%) in the VO group and 11/15 (73%) in the 3DM group.

Students in the 3DM group generally commented that the models helped them to understand echocardiographic anatomy more clearly. One student commented:

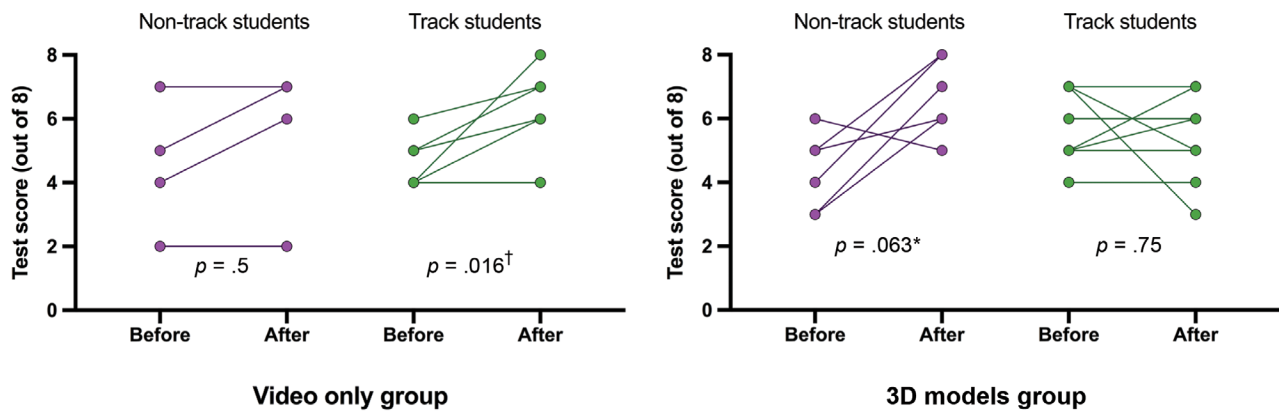


**Figure 4:** Paired dot plot to show pre- and post-intervention test scores for students undertaking the different echocardiographic anatomy learning exercises, split into non-track and track groups

\* trend toward statistical significance  $p < .1$

† statistically significant at  $p < .05$

Note: The data suggest that 3D models were most beneficial for non-track students, but the video tutorial was more helpful for those undertaking the track rotation.

**Table 2:** Responses to the feedback questions on students' experiences of using the learning materials

Aspect of using learning materials	Video only group ( $n = 13$ )			3D models & video group ( $n = 15$ )		
	Positive (4&5)	Neutral (3)	Negative (1&2)	Positive (4&5)	Neutral (3)	Negative (1&2)
Materials were enjoyable to use	13	0	0	15	0	0
Materials improved my confidence	11	2	0	15	0	0
Materials improved my knowledge	11	0	2	13	1	1
Materials were easy to understand	13	0	0	14	0	1
Sufficient time was allowed for learning	3	5	5	7	3	5
More clinical material should be used in teaching anatomy	12	1	0	14	1	0
3D models should be used more in teaching anatomy	11	2	0	14	1	0
Learning echo anatomy has helped me to become a better vet	11	0	1	13	1	1

Note: Likert scores ranged from 1 to 5 (1 = *strongly disagree*, 2 = *partially disagree*, 3 = *mixed feelings*, 4 = *partially agree*, 5 = *strongly agree*).

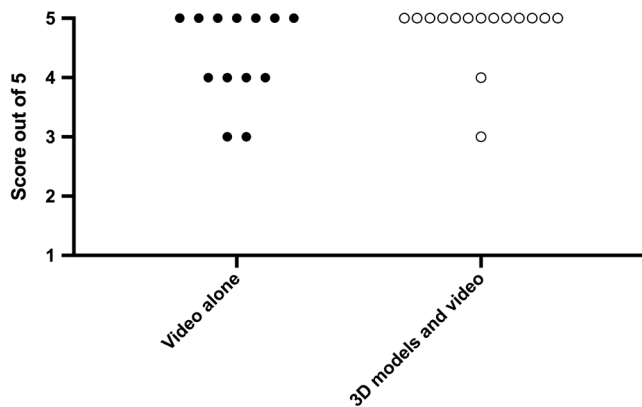


**Figure 5:** Breakdown of responses to the feedback questionnaire statement “I would like to use more 3D models in learning anatomy”

Note: Likert scores ranged from 1 to 5 (1 = *strongly disagree*, 2 = *partially disagree*, 3 = *mixed feelings*, 4 = *partially agree*, 5 = *strongly agree*). A greater proportion of students strongly agreed with the statement if they had used the 3D models in the learning session.

The use of 3D models alongside the echo loops allowed for proper orientation and allowed the whole architecture of the heart to be appreciated.

Another student stated:

The models helped visualize the layers of the heart being observed when using M mode and helped me to see why the papillary muscles ...

One student considered that the models may specifically help people who would consider themselves to be of a particular learning preference:

For practical and visual learners, the 3D model is amazing alongside the videos of the echos [sic].

Some more negative comments included a thought that perhaps the 3D printed models were not as good as using cadavers:

Combining reviewing actual cardiac anatomy, i.e., dissecting real hearts in the views that you take on each may be easier than 3D models.

In addition, one student commented that the models did not always look exactly like the images on videos of the echocardiogram:

The left atrium to aortic view model did not match very well with the echo used in the video, which made it slightly confusing to learn from.

Students also commented positively on the video tutorial:

The video teaching material was really good, especially the echo clips.

Students in the VO group generally found the video helpful in their learning:

[It was] really useful; we had nothing like this in years 1–4, and the video made echo anatomy much clearer, especially for the second and third views/probe orientations.

Another student commented:

This was a really good and fun additional learning resource!

More than one student felt that the video moved too quickly:

[I] really enjoyed the commentary on top of the video to explain the different views, but I think the video should give the viewer more time to adjust to the different views and work out the anatomy before explaining the reason for the view.

In addition, some comments were made to express a desire to have a 3D model alongside the video:

I also feel like having a 3D model in front of me while watching the video would help orientate myself and create a better understanding of the anatomy and how they correlate to the image seen on the echo screen.

## DISCUSSION

We have shown that 3D printed cardiac models that are recognizable to undergraduate veterinary students can be easily produced from a canine CT data set. Data from our study suggest that using 3D printed models alongside more traditional learning resources may be helpful for a subgroup of students to study cardiac anatomy in a clinical context, and users of the models strongly believed that they should be used in teaching more often.

In this trial, the 3D models seemed to improve test scores in students not undertaking the cardiology track rotation. For students on the track rotation, no difference in test scores was identified. In contrast, test scores improved for track students in the VO group but not for non-track students. Feedback overall was positive for both video and models, which students found enjoyable and useful for improving their knowledge and confidence. Students in the 3DM group felt more strongly that anatomy teaching should utilize more 3D models. Interestingly, the VO group’s dropout rate was high, and a lower proportion of students left free-text feedback comments, which may suggest that students in the 3DM group were more engaged in the process than those in VO.

Lim et al. reported that undergraduate test scores increased after the use of 3D printed models as an adjunct teaching aid,<sup>6</sup> and Su et al. reported improved structural conceptualization in students taught using a set of 3D models.<sup>7</sup> Our data show that some students score higher on a test after using 3D heart models, but this benefit was not consistent across our small group of participants. Students on the track rotation—an electively chosen week of further cardiology study, during which students receive echocardiographic anatomy teaching around cases seen every day—did not seem to gain the same benefit from using 3D models as students not choosing to undertake the cardiology track rotation (non-track students). In fact, the test scores of two track students using 3D models decreased by 25% or more after using the learning materials. It is possible that the track students were more confident visualizing echocardiographic anatomy in two dimensions, as this method was familiar to them, and the 3D models provided another level of complexity and thereby potential confusion. This is supported by the observation that the test scores of track students in the VO group significantly improved, where having to rethink anatomy in three dimensions was not required. Non-track students’ test scores seemed to improve after using 3D printed models, perhaps because they did not begin the session with a strong cognitive map of how they visualized echocardiographic anatomy. If this were the case, it argues for the introduction of anatomy teaching using 3D printed models early in the veterinary undergraduate curriculum.

Another aspect of this finding is that using 3D printed models may help foster inclusive learning by allowing students with less background knowledge or less confidence in a particular topic to engage with a subject in a different manner because of the novelty of the models compared with standard imaging-based teaching material and the authenticity of the models—they are from a real dog, not a theoretical ideal. Using novel devices and technology can help to trigger situational interest, the first step on the four-phase model of interest,<sup>16</sup> which in turn can bring students into a subject and facilitate engagement with the topic, seeking meaning and leading to better outcomes.<sup>17</sup> However, an interest-based study is often perceived as more time-consuming by students,<sup>17</sup> which may account for our observation that several students felt short on time to use the learning resources, despite no time limit being set.

Despite these differences between the track and non-track students, the student feedback for using 3D printed models was broadly positive, in concordance with reports from similar studies in medical<sup>5-7,10</sup> and veterinary students.<sup>11-14</sup> Although most students in both groups agreed that 3D printed models should be used more in anatomy teaching, those who had actually used the 3D printed heart models showed a stronger agreement. This suggests that students believed the models to be useful when they had not used them, and this belief was affirmed by their use for most students. Also, students in the 3DM group showed evidence of being more engaged in the process of the study, with no students failing to complete any study tasks (compared with five students in the VO group) and a higher proportion of 3DM students completing free-text feedback. Engagement, defined as the “time and effort students dedicate to educationally purposeful activities,”<sup>18 (p.1)</sup> is vital in the development of deeper learning.<sup>19</sup> Although multifactorial, immediate feelings such as enjoyment and interest can stimulate students to become engaged,<sup>20</sup> which may be the basis of our observation in this study. Also, the authentic nature of 3D printed anatomy<sup>1</sup> provides an engaging learning environment for students,<sup>21</sup> which may also explain our finding. Student engagement is a consideration for higher education quality assurance programs,<sup>22,23</sup> so using learning technology such as 3D printed models may impact the wider university beyond students on the veterinary course.

This study is subject to several limitations. First, the population of students is relatively small. Since less than 30% of the final year accepted the invitation to take part in the study, it may not be a representative sample. It is possible that for these final-year students, where demands on their time are high, only a small proportion had intrinsic motivation to learn more about cardiac anatomy by volunteering to take part in a study. As we know, many students are extrinsically motivated to learn, with a focus on exam success and learning core material, rather than developing knowledge “for its own sake.”<sup>24</sup> In future, more could be done to raise awareness of a study like this within the student body, such as incentives (e.g., an entry in a prize draw) to help motivate people to participate or liaising with student-led relevant societies (e.g., <https://www.m3dicube.co.uk>). Also, the inclusion of 3D models as part of a core curriculum tutorial would probably motivate more students to participate, as they might perceive the use of models as “more important” to their learning rather than a distraction. Additionally, only students from a single institution were included in the present study, while a multicenter study would broaden inclusion and increase relevance to the wider veterinary student body. The self-selection of students into track rotation groups adds a possible confounding

factor—although these data raise some interesting points about inclusive learning opportunities.

It is possible that the present study investigated the utility of 3D printed models to help learn cardiac anatomy too late in the veterinary course. At our center, students first are taught cardiac anatomy in the early months of the degree course. This may be a better point to study the effect of 3D printed models on academic scores and student confidence. At that time, students are less likely to have preconceived ideas of cardiac anatomy and may correct errors in factual learning more easily as a result. Also, at that point, the level of knowledge among the student body may be more uniform. Their own preferences of career path (influencing their track rotation choices) may be less robust, thus removing a confounding factor in evaluating the overall effect of using 3D printed models.

An obvious way to improve our models would be to increase the authenticity by not printing in a single color (white) but printing a composite of a more realistic color (red/pink material) or using colors to help label anatomic structures (e.g., right side of the heart blue, left side of the heart red). We may also be able to add notation to the computer model, so that text labels would be printed on the physical models to aid students in identifying important structures. A set of virtual models could also be tested or provided as well as the physical 3D models, whereby the STL files can be displayed in the form of user-friendly 3D PDF files that students could navigate, rotate, and label.

Despite these drawbacks, our systematic approach to assessing the utility of 3D printed heart models in helping students approach learning the complexities of echocardiographic anatomy is a starting point for larger-scale projects evaluating the use of this technology for veterinary student education. Our hypothesis that using 3D printed models would positively impact test scores and student feedback is supported by these data, but only in particular groups or aspects of feedback. This area merits further study, and a larger study evaluating the use of 3D cardiac models at the time of initial teaching in cardiac anatomy would be a logical next step. A crossover study design may be useful, whereby students are randomized to take part in both study groups sequentially and are tested after each. If this could be standardized in a multicenter study or undertaken over several sequential year groups, the population size is more likely to be representative than the current data set.

## CONCLUSIONS

The creation of 3D printed canine cardiac models was feasible using a clinic-derived CT data set. Using 3D printed heart models may benefit veterinary students learning echocardiographic anatomy by engaging them in the learning process and offering a learning technology that fosters inclusive learning.

## ACKNOWLEDGMENT

Authors Andrew I.U. Shearn and Giovanni Biglino gratefully acknowledge the generous support of the Grand Appeal (The Bristol Children’s Hospital Charity).

## NOTES

- a Siemens Somatom eMotion 16-slice scanner, Siemens Healthcare Ltd., Camberley, UK
- b Materialise NV, Leuven, Belgium, <https://www.materialise.com/en>
- c Formlabs, Somerville, MA, USA
- d Microsoft Forms, Microsoft Inc., Redmond, WA, USA

## REFERENCES

- 1 Silén C, Wirell S, Kvist J, Nylander E, Smedby O. Advanced 3D visualization in student-centred medical education. *Med Teach*. 2008;30(5):e115–24. <https://doi.org/10.1080/01421590801932228>. [Medline:18576181](https://pubmed.ncbi.nlm.nih.gov/18576181/)
- 2 Smerling J, Marboe CC, Lefkowitz JH, et al. Utility of 3D printed cardiac models for medical student education in congenital heart disease: across a spectrum of disease severity. *Pediatr Cardiol*. 2019;40(6):1258–65. <https://doi.org/10.1007/s00246-019-02146-8>. [Medline:31240370](https://pubmed.ncbi.nlm.nih.gov/31240370/)
- 3 Valverde I, Gomez-Ciriza G, Hussain T, et al. Three-dimensional printed models for surgical planning of complex congenital heart defects: an international multicentre study. *Eur J Cardiothorac Surg*. 2017;52(6):1139–48. <https://doi.org/10.1093/ejcts/ezx208>. [Medline:28977423](https://pubmed.ncbi.nlm.nih.gov/28977423/)
- 4 Lau IWW, Sun Z. Dimensional accuracy and clinical value of 3D printed models in congenital heart disease: a systematic review and meta-analysis. *J Clin Med*. 2019;8(9):1483. <https://doi.org/10.3390/jcm8091483>. [Medline:31540421](https://pubmed.ncbi.nlm.nih.gov/31540421/)
- 5 Smith CF, Tollemache N, Covill D, Johnston M. Take away body parts! An investigation into the use of 3D-printed anatomical models in undergraduate anatomy education. *Anat Sci Educ*. 2018;11(1):44–53. <https://doi.org/10.1002/ase.1718>. [Medline:28753247](https://pubmed.ncbi.nlm.nih.gov/28753247/)
- 6 Lim KH, Loo ZY, Goldie SJ, Adams JW, McMenamin PG. Use of 3D printed models in medical education: A randomized control trial comparing 3D prints versus cadaveric materials for learning external cardiac anatomy. *Anat Sci Educ*. 2016;9(3):213–21. <https://doi.org/10.1002/ase.1573>. [Medline:26468636](https://pubmed.ncbi.nlm.nih.gov/26468636/)
- 7 Su W, Xiao Y, He S, Huang P, Deng X. Three-dimensional printing models in congenital heart disease education for medical students: a controlled comparative study. *BMC Med Educ*. 2018;18(1):178. <https://doi.org/10.1186/s12909-018-1293-0>. [Medline:30068323](https://pubmed.ncbi.nlm.nih.gov/30068323/)
- 8 Biglino G, Capelli C, Wray J, et al. 3D-manufactured patient-specific models of congenital heart defects for communication in clinical practice: feasibility and acceptability. *BMJ Open*. 2015;5(4):e007165. <https://doi.org/10.1136/bmjopen-2014-007165>. [Medline:25933810](https://pubmed.ncbi.nlm.nih.gov/25933810/)
- 9 Wang Z, Liu Y, Luo H, Gao C, Zhang J, Dai Y. Is a three-dimensional printing model better than a traditional cardiac model for medical education? A pilot randomized controlled study. *Acta Cardiol Sin*. 2017;33(6):664–9. <https://doi.org/10.6515/ACS20170621A>. [Medline:29167621](https://pubmed.ncbi.nlm.nih.gov/29167621/)
- 10 Keedy AW, Durack JC, Sandhu P, Chen EM, O'Sullivan PS, Breiman RS. Comparison of traditional methods with 3D computer models in the instruction of hepatobiliary anatomy. *Anat Sci Educ*. 2011;4(2):84–91. <https://doi.org/10.1002/ase.212>. [Medline:21412990](https://pubmed.ncbi.nlm.nih.gov/21412990/)
- 11 Preece D, Williams SB, Lam R, Weller R. "Let's get physical": advantages of a physical model over 3D computer models and textbooks in learning imaging anatomy. *Anat Sci Educ*. 2013;6(4):216–24. <https://doi.org/10.1002/ase.1345>. [Medline:23349117](https://pubmed.ncbi.nlm.nih.gov/23349117/)
- 12 Sunol A, Aige V, Morales C, Lopez-Beltran M, Feliu-Pascual AL, Puig J. Use of three-dimensional printing models for veterinary medical education: impact on learning how to identify canine vertebral tracts. *J Vet Med Educ*. 2019;46(4):523–32. <https://doi.org/10.3138/jvme.0817-109r>. [Medline:30418815](https://pubmed.ncbi.nlm.nih.gov/30418815/)
- 13 Li F, Liu C, Song X, Huan Y, Gao S, Jiang Z. Production of accurate skeletal models of domestic animals using three-dimensional scanning and printing technology. *Anat Sci Educ*. 2018;11(1):73–80. <https://doi.org/10.1002/ase.1725>. [Medline:28914982](https://pubmed.ncbi.nlm.nih.gov/28914982/)
- 14 Schoenfeld-Tacher RM, Horn TJ, Scheviak TA, Royal KD, Hudson LC. Evaluation of 3D additively manufactured canine brain models for teaching veterinary neuroanatomy. *J Vet Med Educ*. 2017;44(4):612–9. <https://doi.org/10.3138/jvme.0416-080R>. [Medline:28534721](https://pubmed.ncbi.nlm.nih.gov/28534721/)
- 15 Schievano S, Migliavacca F, Coats L, et al. Percutaneous pulmonary valve implantation based on rapid prototyping of right ventricular outflow tract and pulmonary trunk from MR data. *Radiology*. 2017;242(2):490–7. <https://doi.org/10.1148/radiol.2422051994>
- 16 Hidi S, Renninger KA. The four-phase model of interest development. *Educ Psychol*. 2006;41(2):111–27. [https://doi.org/10.1207/s15326985ep4102\\_4](https://doi.org/10.1207/s15326985ep4102_4)
- 17 Renninger KA, Hidi SE. Interest development and learning. In: Renninger KA, Hidi SE, editors. *The Cambridge handbook of motivation and learning*. Cambridge Handbooks in Psychology. Cambridge, UK: Cambridge University Press; 2019. p. 265–90.
- 18 Australasian Council for Educational Research (ACER). *Doing more for learning: enhancing engagement and outcomes*. Australasian Student Engagement Report. Camberwell, AU: ACER; 2010.
- 19 Cake MA. Deep dissection: motivating students beyond rote learning in veterinary anatomy. *J Vet Med Educ*. 2006;33(2):266–71. <https://doi.org/10.3138/jvme.33.2.266>. [Medline:16849308](https://pubmed.ncbi.nlm.nih.gov/16849308/)
- 20 Furlong MJ, Whipple AD, St Jean G, Simental J, Soliz A, Punthuna S. Multiple contexts of school engagement: moving towards a unifying framework for educational research and practice. *Calif School Psychol*. 2003;8:99–113. <https://doi.org/10.1007/BF03340899>
- 21 Lombardi MM. *Authentic learning for the 21st century: an overview* [Internet]. ELI paper 1: 2007. Louisville, CO: EDUCAUSE Learning Initiative; 2007 May. Available from: <https://library.educause.edu/-/media/files/library/2007/1/eli3009-pdf.pdf>
- 22 Coates H. The value of student engagement for higher education quality assurance. *Qual High Educ*. 2005;11(1):25–36. <https://doi.org/10.1080/13538320500074915>
- 23 Quality Assurance Agency for Higher Education (QAA). *UK quality code for higher education*. Chapter B5: student engagement [Internet]. Gloucester, UK: QAA; 2011 [cited 2018 May 3]. Available from: [https://www.qaa.ac.uk/docs/qaa/quality-code/chapter-b5\\_-\\_student-engagement.pdf?sfvrsn=cd01f781\\_8](https://www.qaa.ac.uk/docs/qaa/quality-code/chapter-b5_-_student-engagement.pdf?sfvrsn=cd01f781_8)
- 24 Lepper MR, Henderlong J. Turning play into work and work into play: 25 years of research on intrinsic versus extrinsic motivation. In: Sansone C, Harakiewicz JM, editors. *Intrinsic and extrinsic motivation: a volume in educational psychology*. Cambridge, MA: Academic Press; 2000. p. 257–307.

## AUTHOR INFORMATION

**Kieran Borgeat**, BSc, BVSc, MVetMed, CertVC, FHEA, MRCVS, DipACVIM, DipECVIM-CA, is Clinical Lead in Cardiology, Small Animal Hospital, Langford Vets, University of Bristol, Stock Lane, Lower Langford, North Somerset, BS40 5DU UK. Email: [k.borgeat@bristol.ac.uk](mailto:k.borgeat@bristol.ac.uk)

**Andrew I.U. Shearn**, BSc, MSc, PhD, is a Research Technician, Bristol Heart Institute, University Hospitals Bristol & Weston NHS Foundation Trust, Bristol Royal Infirmary, Upper Maudlin St., Bristol, BS2 8HW UK.

**Jessie Rose Payne**, BVetMed, MVetMed, PhD, MRCVS, DipACVIM, is a Cardiology Clinician, Langford Vets, University of Bristol, Stock Lane, Lower Langford, North Somerset, BS40 5DU UK.

**Melanie Hezzell**, MA, VetMB, PhD, CertVDI, CertVC, FHEA, MRCVS, DipACVIM, is a Senior Lecturer in Cardiology, Bristol Veterinary School, University of Bristol, Stock Lane, Lower Langford, North Somerset, BS40 5DU UK.

**Giovanni Biglino**, BEng, PhD, is a Senior Lecturer in Biostatistics and EDI Chair, Bristol Heart Institute, University Hospitals Bristol & Weston NHS Foundation Trust, Bristol Royal Infirmary, Upper Maudlin St., Bristol, BS2 8HW UK. He is also an Honorary Clinical Senior Lecturer, National Heart and Lung Institute, Imperial College London, UK.

## ORIGINAL RESEARCH

# Field application of a combined serological-molecular testing protocol for diagnosing genital leptospirosis in naturally infected cows with gestational losses

Luiza Aymée<sup>1</sup> | José Azael Zambrano<sup>2</sup> | Rafael Pérez Escalona<sup>2</sup> | Karina Palhares<sup>1</sup> | Maria Isabel Nogueira Di Azevedo<sup>1</sup>  | Walter Lilenbaum<sup>1</sup>

<sup>1</sup>Laboratory of Veterinary Bacteriology, Biomedical Institute of Fluminense Federal University, Niterói, Brazil

<sup>2</sup>Veterinary Practitioner, Goiás, Brazil

## Correspondence

Walter Lilenbaum, Laboratory of Veterinary Bacteriology, Biomedical Institute of Fluminense Federal University, Niterói, Brazil.

Email: [wlilenbaum@id.uff.br](mailto:wlilenbaum@id.uff.br)

## Funding information

Conselho Nacional de Desenvolvimento Científico e Tecnológico (CNPq); Fundação Carlos Chagas Filho de Amparo à Pesquisa do Estado do Rio de Janeiro (FAPERJ)

## Abstract

**Background:** Bovine genital leptospirosis (BGL) causes chronic reproductive disease in cattle. This study aimed to apply a combined serological-molecular testing protocol under field conditions for diagnosing BGL in cows with gestational losses.

**Methods:** Three beef herds with reproductive failures were studied, and 60 cows with gestational losses (20 from each herd) were randomly selected for laboratory diagnosis of BGL. In addition, 40 cows with normal pregnancy were included as a control. Blood samples were collected from all 100 cows for microscopic agglutination testing, and cervicovaginal mucus (CVM) samples were collected from 28 cows with gestational losses and 20 control cows for *lipL32*-PCR.

**Results:** All herds had high *Leptospira* seroreactivity (>65%), mainly against serogroup Sejroe. Ten of the 28 CVM samples from cows with gestational losses were PCR-positive, while all samples from the control group were negative ( $p < 0.05$ ).

**Limitations:** Unfortunately, the positive samples did not amplify in *secY*-PCR for nucleotide sequencing, which would allow the identification of leptospiral strains.

**Conclusion:** Serology was sufficient to indicate leptospirosis at the herd level, but the definitive diagnosis of BGL was only possible using CVM PCR. Although seroreactivity against serogroup Sejroe has been associated with gestational losses, this is the first study to conduct CVM PCR as a confirmatory test for BGL diagnosis in extensive beef herds under field conditions.

## KEYWORDS

beef cattle, genital infection, *Leptospira* spp, microscopic agglutination testing, PCR

## INTRODUCTION

Leptospirosis is a zoonotic disease that is present worldwide.<sup>1,2</sup> Cattle are one of several animal species that can be infected by *Leptospira* spp. and develop illness.<sup>3</sup> Indeed, leptospirosis is one of the most important reproductive diseases in cattle, resulting in considerable economic losses.<sup>2</sup> Although leptospirosis occurs worldwide, it is endemic in tropical countries such as Brazil.<sup>4</sup>

The clinical signs of bovine leptospirosis include abortions, embryonic death (ED), estrus repetition, stillbirth or the birth of weak calves.<sup>3,5</sup> These manifestations are frequently associated with genital infection by leptospires, which was recently characterised as a particular chronic and silent syndrome named bovine

genital leptospirosis (BGL).<sup>5</sup> Gestational losses in the first trimester of gestation have been reported as one of the more frequent signs of chronic bovine leptospirosis.<sup>3,6</sup> It has been hypothesised that the presence of leptospires in the genital tract causes ED, leading to estrus repetition.<sup>5,7</sup> Nevertheless, the studies that associated gestational losses in the first trimester of gestation with leptospirosis were all conducted in small dairy herds using intensive production systems.

Regarding the diagnosis of BGL, Loureiro and Lilenbaum<sup>5</sup> recently recommended a two-step protocol based on serological screening of the herds followed by an individual diagnosis of the animals based on PCR of a genital sample, preferentially uterine fragments or cervicovaginal mucus (CVM).

Although Oliveira et al.<sup>7</sup> reinforced the association of gestational losses in the first trimester of gestation with leptospirosis, they only performed the serological screening of the herds, which does not confirm genital colonisation. The microscopic agglutination test (MAT) is an indirect method that is reliable at the herd level,<sup>8</sup> while CVM PCR has been used in studies involving slaughtered sheep<sup>9</sup> and in the individual diagnosis of cows.<sup>10,11</sup> Until now, only one study used the approach of herd serology combined with individual PCR of cows with reproductive disorders<sup>11</sup>; however, the genital sample used was vaginal fluid and not CVM, which may not be free of urine contamination of the sample. Thus, the two-step BGL diagnosis approach of herd serological screening (MAT) followed by confirmatory individual CVM PCR has never been performed in cows under field conditions. Therefore, the present study aimed to apply a combined serological-molecular protocol under field conditions for diagnosing BGL in cows with gestational losses.

## MATERIALS AND METHODS

Samples were collected as part of the sanitary programme of the herds for routine diagnosis of leptospirosis. They were sent to the Laboratory of Veterinary Bacteriology of Federal Fluminense University, Brazil. Field procedures were performed by the veterinary practitioners responsible for the sanitary section of the studied herds. The study followed the REFLECT statement checklist.

### Herds

Three herds were included in this study, selected due to their history of reproductive problems and the reliability of their registers. They were herein named A, B and C. Herd A had 1086 Nellore cows, herd B had 1144 Nellore cows and herd C had 755 embryo recipient cows from different breeds, totalling 2985 cows. All herds have extensive beef cattle breeding and were located in the same region of Southern Goiás State in the central region of Brazil. The last vaccination against leptospirosis was performed over a year before the sampling. At that moment, cows from herds A and B were vaccinated with a polyvalent commercial vaccine including strains of *Leptospira* serogroups Canicola, Grippothyphosa, Hardjo, Icterohaemorrhagiae and Pomona (Leptoferm, Zoetis). Animals from herd C were vaccinated against all leptospiral serogroups and also infectious bovine rhinotracheitis, bovine viral diarrhoea virus, bovine parainfluenza-3 and bovine respiratory syncytial virus (CattleMaster Gold, Zoetis).

### Cows

All 2230 cows from farms A and B were submitted to fixed time artificial insemination (FTAI), while the

755 animals from farm C were submitted to embryo transfer (ET). Cows were pregnancy checked 30 days after FTAI or ET by the detection of embryonic vesicles through transrectal ultrasonography, always by the same experienced practitioner. A total of 2681 (89.8%) presented as pregnant after three attempts of FTAI or ET. One month after the first pregnancy diagnosis, the animals were re-examined by ultrasonography. Then, 137 (5.1%) cows that were confirmed as pregnant in the first examination (30 days after FTAI or ET) but not at the second point (60 days after FTAI or ET) were diagnosed with a gestational loss after 30 days, suggesting ED.

### Sampling

From the 137 cows with gestational loss, 60 cows (20 from each herd) were randomly selected for laboratory diagnosis of BGL. In addition, another 40 cows with normal pregnancies (20 from herd A and 20 from herd B) were included as controls. The 40 cows selected from herd A had an average age of 2–3 years, the 40 cows from herd B had an average age of 4–8 years and the 20 cows from herd C had an average age of 2–5 years.

Blood samples were collected from all 100 cows for serology (MAT), while CVM samples were collected from 28 cows with gestational loss and 20 from the control group for *lipL32*-PCR. Since extensively bred beef cattle are aggressive, cows were selected for CVM sampling due to their docility, allowing adequate sample collection. CVM was collected using cytology brushes (Kolplast) in a cytological device (Botupharma), as previously recommended.<sup>5</sup> All collected samples were immediately refrigerated and transported to the Universidade Federal Fluminense in Rio de Janeiro. The samples were then processed and submitted for serology and molecular analysis.

### Serology

Serum samples were tested for antibodies against leptospirosis by MAT using an antigen panel composed of 11 reference strains: *Leptospira interrogans* serovars Copenhageni (strain M20), Hardjoprajitno (strain OMS), Pomona (strain Pomona), Icterohaemorrhagiae (strain Verdun), Canicola (strain Hund Utrecht), Bratislava (strain Jez Bratislava), Australis (strain Ballico), Autumnalis (strain Akiyami A) and Grippothyphosa (strain Moskva V), and *Leptospira borgpetersenii* serovar Hardjobovis (strain Sponselee), all originating from Institut Pasteur, plus *Leptospira santarosai* serovar Guaricura (strain FV52) originating from Universidade Federal Fluminense. The strains selected for the antigen panel are known to be prevalent in cattle in Brazil<sup>8</sup> and represent seven serogroups: Australis, Autumnalis, Icterohaemorrhagiae, Canicola, Sejroe, Pomona and Grippothyphosa. The reaction titre with 50% agglutinated leptospire corresponded to the

**TABLE 1** Results of serological screening and *lipL32*-PCR of cervicovaginal mucus (CVM)

Herd	Serology		CVM <i>lipL32</i> -PCR	
	Sampling	Results	Sampling	Results
A	40 animals—20 control group, 20 gestational losses	65% seroreactive: 27.5% against Australis and 27.5% against Sejroe	8 animals (all with gestational losses)	3 positive (all with gestational losses)
B	40 animals—20 control group, 20 gestational losses	100% seroreactive: 82.5% against Sejroe	20 animals (10 of control group, 10 with gestational losses)	4 positive (all with gestational losses)
C	20 animals—all with gestational losses	65% seroreactive: 50% against Sejroe	20 animals (10 of control group, 10 with gestational losses)	3 positive (all with gestational losses)

reciprocal of the highest dilution of serum and animals were considered reactive when the titre was 200 or more, as suggested for tropical endemic areas.<sup>8</sup>

## Molecular analysis

DNA was extracted from the 48 CVM samples using a DNeasy Blood & Tissue Kit (Qiagen) according to the manufacturer's instructions. PCR was performed targeting the *lipL32* gene for *Leptospira* spp. detection using primers and conditions described in Hammond et al.<sup>12</sup> For each set of samples, ultrapure water was used as the negative control in all reactions, while 10 fg of DNA extracted from *L. interrogans* serovar Copenhageni (Fiocruz L1-130) was used as the positive control. PCR products were analysed by electrophoresis in 1.5%–2% agarose gel and visualised under ultraviolet light after gel red staining. Platinum Taq DNA Polymerase (Invitrogen) was used for the reactions.

## Statistics

The chi-squared goodness of fit test was performed to compare MAT results between the gestational loss group and control group, as well as to compare the CVM PCR results between groups.

## RESULTS

### Serology

Of the 100 tested sera, 79 (79%) were positive, distributed among herd A (26/40, 65%), herd B (40/40, 100%) and herd C (13/20, 65%) (Table 1). Although seroreactivity against serogroups Australis and Sejroe (11/40, 27.5% each) was observed in herd A, in herds B and C, the major serogroup was Sejroe, with rates of 82.5% (33/40) and 50% (10/20), respectively.

Titres of the positive animals were distributed as 200 (17 sera, 21.5%), 400 (29 sera; 36.8%), 800 (30 sera; 37.9%) and 1600 (3 sera; 3.8%). Considering the distribution by serogroups, it was observed that Sejroe was the most frequent (53 sera, 67.1%), followed by Australis (13 sera; 16.4%), Icterohaemorrhagiae (6 sera; 7.6%), Pomona (4 sera; 5.1%) and Grippotyphosa (3

sera; 3.8%). Cows with gestational loss were more frequently ( $p < 0.05$  on the chi-square goodness of fit test) seroreactive than the control group (86.7% vs. 67.5%).

## Molecular analysis

Of the 48 CVM samples, 10 (20.8%) were positive, all of which were from cows with gestational loss ( $p < 0.05$  on the chi-square goodness of fit test). Of these 10 animals, three belonged to herd A, four to herd B and three to herd C. The 20 CVM samples from cows in the control group were all PCR-negative.

## DISCUSSION

ED has been reported as the most frequent reproductive sign of bovine leptospirosis in dairy herds with semi-intensive or intensive production systems.<sup>6,7</sup> Our study represents a step forward from the previous studies<sup>7,13</sup> that suggested the association between gestational losses and leptospirosis, since they did not perform confirmatory tests (PCR) of genital samples. Although there is a difference in production systems between our study and the previous ones, all of them agree that the Sejroe serogroup is the most frequently associated with pregnancy losses in Brazilian cattle.<sup>7,13</sup> Thus, the predominance of Sejroe on MAT was not a surprising result, since strains from the Sejroe serogroup are known as the main agents of BGL, with a preference for uterine colonisation.<sup>5</sup>

BGL is a silent syndrome characterised by inapparent reproductive losses that occur in a silent chronic form.<sup>5</sup> Regarding the reproductive signs of the studied cows, ED was the main failure found in our study. ED leads to estrus repetition due to the absence of embryo implantation or embryo death.<sup>6</sup> In this study, we tested cows that were pregnant at day 30 and presented gestational loss between days 30 and 60, which suggests late ED (LED). In their recent study, Oliveira et al.<sup>7</sup> reported a high frequency of LED in Sejroe-seroreactive dairy herds. Likewise, our study demonstrated that 84.4% of the cows that presented LED were seroreactive against Sejroe. These results reinforce the suggested hypothesis<sup>5</sup> that the critical point of BGL is gestational losses in the first trimester of pregnancy and that Sejroe strains are the main agent

of LED in both beef and dairy cattle. Although gestational losses by LED have multifactorial causes, BGL has been suggested as an important cause of those failures.

It is noteworthy to highlight that the occurrence of different titres at MAT was not related to reproductive failure. It emphasises that, although adequate at a herd level, MAT is not a reliable method to predict reproductive failures when performed at an individual level.<sup>8</sup> We observed that all herds had over 65% seroreactive animals, indicating the presence of leptospirosis. Not surprisingly, the herd that presented the oldest animals had 100% seroreactive cows in the sampling, probably due to the long exposure to the agents in the field. All those animals were seroreactive to Sejroe, whose infections are characterised by a chronic course. However, some of the analysed cows presented titres as high as 800 and 1600, indicating active circulation of leptospire in the herd and recent infections. It has been reported that the bovine humoral response induced by commercial vaccines against leptospirosis remains with high titres between 2 and 6 months after vaccination.<sup>14,15</sup> Therefore, we have discarded the possibility of vaccine reactions to justify the high titres since the last vaccination occurred over a year before the sampling.

To confirm leptospiral infection and diagnose BGL at an individual level, PCR is the recommended method.<sup>5</sup> The use of CVM samples was recommended<sup>5</sup> since it represents a mirror of the uterine environment. It is a less invasive method of sampling than a uterine biopsy, is not affected by potential urine contamination and has the potential to identify animals with genital colonisation by leptospire.<sup>10</sup> However, in the present study, despite the significant difference from the control group, not all cows with pregnancy loss had positive PCR results, even when presenting high titres on the MAT (>800). As has been well as demonstrated for urine, an intermittent release of leptospire from the uterus has been hypothesised<sup>10</sup> and could justify that finding. On the other hand, it is important to highlight that 100% of the cows from the control group were negative, which indicates a high specificity of CVM PCR and its reliability as a tool for diagnosing BGL at the animal level.

To our knowledge, only one previous study combined herd serological screening and PCR of genital samples to diagnose leptospirosis in cows with a history of reproductive problems, with significant results.<sup>11</sup> Although extremely important, that study tested vaginal samples instead of CVM, and urinary contamination of the samples cannot be discarded. To truly demonstrate genital colonisation, it has been recommended that CVM samples should be collected in the vaginal fornix to avoid urine contamination.<sup>5</sup> The limited number of animals submitted to molecular diagnosis and the absence of nucleotide sequences to investigate the leptospiral species involved in those infections are certainly limitations of our study. Furthermore, since it was a field

study with three different herds, there are some variables that could not be controlled, such as possible environmental differences between the farms and reproductive management or nutritional differences between the cows, that may have influenced the results. However, although those variables may interfere with the outcomes, we believe that we could successfully apply the combined collective herd diagnostic (MAT) with the individual cow diagnostic (CVM PCR) to provide a reliable BGL diagnosis under field conditions.

## CONCLUSION

Gestational losses in the first trimester of pregnancy due to ED were confirmed as a cause of reproduction failures in beef herds with an extensive breeding system. Sejroe was the most frequently observed serogroup in all herds (>65%) and was associated with gestational losses at the herd level. At an individual level, genital infection was confirmed by CVM PCR exclusively in cows with gestational losses ( $p < 0.05$ ), reinforcing that BGL was present in all three herds, leading to gestational losses.

## AUTHOR CONTRIBUTIONS

*Conceptualisation, data curation, methodology, writing—original draft and writing—review and editing:* Luiza Aymée. *Investigation, methodology and writing—original draft:* José Azael Zambrano. *Investigation and methodology:* Rafael Pérez Escalona. *Methodology and conceptualisation:* Karina Palhares da Silva. *Conceptualisation, investigation, validation and methodology:* Maria Isabel Nogueira Di Azevedo. *Formal analysis, funding acquisition, project administration, resources, supervision, writing—original draft and writing—review and editing:* Walter Lilenbaum.

## ACKNOWLEDGEMENTS

The authors are thankful to Ana Luiza dos Santos Baptista Borges for her assistance with laboratory tests. This study was supported by Conselho Nacional de Desenvolvimento Científico e Tecnológico (CNPq) and Fundação Carlos Chagas Filho de Amparo à Pesquisa do Estado do Rio de Janeiro (FAPERJ).

## CONFLICT OF INTEREST STATEMENT

The authors declare they have no conflicts of interest.

## DATA AVAILABILITY STATEMENT


The datasets used and/or analysed during the current study are available from the corresponding author upon reasonable request.

## ETHICS STATEMENT

The ethics committee's approval was not necessary for our work since our study was performed on diagnostic samples sent to the Laboratory of Veterinary Bacteriology of Federal Fluminense University, Brazil.



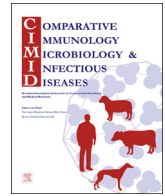
**ORCID**

Maria Isabel Nogueira Di Azevedo  <https://orcid.org/0000-0002-9882-3130>

**REFERENCES**

1. Adler B. *Leptospira* and Leptospirosis. *Vet Microbiol.* 2010;140(3–4):286–97.
2. Delooz L, Czaplicki G, Gregoire F, Dal Pozzo F, Pez F, Kodjo A, Saegerman C. Serogroups and genotypes of *Leptospira* spp. strains from bovine aborted foetuses. *Transbound Emerg Dis.* 2018;65(1):158–65.
3. Ellis WA. Animal Leptospirosis. *Curr Top Microbiol Immunol.* 2015;387:99–137.
4. Orjuela AG, Parra-Arango JL, Sarmiento-Rubiano LA. Bovine leptospirosis: effects on reproduction and an approach to research in Colombia. *Trop Anim Health Prod.* 2022;54(5):251.
5. Loureiro AP, Lilenbaum W. Genital bovine leptospirosis: a new look for an old disease. *Theriogenology.* 2020;141:41–7.
6. Alfieri AA, Leme RA, Agnol AMD, Alfieri AF. Sanitary program to reduce embryonic mortality associated with infectious diseases in cattle. *Anim Reprod.* 2019;16(3):386–93.
7. Oliveira GDM, Garcia LAN, Soares LAP, Lilenbaum W, Souza GN. Leptospirosis caused by Sejroe strains leads to embryonic death (ED) in herds with reproductive disorders. *Theriogenology.* 2021;174:121–3.
8. Pinto PS, Libonati H, Penna B, Lilenbaum W. A systematic review of the microscopic agglutination test seroepidemiology of bovine leptospirosis in Latin America. *Trop Anim Health Prod.* 2016;48(2):239–48.
9. Nogueira DB, Costa FTR, Bezerra CS, Silva MLCR, Costa DF, Viana MP, et al. Use of serological and molecular techniques for detection of *Leptospira* sp. carrier sheep under semiarid conditions and the importance of genital transmission route. *Acta Trop.* 2020;207:105497.
10. Aymée L, Di Azevedo MIN, Pedrosa JS, Melo JLS, Carvalho-Costa FA, Lilenbaum W. The role of *Leptospira santarosai* serovar Guaricura as agent of bovine genital leptospirosis. *Vet Microbiol.* 2022;268:e109413.
11. Gonçalves DD, Pastre GB, Rey LMR, Fazoli KGZ, Silva LL, Ferreira LRP, et al. *Leptospira* spp. in naturally infected dairy cow from a Brazilian border region. *Vector Borne Zoonotic Dis.* 2021;21(11):864–9.
12. Hammond C, Martins G, Loureiro AP, Pestana C, Lawson-Ferreira R, Medeiros MA, et al. Urinary PCR is an increasingly useful tool for an accurate diagnosis of leptospirosis in live-stock. *Vet Res Commun.* 2015;38(1):81–5.
13. Fávero JF, Araújo HL, Lilenbaum W, Machado G, Tonin AA, Baldissera MD, et al. Bovine leptospirosis: prevalence, associated risk factors for infection and their cause-effect relation. *Microb Pathog.* 2017;107:149–54.
14. Arduino GGC, Giro RJS, Magajevski FS, Pereira GT. Agglutinating antibody titers induced by commercial vaccines against bovine leptospirosis. *Pes Vet Bra.* 2009;29(7):575–82.
15. Balakrishnan G, Roy P. Comparison of efficacy of two experimental bovine *Leptospira* vaccines under laboratory and field. *Vet Immunol Immunopathol.* 2014;159(1–2):11–5.

**How to cite this article:** Aymée L, Zambrano JA, Escalona RP, Palhares K, Di Azevedo MIN, Lilenbaum W. Field application of a combined serological-molecular testing protocol for diagnosing genital leptospirosis in naturally infected cows with gestational losses. *Vet Rec.* 2023;e3309. <https://doi.org/10.1002/vetr.3309>



## Asymptomatic leptospiral infection is associated with canine chronic kidney disease

R. Sant'Anna<sup>a</sup>, A.S. Vieira<sup>a</sup>, J. Oliveira<sup>b</sup>, W. Lilenbaum<sup>a,\*</sup>

<sup>a</sup> Department of Microbiology and Parasitology, Biomedical Institute of the Fluminense Federal University, Brazil

<sup>b</sup> Department of Pathology and Clinics, Fluminense Federal University, Brazil

### ARTICLE INFO

#### Keywords:

Canine  
Renal function  
CKD  
Leptospirosis

### ABSTRACT

Canine leptospirosis is characterized by an acute or chronic disease. Some dogs may act as asymptomatic carriers, keeping the agent in the renal tubules and eliminating it in the urine for an extended period. Chronic kidney disease (CKD) is multifactorial and pathophysiology has been widely discussed. The aim of the study was to investigate whether the occurrence of CKD may possibly be associated with asymptomatic leptospiral infection in dogs in endemic regions. Serology and urine PCR were performed in 16 dogs with CKD and 48 healthy dogs from an endemic area. Dogs with CKD were more frequently shedders (75%) than non-CKD animals (20.8%). Therefore, our results demonstrate that asymptomatic leptospiral infection is associated with canine chronic kidney disease and that differential diagnosis is important for dogs from endemic areas presenting CKD. The early detection of shedders, besides the obvious impact on Public health may also help to improve the animal health and avoid the development of CKD.

### 1. Introduction

Leptospirosis is a worldwide infection caused by pathogenic spirchetes of the genus *Leptospira*. It affects domestic animals as well as wildlife and is also a major zoonosis [1]. The transmission of leptospirosis occurs mainly by exposure to water or soil contaminated with urine from animal carriers [2].

Canine leptospirosis is a disease characterized by an icteric severe form causing damage to the liver, renal involvement leading to acute renal failure and severe pulmonary form, which can lead to acute respiratory failure and death; and by an anicteric form with sudden onset and milder symptoms [3]. Despite the previous occurrence of the acute course of infection, some dogs may act as asymptomatic carriers, maintaining the agent in their renal tubules and eliminating it in the urine for a prolonged period [4,5]. It has recently been demonstrated that in endemic regions up to 20% of asymptomatic dogs may shed leptospires in urine [6].

Acute leptospirosis is usually diagnosed by serology (Microscopic Agglutination Test - MAT) and is based on the increase in titers of two paired samples [7]. The most frequent serovars in canine populations are Icterohaemorrhagiae and Canicola [8]. In contrast, asymptomatic animals present low titres, and other diagnostic methods, such as PCR, are necessary to detect carriers through detection of leptospiral DNA in

the urine [2,9,10].

The chronic kidney disease (CKD) refers to a pathological process involving functional and / or structural damage of renal tissue, with loss of function, usually lasting more than three months [11,12]. CKD is known to be multifactorial and primary diseases (as infectious agents), age, race and genetic load may be related to this affection [11,13]. Among the affections of the urinary system, CKD is the most common in dogs [14] and has high and increasing worldwide prevalence [15].

Although to date there are scarce studies associating asymptomatic leptospiral infection with CKD in dogs, recent research has suggested that in human being asymptomatic renal colonization by leptospires is a neglected risk for renal fibrosis and CKD, especially in endemic areas [10].

Considering these aspects, the objective of this study was to investigate the hypothesis that the occurrence of CKD might be associated with asymptomatic leptospiral infection in dogs in endemic regions (Table 1).

### 2. Material and methods

This study was approved by the Animal Use Ethics Committee of the Federal Fluminense University under number 709/2015.

\* Corresponding author at: Departamento de Microbiologia e Parasitologia, Instituto Biomédico, Universidade Federal Fluminense, Rua Professor Hernani Melo, 101 - São Domingos, Niterói, RJ, CEP: 24210-130, Brazil.

E-mail address: [wlilenbaum@id.uff.br](mailto:wlilenbaum@id.uff.br) (W. Lilenbaum).

<https://doi.org/10.1016/j.cimid.2018.11.009>

Received 22 November 2017; Received in revised form 4 April 2018; Accepted 20 November 2018

0147-9571/© 2018 Elsevier Ltd. All rights reserved.

**Table 1**  
Serology and urine PCR of dogs with (A) and without (B) Chronic Kidney Disease from high-prevalence region.

Test\Group	Group A	Group B
Serology (MAT)	12/16 (75%) <sup>a</sup>	12/48 (25%) <sup>b</sup>
Urine PCR	12/16 (75%) <sup>c</sup>	10/48 (20.8%) <sup>d</sup>

\*Different letters indicate significantly different results, according to Fisher's exact test.

### 2.1. Animals and study groups

A total of 64 dogs were studied, divided into two groups, A and B. Group A refers to adult (age 6–16 years) dogs with a confirmed diagnosis of CKD. Group B is a control group of clinically healthy dogs. First, dogs with CKD were identified based on abdominal ultrasonography, hematological (CBC) and biochemical tests. Briefly, alanine aminotransferase (ALT), aspartate aminotransferase (AST), alkaline phosphatase (AP), as well as serum levels of urea (U), creatinine (C), phosphorus (P); calcium (Ca), albumin (A) and total proteins (TP) were performed. Urine samples were tested for Glutamyl Transpeptidase (GGT) and urinalysis. All samples were analyzed in the laboratory within four hours of collection. Then, for each dog defined as CKD (Group A), three healthy dogs of the same age, gender and neighborhood were studied (Group B) and submitted to the same tests of Group A.

The study was conducted on a region known to present high prevalence for leptospirosis (São Gonçalo - RJ, Brazil). Main inclusion criteria for Group A followed the recommendations of the International Renal Interest Society [11], i.e., for CKD it was required  $U \geq 60$  mg l/dL,  $C \geq 1.4$  mg/dL, Urine density  $\leq 1025$  and presence of changes in the medullary cortical relationship and uni or bilateral renal architecture for imaging by abdominal ultrasonography. For dogs of control group (B), the same tests were conducted and dogs with any altered exam were excluded from the study. Population sampling analysis was not performed, since determining the prevalence of CKD or leptospiral infection on the studied regions was not one of the objectives of the study.

For all groups, the exclusion criteria included the recent use (< 30 days) of antimicrobials and the systematic use of angiotensin converting enzyme inhibitors, since this short-term medication causes a decrease in glomerular filtration and consequently an increase in azotemia, which may mask the DRC. Besides, it was excluded dogs immunized against leptospirosis for less than one year, with unknown vaccine history and all dogs that presented seropositive in the screening exams.

### 2.2. Sampling

Blood and urine samples were collected from all dogs. For blood counts, biochemistry and serology, 5 mL of blood were collected in a single tube and with anticoagulant EDTA (Vacutainer, BD, SP, São Paulo, Brazil), by jugular vein puncture. Blood samples were centrifuged at 3500 rpm for 10 min and the serum was separated in 100  $\mu$ L aliquots each into microtubes (1.5 mL). Serum samples were conditioned at -20 °C until processing, while whole blood samples were sent immediately after collection to perform the blood count. Urine samples were collected by ultrasound-guided cystocentesis. An amount of 10 mL of urine was collected and a 1 mL aliquot was transferred to microtubes containing 100  $\mu$ L of 10x PBS. Urine samples were also conditioned at -20 °C until processing.

From all animals, blood and urine samples were collected at the same day of the ultrasonography, and then once a month, performing the same tests in all the collections. Overall, three samplings for a minimum period of three months were conducted.

### 2.3. Serology

For the detection of anti-*Leptospira* antibodies, microscopic agglutination test (MAT) was conducted according to international recommendations [7] using a panel including eight serovars representing seven serogroups. The antigens used were *Leptospira interrogans* serovars Autumnalis (Akiyami A), Bratislava (Jez-Bratislava), Bataviae (Van Tienen), Canicola (Hond Utrecht IV), Grippotyphosa (Moska V), Icterohaemorrhagiae (RGA), Copenhageni (M 20) and Pomona (Pomona). The reaction titer with 50% of agglutinated leptospire corresponded to the reciprocal of the highest dilution of serum. Since it is an endemic region, titres of 50 a 200 was considered as exposure and > 200 as active infection [16]. Serology was paired with a monthly serological examination for three months of each animal.

### 2.4. Molecular analysis

PCR was performed as described [17]. Briefly, DNA of the urine samples was extracted using the Promega Wizard SV Genomic DNA Purification System (Promega, Madison, USA). (LipL32\_45F-5'AAG CAT TAC TTG CGC TGG TG 3'and LipL32\_286R-5'TTT CAG CCA GAA CTC CGA TT 3'), which generated a fragment of 242 bp. The total volume of each sample was analyzed by agarose gel electrophoresis (1.5%), stained with Redgel solution 3% (Biotium, Hayward, USA) and the bands (240 bp) of DNA were visualized under ultraviolet light. As positive control, a strain of *Leptospira interrogans* serovar Copenhageni strain Fiocruz L1-130 was used, and ultrapure water was used as negative control.

To confirm the identity of the amplicons, PCR products from five samples were randomly selected and submitted to nucleotide sequencing of gene *lipL32* in order to confirm the diagnosis of *Leptospira*. Amplicons were purified with GFX PCR DNA Gel Band Purification Kit (GE HealthCare). The sequencing reaction was performed using the Big Dye Terminator v3.1 kit (Applied Biosystems) and capillary electrophoresis was performed in both directions on an ABI 3730 automatic sequencer (Applied Biosystems). The sequences were edited using the BioEdit v.7.0.4 programs [18] and MEGA v.6 [19].

### 2.5. Statistical analysis

Positivity at PCR and exposition identified by serology (titres of 50–200) were defined as the dependent variables. Thus, Fisher's exact test was used to investigate the association between these variables and dogs with CKD. A confidence interval of 95% ( $p < 0.05$ ) was used in all analyzes.

## 3. Results

### 3.1. Serology

In group A, all dogs presented exposure, defined by low titres of 50 (4/16, 25%) or 100 (12/16, 75%). On Group B, 25% were exposed (12/48) and presented titers of 100. For both groups, the observed reactions were directed against serogroups Icterohaemorrhagiae (58.4%) and Canicola (41.6%).

### 3.2. Molecular analysis (PCR and sequencing)

Regarding urine PCR, in Group A 12/16 animals (75%) were positive, while on Group B, 10/48 animals (20.8%) presented positive, a significant difference ( $p = 0.0002$ , RR 3.3). Regarding sequencing of amplicons, all the five amplicons that were sequenced were confirmed as *Leptospira* sp.

### 3.3. Hematologic and biochemical results

All animals in Group A presented their altered hematology tests with results above the reference values proposed in all three samples during three months of medical follow-up confirming the diagnosis of chronic kidney disease. Results of Group A ranged from: CBC 11.4–36.5%, Urea 78–598.4 mg/l/dL, Creatinin 2–10.8 mg/dL and Urine density 1005–1020 (Supplementary material Table 1).

### 3.4. Abdominal ultrasonography

All three ultrasound examinations performed during the three months of follow-up showed both the cortex and the medulla hyper-echoic, heterogeneous and poorly delimited images altering the medullary cortical relationship. Kidneys with altered renal architecture, of diminished size and irregular contour. All these changes characterize chronic nephropathy.

## 4. Discussion

The seroprevalence observed in this study agrees with previous studies in which it is shown that the studied region presents high prevalence of leptospirosis [6]. Similarly, the distribution by serogroups agrees not only to the studied region, but throughout the country [8]. It is noteworthy that the serogroup Icterohaemorrhagiae is composed not only by serovar Icterohaemorrhagiae, but also by serovar Copenhageni. This serovar, particularly the strain FIOCRUZ L1-130, is known as the more prevalent strain in human leptospirosis [20] as well as in dogs [21]. In addition, the Canicola is a serovar cited as one of the most commonly found in dogs [4], being the dog its main natural reservoir [22].

Seroreactivity of dogs affected by CKD in regions of high prevalence was significantly higher than that of dogs of the same age, sex and neighborhood, but without CKD. In addition, most dogs with CKD presented low titers (100), suggesting only exposure [23,16] but no clinical active infection.

The most important outcome of the study regards to the differences on urine PCR positivity on the groups and the association of PCR positivity with CKD. Dogs with CKD were significantly more frequently infected (as detected by urine PCR) than dogs without CKD. In fact, dogs with CKD are three times more likely to be seroreactive and 3.3 times more likely to be infected by leptospires than non-CKD animals of the same area, sex, and age. Although there are scarce studies in dogs referring to the association of leptospiral infection and CKD, in humans it has recently been shown a high prevalence of CKD in areas endemic to leptospirosis [10].

It is widely known that acute leptospirosis might lead to tubulointerstitial nephritis and interstitial fibrosis [24,25], and when treated improperly or untreated in time can progress to CKD [10,26]. Besides, it is known that animals living in endemic areas can infect and maintain leptospires in the renal tubules and interstices for a long time, developing a silent asymptomatic infection by eliminating leptospires in the urine [6]. Considering the two points, the present study demonstrated that even asymptomatic shedders from endemic regions are more susceptible to develop CKD. Noteworthy that leptospiral infection is treatable with antimicrobials. Considering this, we suggest that animals from endemic regions should be investigated for renal carrier status by urine PCR. The early detection of shedders, besides the obvious impact on Public health [6] may also help to improve the animal health and avoid the development of CKD.

## 5. Conclusion

Our results demonstrate that in dogs of endemic area there is an association between leptospiral infection and CKD. Acute leptospirosis is not a pre-requisite for the development of CKD, which may also occur

due to the long-term silent leptospiral infection of these animals. The early detection of shedders, besides the obvious impact on Public health may also help to improve the animal health and avoid the development of CKD.

## Conflict of interest

None of the authors of this paper has a financial or personal relationship with other people or organisations that could inappropriately influence or bias the content of the paper.

## Acknowledgements

The authors thank the owners who allowed sampling on their dogs. They also thank Dr G. Martins (UFF) for the help with statistics and the veterinary team of “SOS Focinhos Animal Clinics” for the help during sampling. This study was supported by FAPERJ (Fundação de Amparo à Pesquisa do Estado do Rio de Janeiro). R.S. and A.V. are CAPES Fellows. W.L. is a FAPERJ and CNPQ Fellow.

## Appendix A. Supplementary data

Supplementary material related to this article can be found, in the online version, at doi:<https://doi.org/10.1016/j.cimid.2018.11.009>.

## References

- [1] B. Adler, *Leptospira* and Leptospirosis, Springer, Berlin, 2015, pp. 1–10.
- [2] D.A. Haake, P.N. Levett, Leptospirosis in humans, *Curr. Top. Microbiol. Immunol.* 387 (2015) 65–97.
- [3] W.A. Ellis, Animal leptospirosis, *Curr. Top. Microbiol. Immunol.* 387 (2015) 99–137.
- [4] M. Lelu, C. Muñoz-Zanzi, B. Higgins, R. Galloway, Seroepidemiology of leptospirosis in dogs from rural and slum communities of Los Rios Region, Chile, *BMC Vet. Res.* 11 (2015) 1–8.
- [5] S.E. Grayzel, E.E. De Bess, Characterization of leptospirosis among dogs in Oregon, 2007–2011, *J. Am. Vet. Med. Assoc.* 248 (2016) 908–915.
- [6] R. Sant'anna, A.S. Vieira, J. Grapiglia, W. Lilienbaum, High number of asymptomatic dogs as leptospiral carriers in an endemic area indicates a serious public health concern, *Epidemiol. Infect.* 145 (2017) 1852–1854.
- [7] OIE, Manual of Diagnostic Tests and Vaccines for Terrestrial Animals, pp. 1–15 World Organization for Animal Health, Paris, 2014.
- [8] P.S. Pinto, H. Libonati, W. Lilienbaum, Systematic review of leptospirosis on dogs, pigs, and horses in Latin America, *Trop. Anim. Health Prod.* 49 (2017) 231–238.
- [9] M.A. Inkelmann, G.D. Kommers, M.E. Trost, C.S.L. Barros, R.A. Figuera, L.F. Irigoyen, I.P. Silveira, Urinary system injuries in 1,063 dogs, *Braz. J. Vet. Res.* 32 (2012) 761–771.
- [10] C.W. Yang, Leptospirosis renal disease: emerging culprit of chronic kidney disease unknown etiology, *Nephron* (2018) 129–136.
- [11] IRIS International Renal Interest Society, IRIS Guidelines, (2013) (Accessed 15 December 2016), <http://www.iris-kidney.com/guidelines/>.
- [12] L.D. Cowgill, D.J. Polzin, J. Elliott, M.B. Nabity, G. Segev, G.F. Grauer, S. Brown, C. Langston, A.M. Van Dongen, Is progressive chronic kidney disease a slow acute kidney injury? *Vet. Clin. North Am. Small Anim. Pract.* 46 (2016) 995–1013.
- [13] V. Meucci, G. Luci, M. Vanni, G. Guidi, F. Perondi, L. Intorre, Serum levels of ochratoxin A in dogs with chronic kidney disease (CKD): a retrospective study, *J. Vet. Med. Sci.* 79 (2017) 440–447.
- [14] D.G. O'Neill, J. Elliott, D.B. Church, P.D. McGreevy, P.C. Thomson, D.C. Brodbelt, Chronic kidney disease in dogs in UK veterinary practices: prevalence, risk factors, and survival, *J. Vet. Intern. Med.* 27 (July–August (4)) (2013) 814–821.
- [15] H.Y. Yang, C.C. Hung, S.H. Liu, Y.G. Guo, Y.C. Chen, Y.C. Ko, C.T. Huang, L.F. Chou, Y.C. Tian, M.Y. Chang, H.H. Hsu, M.Y. Lin, S.J. Hwang, C.W. Yang, Overlooked risk for chronic kidney disease after leptospiral infection: a population-based survey and epidemiological cohort evidence, *PLoS Negl. Trop. Dis.* 10 (2015) e0004105.
- [16] G. Martins, W. Lilienbaum, The panorama of animal leptospirosis in Rio de Janeiro, Brazil, regarding the seroepidemiology of the infection in tropical regions, *BMC Vet. Res.* 9 (2013) 237.
- [17] C. Hamond, G. Martins, A.P. Loureiro, C. Pestana, R. Lawson-Ferreira, M.A. Medeiros, W. Lilienbaum, Urinary PCR as an increasingly useful tool for an accurate diagnosis of leptospirosis in livestock, *Vet. Res. Commun.* 38 (2014) 81–85.
- [18] T.A. Hall, Bio Edit: a user-friendly biological sequence alignment editor and analysis program for Windows 95/98/NT, *Nucleic Acids Symp.* 41 (1999) 95–98.
- [19] K. Tamura, G. Stecher, D. Peterson, A. Filipski, S. Kumar, MEGA 6: molecular evolutionary genetics analysis version 6.0, *Mol. Biol. Evol.* 30 (2013) 2725–2729.
- [20] K.P. Patra, B. Choudhury, M.M. Matthias, S. Baga, K. Bandyopadhyay, J.M. Vinet, Comparative analysis of lipopolysaccharides of pathogenic and intermediately

- pathogenic *Leptospira* species, BMC Microbiol. 15 (2015) 244.
- [21] E.F. Silva, C.S. Santos, D.A. Athanzio, N. Seiffert, F.K. Seixas, G.M. Cerqueira, M.Q. Fagundes, C.S. Brod, M.G. Reis, O.A. Dellagostin, A.L. Ko, Characterization of virulence of *Leptospira* isolates in a hamster model, Vaccine 26 (2008) 3892–3896.
- [22] M. Matsui, L. Roche, S. Geroult, S. Geroult, M.E. Soupé-Gilbert, D. Monchy, M. Huerre, C. Goarant, Cytokine and chemokine expression in kidneys during chronic leptospirosis in reservoir and susceptible animal models, PLoS One 11 (2016) 1–20.
- [23] H. Langoni, M.C. Ponte, D. Barbosa, M.P. Manzi, R.C. Silva, B.D. Menozzi, Research antibody and DNA *Leptospira* spp. In canine serum, Vet. Zootec. 22 (2015) 429–436.
- [24] E.M. Atasoyu, V. Turhan, S. Unver, T.R. Evrenkaya, S. Yildirim, A case of leptospirosis presenting with end-stage renal failure, Nephrol. Dial. Transplant. 20 (2005) 2290–2292.
- [25] H.Y. Yang, P.Y. Hsu, M.J. Pan, M.S. Wu, C.H. Lee, C.C. Yu, C.C. Hung, C.W. Yang, Clinical distinction and evaluation of leptospirosis in Taiwan—a case-control study, J. Nephrol. 18 (2005) 45–53.
- [26] N.J. Herath, S.A. Kularatne, K.G. Weerakoon, A. Wazil, N. Subasinghe, V.I.N. Ratnatunga, Long term outcome of acute kidney injury due to leptospirosis? A longitudinal study in Sri Lanka, BMC Res. Notes 7 (2014) 398.



## RESEARCH ARTICLE

### Computed Tomography-Based Evaluation of Skull Measurements and Eye Biometrics in Brachycephalic vs. Non-Brachycephalic Cats

Ermış Özkan<sup>1</sup>, Gülsün Pazvant<sup>1</sup>, Didar Aydın Kaya<sup>2\*</sup>, Simge Uğur<sup>2</sup>, Zeynep Nilüfer Akçasız<sup>2</sup>, Ebru Eravci Yalin<sup>2</sup>, Murat Karabağlı<sup>3</sup> and Tuğba Kurt<sup>4</sup>

<sup>1</sup>Department of Anatomy, Faculty of Veterinary Medicine, Istanbul University-Cerrahpaşa, 34320, Istanbul, Türkiye;

<sup>2</sup>Department of Surgery, Faculty of Veterinary Medicine, Istanbul University-Cerrahpaşa, 34320, Istanbul, Türkiye;

<sup>3</sup>Department of Radiology, Faculty of Veterinary Medicine, Istanbul University-Cerrahpaşa, 34320, Istanbul, Türkiye;

<sup>4</sup>Ada Veterinary Polyclinic, 34330, Istanbul, Türkiye.

\*Corresponding author: [didar@iuc.edu.tr](mailto:didar@iuc.edu.tr)

#### ARTICLE HISTORY (24-414)

Received: July 20, 2024  
Revised: August 15, 2024  
Accepted: August 19, 2024  
Published online: August 27, 2024

#### Key words:

Cranium  
Orbita  
Ocular  
Feline  
Shorthair Brachycephaly

#### ABSTRACT

Brachycephaly in cats, characterized by shortened facial and skull length and a rounder head due to inherited defects in skull bone development, can lead to respiratory and ocular problems, particularly in popular breeds like Exotic Shorthair, British Shorthair, Persian and Scottish Fold. Eye diseases in cats and dogs can result from various factors, including infectious agents, metabolic disorders, physical trauma and breed-specific congenital abnormalities, with brachycephalic cats being particularly prone to chronic corneal diseases and glaucoma due to their anatomical features. Despite challenges such as cost, the need for anesthesia and radiation exposure, understanding normal eye measurements and biometrics through imaging techniques like ultrasound, MRI and CT is essential for diagnosing eye diseases in veterinary ophthalmology. This study aimed to utilize computed Tomography (CT) images to measure intraocular structures in healthy cats with varying skull structures and establish the correlation between these measurements and skull morphometric data. In the study, a total of 24 cats from brachycephalic and 27 cats from non-brachycephalic breeds (both sexes) were included. Two-dimensional CT scans of cats were reconstructed into 3D models using the 3D Slicer 5.4.0 program, which was also used for intraocular and skull measurements. Results demonstrated that the antero-posterior distance of the lens and postorbital breadth measurements were higher, while greatest length of the skull was lower, in brachycephalic than in non-brachycephalic cats ( $p < 0.05$ ). According to the results of Discriminant Function analysis, when considering head types, it was observed that 92.6% of animals with non-brachycephalic head and 79.2% of animals with brachycephalic head types were accurately classified. These findings emphasize the importance of considering anatomical variations in brachycephalic and non-brachycephalic cats for accurate diagnosis of eye health issues in these cats.

**To Cite This Article:** Özkan E, Pazvant G, Kaya DA, Uğur S, Akçasız ZN, Yalin EE, Karabağlı M and Kurt T, 2024. Computed tomography-based evaluation of skull measurements and eye biometrics in brachycephalic vs. non-brachycephalic cats. Pak Vet J, 44(3): 910-916. <http://dx.doi.org/10.29261/pakvetj/2024.238>

#### INTRODUCTION

Brachycephaly in cats is characterized by a decrease in facial and skull length and a more rounded head (Künzel *et al.*, 2003). This head shape stems from an inherited defect in the development of skull bones (Gündemir *et al.*, 2024). In brachycephalic cats, facial and nasal bone shortening alters anatomy of the face. This condition usually results in breathing difficulties and

various eye problems in cats. Brachycephalic cat breeds are widespread globally and have become increasingly popular in recent years. Among these, the most common are Exotic Shorthair, British Shorthair, Persian breeds and Scottish Fold (Künzel *et al.*, 2003; Schlueter *et al.*, 2009; Schmidt *et al.*, 2017; Şenol *et al.*, 2022).

The eye is a crucial sensory organ for the continuation of a quality life, as well as for safety, in most animals. It consists of the eyeball and the soft tissues

responsible for its movement. However, in carnivores, the absence of the arcus orbitalis results in the eye being surrounded by various anatomical structures (Dursun, 2007).

Eye diseases in cats and dogs can be congenital or acquired, stemming from factors such as infectious agents, metabolic disorders and physical trauma. Additionally, congenital abnormalities specific to species and breeds may also occur (Gültekin *et al.*, 2022; Demir *et al.*, 2023). Congenital or acquired eye and eyelid diseases are commonly encountered in both cats and dogs (Narfström, 1999).

According to Schlueter *et al.* (2009), cats with severe or extreme brachycephaly (category III or IV) should not be used for breeding purposes, while cats with broader facial bones should be selected. Cats with brachycephalic skull shapes, which can lead to respiratory, cardiac and ophthalmological problems, may encounter these problems throughout their lives, or even experience recurrence despite treatment. Brachycephalic cats are susceptible to a range of eye diseases due to their prominent and protruding eyeballs, which can cause permanent damage to all components of the eye. Among these, corneal diseases hold significant importance in veterinary ophthalmology due to their persistent and recurrent nature (Stiles, 1995). Particularly, chronic corneal diseases are commonly observed in brachycephalic cats (Pentlarge, 1989; Nasisse *et al.*, 1998). As a result of shallow eye sockets and prominent eyeballs, decreased corneal sensitivity and ulcerative keratitis are frequently encountered in these breeds (Appelboom, 2016). Glaucoma is a condition characterized by increased intraocular pressure, which can alter eye biometrics and damage the optic nerve (Evangelho *et al.*, 2024). In cats, glaucoma is mostly associated with intraocular tumors and chronic uveitis (Blocker and Van Der Woerd, 2001; McLellan and Teixeira, 2015), and can lead to blindness as it progresses. Because the disease progresses insidiously and develops gradually, cats are often not presented for clinical evaluation until later stages of the disease.

The knowledge about normal measurements for ocular structures can assist in identifying structural abnormalities and diagnosing ocular disorders. The identification of eye diseases according to breeds can positively support treatment processes and also help inform animal owners, thereby aiding veterinarians (Ermutlu *et al.*, 2024). For these reasons, knowledge of normal eye biometrics is effective in diagnosing many eye diseases. Eye biometrics involves the detailed evaluation of anatomical measurements and features of the eye and is an essential medical and scientific method for assessing eye health and diagnosing eye problems. Some of these technologies commonly used in determining eye biometrics are the use of ultrasound, MRI (magnetic resonance imaging) and CT (computed tomography) scanning. CT and MRI can provide cross-sectional and three-dimensional images, facilitating the evaluation of spatial relationships among anatomical structures (Akbaş *et al.*, 2023; Gundemir *et al.*, 2023; Manuta *et al.*, 2023). MRI and CT have been identified as excellent imaging methods for diagnosing a range of ophthalmic diseases. CT is used to evaluate anatomical differences between

brachycephalic and non-brachycephalic cats. However, there is limited information available regarding normal eye sizes in different cat breeds and the relationship between eye size and skull measurements. Nevertheless, the most detailed measurement of eye biometrics and the diagnosis of eye diseases are possible with CT and require less scanning time than MRI. However, the cost and the need for anesthesia and exposure of animal to radiation during CT scanning present disadvantages.

In veterinary anatomical literature, the dog has predominantly been the focus as the representative of the Carnivora order, resulting in a relative neglect of feline anatomy (Abouelela *et al.*, 2022; Jashari *et al.*, 2022). Therefore, anatomical studies of cats employing advanced imaging techniques such as CT are of significant value (Yılmaz, 2021). The aim of this study was to use CT images to measure intraocular structures in healthy cats with different skull structures and to define the relationship between these measurements and skull morphometric data. Knowledge about the CT appearance of the eye and the normal intraocular dimensions in brachycephalic and non-brachycephalic cats forms the basis for evaluating CT in patients with diseases that may cause changes in the appearance and dimensions of the eye due to eye diseases.

## MATERIALS AND METHODS

**Study population:** In the study, a total of 24 cats (11 males and 13 females) from brachycephalic breeds and 27 cats (15 males and 12 females) from non-brachycephalic breeds were included. The brachycephalic group consisted of 14 British Shorthairs, 7 Scottish Folds, and one each of Exotic Shorthair, Persian and Chinchilla. The non-brachycephalic group included 22 mixed-breed cats, 2 Ankara cats, and one each of Siamese, Russian Blue and Bombay. These experimental cats used in the study were over one year in age. CT images of the head, obtained from the archive records of the Department of Radiology at Istanbul University-Cerrahpaşa Faculty of Veterinary Medicine, during the year 2023 were used in the study. Cats with eye-related complaints documented in their medical history or those with any eye-related abnormalities identified in the CT images by the veterinarian were excluded from the study. Moreover, for consistency, only left eyes were included in the study, resulting in a total of 51 eyeballs being used. As the study utilized archive data, there were no requirements for approval from an animal welfare committee.

**Intraocular and skull measurements:** The CT imaging was conducted using the Siemens SOMATOM Scope VB30 machine with the following parameters: slice thickness of 0.6mm, tube voltage of 110kV, and tube current of 28mA, with an exposure time of 14 seconds. During data processing, patients were excluded if the slice thickness exceeded 0.6mm, as this could lead to measurement calculation errors.

For brachycephalic and non-brachycephalic cats, intraocular measurements were obtained from multi-planar reformatting parasagittal images optimized for globe size. Measurements taken from 2D CT images were performed by a single veterinarian for consistency.

Intraocular measurements were separately recorded for brachycephalic and non-brachycephalic cats, as well as for males and females. These measurements were: Anterio-posterior distance of the globe, anterio-posterior distance of the anterior chamber, anterio-posterior distance of the lens, anterio-posterior distance of the vitreous chamber, latero-medial distance of the lens and globe height (Fig. 1). Three-dimensional reconstructions of the skull of the same animal were created using their head CT scans, and measurements related to the skull, including greatest length of the skull (GLS), skull width (SW), zygomatic breadth (ZB), postorbital breadth (POB) and greatest breadth of braincase (GBB), were taken from these reconstructions (Fig. 2). Intraocular measurements were made from 2D CT images, followed by 3D modeling using the 3D Slicer 5.4.0 program, and skull measurements were taken from these models.

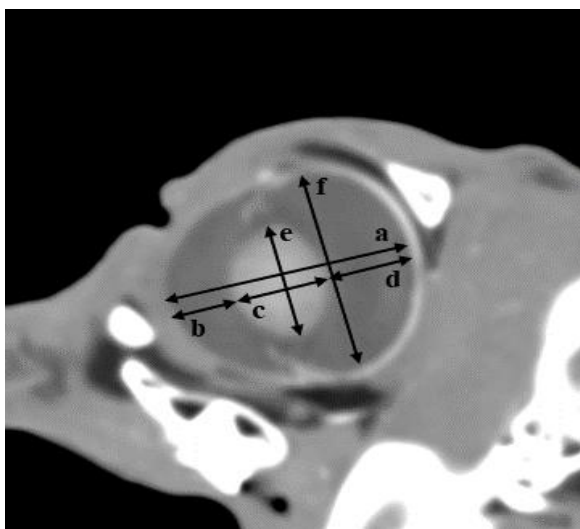


**Fig. 1:** Showing the intraocular measurements taken from the 2D CT images made from parasagittal sections. Note: a: The anterio-posterior distance of the globe, b: The anterio-posterior distance of the anterior chamber, c: The anterio-posterior distance of the lens, d: The anterio-posterior distance of the vitreous chamber, e: The latero-medial distance of the lens, f: Globe height.

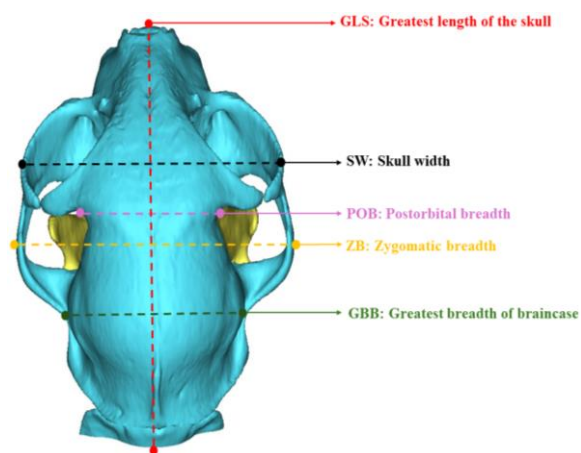


**Fig. 2:** Measurements of the skull taken via three-dimensional modeling (The distances between points of the same color were measured when calculating the length and width).

**Statistical analysis:** Statistical analyses were performed using IBM SPSS Statistics 21 after the data were saved in Excel format. Means, standard deviations, and

comparisons between groups were conducted using this program. T-tests and Discriminant Function (DF) analyses were utilized for intergroup comparisons for brachycephalic and non-brachycephalic head types and between male and females. The Pearson correlation coefficients between intra-ocular and cranial measurements were calculated utilizing the same statistical software program.

## RESULTS

In the present research, statistical evaluations were performed, taking into consideration intraocular (Fig. 1) and cranial measurements (Fig. 2), while considering the head types and sex of cats. For intraocular measurement “anterio-posterior distance of the lens”, the mean for brachycephalic cats was significantly higher ( $p < 0.05$ ) than for non-brachycephalic cats (Table 1). When examining cranial measurements, it was observed that in cats with brachycephalic skull type, the mean value for GLS was significantly lower, while the mean value for POB was higher compared to cats with non-brachycephalic skull type ( $p < 0.05$ ). The differences in mean values for other intraocular and cranial measurements were statistically non-significant (Table 1).

In the second phase of our results, all measured values were separated into female and male groups, both within each group (brachycephalic or non-brachycephalic) and across all cats regardless of head type (Table 2). Considering cranial measurements in cats with non-brachycephalic head types, the values for GLS, ZB and GBB were higher in male than those in female cats ( $p < 0.05$ ). When examining cranial measurements in brachycephalic cats, male animals showed significantly higher SW compared to females ( $p < 0.05$ ). When evaluating female and male groups for the total population regardless of skull type, statistically significant differences ( $P < 0.05$ ) were observed in the mean values between groups for intraocular measurement “anterio-posterior distance of the globe” and cranial measurements for SW, ZB and GBB, values being higher in males than in females. For all other intraocular and cranial measurements, the differences in mean values between female and male groups were statistically non-significant (Table 2).

In the present study, correlation analysis was conducted between intraocular and cranial measurements, considering skull types. In cats with brachycephalic skull types (Table 3), significant positive correlations were observed between intraocular measurement “anterio-posterior distance of the globe” and cranial measurements GLS, SW, ZB ( $p < 0.01$ ), POB and GBB ( $p < 0.05$ ). For cats with non-brachycephalic skull types (Table 4), significant positive correlations ( $p < 0.01$ ) were observed between intraocular measurement “anterio-posterior distance of the globe” and cranial measurements ZB and GBB. Additionally, in these cats, a positive correlation at the  $p < 0.01$  level was also observed between intraocular measurement “globe height” and cranial measurement GLS. Correlations of  $p < 0.05$  level were observed between various intraocular and cranial measurements in cats with both brachycephalic and non-brachycephalic skull types, as shown in Table 3 and Table 4.



Discriminant Function (DF) analyses were conducted in addition to the analyses mentioned above, based on the measurements taken. According to the results of DF analysis, when considering head types, it was observed that 92.6% of animals with non-brachycephalic head types and 79.2% of animals with brachycephalic head types were accurately classified. The analysis was conducted

using the stepwise method, and the most suitable parameters for distinguishing head types were selected. The measurements that were most discriminatory in determining the head type among the measured values were transformed into formulas using Canonical Discriminant Function Coefficients results of DF analysis. The formulated equation is given below:

**Table 1:** The mean values ( $\pm$ SD) of the intra-ocular and cranial measurements for cats of two groups.

Measurements (mm)	Brachycephalic (n=24)	Non-brachycephalic (n=27)
AP distance of the globe	20.92 $\pm$ 1.30	21.17 $\pm$ 0.95
AP distance of the anterior chamber	4.88 $\pm$ 0.66	4.77 $\pm$ 0.47
AP distance of the vitreous chamber	8.80 $\pm$ 0.87	8.98 $\pm$ 0.73
AP distance of the lens	8.00 $\pm$ 0.89*	7.50 $\pm$ 0.69*
LM distance of the lens	10.98 $\pm$ 1.15	10.99 $\pm$ 0.92
Globe height	20.60 $\pm$ 1.00	20.77 $\pm$ 0.96
Greatest length of the skull	80.68 $\pm$ 8.95*	88.60 $\pm$ 8.84*
Skull width	62.81 $\pm$ 5.89	60.33 $\pm$ 4.50
Zygomatic breadth	64.65 $\pm$ 5.97	65.60 $\pm$ 5.33
Postorbital breadth	36.29 $\pm$ 4.67*	33.03 $\pm$ 2.94*
Greatest breadth of braincase	41.58 $\pm$ 1.97	41.16 $\pm$ 1.88

\*: The difference between the mean values within the same row is statistically significant ( $P < 0.05$ ); AP=Anterio-posterior; LM= Latero-medial.

**Table 2:** The mean ( $\pm$ SD) values for intra-ocular and cranial measurements in females and males

Measurements (mm)	Head Type	Female		Male	
		N	Mean $\pm$ SD	N	Mean $\pm$ SD
AP distance of the globe	Brachycephalic	13	20.67 $\pm$ 1.40	11	21.22 $\pm$ 1.16
	Non-brachycephalic	12	20.80 $\pm$ 0.87	15	21.46 $\pm$ 0.94
	Total	25	20.73 $\pm$ 1.15*	26	21.36 $\pm$ 1.02*
AP distance of the anterior chamber	Brachycephalic	13	4.69 $\pm$ 0.67	11	5.10 $\pm$ 0.61
	Non-brachycephalic	12	4.73 $\pm$ 0.48	15	4.81 $\pm$ 0.48
	Total	25	4.71 $\pm$ 0.58	26	4.93 $\pm$ 0.55
AP distance of the lens	Brachycephalic	13	8.81 $\pm$ 0.91	11	8.79 $\pm$ 0.86
	Non-brachycephalic	12	8.85 $\pm$ 0.87	15	9.08 $\pm$ 0.61
	Total	25	8.83 $\pm$ 0.87	26	8.96 $\pm$ 0.72
AP distance of the vitreous chamber	Brachycephalic	13	7.98 $\pm$ 0.57	11	8.03 $\pm$ 1.20
	Non-brachycephalic	12	7.43 $\pm$ 0.79	15	7.56 $\pm$ 0.62
	Total	25	7.72 $\pm$ 0.72	26	7.76 $\pm$ 0.92
LM distance of the lens	Brachycephalic	13	10.84 $\pm$ 1.17	11	11.14 $\pm$ 1.17
	Non-brachycephalic	12	10.96 $\pm$ 0.84	15	11.01 $\pm$ 1.00
	Total	25	10.9 $\pm$ 1.01	26	11.06 $\pm$ 1.05
Globe height	Brachycephalic	13	20.80 $\pm$ 0.93	11	20.37 $\pm$ 1.07
	Non-brachycephalic	12	20.42 $\pm$ 0.77	15	21.06 $\pm$ 1.02
	Total	25	20.62 $\pm$ 0.86	26	20.77 $\pm$ 1.08
Greatest length of the skull	Brachycephalic	13	79.01 $\pm$ 9.97	11	82.66 $\pm$ 7.55
	Non-brachycephalic	12	86.55 $\pm$ 2.93*	15	90.24 $\pm$ 5.50*
	Total	25	82.63 $\pm$ 8.27	26	87.04 $\pm$ 7.37
Skull width	Brachycephalic	13	60.64 $\pm$ 3.96*	11	65.37 $\pm$ 6.89*
	Non-brachycephalic	12	58.82 $\pm$ 2.50	15	61.54 $\pm$ 5.40
	Total	25	59.76 $\pm$ 3.40*	26	63.16 $\pm$ 6.25*
Zygomatic breadth	Brachycephalic	13	62.62 $\pm$ 3.06	11	67.05 $\pm$ 7.69
	Non-brachycephalic	12	62.73 $\pm$ 2.54*	15	67.90 $\pm$ 5.92*
	Total	25	62.67 $\pm$ 2.76*	26	67.54 $\pm$ 6.59*
Postorbital breadth	Brachycephalic	13	34.64 $\pm$ 4.80	11	38.24 $\pm$ 3.85
	Non-brachycephalic	12	32.27 $\pm$ 3.26	15	33.64 $\pm$ 2.61
	Total	25	33.54 $\pm$ 4.23	26	35.58 $\pm$ 3.89
Greatest breadth of braincase	Brachycephalic	13	41.22 $\pm$ 2.07	11	42.01 $\pm$ 1.85
	Non-brachycephalic	12	40.22 $\pm$ 1.42*	15	41.90 $\pm$ 1.91*
	Total	25	40.74 $\pm$ 1.83*	26	41.95 $\pm$ 1.85*

AP=Anterio-posterior; LM= Latero-medial.

**Table 3:** The correlation coefficients between intra-ocular and cranial measurements in the brachycephalic head type cats.

Measurements	a	b	d	c	e	f	GLS	SW	ZB	POB	GBB
a		0.439*	0.551**	0.411*	0.538**	0.620**	0.529**	0.726**	0.634**	0.463*	0.429*
b	0.439*		0.055	-0.067	0.241	0.120	0.362	0.305	0.308	0.041	0.080
d	0.551**	0.055		0.068	0.068	0.580**	0.216	0.271	0.146	0.170	0.081
c	0.411*	-0.067	0.068		0.556**	0.268	0.071	0.419*	0.407*	0.472*	0.288
e	0.538**	0.241	0.068	0.556**		0.320	0.259	0.481*	0.402	0.508*	0.295
f	0.620**	0.120	0.580**	0.268	0.320		0.402	0.330	0.226	0.156	0.225
GLS	0.529**	0.362	0.216	0.071	0.259	0.402		0.420*	0.454*	-0.034	-0.089
SW	0.726**	0.305	0.271	0.419*	0.481*	0.330	0.420*		0.961**	0.761**	0.573**
ZB	0.634**	0.308	0.146	0.407*	0.402	0.226	0.454*	0.961**		0.676**	0.459*
POB	0.463*	0.041	0.170	0.472*	0.508*	0.156	-0.034	0.761**	0.676**		0.809**
GBB	0.429*	0.080	0.081	0.288	0.295	0.225	-0.089	0.573**	0.459*	0.809**	

\*: The correlation is statistically significant ( $P < 0.05$ ). \*\*: The correlation is statistically significant ( $P < 0.01$ ). a: The antero-posterior distance of the globe, b: The antero-posterior distance of the anterior chamber, c: The antero-posterior distance of the lens, d: The antero-posterior distance of the vitreous chamber, e: The latero-medial distance of the lens, f: Globe height, GLS: Greatest length of the skull, SW: Skull width, ZB: Zygomatic breadth, POB: Postorbital breadth, GBB: Greatest breadth of braincase.

**Table 4:** The correlation coefficients between intra-ocular and cranial measurements in the non-brachycephalic head type cats.

Measurements	a	b	d	c	e	f	GLS	SW	ZB	POB	GBB
a		0.350	0.272	0.106	0.327	0.482*	0.302	0.332	0.659**	0.359	0.551**
b	0.350		0.100	-0.094	-0.121	-0.055	0.018	0.110	0.208	0.085	0.181
d	0.272	0.100		-0.624**	-0.349	0.238	0.211	0.367	0.204	-0.018	0.339
c	0.106	-0.094	-0.624**		0.663**	-0.016	-0.139	-0.250	0.057	0.165	-0.211
e	0.327	-0.121	-0.349	0.663**		0.315	0.223	0.094	0.176	0.371	0.031
f	0.482*	-0.055	0.238	-0.016	0.315		0.507**	0.412*	0.430*	0.349	0.399*
GLS	0.302	0.018	0.211	-0.139	0.223	0.507**		0.753**	0.596**	0.457*	0.481*
SW	0.332	0.110	0.367	-0.250	0.094	0.412*	0.753**		0.502**	0.541**	0.461*
ZB	0.659**	0.208	0.204	0.057	0.176	0.430*	0.596**	0.502**		0.581**	0.633**
POB	0.359	0.085	-0.018	0.165	0.371	0.349	0.457*	0.541**	0.581**		0.297
GBB	0.551**	0.181	0.339	-0.211	0.031	0.399*	0.481*	0.461*	0.633**	0.297	

\*: The correlation is statistically significant ( $P < 0.05$ ); \*\*: The correlation is statistically significant ( $P < 0.01$ ); a: The antero-posterior distance of the globe, b: The antero-posterior distance of the anterior chamber, c: The antero-posterior distance of the lens, d: The antero-posterior distance of the vitreous chamber, e: The latero-medial distance of the lens, f: Globe height, GLS: Greatest length of the skull, SW: Skull width, ZB: Zygomatic breadth, POB: Postorbital breadth, GBB: Greatest breadth of braincase.

$$D = GLS * 0.159 - SW * 0.167 - 3.179$$

$D > 0$  for non-brachycephalic;  $D < 0$  for brachycephalic  
(centroid 0.785 for non-brachycephalic,  $-0.884$  for brachycephalic)

## DISCUSSION

Brachycephaly is characterized by a decrease in the length of the face and skull of the affected individual and the skull becomes more rounded, “dome-shaped” (Künzel *et al.*, 2003). Despite the decrease in the size of the face, there is no corresponding decrease in the size of the soft tissues of the head. Externally, the skin of the face tends to appear folded, whereas internally, the mucous membranes of the nose and respiratory passages are disproportionately large. This disproportionate structuring leads to respiratory, cardiac, and ophthalmological problems in brachycephalic breeds. Schlueter *et al.* (2009) categorized brachycephalic skull deformities in cats into 4 categories based on the severity (mild, moderate, profound and severe). The risk of diseases associated with brachycephalic skull structure may increase in parallel with the degree of brachycephaly (degree of abnormality in head shape). Understanding the relationships between skull type and ocular measurements in brachycephalic and non-brachycephalic cat breeds will shed light on important issues such as disease diagnosis.

In our study, the mean “anterio-posterior distance of the globe” evaluated from the eye measurements was measured as  $20.92 \pm 1.30$  mm for brachycephalic and  $21.17 \pm 0.95$  mm for non-brachycephalic cat breeds. Salgüero *et al.* (2015) reported an average value of  $20.90 \pm 0.14$  mm for the same measurement in the left eye of different dog breeds regardless of skull types. In a study conducted on humans (Igbinedion and Ogbeide, 2013), it was noted that the gender factor affected eye measurements. In our study, it was observed that, in general, males had higher values than females for most of the ocular measurements in both brachycephalic and non-brachycephalic cats. When a t-test was applied without distinguishing skull types, a statistically significant difference was observed for measurement “anterio-posterior distance of the globe” ( $P < 0.05$ ). However, when differences between female and male groups were examined within skull types, there was no difference. The fact that sex differences yield statistically different results suggests that studies investigating these differences should consider skull types when conducting research.

Yuwatanakorn *et al.* (2021) reported an average value of  $20.2 \pm 0.04$  mm for the same measurement (anterio-posterior distance of the globe) for brachycephalic and non-brachycephalic cats. In the same study, it was reported that the differences between skull types were statistically non-significant when the mean values of the “anterio-posterior distance of the anterior chamber”, “anterio-posterior distance of the vitreous” and “globe height” were examined. When comparing the results, it can be concluded that our study reached the same conclusion that the difference between the two skull types is statistically non-significant.

According to Yuwatanakorn *et al.* (2021), no difference was observed between brachycephalic and non-brachycephalic skull types for the “anterio-posterior distance of the lens”. However, in our study, a statistically significant difference ( $P < 0.05$ ) was found between these two skull types for this measurement, mean value was higher for brachycephalic than non-brachycephalic cats. The reason for this discrepancy between the two studies regarding measurement “anterio-posterior distance of the lens” is believed to be due to differences in the brachycephalic cats used in the two studies. Brachycephalic cat breeds used in our study predominantly included British Shorthair and Scottish Fold. We also included Exotic Shorthair and Persian breeds which are categorized as severe (extreme) brachycephalic, while Yuwatanakorn *et al.* (2021) included American Shorthair and mixed breeds in their study. At this point, it is considered important to take into account the categorization of brachycephalic skull types into subgroups and the statistical diversity it creates when evaluating brachycephalic and non-brachycephalic skull types.

Mirshahi *et al.* (2014) evaluated the relationship between cranial morphometrics and ocular biometrics using a method commonly employed in clinics such as ultrasonography. These workers indicated that one of the primary factors influencing feline ocular biometrics via ultrasonography was cranial circumference. Cats of Persian breed were included in their study, and a positive correlation was noted between cranial circumference and eye measurements “anterio-posterior distance of the globe” and “anterio-posterior distance of the lens”. In our investigation, while focusing on brachycephalic cat breeds, it was observed that ocular measurements, particularly “anterio-posterior distance of the globe”, exhibited a positive correlation with all cranial vault

measurements, while measurement “anterio-posterior distance of the lens” demonstrated a positive correlation with three specific cranial vault measurements SW, ZB and POB ( $p < 0.05$ ). Conversely, in non-brachycephalic cat breeds, measurement “anterio-posterior distance of the globe” displayed a positive correlation with two cranial measurement points ZB and GBB ( $p < 0.01$ ), whereas measurement “anterio-posterior distance of the lens” showed no correlation with any of the cranial measurements. Both Mirshahi *et al.* (2014) and our study suggest that cranial measurements exert an influence on eye measurements “anterio-posterior distance of the globe” and “anterio-posterior distance of the lens”. However, when considering the measurement of the “anterio-posterior distance of the anterior chamber”, both studies observed that the type of skull did not affect this measurement.

Another method used in our study to elucidate the relationship between groups is DFA (Discriminant Function Analysis), which is a statistical technique used to differentiate or classify groups by utilizing multiple variables to determine differences between groups. It identifies the variables that best distinguish groups by creating models and then evaluates the accuracy and effectiveness of the model. DFA is used to predict the group to which individuals in the study belong to (Gündemir *et al.*, 2020; Pazvant *et al.*, 2022). Using the Stepwise discriminant functions, we found that cranial measurements GLS and SW were useful variables. In the study conducted by Pazvant *et al.* (2022) on seagulls, discriminant functions were derived from measurements obtained from head metrics, resulting in four functions with high separation rates. In all four functions, the head length measurement (which is GLS in our study) was included in the formula, which parallels our study. In both studies, head length measurements were observed to have highly discriminative features in the DF analyses.

In our study, results of DFA results showed a separation rate of 92.6% in non-brachycephalic cat breeds, while this rate was found to be 79.2% in brachycephalic cat breeds. The lower separation rate in brachycephalic cat breeds is thought to be due to the different degrees of brachycephaly within these breeds. Since there are various types of brachycephalic skull shapes with different degrees of brachycephaly (Schlueter *et al.*, 2009), it is considered important to apply DFA to brachycephalic cat breeds with different degrees of brachycephaly to make brachycephalic cat categorization more distinct.

**Conclusions:** In conclusion, our findings indicate that skull type influences the size and structure of the eyes at certain points, including antero-posterior distance of the lens, greatest length of the skull and postorbital breadth. At these points, the difference between brachycephalic and non-brachycephalic skulls was significant ( $P < 0.05$ ). Additionally, with DF analysis, it was observed that 92.6% of skulls with non-brachycephalic head types and 79.2% of skulls with brachycephalic head types were accurately classified. These data serve as an important guide for understanding the relationship between eye measurements and skull type in brachycephalic and non-brachycephalic cats.

**Authors contributions:** EÖ and GP conceived the idea and designed the study. MK managed acquisition of images. DAK, SU, ZNA, EEY and TK carried out image evaluation and measurements. EÖ and GP performed statistical analysis of data. All authors reviewed the manuscript for important intellectual contents and approved the final version.

## REFERENCES

- Abouelela YS, Farghali HA, Ahmed ZSO, *et al.*, 2022. Anatomy and morphometry of major salivary glands of domestic cats with relation to their histological features. *Pak Vet J* 42:81-87.
- Akbaş ZS, Duro S, Yalin EE, *et al.*, 2023. Detection of sexual dimorphism of the foramen magnum in cats using computed tomography. *Anat Histol Embryol* 52:595-602.
- Appelboom H, 2016. Pug appeal: brachycephalic ocular health. *Companion Anim* 21:29-36.
- Blocker T and Van Der Woerdt A, 2001. The feline glaucomas: 82 cases (1995-1999). *Vet Ophthalmol*, 4:81-85.
- Demir A, Akcasiz ZN and Erdoğan Bamaç Ö, 2023. Progressive ocular histiocytosis in a cat. *Kafkas Univ Vet Fak Derg* 29:305-9.
- Dursun N, 2007. Veteriner Anatomi 1. 11th Ed, Medisan Yayınevi, Ankara, Türkiye.
- Ermütlu ÇŞ, Balyen L, Özyaydin İ, *et al.*, 2024. Anterior and posterior segment parameters of the eye in eagle owls (*Bubo bubo*). *Kafkas Univ Vet Fak Derg* 30:81-86.
- Evangelho KDS, Cifuentes-González C, Rojas-Carabali W, *et al.*, 2024. Early detection of functional changes in an intraocular hypertension rabbit model treated with human wharton jelly mesenchymal stem cells (hWJ-MSCs) using chromatic pupillometry. *Pak Vet J* 44:29-37.
- Gültekin Ç, Sayiner S and Özgencil FE, 2022. Serology-based approach in the clinical evaluation of neonatal viral eye diseases in kittens: Calicivirus, Herpesvirus, and Panleukopenia virus. *Kafkas Univ Vet Fak Derg* 28:773-79.
- Gündemir O, Akcasiz ZN, Yılmaz O, *et al.*, 2023. Radiographic analysis of skull in Van cats, British shorthairs and Scottish folds. *Anat Histol Embryol* 52:512-18.
- Gündemir O, Pazvant G and İnce NG, 2020. The morphometric examination of head area of black headed gulls (*Larus Ridibundus*) from Marmara Region. *J Res Vet Med* 39:49-53.
- Gündemir O, Michaud M, Altundağ Y, *et al.*, 2024. Chewing asymmetry in dogs: Exploring the importance of the fossa masseterica and first molar teeth morphology. *Anat Histol Embryol* 53:e13050.
- Igbinedion BO and Ogbeide OU, 2013. Measurement of normal ocular volume by the use of computed tomography. *Niger J Clin Pract* 16:315-19.
- Jashari T, Kahvecioğlu O, Duro S, *et al.*, 2022. Morphometric analysis for the sex determination of the skull of the Deltari Ilir dog (*Canis lupus familiaris*) of Kosovo. *Anat Histol Embryol* 51:443-51.
- Künzel W, Breit S and Oppel M, 2003. Morphometric investigations of breed-specific features in feline skulls and considerations on their functional implications. *Anat Histol Embryol* 32:218-23.
- Manuta N, Gündemir O, Yalin EE, *et al.*, 2023. Pelvis shape analysis with geometric morphometry in crossbreed cats. *Anat Histol Embryol* 52:611-18.
- McLellan GJ and Teixeira LB, 2015. Feline glaucoma. *Vet Clin: Small Anim Pract* 45:1307-33.
- Mirshahi A, Shafiq SH and Azzadeh M, 2014. Ultrasonographic biometry of the normal eye of the Persian cat. *Aust Vet J* 92:246-49.
- Narfström K, 1999. Hereditary and congenital ocular disease in the cat. *J Feline Med Surg* 1:135-41.
- Nasise MP, Glover TL, Moore CP, *et al.*, 1998. Detection of feline herpesvirus 1 DNA in corneas of cats with eosinophilic keratitis or corneal sequestration. *Am J Vet Res* 59:856-58.
- Pazvant G, İnce NG, Özkan E, *et al.*, 2022. Sex determination based on morphometric measurements in yellow-legged gulls (*Larus michahellis*) around Istanbul. *BMC Zool* 7:1-7.
- Pentlidge VW, 1989. Corneal sequestration in cats. *Compend Contin Edu* 11:24-32.
- Salgüero R, Johnson V, Williams D, *et al.*, 2015. CT dimensions, volumes and densities of normal canine eyes. *Vet Rec* 176:386.


- Schlueter C, Budras KD, Ludwig E, *et al.*, 2009. Brachycephalic feline noses: CT and anatomical study of the relationship between head conformation and the nasolacrimal drainage system. *J Feline Med Surg* 11:891-900.
- Schmidt MJ, Kampschulte M, Enderlein S, *et al.*, 2017. The relationship between brachycephalic head features in modern Persian cats and dysmorphologies of the skull and internal hydrocephalus. *J Vet Intern Med* 31:1487-1501.
- Stiles J, 1995. Treatment of cats with ocular disease attributable to herpesvirus infection: 17 cases (1983–1993). *J Am Vet Med Assoc* 207:599-603.
- Şenol E, Gündemir O, Duro S, *et al.*, 2022. A pilot study: Can calcaneus radiographic image be used to determine sex and breed in cats? *Vet Med Sci* 8:1855-61.
- Yılmaz O, 2021. Computed tomographic imaging characteristics of the thyroid glands in clinically normal Van cats. *Kafkas Univ Vet Fak Derg* 27:617-24.
- Yuwatanakorn K, Thanaboonipat C, Tuntivanich N, *et al.*, 2021. Comparison of computed tomographic ocular biometry in brachycephalic and non-brachycephalic cats. *Vet World* 14:727.

RESEARCH ARTICLE

Open Access



# Non-invasive sampling in Itatiaia National Park, Brazil: wild mammal parasite detection

Laís Verdan Dib<sup>1</sup>, João Pedro Siqueira Palmer<sup>1</sup>, Camila de Souza Carvalho Class<sup>1</sup>, Jessica Lima Pinheiro<sup>1</sup>, Raissa Cristina Ferreira Ramos<sup>1</sup>, Claudijane Ramos dos Santos<sup>1</sup>, Ana Beatriz Monteiro Fonseca<sup>2</sup>, Karen Gisele Rodríguez-Castro<sup>3</sup>, Camila Francisco Gonçalves<sup>3</sup>, Pedro Manoel Galetti Jr.<sup>3</sup>, Otilio Machado Pereira Bastos<sup>1</sup>, Claudia Maria Antunes Uchôa<sup>1</sup>, Laís Lisboa Corrêa<sup>1</sup>, Augusto Cezar Machado Pereira Bastos<sup>1</sup>, Maria Regina Reis Amendoeira<sup>4</sup> and Alynne da Silva Barbosa<sup>1,4\*</sup> 

## Abstract

**Background:** Non-invasive sampling through faecal collection is one of the most cost-effective alternatives for monitoring of free-living wild mammals, as it provides information on animal taxonomy as well as the dynamics of the gastrointestinal parasites that potentially infect these animals. In this context, this study aimed to perform an epidemiological survey of gastrointestinal parasites using non-invasive faecal samples from carnivores and artiodactyls identified by stool macroscopy, guard hair morphology and DNA sequencing in Itatiaia National Park. Between 2017 and 2018, faeces from carnivores and artiodactyls were collected along trails in the park. The host species were identified through macroscopic and trichological examinations and molecular biology. To investigate the parasites, the Faust, Lutz and modified Ritchie and Sheather techniques and enzyme immunoassays to detect *Cryptosporidium* sp. antigens were used.

**Results:** A total of 244 stool samples were collected. The species identified were *Chrysocyon brachyurus*, *Leopardus guttulus*, *Canis familiaris*, *Cerdocyon thous*, *Puma yagouaroundi*, *Leopardus pardalis*, *Puma concolor* and *Sus scrofa*. There were 81.1% samples that were positive for parasites distributed mainly in the high part of the park. Helminths, especially eggs of the family Ascarididae, were more frequently detected in carnivore faeces (70.9%). Protozoa, especially *Cryptosporidium* sp., represented the highest frequency of infection in artiodactyl faeces (87.1%). This zoonotic protozoon was detected in eight mammalian species, including in a wild boar. High values of structural richness and Shannon and Simpson diversity indices were observed for the parasites, especially in the faeces of *C. brachyurus*. Significant differences in parasite diversity were observed between wild and domestic animals, such as *C. brachyurus* and *C. familiaris*, respectively, and between taxonomically distant species, such as *C. brachyurus* and *S. scrofa*. The highest values for parasite similarity were found among the species that frequented similar areas of the park, such as *C. brachyurus* and *L. guttulus*.

(Continued on next page)

\* Correspondence: [alynnedsb@gmail.com](mailto:alynnedsb@gmail.com)

<sup>1</sup>Department of Microbiology and Parasitology, Laboratory of Parasitology, Federal Fluminense University, Biomedical Institute, Professor Hernani Mello Street, São Domingos, Niterói, Rio de Janeiro 24210-130, Brazil

<sup>4</sup>Laboratory of Toxoplasmosis and Other Protozoan Diseases, Oswaldo Cruz Foundation (Fiocruz, Rio de Janeiro), Oswaldo Cruz Institute, Avenue Brazil, 4365, Manguinhos, Rio de Janeiro 21040-360, Brazil

Full list of author information is available at the end of the article



© The Author(s). 2020 **Open Access** This article is licensed under a Creative Commons Attribution 4.0 International License, which permits use, sharing, adaptation, distribution and reproduction in any medium or format, as long as you give appropriate credit to the original author(s) and the source, provide a link to the Creative Commons licence, and indicate if changes were made. The images or other third party material in this article are included in the article's Creative Commons licence, unless indicated otherwise in a credit line to the material. If material is not included in the article's Creative Commons licence and your intended use is not permitted by statutory regulation or exceeds the permitted use, you will need to obtain permission directly from the copyright holder. To view a copy of this licence, visit <http://creativecommons.org/licenses/by/4.0/>. The Creative Commons Public Domain Dedication waiver (<http://creativecommons.org/publicdomain/zero/1.0/>) applies to the data made available in this article, unless otherwise stated in a credit line to the data.

(Continued from previous page)

**Conclusions:** The animals and parasite infections were identified through the combination of three techniques. High frequency parasite structures were diagnosed. Zoonotic protozoa were found and mainly occurred in samples from introduced species.

**Keywords:** Gastrointestinal parasites, Wild animals, Coproparasitologic, Trichology, DNA sequencing

## Background

Over the years, wild mammalian fauna have been declining around the world for different reasons, including vehicle fatalities, agricultural frontier expansion, pasture formation, deforestation, environmental pollution and fur trafficking [1, 2]. Another factor that may result in declines in mammalian fauna is the parasite load of different aetiological agents, such as gastrointestinal parasites. These agents infect a myriad of hosts and make important alterations to community structure, directly impacting biodiversity and ecosystem dynamics [3]. The susceptibility of hosts to these infections is related to their phylogenetic proximity, body morphology and dietary habits [4]. Parasitism may result in weight loss, metabolic imbalance, reproductive disorders, anaemia, dehydration, foetal malformations, locomotor injuries, and even death among wild animals [5, 6]. When parasitized, many wild mammals end up presenting behavioural and functional alterations in their niche [7–9]. Therefore, studies on the prevalence of parasites in both wild and sympatric domestic animals are important for better understanding the possible effects on wildlife, the parasitic distribution dynamics among the hosts and possible parasitic sources for fauna.

There are three main types of sampling for wild mammal studies: destructive sampling from dead animals; non-destructive sampling from captured animals; and non-invasive sampling, in which samples, such as traces in the environment, loose hair or feathers, faeces and other remnants, are obtained without catching or handling the animal [10, 11]. It is worth mentioning that non-invasive sampling has become an alternative strategy for species monitoring and conservation, especially for those species with low population density and elusive nocturnal habits, such as carnivores [12]. Through non-invasive faecal sampling, it is possible to obtain data about biodiversity, including identification of the species inhabiting a region, their diet composition and their role in the ecosystem, as well as information about potentially infectious gastrointestinal parasites of these animals [13].

Brazil harbours high mammal biodiversity that includes different species of carnivores and artiodactyls [14], many of which are endangered [15]. However, very little is known about the parasite distribution in Brazilian wild mammal fauna, especially in conservation areas [16]. To obtain reliable information about the mammalian fauna

from non-invasive samples and to correlate it to parasite biodiversity, it is essential to precisely identify the host, which is possible through the association of faecal macroscopy, trichology of guard hairs (syn: overhairs), and DNA sequencing.

The use of morphological analysis to study faeces from free-living wild animals is very important since it serves as an initial screening of the samples to be collected, allowing reliable host taxonomic classification at the order level [17]. On the other hand, the trichology of mammalian guard hairs can provide specific information about the host species by associating the guard hair colour pattern (macroscopic guard-hair morphology) and the analysis of its cuticle and medullary designs (microscopic guard-hair morphology). Moreover, DNA sequencing is widely used in studies of free-living wild mammals; similar to trichology, it can also identify the host species.

To avoid possible ecological imbalances, it is important to perform constant monitoring of the wildlife in conservation areas. In this context and while any parasitological study was performed with mammals in the first Brazilian national park, this study aimed to perform an epidemiological survey of gastrointestinal parasites in non-invasive faecal samples from carnivores and artiodactyls identified by stool macroscopy, guard-hair trichology and DNA sequencing in Itatiaia National Park (PNI).

## Results

### Host identification

Three identification techniques, macroscopy, trichology and DNA sequencing, were used to analyse 244 faecal samples (S1, supplementary material and Table 1). It was possible to confirm eight mammal species, which included seven carnivores and one artiodactyl. The host species were identified for 180 of the samples. However, the three techniques did not achieve the same results in 110 of the samples for which the species were identified.

Therefore, Pearson's correlation was performed and established a very strong relationship ( $\rho > 0.9$ ) in most cases for the information associated with the *C. brachyurus* and *L. guttulus* samples and a moderate relationship ( $0.5 \leq \rho \leq 0.7$ ) for the *P. yagouaroundi* samples. The other samples in this group did not show significant degrees of correlation ( $\rho < 0.5$ ). After associating the

**Table 1** Hosts classification based on the association of faecal macroscopy, guard hair trichology and DNA sequencing

Taxonomy	Macroscopy	Trichology	DNA sequencing	Pearson's correlation coefficiente ( $\rho$ )	Total fecal samples (n = 244)
<b>Order Carnivora</b>					<b>168 (68.8%)</b>
<b>Family Canidae</b>					<b>112 (45.9%)</b>
<i>Chrysocyon brachyurus</i>					97 (39.7%)
	Order Carnivora	<i>C. brachyurus</i>	<i>C. brachyurus</i>	<sup>c</sup>	42
	Order Carnivora	Family Mustelidae	<i>C. brachyurus</i>	0.95	11
	Order Carnivora	Family Mephitidae	<i>C. brachyurus</i>	0.95	2
	Order Carnivora	<i>C. brachyurus</i>	Low quality gene sequence	0.97	6
	Order Carnivora	Family Canidae	<i>C. brachyurus</i>	<sup>c</sup>	1
	Order Carnivora	Absent guard hair	<i>C. brachyurus</i>	0.95	24
	Family Canidae	<i>C. brachyurus</i>	<i>C. brachyurus</i>	<sup>c</sup>	3
	Family Felidae	<i>C. brachyurus</i>	<i>C. brachyurus</i>	0.99	7
	Family Felidae	Family Canidae	<i>C. brachyurus</i>	–	1
<i>Canis familiaris</i>					13 (5.3%)
	Order Carnivora	Family Canidae	<i>C. familiaris</i>	<sup>c</sup>	8
	Order Carnivora	<i>Procyon cancrivorus</i>	<i>C. familiaris</i>	–	1
	Order Carnivora	Family Mephitidae	<i>C. familiaris</i>	–	1
	Order Carnivora	Absent guard hair	<i>C. familiaris</i>	–	2
	Family Canidae	Family Canidae	<i>C. familiaris</i>	<sup>c</sup>	1
<i>Cerdocyon thous</i>					2 (0.8%)
	Order Carnivora	<i>C. thous</i>	<i>C. thous</i>	<sup>c</sup>	1
	Order Carnivora	Absent guard hair	<i>C. thous</i>	–	1
<b>Family Felidae</b>					56 (22.9%)
<i>Leopardus guttulus</i>					52 (21.3%)
	Family Felidae	<i>L. guttulus</i>	<i>L. guttulus</i>	<sup>c</sup>	3
	Family Felidae	<i>L. guttulus</i>	Low quality gene sequence	0.97	1
	Family Felidae	Absent guard hair	<i>L. guttulus</i>	0.94	24
	Family Felidae	Family Canidae	<i>L. guttulus</i>	0.94	6
	Family Felidae	<i>Procyon cancrivorus</i>	<i>L. guttulus</i>	0.94	2
	Family Felidae	Family Mustelidae	<i>L. guttulus</i>	0.94	2
	Family Felidae	Family Mephitidae	<i>L. guttulus</i>	0.94	5
	Order Carnivora	Absent guard hair	<i>L. guttulus</i>	–	7
	Order Carnivora	<i>L. pardalis</i>	<i>L. guttulus</i>	–	1
	Order Carnivora	<i>P. yagouaroundi</i>	<i>L. guttulus</i>	–	1
<i>Puma yagouaroundi</i>					2 (0.8%)
	Family Felidae	<i>P. yagouaroundi</i>	Low quality gene sequence	0.68	2
<i>Leopardus pardalis</i>					1 (0.4%)
	Order Carnivora	<i>L. pardalis</i>	Low quality gene sequence	–	1
<i>Puma concolor</i>					1 (0.4%)
	Order Carnivora	Familia Mustelidae	<i>P. concolor</i>	–	1
<b>Order Artiodactyla</b>					<b>31 (12.7%)</b>
<b>Family Suidae</b>					<b>12 (4.9%)</b>
<i>Sus scrofa</i>					12 (4.9%)
	Order Artiodactyla	Absent guard hair	<i>S. scrofa</i>	–	1
	Order Artiodactyla	Order Artiodactyla	<i>S. scrofa</i>	<sup>c</sup>	11

**Table 1** Hosts classification based on the association of faecal macroscopy, guard hair trichology and DNA sequencing (Continued)

Taxonomy	Macroscopy	Trichology	DNA sequencing	Total faecal samples (n = 244)
<b>Order Carnivora</b>				<b>168 (68.8%)</b>
Order Carnivora US <sup>a</sup>				45 (18.4%)
	Order Carnivora	<i>L. guttulus</i>	<i>C. familiaris</i>	1
	Order Carnivora	<i>L. pardalis</i>	<i>C. brachyurus</i>	2
	Order Carnivora	<i>P. yagouaroundi</i>	<i>C. brachyurus</i>	1
	Order Carnivora	Absent guard hair	Low quality gene sequence	9
	Order Carnivora	Family Mephitidae	Low quality gene sequence	1
	Order Carnivora	<i>C. brachyurus</i>	<i>L. guttulus</i>	5
	Order Carnivora	<i>Leopardus wiedii</i>	<i>C. thous</i>	1
	Order Carnivora	<i>Nasua nasua</i>	Low quality gene sequence	1
	Order Carnivora	Family Mustelidae	Low quality gene sequence	1
	Order Carnivora	Family Canidae	Low quality gene sequence	4
	Family Felidae	<i>C. brachyurus</i>	<i>L. guttulus</i>	1
	Family Felidae	Family Canidae	Low quality gene sequence	3
	Family Felidae	<i>Nasua nasua</i>	Low quality gene sequence	1
	Family Felidae	Family Mustelidae	Low quality gene sequence	3
	Family Felidae	Absent guard hair	Low quality gene sequence	6
	Family Felidae	Family Mephitidae	Low quality gene sequence	4
	Family Felidae	<i>C. brachyurus</i>	Low quality gene sequence	1
<b>Order Artiodactyla</b>				<b>31 (12.7%)</b>
Order Artiodactyla US <sup>b</sup>				19 (7.8%)
	Order Artiodactyla	Absent guard hair	Low quality gene sequence	6
	Order Artiodactyla	Order Artiodactyla	Low quality gene sequence	13

<sup>a</sup> Order Carnivora Unidentified Species; <sup>b</sup> Order Artiodactyla Unidentified Species. <sup>c</sup> Total agreement among the three identification techniques

three identification techniques, a final classification of host species was conducted using the highlighted information (Table 1).

### Parasitological diagnosis

In the faeces of the animals, several parasitic taxa were identified, including the phyla Nematoda, Platyhelminthes and Protozoa. These were characterized into morphotypes by their different sizes, colours and shapes. Out of the 244 faecal samples collected, structures of gastrointestinal parasites were revealed in 198 (81.1%) through the combined use of microscopic coproparasitological techniques and ELISA. In general, helminths were observed more frequently than protozoa and were mainly seen in faeces from carnivores. The inverse was observed in relation to the stool samples from artiodactyls (Table 2).

Among the 213 faecal samples from animals of the order Carnivora that were analysed, 171 (80.3%) showed structures from gastrointestinal parasites, among which eggs of the families Ascarididae and Diphylobothriidae and coproantigens of *Cryptosporidium* sp. can be highlighted. Among the samples from the animals of the order Artiodactyla, the total number positive for

gastrointestinal parasites was 27 samples (87.1%). Antigens of *Cryptosporidium* sp. were the most frequently detected structure, followed by cysts of *Balantioides coli* and nematode larvae (Table 2).

Out of the 244 faecal samples retrieved from the park, most were identified as belonging to *C. brachyurus* (97) and *L. guttulus* (52). Among these, structures of gastrointestinal parasites were detected in 79 (81.4%) samples from *C. brachyurus* and in 43 (82.7%) from *L. guttulus* (Figs. 1 and 2). Such parasites were also observed in other faecal samples of carnivores and artiodactyls that had been collected along the park trails (Figs. 1 and 2).

In addition, a difference in the distribution of parasitic structures can be observed in the three areas of the park. The High Part was the region where all parasitic taxa were detected, except for *Eimeria* sp. However, the Lower Part was the region that presented the least diversity of parasitic structures, being detected 7 out of 15 taxa. In Visconde de Mauá, 10 out of 15 taxa were detected, highlighting the presence of antigens of *Cryptosporidium* sp. which was quite evident (Fig. 3).

Eggs of the family Ascarididae, especially those classified as morphotype 1, that were similar to *Toxocara* sp. were



**Table 2** Frequency of gastrointestinal parasites in carnivorous and artiodactyls faecal samples surveyed in Itatiaia National Park, Brazil

Helminth and protozoan structures	Order Carnivora (n = 213)	Order Artiodactyla (n = 31)	Total (n = 244)
<b>Helminths</b>			
Family Ascarididae	71 (33.3%)	4 (12.9%)	75 (30.8%)
<i>Trichuris</i> sp.	31 (14.5%)	–	31 (12.7%)
<i>Capillaria</i> sp.	29 (13.6%)	–	29 (11.9%)
Nematode larvae	25 (11.7%)	6 (19.4%)	31 (12.7%)
Thin-shelled nematode egg	21 (9.8%)	3 (9.7%)	24 (9.8%)
<i>Physaloptera</i> sp.	12 (5.6%)	–	12 (4.9%)
Family Diphylobothriidae	52 (24.1%)	–	52 (21.3%)
Order Cyclophyllidea	8 (3.7%)	–	8 (3.3%)
Family Dicrocoeliidae	10 (4.7%)	–	10 (4.1%)
Phylum Acanthocephala	1 (0.5%)	–	1 (0.4%)
Subtotal of helminths positive samples	151 (70.9%)	10 (32.2%)	161 (66%)
<b>Protozoan</b>			
Non-sporulated coccidian	10 (4.7%)	–	10 (4.1%)
<i>Eimeria</i> sp.	–	1 (3.2%)	1 (0.4%)
<i>Balantioides coli</i>	–	6 (19.4%)	6 (2.4%)
Amoebae	3 (1.4%)	–	3 (1.2%)
Coproantigens of <i>Cryptosporidium</i> sp.	42 (19.7%)	25 (80.6%)	67 (27.4%)
Subtotal of protozoan positive samples	54 (25.3%)	27 (87.1%)	81 (33.2%)
<b>Total of positive samples</b>	<b>171 (80.3%)</b>	<b>27 (87.1%)</b>	<b>198 (81.1%)</b>

detected mainly in faecal samples from carnivores, except from *L. pardalis* and *P. concolor*. Parasite structures that matched the typical morphology of infertile *Ascaris* eggs (morphotype 2) were only observed in samples from *S. scrofa*. A third morphotype of ascarid was detected in 11.9% of the samples, including the faeces from *C. brachyurus*, *C. familiaris* and *L. guttulus* (Table 3 and Fig. 4).

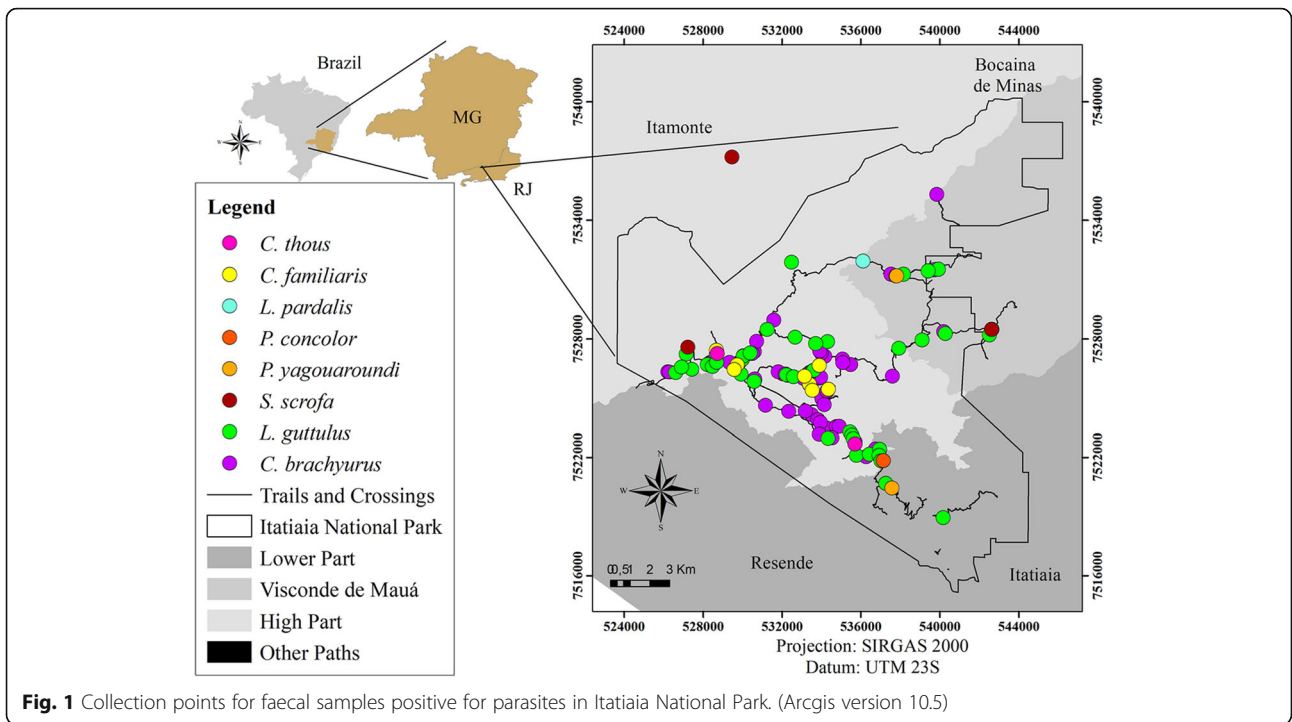
Eggs of the family Diphylobothriidae were the second most frequent parasite among the helminths and were detected only in the faecal samples from carnivores. Nematode larvae and *Trichuris* sp. eggs were observed in 12.7% of the stool samples. Nematode larvae were detected in faeces from both carnivores and artiodactyls and were not classified into different morphotypes. Eggs of *Trichuris* sp. were only diagnosed in samples from carnivores, and these were morphologically classified as morphotypes 1 and 2. *Capillaria* sp. eggs were diagnosed in 11.9% of the faecal samples analysed. These were classified into morphotypes 1 and 2 and were detected in faeces from *C. brachyurus*, *L. guttulus*, *P. yagouaroundi* and *L. pardalis* (Table 3 and Fig. 4).

Thin-shelled nematode eggs were observed in 9.8% of the samples. Among these, the eggs were classified into morphotype 1, which were similar to those of the superfamily Strongyloidea, and morphotype 2, which were similar to strongylids (superfamilies Trichostrongyloidea and Strongyloidea). Morphotype 1 eggs were detected in

faeces from *C. brachyurus*, *C. familiaris* and *L. guttulus*, and morphotype 2 eggs were detected in samples from *L. guttulus*, *C. thous* and *S. scrofa*. Thin-shelled eggs with tapered ends were diagnosed in the faeces of both *C. familiaris* and unidentified artiodactyls (Table 3 and Fig. 4).

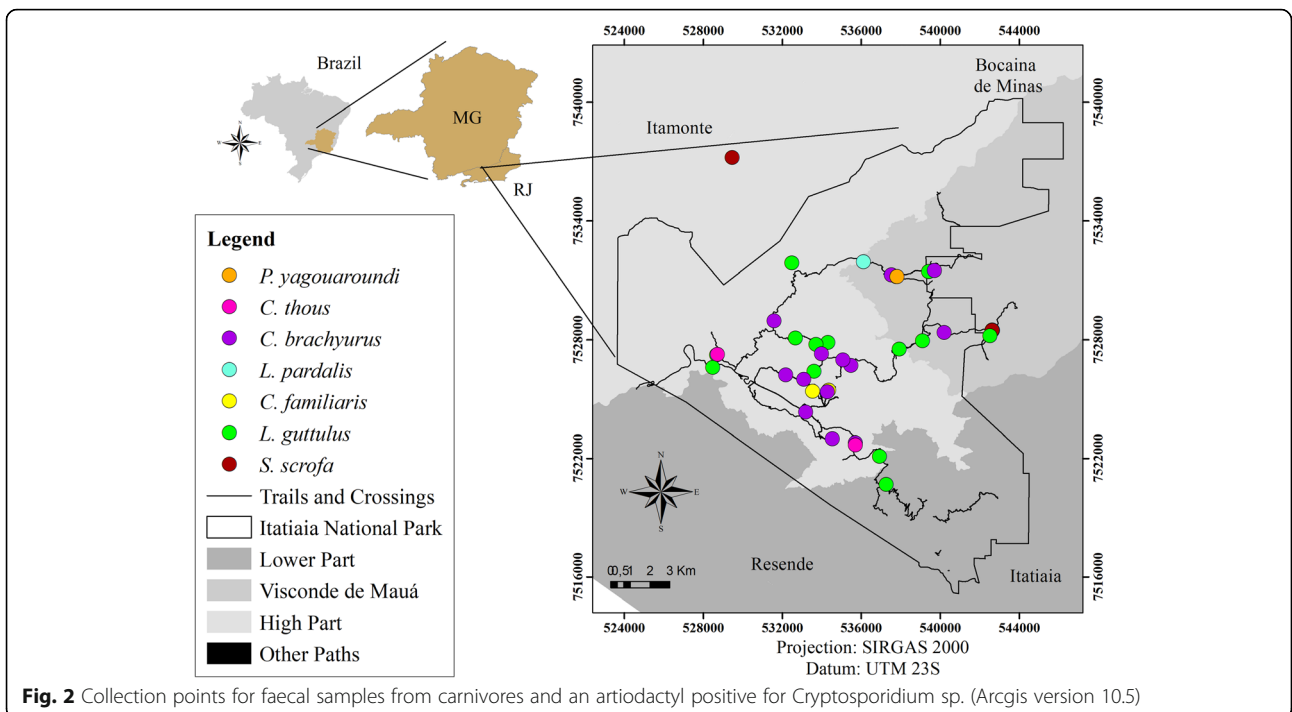
In the faeces from carnivores, eggs of other helminths, such as *Physaloptera* sp. and the family Dicrocoeliidae were also observed. Cestode eggs of the order Cyclophyllidea, which were classified as morphotype 1, were detected in 2.9% of the faeces analysed. Eggs from the family Taeniidae, which were named morphotype 2, were detected in one sample from *C. brachyurus*. In a faecal sample that was positive for eggs of the phylum Acanthocephala, the host was only characterized down to the taxonomic group of the order Carnivora (Table 3 and Fig. 4).

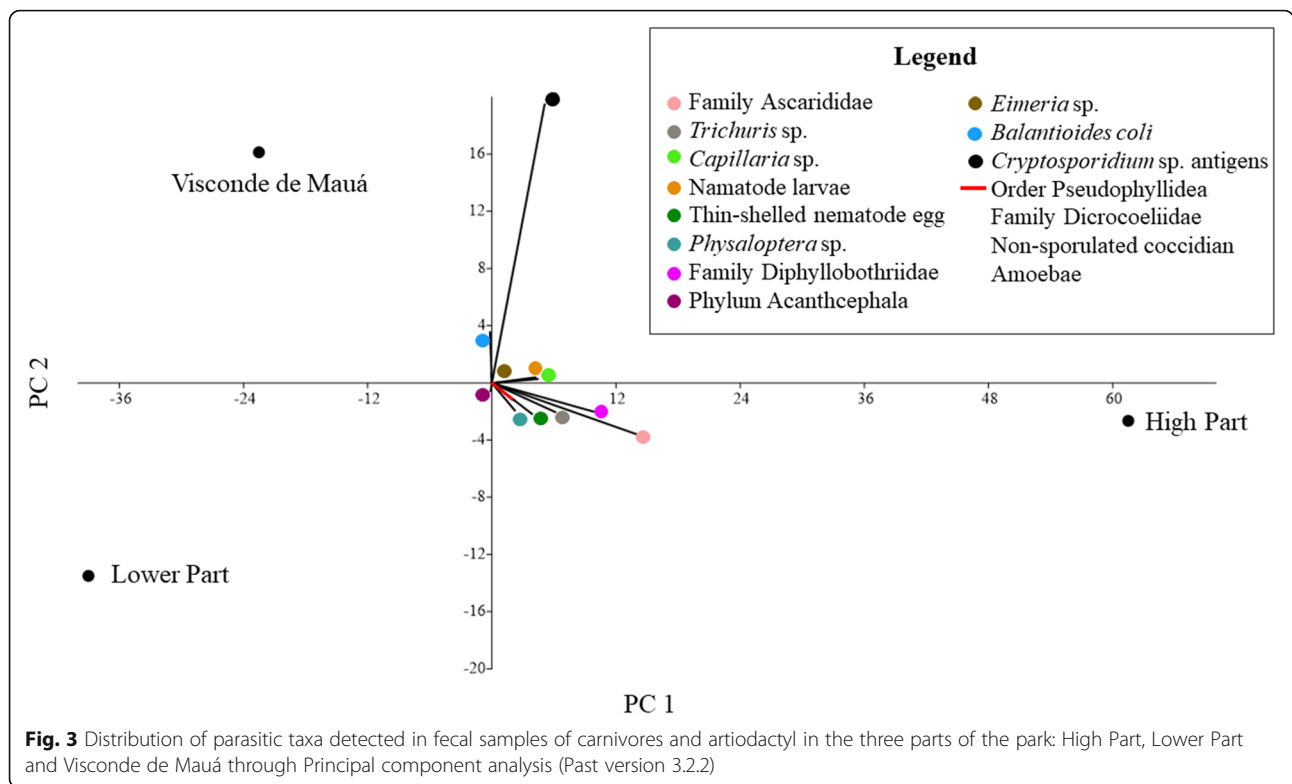
Among the protozoa detected, *Cryptosporidium* sp. was diagnosed through antigens in the faeces of all animals that were identified to the species level except for *P. concolor* (Fig. 2). Unsporulated coccidia oocysts and tetranucleated amoeba cysts were detected in faeces that were identified as from *C. brachyurus*, and the latter were also found in faeces from *L. guttulus*. Sporulated coccidian oocysts with the typical morphological pattern of *Eimeria* sp. and *Balantioides coli* cysts were detected only in faeces from artiodactyls (Table 3 and Fig. 5). All different morphotypes of protozoa structures detected presented similar morphology and varied only in size.



Regarding parasitic associations, polyparasitism was observed in 94 samples (38.5%), which had two to eight parasite structures. Associations were found between helminths alone, between helminths and protozoa and between protozoa alone. The most frequently detected parasitic associations occurred between eggs of the

families Ascarididae and Diphylobothriidae and between eggs of Ascarididae and *Trichuris* sp.; both combinations were present in five samples from carnivores (2.3%). In the faeces from artiodactyls, the most frequent association occurred between nematode larvae and *Cryptosporidium* sp. coproantigens in three samples (9.7%).





To analyse the richness, diversity, and similarity indices, the sample sufficiency for each host species (relationship between the faecal samples and the different parasitic taxa detected) was analysed and plotted on accumulation curves. The accumulation curves of *C. brachyurus*, *L. guttulus*, and *C. familiaris* stabilized, which means that the number of samples recovered for each of these hosts was enough to estimate the richness and diversity indices of the parasitic fauna. It was not possible to establish accumulation curves for *L. pardalis* and *P. concolor* since only one faecal sample was collected from each of these species (Fig. 6).

The faecal samples from *C. brachyurus* and *L. guttulus* presented the highest richness and were positive for a great number of different parasite taxa, and similarity, as demonstrated by the parasitic likeness between the hosts (Table 4 and Fig. 7). However, despite the detection of common parasites between artiodactyls and carnivores, many agents were detected in only one of these hosts, which justified the low parasite similarity index between them (Fig. 7). In the pooled t test, the Shannon diversity index ( $H'$ ) of the parasites was significant ( $p < 0.05$ ) between *C. brachyurus* and *C. familiaris* and between *S. scrofa* and *C. brachyurus* (Table 5). Thus, it was demonstrated that the parasitic taxa and their distribution differed considerably among hosts.

### Discussion

From the association of the macroscopic, trichological and DNA sequencing results, a final identification of the host species was obtained. Through macroscopic examination of the faeces, problems in identification occurred with canid samples when seeds, which are common in the diet of neotropical canids such as *C. brachyurus*, were not observed. In addition, there is no consensus among authors regarding the shape of mammalian stool. Thus, to minimize misidentification of the host by macroscopy, the samples were classified only into high-level taxonomic categories, such as order, in most cases. Despite the low resolution of host identification, this is a low-cost technique and can be used by any researcher during field work.

In this study, host species were not identified through trichological analysis in most of the samples. As pointed out at Serra dos Órgãos National Park, one of the limitations in mammalian identification through trichology is that faeces often presents many hairs, but not all are guard hairs [16]. In addition, some guard hair had deteriorated, making it impossible to assess their cuticles. In this case, since only the medullary patterns were observed, it was only possible to identify the animals down to the family level, such as the family Canidae. On the other hand, the guard hairs recovered from artiodactyl samples did not have cuticles, and only the internal layer was composed of

**Table 3** Frequency of gastrointestinal parasite morphotypes in mammal faecal samples from Itatiaia National Park, Brazil

Morphotypes of helminth and protozoan structures	Chrysocyon brachyurus (n = 97)	Canis familiaris (n = 13)	Cerdocyon thous (n = 2)	Leopardus guttulus (n = 52)	Puma yagouaroundi (n = 2)	Leopardus pardalis (n = 1)	Puma concolor (n = 1)	Order Carnivora US (n = 45)	Sus scrofa (n = 12)	Order Artiodactyla US (n = 19)	Total (n = 244)
<b>Helminths</b>											
Family Ascaridae	25 (25.8%)	4 (30.8%)	1 (50%)	20 (38.5%)	1 (50%)	-	-	21 (46.7%)	4 (33.3%)	-	75 (30.8%)
Morphotype 1 - <b>C:</b> 92.5 ± 5.8 × 81.4 × 7.1; <b>F:</b> 92.5 ± 6 × 81.4 × 6.2; <b>S:</b> 88.8 ± 8.7 × 85.1 × 7.6	20 (20.6%)	2 (15.4%)	1 (50%)	19 (36.5%)	1 (50%)	-	-	15 (33.3%)	3 (25%)	-	61 (25%)
Morphotype 2 - <b>C:</b> 111 ± 18.5 × 107.3 ± 23.2; <b>F:</b> 107.3 ± 8.9 × 83.2 ± 12.9	-	-	-	-	-	-	-	-	1 (8.3%)	-	1 (0.4%)
Morphotype 3 - <b>S:</b> 114.7 ± 4.8 × 74 ± 1.6	11 (11.3%)	3 (23.1%)	-	10 (19.2%)	-	-	-	4 (8.9%)	-	-	29 (11.9%)
Trichuris sp.	19 (19.6%)	-	-	4 (7.7%)	2 (100%)	-	-	6 (13.3%)	-	-	31 (12.7%)
Morphotype 1 - <b>C:</b> 88.8 ± 8 × 37 ± 2.8; <b>F:</b> 81.4 ± 4.5 × 40.7 ± 4.2	12 (12.4%)	-	-	1 (1.9%)	2 (100%)	-	-	5 (11.1%)	-	-	18 (7.4%)
Morphotype 2 - <b>C:</b> 107.3 ± 7.3 × 40.7 ± 4.9; <b>F:</b> 107.3 ± 7.6 × 42.5 ± 3.7	10 (10.3%)	-	-	4 (7.7%)	-	-	-	2 (4.4%)	-	-	18 (7.4%)
Capilaria sp.	14 (14.4%)	-	-	11 (21.1%)	1 (50%)	1 (100%)	-	2 (4.4%)	-	-	29 (11.9%)
Morphotype 1 - <b>C:</b> 85.1 ± 5.1 × 44.4 ± 4.9; <b>F:</b> 85.1 ± 6.4 × 44.4 ± 3.9	8 (8.2%)	-	-	6 (11.5%)	1 (50%)	1 (100%)	-	-	-	-	15 (6.1%)
Morphotype 2 - <b>C:</b> 99.9 ± 8.1 × 44.4 ± 6.1; <b>F:</b> 101.7 ± 5.6 × 51.8 ± 6.5	9 (9.3%)	-	-	10 (19.2%)	-	1 (100%)	-	2 (4.4%)	-	-	23 (9.4%)
Nematode larvae	13 (13.4%)	-	-	5 (9.6%)	-	-	1 (100%)	6 (13.3%)	1 (8.3%)	5 (26.3%)	31 (12.7%)
Thin-shelled nematode egg	9 (9.3%)	3 (23.1%)	1 (50%)	4 (7.7%)	-	-	-	4 (8.9%)	2 (16.7%)	1 (5.3%)	24 (9.8%)
Morphotype 1 - <b>C:</b> 85.1 ± 4.2 × 55.5 ± 3.7; <b>F:</b> 96.2 × 40.7	7 (7.2%)	1 (7.7%)	-	1 (1.9%)	-	-	-	3 (6.7%)	-	-	12 (4.9%)
Morphotype 2 - <b>C:</b> 107.3 ± 5.5 × 57.3 ± 4.8; <b>F:</b> 109.1 ± 2.6 × 85.1 ± 31.4; <b>S:</b> 172 ± 29.8 × 79.5 ± 10.6	2 (2.1%)	1 (7.7%)	1 (50%)	3 (5.8%)	-	-	-	1 (2.2%)	2 (16.7%)	-	10 (4.1%)
Morphotype 3 - <b>C:</b> 92.5 ± 6.1 × 55.5 ± 5.6	-	1 (7.7%)	-	-	-	-	-	-	-	1 (5.3%)	2 (0.8%)
Physaloptera sp. - <b>C:</b> 70.3 ± 10 × 46.2 ± 9.7; <b>F:</b> 70.3 × 51.8	9 (9.3%)	-	-	1 (1.9%)	-	-	-	2 (4.4%)	-	-	12 (4.9%)
Family Dipyllobothriidae - <b>C:</b> 88.8 ± 9.3 × 48.1 ± 6.3; <b>F:</b> 85.1 ± 7.1 × 48.1 ± 4	31 (32%)	-	1 (50%)	10 (19.2%)	-	-	-	10 (22.2%)	-	-	52 (21.3%)
Order Cyclophyllidea	4 (4.1%)	1 (7.7%)	-	1 (1.9%)	-	-	-	2 (4.4%)	-	-	8 (3.3%)
Morphotype 1 - <b>C:</b> 83.2 ± 8.1 × 77.7 ± 12.3; <b>F:</b> 81.4 ± 15.7 × 75.8 ± 7.8	3 (3.1%)	1 (7.7%)	-	1 (1.9%)	-	-	-	2 (4.4%)	-	-	7 (2.9%)
Morphotype 2 - <b>C:</b> 48.1 × 37	1 (1%)	-	-	-	-	-	-	-	-	-	1 (0.4%)
Family Dicrocoeliidae - <b>C:</b> 55.5 ± 11.3 × 33.3 ± 3.7; <b>F:</b> 51.8 ± 1.5 × 33.3 ± 3.3	5 (5.1%)	-	-	3 (5.8%)	-	-	-	2 (4.4%)	-	-	10 (4.1%)
Phylum Acanthocephala	-	-	-	-	-	-	-	1 (2.2%)	-	-	1 (0.4%)
Morphotype 1 - 88.8 ± 9.5 × 74 ± 3.3	-	-	-	-	-	-	-	1 (2.2%)	-	-	1 (0.4%)
Morphotype 2 - 85.1 × 66.7	-	-	-	-	-	-	-	1 (2.2%)	-	-	1 (0.4%)
Helminths positive samples	72 (74.2%)	7 (53.8%)	1 (50%)	35 (67.3%)	2 (100%)	1 (100%)	1 (100%)	31 (68.9%)	5 (41.7%)	5 (26.3%)	161 (66%)

**Table 3** Frequency of gastrointestinal parasite morphotypes in mammal faecal samples from Itatiaia National Park, Brazil (Continued)

Morphotypes of helminth and protozoan structures	<i>Chrysocyon brachyurus</i> (n = 97)	<i>Canis familiaris</i> (n = 13)	<i>Cerdocyon thous</i> (n = 2)	<i>Leopardus guttulus</i> (n = 52)	<i>Puma yagouaroundi</i> (n = 2)	<i>Leopardus pardalis</i> (n = 1)	<i>Puma concolor</i> (n = 1)	Order Carnivora US (n = 45)	<i>Sus scrofa</i> (n = 12)	Order Artiodactyla US (n = 19)	Total (n = 244)
<b>Protozoa</b>											
Non-sporulated coccidian	9 (9.3%)	-	-	-	-	-	-	1 (2.2%)	-	-	10 (4.1%)
Morphotype 1 - <b>C</b> : 25.9 ± 2.4 × 22.2 ± 2.5	7 (7.2%)	-	-	-	-	-	-	-	-	-	7 (2.9%)
Morphotype 2 - <b>C</b> : 37 ± 6.9 × 33.3 ± 5.6	5 (5.1%)	-	-	-	-	-	-	-	-	-	5 (2%)
<i>Eimeria</i> sp. - <b>S</b> : 37 × 37	-	-	-	-	-	-	-	-	1 (8.3%)	-	1 (0.4%)
<i>Balantoides coli</i> - <b>S</b> : 48.1 ± 38.8 × 44.4 ± 35.5	-	-	-	-	-	-	-	-	2 (16.7%)	4 (21%)	6 (2.4%)
Amoebae - <b>C</b> : 18.5 ± 5.8 × 18.5 ± 3.6; <b>F</b> : 18.5 ± 3.2 × 18.5 ± 2	2 (2.1%)	-	-	1 (1.9%)	-	-	-	-	-	-	3 (1.2%)
<i>Cryptosporidium</i> sp. coproantigens	13 (13.4%)	2 (15.4%)	2 (100%)	14 (26.9%)	1 (50%)	1 (100%)	-	9 (20%)	10 (83.3%)	15 (78.9%)	67 (27.4%)
Protozoan positive samples	22 (22.7%)	2 (15.4%)	2 (100%)	15 (28.8%)	1 (50%)	1 (100%)	-	10 (22.2%)	10 (83.3%)	17 (89.5%)	81 (33.2%)
<b>Total positive samples</b>	79 (81.4%)	8 (61.5%)	2 (100%)	43 (82.7%)	2 (200%)	1 (100%)	1 (100%)	35 (77.8%)	10 (83.3%)	17 (89.5%)	198 (81.1%)

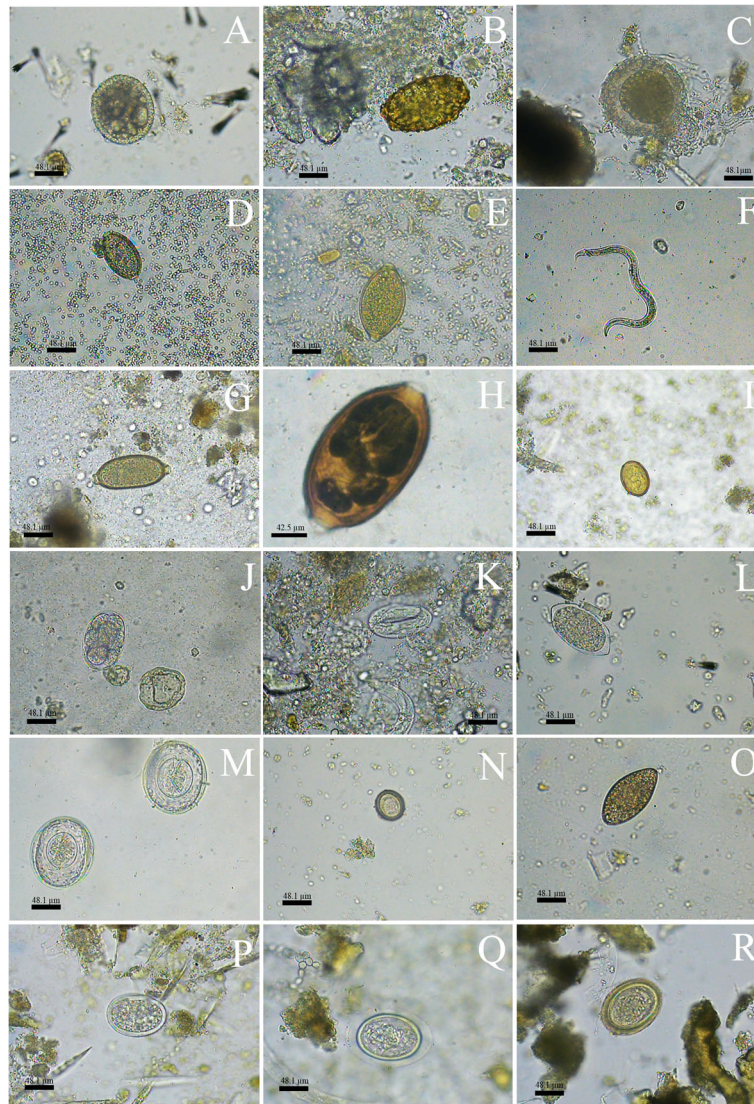


**Fig. 4** Morphotypes of helminths eggs in 400 x (A to F; H to S) and 1000 x (G) detected in faecal samples of carnivores and artiodactyls from Itatiaia National Park, Brazil. **a** Ascarididae family 1. **b** Ascarididae family 2. **c** Ascarididae family 3. **d** *Trichuris* sp. 1. **e** *Trichuris* sp. 2. **f** Nematode larvae. **g** *Capillaria* sp. 1. **h** *Capillaria* sp. 2. **i** Dicrocoelidae family. **j** Thin-shelled nematode egg 1. **k** Thin-shelled nematode egg 2. **l** Thin-shelled nematode egg 3. **m** Cyclophyllidea order 1. **n** Cyclophyllidea order 2. **o** Diphyllbothriidae family. **p** *Physaloptera* sp. **q** Acanthocephala phylum 1. **r** Acanthocephala phylum 2

fibres. The loss of the cuticular layer may have occurred during laboratory processing or by the passage of the guard hairs through the gastrointestinal tract. Nevertheless, the cuticle may have been rubbed off when artiodactyls rubbed their bodies on natural substrates, such as trees. It is noteworthy that trichological processing is time-consuming, and the assessment of guard hairs requires trained professionals. Moreover, it is important to make controls with guard hairs that were taken directly from animals to achieve greater accuracy in host identification from the non-invasive samples. Nevertheless, this methodology is also very advantageous since it is inexpensive

and allows a very specific taxonomic classification of the animal.

DNA sequencing was also used for host identification. It is important to highlight that genetic sequences do not ensure that it is the true host due to the possibility of countermarking by other animals with territorial behaviour. Nonetheless, the use of DNA sequencing may be the only alternative for the identification of *S. scrofa*, for which faecal hair release in feces is not common. However, this technique was the most expensive among those used in this study, and it does not always provide satisfactory results due to many faecal inhibitors. Thus, the association among macroscopy, trichology, and DNA sequencing is

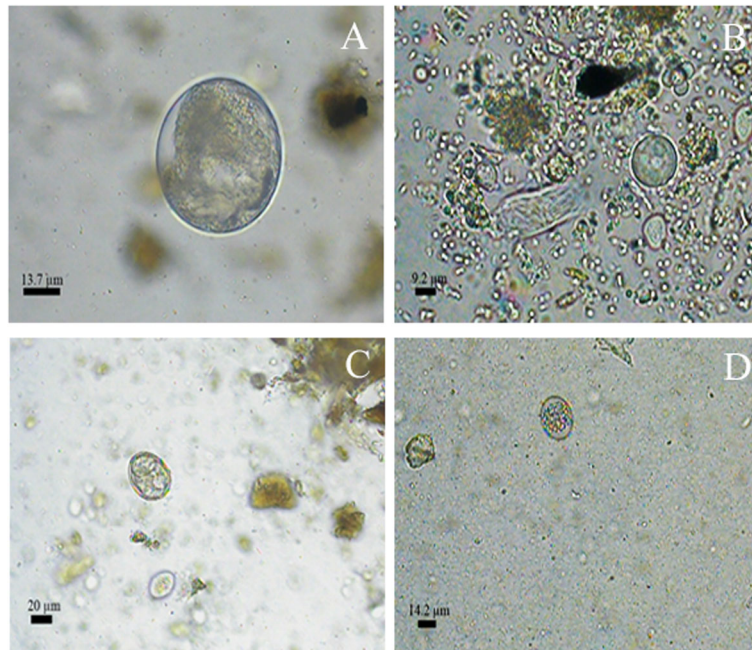


**Fig. 5** Morphotypes of protozoa cysts and oocysts in 1000 x detected in faecal samples of carnivores and artiodactyls from Itatiaia National Park, Brazil. **a** *Balantioides coli*. **b** Amoebae. **c** *Eimeria* sp. **d** Non-sporulated coccidia

essential to provide the most trustworthy identification from non-invasive samples.

The overall positive rate for gastrointestinal parasites was 81.1%. In this study, from all the 244 samples, the positive rates were 36.5% for Canidae family, 19.3% for Felidae and 4.1 for Suidae. Lower overall frequencies have

been reported in other studies, varying from 58 to 74.7% for feline faeces from reserves and forests in Mexico [18–20], 75% for feline and artiodactyl faeces from a reserve in Bolivia [21], 53.3% for faeces from canids, felids, mustelids and procyonids collected in a reserve in Minas Gerais, Brazil [22], and 70% for feline faeces found in a

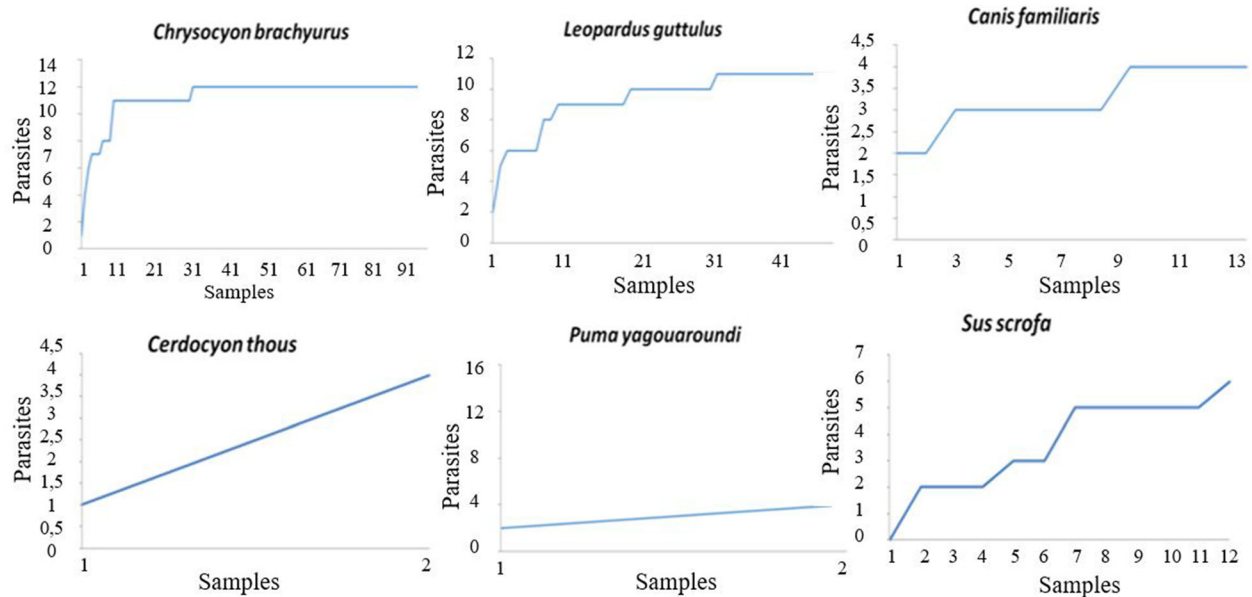


**Fig. 6** Accumulation curves for gastrointestinal parasite structures detected in faecal samples from carnivores and an artiodactyl from Itatiaia National Park, Brazil

**Table 4** Richness and diversity of gastrointestinal parasites in mammal faeces from Itatiaia National Park, Brazil

Host	Richness	Shannon (H')	Simpson
Family Canidae			
<i>Chrysocyon brachyurus</i>	12	2.2761	0.887
<i>Canis familiaris</i>	4	1.2799	0.778
<i>Cerdocyon thous</i>	4	1.3297	0.867
Family Felidae			
<i>Leopardus guttulus</i>	11	1.9662	0.850
<i>Puma yagouaroundi</i>	4	1.3322	0.900
<i>Leopardus pardalis</i>	2	0.6931	1
<i>Puma concolor</i>	2	0.6931	1
Family Suidae			
<i>Sus scrofa</i>	6	1.4286	0.721

reserve in Espírito Santo, Brazil [23]. In contrast, the frequency of parasites detected in faeces from Serra dos Órgãos National Park was 86.6%, which was slightly higher than that observed in Itatiaia National Park [16]. The high frequency of gastrointestinal parasites detected may have occurred since these animals live in natural environments that are rich in abiotic and biotic factors that promote infection through contact with contaminated soil, water, food and infected prey.

In general, helminths were more frequent than protozoa in the faeces from carnivores. High frequencies of helminths have also been observed in stool samples from carnivores in Thailand, Mexico, Bolivia and Brazil [16, 18–29]. In this study, the high frequency of helminths showed that the environment inhabited by the animals presented

conditions that were favourable for maintenance of nematode, cestode, trematode and acanthocephalan life cycles. Unlike in carnivore faecal samples, protozoa were the most frequently detected parasites in the faeces of *S. scrofa*. Among the studies that analysed samples of free-living *S. scrofa*, *Tayassu pecari* and *Pecari tajacu*, only one conducted in Texas, USA, reported protozoa in faeces from pigs [30].

Eggs from the family Ascarididae were the most frequently observed group in the faecal material of carnivorous hosts. Most of the eggs detected were similar to *Toxocara* sp. (morphotype 1) and were consistent with *T. canis* and *T. cati*. Brownish ascarid eggs with very thick shells (morphotype 3) were also detected. These eggs may have belonged to another species that has not yet been reported or may even have resulted from parasitic adaptation. In Itatiaia, the high positivity for *Toxocara* sp. may have been favoured due to the extreme resistance of these ascarid eggs the park's abundant edaphic environment and humid tropical climate, which contribute towards larval development within the egg. Moreover, predation can be cited as a possible form of transmission due to paratenic hosts [24] and pseudoparasitism, in which the animal does not truly become infected.

Eggs of the family Diphyllbothriidae were the second most frequently detected parasite structures among helminths in faeces from carnivores. Morphologically, the eggs were consistent with *Spirometra* sp. [31]. The high frequency of these parasites seemed to be related to the abundance of rivers and waterfalls in the park, where copepods, fish, amphibians and snakes (intermediate hosts) can be found.

Nematode larvae were detected in the faeces of *C. brachyurus*, *L. guttulus*, *P. concolor* and *S. scrofa*. These species have also been reported in faeces from felids at a reserve in São Paulo and in the Serra dos Órgãos National Park in Rio de Janeiro, both of which are in Brazil [16]. Although no specific classification of the larvae was made, it was verified if the larvae detected belonged to the genus *Aelurostrongylus* and none presented a subterminal spine structure. Since the faecal samples were collected directly from the ground, the larvae observed may have been free-living nematodes. In addition, these larvae could have developed from pathogenic parasites such as hookworm eggs, *Strongyloides* eggs or even, in the case of artiodactyls, strongylid eggs if the samples were collected from the rectum of the animals or immediately after they defecated.

Thin-shelled nematode eggs were observed in faecal material from both the carnivores and the artiodactyls and appeared similar to hookworm eggs (morphotype 1). Strongylid-like eggs (morphotype 2) were specifically detected in artiodactyl faeces. This finding was expected and corroborated the host identification. Strongylid eggs

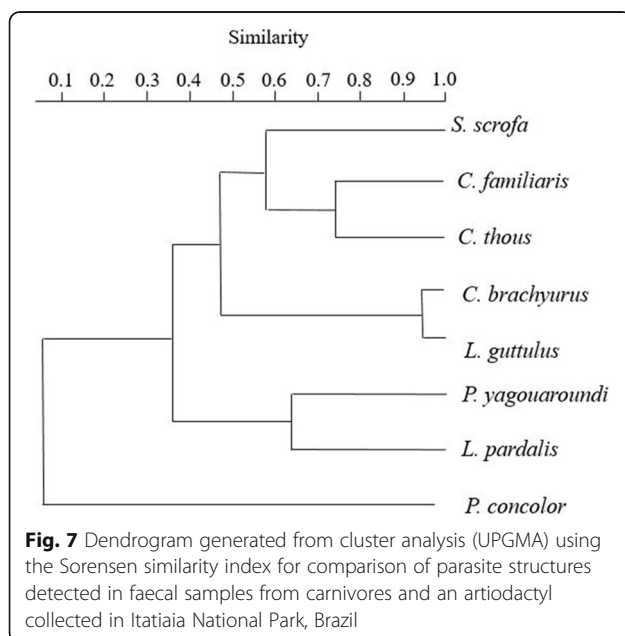




**Table 5** Statistical significance of Poole t test of identified hosts from Itatiaia National Park, Brazil

pvalue	<i>Leopardus guttulus</i>	<i>Chrysocyon brachyurus</i>	<i>Canis familiaris</i>	<i>Cerdocyon thous</i>	<i>Leopardus pardalis</i>	<i>Sus scrofa</i>	<i>Puma yagouaroundi</i>	<i>Puma concolor</i>
<i>Leopardus guttulus</i>		0.05	0.12	0.34	0.46	0.1	0.43	0.46
<i>Chrysocyon brachyurus</i>			0.03*	0.17	0.38	0.01*	0.26	0.38
<i>Canis familiaris</i>				0.94	0.72	0.76	0.95	0.72
<i>Cerdocyon thous</i>					0.7	0.88	1	0.7
<i>Leopardus pardalis</i>						0.66	0.7	1
<i>Sus scrofa</i>							0.9	0.66
<i>Puma yagouaroundi</i>								0.6
<i>Puma concolor</i>								

\*p value &lt;0.05

have been reported in faeces of artiodactyls in a reserve in the Pantanal and in a park in Piauí, Brazil [25, 32]. It is important to highlight that strongylid-like eggs were also diagnosed in faeces from carnivores. This may have occurred due to ungulate or wild artiodactyl predation, farms that had not yet been removed from the park, or ingestion of contaminated water or food. It is important to highlight that those remained farms in PNI can be the source for the introduction of new parasites among the wild fauna that can disseminate the eggs in the park causing an environmental imbalance in the future.

Eggs of *Trichuris* sp. and *Capillaria* sp. were exclusively detected in faeces from carnivores. The *Trichuris* sp. morphotype 1 eggs detected in the *C. brachyurus* samples were consistent with *Trichuris vulpis*, and those diagnosed in the faeces of *L. guttulus* were similar to *Trichuris campanula*. The morphotype 1 and 2 eggs of *Capillaria* sp. and morphotype 2 eggs of *Trichuris* sp. were much larger than the eggs already described as infecting canids and felids in the literature. This demonstrated that other enoplids were probably infecting these animals. It should also be pointed out that these species of *Trichuris* and *Capillaria* may have been ingested during the predation of infected rodents and represent cases of pseudoparasitism. Overall, the diagnosis of *Capillaria* sp. in the biological material of wild animals seems to be directly related to predation on rodents [33]. This may have occurred in the present study, since rodent guard hairs were observed in most of the faecal samples that were positive for *Capillaria* sp.

Eggs of other helminths were also detected in fecal samples from the park, such as the nematode *Physaloptera* sp., microcoelids similar to *Platynosomum illiciens*, cestodes of the order Cyclophyllidea and acanthocephalans.

In general, the biological life cycles of these parasites require the existence of different intermediate and paratenic hosts. In Itatiaia National Park, the animals that can be intermediate and paratenic hosts for these parasites are very prevalent, especially arthropods, rodents and reptiles, thus demonstrating that this is an appropriate environment for

the maintenance of heteroxenic life cycles in which different host species participate.

Among the protozoa, the phylum Apicomplexa was most frequently diagnosed in Itatiaia National Park, including non-sporulated coccidian oocysts in faeces from *C. brachyurus*. Sporulated coccidian oocysts of *Eimeria* sp. (which were detected in faeces from *S. scrofa*) and coproantigens of *Cryptosporidium* sp. were proportionally more frequently detected in the faeces from artiodactyls.

The unsporulated coccidian oocysts that were detected in faecal material from *C. brachyurus* presented different sizes. The smallest was morphotype 1, which was consistent with *Cystoisospora ohioensis*, and the largest was morphotype 2, which was similar to *Cystoisospora canis* [34]. *Cystoisospora* is the most commonly reported genus in the coccidian group in faeces from wild felids in parks and reserves in Mexico and Brazil [16, 20, 22, 35].

The use of an immunoenzymatic assay for the detection of *Cryptosporidium* sp. may have facilitated its diagnosis in the present study due to the greater sensitivity of this technique. It is noteworthy that the artiodactyl diet, i.e., intake of forage, seemed to be a factor that determined a higher frequency of *Cryptosporidium* sp. in this group. It is important to highlight that approximately 31 species of *Cryptosporidium* sp. have been described, among which some have high zoonotic potential to infect mammals [36–39].

The high positivity for *Cryptosporidium* sp. in the carnivores and artiodactyls of Itatiaia National Park is extremely important, since there are very few reports of parasitism in these animals, thus emphasizing the need for further studies to be conducted in wild environments. In addition, it is important to draw attention to the possibility that this protozoon is being introduced to the park by invasive artiodactyls (e.g., *S. scrofa*). It needs to be highlighted that the identification of *Cryptosporidium* sp. in samples of an introduced species should be regarded as a warning, since there are no reports in the Brazilian literature of these parasites infecting these animals.

The identification of protozoan oocysts and coproantigens in faeces from carnivores and artiodactyls is directly associated with the ingestion of sporulated oocysts, mainly through water consumption or through predation. In the case of *Cystoisospora* sp., carnivores and artiodactyls become infected by ingesting cysts containing zoites within the tissues of intermediate hosts, such as mammals, birds and rodents. Both forms of infection may be occurring in Itatiaia National Park given the abundance of possible prey for these hosts, as well as the richness of water resources, such as lakes, rivers and waterfalls.

Protozoan cysts such as amoeboids that were similar to *Entamoeba* sp. were detected in *C. brachyurus* and *L. guttulus* faeces. At Emas National Park in Goiás, Brazil, amoeboid cysts were also detected in the faeces of *C. brachyurus* [40]. Diagnosing these structures in faeces from free-living carnivores in a national park was an unexpected finding. However, this diagnosis needs to be reported, even if it might have resulted from contamination of the sample through contact with the soil or due to pseudoparasitism. The proximity of wild animals to humans, especially tourists visiting and camping in the park, may favour zoonotic transmission. In addition, *Balantioides coli* cysts were detected in the faecal material of artiodactyls in Itatiaia National Park, especially at Visconde de Mauá, where most samples from this group of animals were found. In addition to the macroscopic evaluation, the diagnosis of *B. coli* cysts contributed to confirming that these samples belonged to the order Artiodactyla. It is noteworthy that *S. scrofa* is considered the main reservoir for this protozoan, which has zoonotic transmission potential. Moreover, further surveys in environments proximate to human use should also be made in order to obtain information about the possibility of dissemination of *B. coli* between artiodactyls and humans.

The stabilization of the parasite accumulation curve demonstrated that the amount of samples collected from *C. brachyurus*, *L. guttulus* and *C. familiaris* was sufficient for all parasitological analyses, which is extremely important since it is not known how many individuals of each of these mammals inhabit the park. In Serra da Calçada, Minas Gerais, Brazil, faeces from *C. brachyurus* were found to present a lower richness index ( $R = 6$ ) than that observed for the same species in the present study [28].

High parasite diversity was found for the faeces of *C. brachyurus* and *L. guttulus*, however few studies reported their diversity indices [26]. It is important to highlight that diversity indices, such as Shannon and Simpson's indices, depend on the estimation of parasite abundance. Therefore, one of the major limitations of parasitological surveys through faecal analysis is the lack of an appropriate method for precisely quantifying the parasite abundance since the number of eggs found in non-invasive faecal sampling may not reflect the actual parasite burden [41, 42].

Importantly, not all the parasites detected in faeces from *C. brachyurus* were present in samples from *C. familiaris*, and this may have given rise to significant parasite diversity in the pooled t test for canids. Although circulation of domestic dogs is prohibited in the park, they are sporadically seen on the trails, which increases the chances of this animal becoming infected with the same parasites as *C. brachyurus* and vice versa. Domestic animals have also been seen in or near other Brazilian conservation areas and are potential parasite dispersers [22, 25, 28, 35]. In this study, pets that were present in the park were associated with dog owners properties within or near the park, tourists or even abandonment; these are all situations which the park is not able to handle properly. Although the parasitic similarity between *C. brachyurus* and *C. familiaris* is low, it still denotes the possibility of parasite transmission between these canids, since all the structures detected in dog faeces were also detected in faeces from *C. brachyurus* and some positive samples from both canids were geographically proximate.

It needs to be borne in mind that canids, especially *C. brachyurus*, and *S. scrofa* are omnivorous. This dietary habit expands the feeding options of these animals, and this may have favoured infection by distinct parasitic agents in the present study. The parasite diversity and richness diagnosed in the felid faecal material, mainly in *L. guttulus*, may be directly related to carnivory. Thus, these animals can ingest a large variety of prey and are considered excellent parasite accumulators [43]. Since both felids and canids are territorial animals and travel long distances, they could also participate in the dispersal of parasites in the park environment.

It was also observed that the patterns of parasite structures in the faeces from *C. brachyurus* and *L. guttulus* were similar, as corroborated by the high Sorensen index. This similarity implies the possibility of shared parasites, since most of the samples from *C. brachyurus* were collected geographically proximate to the faeces of *L. guttulus*; both were mainly found in the upper part of Itatiaia National Park and in Visconde de Mauá (Figs. 1, 2 and 3).

In relation to *S. scrofa*, it was found that the accumulation curve for parasite structures did not stabilize, thus suggesting that the number of species could increase if more samples from these animals were collected. In faecal samples from the Serra da Capivara National Park, Piauí, Brazil, a similar picture to that in the present study was also seen with regard to both the richness and the non-stabilization of the *S. scrofa* graph maybe also because this species is omnivorous [25]. In addition, the different parasitism patterns observed between artiodactyls and carnivores seem to be associated with the specificity of the parasites to their hosts, the natural resources available in the park, the behaviour of the animal species

(including their feeding habits) and the dispersal of parasite structures in different areas of Itatiaia National Park.

Importantly, some parasite taxa were shared among native, domestic (*C. familiaris*) and introduced (*S. scrofa*) animals. It was also verified that many of the detected parasites were zoonotic, including *Cryptosporidium* sp. and *Balantioides coli*. These species were mainly detected in the introduced species, especially in omnivorous animals that can move between the park and human dominated landscapes. Both the prospect of similar parasitic taxa between different hosts and that of zoonotic infectious agents should be faced with concern. Therefore, the parasites in introduced and domestic fauna should be frequently monitored, as they may have negative implications for wildlife conservation and even cause public health problems.

## Conclusions

Through the present study, it was possible to confirm the presence of mammalian species, such as carnivores and an artiodactyl, as well as the high richness and diversity of parasite structures in the faeces of these animals. Within this parasite richness, different helminth eggs, cysts, oocysts and protozoan antigens were detected. Our results demonstrated that the park has the elements necessary for the maintenance of complex parasite life cycles that include various hosts, such as intermediate and paratenic hosts. It is important to highlight that several parasites observed in the present study have the potential for zoonotic transmission, given that they may have been transmitted to animals due to their proximity to humans or due to some anthropogenic alterations. So, although it is a hard work, preventing domestic companion and invasive animals from entering and colonize the park would contribute to the maintenance of the environment balance in the park. Even so, the possibility that these parasites truly form part of the parasitic fauna of these animals cannot be ruled out. This scenario emphasizes the importance of constant surveillance of potentially infectious biological agents in the park and reserve environments.

## Methods

### Study site

The study was carried out in Itatiaia National Park, which is a Brazilian protected area covering 28,084,100 ha. It is located in the Serra da Mantiqueira mountain range and encompasses parts of the states of Minas Gerais and Rio de Janeiro. The park is divided into three areas: the lower part, the high part and Visconde de Mauá. The Lower part encompasses the southern area of the park, where vegetation of the Atlantic Forest biome predominates. The high part, where the Maciço das Prateleiras and the Agulhas Negras are located, comprises rock formations and predominantly high-altitude grassland vegetation, and

Visconde de Mauá, which has predominantly Atlantic Forest vegetation and many waterfalls (Fig. 8).

Itatiaia National Park is located in the Atlantic Forest biome and presents a wide range of abiotic factors, such as different types of soil, atmospheric pressure, and temperatures. The relief is mainly mountainous, and the elevation ranges from 540 m in the southern part of the park to 2791.55 m at Pico das Agulhas Negras. The climate is moderate and humid, with temperatures ranging from 10 °C to 18 °C [44]. The park also has a high diversity of biotic factors, including plants, animals, microorganisms and helminths. Regarding biodiversity, many animal species have been catalogued in this park, including reptiles, amphibians, mammals and birds. This includes 111 species of mammals that have been identified.

### Collection of faecal samples

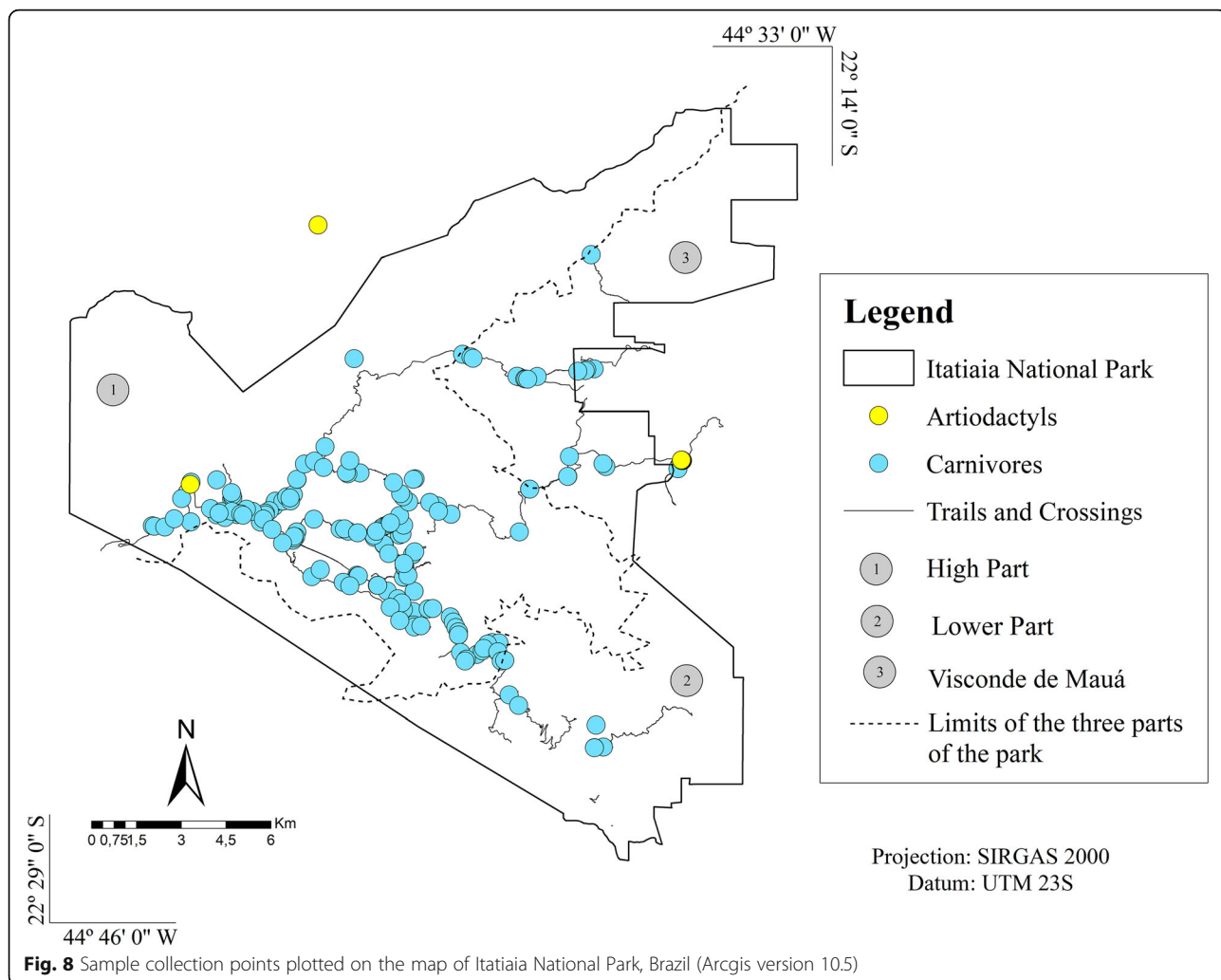
Between June 2017 and April 2018, faecal material was obtained through opportunistic sampling. This material was only collected if it was morphologically consistent with the faeces of carnivores or artiodactyls. Faecal samples that were extremely dehydrated and/or deteriorated were not collected. A total of 352.2 km was surveyed, including 27 trails, 3 crossings and 6 roads. In addition, a sample from a georeferenced artiodactyl outside the park in the municipality of Campo Redondo, Minas Gerais, was also collected. Since this specimen was caught on a trail leading to the park, its sample was also included in this study. During field collection, all samples were georeferenced, identified with the aid of identification keys, photographed, and stored in plastic bags without chemical preservatives in non-refrigerated bags. In addition, the identification number, date, time, and place of collection were registered on each datasheet for each sample. All obtained faeces were sent to the Laboratory of Parasitology at the Biomedical Institute of Fluminense Federal University, where they were refrigerated for 2 days.

### Host identification - macroscopic morphological analysis

The first step in identifying the host species was macroscopic morphological analysis of the stool samples. First, the samples were weighed and then the material was deposited on a white sheet to register the coloration and presence of artefacts and dietary components and measured. After, all this information was compared with the faecal morphology descriptions of the mammalian species of Brazil [12, 45].

### Host identification - guard hair trichology

To retrieve any hair present in the collected faecal samples, half of each sample was washed, dried and stored in plastic bags. The guard hairs were then selected and subjected to cuticular impression and medullary diaphanization [46]. The cuticular and medullary patterns of the guard hairs were examined,



photomicrographed using an Olympus® BX 41 optical microscope, and compared with descriptions in the literature [46–56]. In addition, reference slides were made using guard hairs retrieved from mammal faeces collected at the Rio de Janeiro Zoo, guard hairs deposited in collections in the Serra dos Órgãos National Park and hairs from taxidermized animals from Itatiaia National Park.

**Host identification – DNA sequencing**

**Faecal sample preprocessing and DNA extraction**

The second half of the faecal sample was homogenized in distilled water, and the resulting filtrate was aliquoted into 15 mL conical-bottom centrifuge tubes, which were refrigerated for 3 to 4 days and subjected to faecal suspensions and DNA extraction.

The faecal suspensions were then prepared in sterile tubes using 200 µl of faecal filtrate and 800 µl of 0.01 M Tris-Ca<sup>++</sup> buffer (pH 7.2). After centrifugation at 1500 RPM for 10 min, the supernatant was collected and

transferred to another sterile tube, where 100 µL of chloroform was added. After another centrifugation, the resulting faecal suspension was collected and aliquoted into 1.5 mL microtubes, which were stored at – 20 °C overnight. DNA extraction was then performed from 200 µl of the faecal suspension using the High Pure PCR Template Preparation kit (Roche®) following the manufacturer’s recommendations.

**Polymerase chain reaction (PCR), sequencing and phylogenetic analysis**

PCR was performed on the carnivore faecal samples using the forward primer Car12Ss2 (5 ‘GGTTTGGTCC TRGCCTT 3’) and the reverse primer Car12Ss2 (5 ‘AGCAAGGTGTTATGAGCTAC 3’), which amplify a 12S mitochondrial gene fragment [57]. Samples that presented low-quality electropherograms were also submitted to PCR using the forward primer ATP6-DF3 (5 ‘AACGAAAATCTATTCGCCTCT 3’) and reverse primer ATP6-DR1 (5 ‘CCAGTATTTGTTTTGATGTTAG



TTG 3'), which amplify a fragment of the ATP6 mitochondrial gene. To analyse the samples from the artiodactyls, the forward primer BC-F2 (5' ATCACCCTATTGT TAATATAAAACC 3') and reverse primer HCO2198 (5' TAAACTTCAGGGTGACCAAAAAATCA 3') were used to amplify a fragment of the COI mitochondrial gene. Both PCRs were performed using validated protocols [58]. All amplified products were confirmed through electrophoresis on a 1.5% agarose gel and were purified using the ExoSAP-IT enzyme and sequenced in the forward direction by a 3730 × 1 DNA Analyser automated sequencer (Applied Biosystems). Finally, the sequences were aligned with the reference sequences, which were retrieved from GenBank, using BioEdit software, version 7.2.5. The DNA sequences from the mammalian samples matched the DNA reference sequences at a level of 95% or higher (Table 6).

#### Parasitological techniques - microscopy

The filtrate resulting from the second half of each sample was used for faecal sample preprocessing and DNA extraction and for parasitological techniques. The filtrate was aliquoted into 15 mL conical-bottom centrifuge tubes, which were subjected to centrifuge-sedimentation [59, 60], centrifugal-flotation techniques using zinc at a density of 1.180 g/cm<sup>3</sup> [61] and centrifugal flotation with 1.300 g/cm<sup>3</sup> sucrose solution [62, 63]. The remaining filtrate was transposed to a conical-bottom glass for use with the spontaneous sedimentation technique [64]. The microscopy slides obtained from each parasitological technique were read and photomicrographed using an Olympus® BX 41 optical microscope; slides were initially examined at 100X magnification and, when necessary, at 400X magnification. The morphometry of the parasite structures was evaluated using a 400X and 1000X magnification eyepiece under an Olympus® BX 41 microscope.

#### Parasitological techniques - ELISA for *Cryptosporidium* sp.

The frozen samples in microtubes were subjected to enzyme-linked immunosorbent assay (ELISA) using the "Cryptosporidium antigen detection microwell" kit (IVD Research®). Prior to the enzyme immunoassay, a solution was made using 60 µL of the sample and 60 µL of the diluent provided in the kit. After dilution, 100 µL of this solution was transferred to the assay plate, and thus, the technique was performed as recommended by the manufacturer. The plates were read in an ELISA reader (Thermo plate® TP-reader LGC Biotechnology Ltda.).

#### Analysis of results

The host identification was summarized with the parasitological results. Since the techniques did not provide information with the same degree of precision for the host taxonomy, an association was made between the more

specific results of each method and the final classification of the host (Table 7). Pearson's correlation coefficient ( $\rho$ ) was calculated to support the association of information for the identification of host species. This method was not used for those samples for which all three identification techniques completely agreed.

Through macroscopy, the samples were classified into a taxonomic group of order or family. Using trichology, the samples were classified into a family and species taxonomic group, and DNA sequencing provided taxonomic information about the host species.

Faecal samples were considered positive for gastrointestinal parasite structures when at least one cyst, oocyst, egg or nematode larva was detected and/or antigen of *Cryptosporidium* sp. was shown. The parasitological results were presented descriptively at the lowest possible taxonomic rank and into morphotypes of helminth eggs and protozoan oocysts. These morphotypes were distinguished from each other by their taxonomic rank, morphology (colour and shape) and size. The richness, diversity, and similarity indices and Principal Component Analysis (PCA) were analysed only according to the results obtained from the different taxa parasite structures. The morphotypes detected in the same taxa were not considered in the index analysis.

**Table 7** Criteria used in the association of information obtained from macroscopic analysis of faeces, trichology of guard-hair and DNA sequencing for the final classification of hosts

Host identification
Host species
<ol style="list-style-type: none"> <li>1) Association of the 3 techniques when they completely agreed with each other.</li> <li>2) Association of 2 techniques when one of the methods does not provide taxonomic information about the host.</li> <li>3) Trichology + DNA sequencing when macroscopy provides taxonomic information that does not agree with the obtained by other techniques.</li> <li>4) Macroscopy + DNA sequencing DNA when: <ul style="list-style-type: none"> <li>- Trichology provided information on small carnivores (mustelids and procionids), which are incompatible with the morphology of samples with large fecal volume.</li> <li>- Different species of small felids were identified by trichology and sequencing.</li> </ul> </li> </ol>
Unidentified species of Carnivores / Artiodactyls
<ol style="list-style-type: none"> <li>1) Complete disagreement with all information obtained by the techniques.</li> <li>2) Taxonomic information from the host obtained only by a single identification technique.</li> <li>3) Identification of a feline and a canine by trichology and sequencing.</li> <li>4) Absence of information on gene sequencing and information on small carnivores (mustelids and procionids) by trichology, which are incompatible with the morphology of samples with large fecal volume.</li> <li>5) Absence of taxonomic information on the host species.</li> </ol>

These statistical tests were performed using Past® software, version 3.2.2 [65]. The parasite richness for each host species was determined by counting the different taxa detected in its samples; in addition, the sample sufficiency was plotted on accumulation curves of the parasite species [66].

The parasite diversity was analysed statistically using the Shannon (H') and Simpson© indices [67]. The statistical significance of Shannon's diversity for the parasites was analysed using a pooled t test, with a significance level of 5% [68]. Sorensen's index (S) was also used to compare the similarity of the parasite structures among host species [67].

The Shannon and Simpson diversity indices for the parasites were complementary and were analysed to verify the relative abundances of the species for the set of samples of each host species. The highest parasitic diversity was determined in the hosts that presented high Shannon index and Simpson index values of close to 1.

## Supplementary information

**Supplementary information** accompanies this paper at <https://doi.org/10.1186/s12917-020-02490-5>.

**Additional file 1 S1 Table.** Macro and microscopic morphology of guard hairs and frequency of mammalian taxa identified by trichology in faecal samples collected in Itatiaia National Park, Brazil.

## Abbreviations

*C. brachyurus*: *Chrysocyon brachyurus*; *C. familiaris*: *Canis familiaris*; *C. thous*: *Cerdocyon thous*; ELISA: Enzyme-Linked Immunosorbent Assay; *L. guttulus*: *Leopardus guttulus*; *L. pardalis*: *Leopardus pardalis*; PCA: Principal Components Analysis; *P. concolor*: *Puma concolor*; PNI: Itatiaia National Park; PCR: Polymerase chain reaction; *P. yagouaroundi*: *Puma yagouaroundi*; *S. scrofa*: *Sus scrofa*; Syn: Synonymous; UPGMA: Unweighted Pair Group Method with Arithmetic Mean; US: Unidentified Species

## Acknowledgements

We would like to thank the Parasitology Laboratories of the Fluminense Federal University, the Molecular Biology and Conservation Laboratory of the Federal University of São Carlos and the Laboratory of Toxoplasmosis and Other Protozoan Diseases of the Oswaldo Cruz Institute for their inputs; and, especially, the entire team at Itatiaia National Park.

## Authors' contributions

LVD, ASB - performed the macroscopic analysis of feces, the trichological processing of guard hairs, molecular analysis, and tabulation of results and dissertation of the manuscript. JPSP, CSCCL, JLP, RCFR, CRS - contributed to the macroscopic analysis of feces, guard hairs trichological analysis. ABMF - contributed to the statistical analysis and interpretation of parasitological diversity indices and sample sufficiency. KGRC, CFG and PMGJr - contributed to the performance of molecular techniques, including the PCR and genetic sequencing interpretation of mammalian samples. OMPB, CMAU, ACMPB - contributed to the parasitological processing, interpretation and discussion of parasitological results. LLC - assisted in the molecular classification of hosts and deposition of gene sequences in digital databases. MRRA - provided material for the immunoenzymatic assay and contributed to the interpretation and discussion of parasitological results. All authors contributed to the review of the manuscript.

## Funding

Not applicable.

## Availability of data and materials

The datasets generated in this study from AT6 region are available in the Dryad repository under DOI number <https://doi.org/10.5061/dryad.djh9w0vxx>. The other sequences are available in GenBank-NCBI under accession numbers MN509185, MN509186, MN509187, MN509188, MN509189, MN509190, MN509191, MN509192, MN509193, MN509194, MN509195, MN509196, MN509197, MN509198 for 12S gene and MN608174, MN608175, and MN608176 for COI.

## Ethics approval and consent to participate

This study was approved by Biodiversity Information and Authorization System (SISBIO) under authentication code 25693264 and number 57635-1 on March 24th 2017 in order to comply national guidelines and to obtain authorization to collect feces from wild animals at Itatiaia National Park. This system is responsible for giving permission to every research made in Brazilian national parks. Also, this study was approved by the Animal Ethics Committee of Fluminense Federal University, under license number 930 since all the feces were processed and analyzed in this University.

## Consent for publication

Not applicable.

## Competing interests

The authors declare that they have no competing interests.

## Author details

<sup>1</sup>Department of Microbiology and Parasitology, Laboratory of Parasitology, Federal Fluminense University, Biomedical Institute, Professor Hernani Mello Street, São Domingos, Niterói, Rio de Janeiro 24210-130, Brazil. <sup>2</sup>Statistics Laboratory, Mathematics and Statistics Institute, Fluminense Federal University, Rua Professor Marcos Waldemar de Freitas Reis s/n, bloco G, Gragoatá campus, Niterói, RJ 24210-201, Brazil. <sup>3</sup>Department of Genetics and Evolution, Laboratory of Molecular Biodiversity and Conservation, Federal University of São Carlos, Washington Luis highway, km 235, São Carlos, São Paulo 13565-905, Brazil. <sup>4</sup>Laboratory of Toxoplasmosis and Other Protozoan Diseases, Oswaldo Cruz Foundation (Fiocruz, Rio de Janeiro), Oswaldo Cruz Institute, Avenue Brazil, 4365, Manginhos, Rio de Janeiro 21040-360, Brazil.

Received: 17 February 2020 Accepted: 24 July 2020

Published online: 17 August 2020

## References

- Wilson DE, Mittermeier RA. The mammals of the world. Barcelona: Lynx; 2009.
- Aranda RC, Serrano-Martínez E, Tantaleán VM, Quispe HM, Casas VG. Identificación y frecuencia de parásitos gastrointestinales en félidos silvestres en cautiverio en el Perú. Rev Investig Vet Perú. 2013;24(3):360-8. <https://doi.org/10.15381/rivep.v24i3.2585>.
- Poulin R. The functional importance of parasites in animal communities: many roles at many levels? Int J Parasitol. 1999;29(6):903-14. [https://doi.org/10.1016/S0020-7519\(99\)00045-4](https://doi.org/10.1016/S0020-7519(99)00045-4).
- Freeland WJ. Parasites and the coexistence of animal host species. Am Nat. 1983;121(2):223-36. <https://www.jstor.org/stable/2461124>.
- Azpíri GS, Maldonado FG, González GC. La importancia del estudio de enfermedades en la conservación de fauna silvestre. Vet México. 2000;31(3):223-30. <http://www.redalyc.org/articulo.oa?id=42331308>.
- Barutzki D, Schaper R. Endoparasites in dogs and cats in Germany 1999-2002. Parasitol Res. 2003;90(0):S148-50. <https://doi.org/10.1007/s00436-003-0922-6>.
- Daszak P. Emerging infectious diseases of wildlife- threats to biodiversity and human health. Sci. 2000;287(5452):443-9. <https://doi.org/10.1126/science.287.5452.443>.
- Emmons LH, Feer F. Neotropical rainforest mammals, a field guide. Chicago: University of Chicago Press; 1997.
- Cleveland S, Hess GR, Dobson MK, Laurenson HI, McCallum MG, Roberts MG, Woodroffe R. The role of pathogens in biological conservation. In: Hudson PJ, Rizzoli A, Grenfell BT, Heesterbeek H, Dobson AP, editors. The Ecology of Wildlife Diseases. Nova York: Oxford University Press; 2002. p. 139-50.
- Morin PA, Woodruff DS. Noninvasive Genotyping for Vertebrate. In: Smith TB, Wayne RK, editors. Molecular genetic approaches in conservation. Oxford: University Press; 1996. p. 298-313.

11. Taberlet P, Waits LP, Luikart G. Noninvasive genetic sampling: look before you leap. *Trends Ecol Evol.* 1999;14(8):323–7. [https://doi.org/10.1016/s0169-5347\(99\)01637-7](https://doi.org/10.1016/s0169-5347(99)01637-7).
12. Chame M. Terrestrial mammal feces: a morphometric summary and description. *Mem Inst Oswaldo Cruz.* 2003;98(suppl 1):71–94. <https://doi.org/10.1590/S007402762003000900014>.
13. Dib LV, Palmer JPS, Lima CSCL, Bastos OMP, Uchôa CMA, Amendoeira MRR, Bastos ACMP, Barbosa AS. Noninvasive Sampling: Monitoring of Wild Carnivores and Their Parasites. In: Baker A, editor. *Protected Areas, National Parks and Sustainable Future.* London: IntechOpen; 2019. p. 1–13.
14. Calixto JB, Siqueira JM Jr. The Drug Development in Brazil: Challenges. *Gazeta Médica da Bahia.* 2008;78(Suppl 1):98–106.
15. ICMBio Instituto Chico Mendes de Conservação da Biodiversidade 2016. Carnívoros brasileiros. <http://www.icmbio.gov.br/cenap/carnivoros-brasileiros.html>. Accessed 22 Apr 2019.
16. Dib LV, Cronemberger C, Pereira FA, Bolais PF, Uchôa CMA, Bastos OMP, Amendoeira MRR, Barbosa AS. Gastrointestinal parasites among felids inhabiting the Serra dos Órgãos National Park, Rio de Janeiro, Brazil. *Rev Bras Parasitol Vet.* 2018;27(2):131–40. <https://doi.org/10.1590/S1984-296120180016>.
17. Seton ET. On the study of scatology. *J Mamm.* 1925;6(1):47.
18. Silva-Caballero A. Parasitosis gastrointestinales en felinos silvestres en Nanchitlita, México. 2010; Dissertation, Universidad Autónoma del Estado de México.
19. Contreras MG. Parásitos gastrointestinales de felinos de la Reserva Ecológica El Edén A.C. Quintana Roo, México. 2014; Dissertation, Universidad Veracruzana.
20. Solórzano-García B, White-Day JM, Gómez-Contreras M, Cristóbal-Azkárate J, Osorio-Sarabia D, Rodríguez-Luna E. Coprological survey of free-ranging jaguar (*Panthera onca*) and puma (*Puma concolor*) inhabiting 2 types of tropical forests in Mexico. *Rev Mex Biodivers.* 2017;88(1):146–53. <https://doi.org/10.1016/j.rmb.2017.01.011>.
21. Beltrán-Saavedra LF, Angulo S, Gonzales JL. Uso de metodologías de censos muestrales indirectos de fecas para evaluar endoparásitos en mamíferos silvestres: Un ensayo en la Reserva Privada de San Miguelito, Santa Cruz. *Bolivia Ecol Biol.* 2009;44(1):56–61.
22. Araujo RDS. Enteroparasitos de carnívoros silvestres e *Canis familiaris* (Linnaeus 1758) (Mammalia; Carnivora) na Reserva Particular do Patrimônio Natural Santuário do Caraça, Minas Gerais. 2014. Dissertation, Minas Gerais Federal University.
23. Srbeek-Araujo AC, Santos JLC, Almeida VM, Guimarães MP, Chiarello AG. First record of intestinal parasites in a wild population of jaguar in the Brazilian Atlantic Forest. *Rev Bras Parasitol Vet.* 2014;23(3):393–8. <https://doi.org/10.1590/S1984-29612014065>.
24. Patton S, Rabinowitz AR. Parasites of wild Felidae in Thailand: a Coprological survey. *J Wild Dis.* 1994;30(3):472–5. <https://doi.org/10.7589/0090-3558-30.3.472>.
25. Fiorello CV, Robbins RG, Maffei L, Wade SE. Parasites of free-ranging small canids and felids in the Bolivian Chaco. *J Zoo Wild Med.* 2006;37(2):130–4. <https://doi.org/10.1638/05-075.1>.
26. Brandão ML, Chame M, Cordeiro JLP, Chaves SAM. Diversidade de helmintos intestinais em mamíferos silvestres e domésticos na Caatinga do Parque Nacional Serra da Capivara, Sudeste do Piauí. *Brasil Rev Bras Parasitol Vet.* 2009;18(e1):19–28. <https://doi.org/10.4322/rbvp.018e1004>.
27. Kusma SC, Wrublewski DM, Teixeira VN, Holdefer DR. Parasitos intestinais de *Leopardus wiedii* e *Leopardus tigrinus* (Felidae) da Floresta Nacional de Três Barras, SC. *Luminária.* 2015;17(1):82–95.
28. Massara R, Paschoal A, Chiarello A. Gastrointestinal parasites of maned wolf (*Chrysocyon brachyurus*, Illiger 1815) in a suburban area in southeastern Brazil. *Braz J Biol.* 2015;75(3):643–9. <https://doi.org/10.1590/1519-6984.20013>.
29. Wrublewski DM, Kusma SC, Teixeira VN. Parasitos gastrointestinais em *Puma concolor*, *Puma yagouaroundi* e *Leopardus pardalis* (Carnivora: Felidae) na Floresta Nacional de Três Barras, SC, Brasil. *Rev Acad Cien Anim.* 2018;16:1–8. <https://doi.org/10.7213/1981-4178.2018.16004>.
30. Rodríguez-Rivera LD, Cummings KJ, McNeely I, Suchodolski JS, Scorza AV, Lappin MR, Mesenbrink BT, Leland BR, Bodenchuk MJ. Prevalence and diversity of *Cryptosporidium* and *Giardia* identified among feral pigs in Texas. *Vector-Borne and Zoonotic Dis.* 2016;16(12):765–8. <https://doi.org/10.1089/vbz.2016.2015>.
31. Conboy G. Cestodes of dogs and cats in North America. *Vet Clin North Am Small Anim Pract.* 2009;39(6):1075–90. <https://doi.org/10.1016/j.cvs.2009.06.005>.
32. Souza HCD. Helmintos intestinais de Tayassuidae e Suidae (Mammalia: Artiodactyla) no Pantanal: um estudo sobre a circulação de espécies na Reserva Particular do Patrimônio Nacional SESC Pantanal e seu entorno, Baía de Melgaço. 2014; Dissertation, Oswaldo Cruz Foundation.
33. Ruas JL, Muller G, Farias NAR, Gallina T, Lucas ASG, Pappen F, Sinko AL, Brum JGW. Helmintos do cachorro do campo, *Pseudaloxep gymnocercus* (Fischer, 1814) e do cachorro do mato, *Cerdoconyx thous* (Linnaeus, 1766) no sul do estado do Rio Grande do Sul. *Brasil Rev Bras Parasitol Vet.* 2008; 17(2):87–92. <https://doi.org/10.1590/S1984-29612008000200005>.
34. Lindsay DS, Dubey JP, Blagburn BL. Biology of *Isoospora* spp. from humans, nonhuman primates, and domestic animals. *Clin Microbiol Ver.* 1997;10(1): 19–34 PMID 8993857.
35. Santos JLC, Magalhães NB, Santos HA, Ribeiro RR, Guimarães MP. Parasites of domestic and wild canids in the region of Serra do Cipó National Park, Brazil. *Rev Bras Parasitol Vet.* 2008;21(3):270–7. <https://doi.org/10.1590/S1984-29612008000200005>.
36. Šlapeta J. *Cryptosporidiosis* and *Cryptosporidium* species in animals and humans: a thirty colour rainbow? *Int J Parasitol.* 2013;43(12–13):957–70. <https://doi.org/10.1016/j.ijpara.2013.07.005>.
37. Holubová N, Sak B, Horčíková M, Hlášková L, Květoňová D, Menchaca S, McEvoy J, Kváč M. *Cryptosporidium avium* n. sp. (Apicomplexa: Cryptosporidiidae) in birds. *Parasitol Res.* 2016;115(6):2243–51. <https://doi.org/10.1007/s00436-016-4967-8>.
38. Kváč M, Havrdová N, Hlášková L, Daňková T, Kanděra J, Ježková J, Vítovec J, Sak B, Ortega Y, Xiao L, Modrý D, Chelladurai JR, Prantlová V, McEvoy J. *Cryptosporidium proliferans* n. sp. (Apicomplexa: Cryptosporidiidae): molecular and biological evidence of cryptic species within gastric *Cryptosporidium* of mammals. *PLoS One.* 2016;11(1):1–24. <https://doi.org/10.1371/journal.pone.0147090>.
39. Zahedi A, Papparini A, Jian F, Robertson I, Ryan U. Public health significance of zoonotic *Cryptosporidium* species in wildlife: critical insights into better drinking water management. *Int J Parasitol: Paras Wild.* 2016;5(1):88–109. <https://doi.org/10.1016/j.ijppaw.2015.12.001>.
40. Braga RT, Vynne C, Loyola RD. Fauna parasitária intestinal de *Chrysocyon brachyurus* (lobo-guará) no Parque Nacional das Emas. *Bioikos.* 2012;24(1): 49–55 <https://www.researchgate.net/publication/261795270>.
41. Gillespie TR. Noninvasive assessment of gastrointestinal parasite infections in free-ranging primates. *Int J Primatol.* 2006;27(4):1129–43. <https://doi.org/10.1007/s10764-006-9064-x>.
42. Greiner EC, McIntosh A. Collection methods and diagnostic procedures for primate parasitology. In: Huffman MA, Chapman CA, editors. *Primates parasite ecology. The dynamics and study of host–parasite relationships.* Cambridge: Cambridge University Press; 2009. p. 3–27.
43. Rocha FL. A rede trófica e o papel dos carnívoros silvestres (Ordem Carnivora) nos ciclos de transmissão de *Trypanosoma cruzi*. 2013; Dissertation, Oswaldo Cruz Foundation.
44. ICMBio - Instituto Chico Mendes de Conservação da Biodiversidade. 2013. Plano de Manejo do Parque Nacional do Itatiaia. Encarte 3. Available on : <<http://www.icmbio.gov.br/portal/component/content/article?id=2181:parna-do-itaiaia>>. Access realized at: 11 Apr 2020.
45. Borges PL, Tomás WM. Guia de rastros e outros vestígios de mamíferos do Pantanal. 1st ed. Pantanal com Ciência, SEBRAE MS: Mato Grosso do Sul; 2008.
46. Quadros J. Identificação microscópica de pêlos de mamíferos brasileiros e sua aplicação no estudo da dieta de carnívoros. 2002. Dissertation, Paraná Federal University.
47. Hess WM, Flinders JT, Pritchett CL, Allen JV. Characterization of hair morphology in families Tayassuidae and Suidae with scanning Electron microscopy. *J Mamm.* 1985;66(1):75–84. <https://doi.org/10.2307/1380958>.
48. Teerink BJ. Hair of west European mammals: atlas and identification. Cambridge: University Press; 1991.
49. Martins IA. Identificação dos canídeos brasileiros através dos seus pêlos guarda: Paulista State University; 2005. <http://rgdoi.net/10.13140/RG.2.1.35.96.1760>. Accessed 26 June 2019.
50. Fernandes MAW. Análise comparativa da morfologia dos pelos-guarda de mamíferos com hábito semi-aquático. 2008; Dissertation, Paraná Federal University.
51. Vanstreels RET, Ramalho FP, Adania CH. Microestrutura de pêlos-guarda de felídeos Brasileiros: considerações para a identificação de espécies. *Biota Neotrop.* 2010;10(1):333–7. <https://doi.org/10.1590/S1676-06032010000100029>.



52. Abreu MSL, Christoff AU, Vieira EM. Identificação de marsupiais do Rio Grande do Sul através da microestrutura dos pelos-Guarda. *Biota Neotrop.* 2011;11(3):391–400. <https://doi.org/10.1590/S1676-06032011000300031>.
53. Duarte TDS. Micromorfologia de pelos aristiformes de roedores das famílias Cricetidae e Echimyidae (Mammalia, Rodentia). 2013;Dissertation, Viçosa Federal University.
54. Silveira F, Sbalqueiro IJ, Monteiro-Filho ELA. Identificação das espécies brasileiras de *Akodon* (Rodentia: Cricetidae: Sigmodontinae) através da microestrutura dos pelos. *Biota Neotrop.* 2013;13(1):339–45. <https://doi.org/10.1590/S1676-06032013000100033>.
55. Miranda GHB, Rodrigues FHG, Paglia AP. Guia de Identificação de Pelos de Mamíferos Brasileiros. Brasília: Ciências Forenses; 2014.
56. Alberts CC, Saranholi BH, Frei F, Galetti PM. Comparing hair-morphology and molecular methods to identify fecal samples from Neotropical felids. *PLoS ONE.* 2017;12(9):e0184073:1–24. <https://doi.org/10.1371/journal.pone.0184073>.
57. Rodriguez-Castro KG, Saranholi BH, Bataglia L, Blanck DV, Galetti PM Jr. Molecular species identification of scat samples of south American felids and canids. *Conserv Genet Resour.* 2018:1–6. <https://doi.org/10.1007/s12686-018-1048-6>.
58. Chaves PB, Graeff VG, Lion MB, Oliveira LR, Eizirik E. DNA barcoding meets molecular scatology: short mtDNA sequences for standardized species assignment of carnivore noninvasive samples: carnivore dna mini-barcodes. *Mol Ecol Resour.* 2012;12(1):18–35. <https://doi.org/10.1111/j.1755-0998.2011.03056.x>.
59. Ritchie LS. An ether sedimentation technique for routine stool examinations. *Unit S Arm Med Depart Bull.* 1948;8:326 PMID 18911509.
60. Young KH, Bullock SL, Melvin DM, Spruill CL. Ethyl Acetate as a Substitute for Diethyl Ether in the Formalin-Ether Sedimentation Technique. *J Clin Microbiol.* 1979;10(6):852–3 PMID 574877.
61. Faust EC, D'Antoni JS, Odon V, Miller MJ, Perez C, Sawitz W, Thomen F, Tobie JE, Walker JH. A critical study of clinical laboratory techniques for the diagnosis of protozoan cysts and helminth eggs in feces. I. Preliminary communication. *Am J Trop Med.* 1938;18:169–83. <https://doi.org/10.4269/ajtmh.1938.s1-18.169>.
62. Sheather AL. The detection of intestinal protozoa and mange parasites by a floatation technique. *J Comp Pathol Therap.* 1923;36:266–75. [https://doi.org/10.1016/S0368-1742\(23\)80052-2](https://doi.org/10.1016/S0368-1742(23)80052-2).
63. Huber F, Bomfim TC, Gomes RS. Comparação da eficiência da técnica de sedimentação pelo formaldeído-éter e da técnica de centrifugo-flutuação modificada na detecção de cistos de *Giardia* sp. e oocistos de *Cryptosporidium* sp. em amostras fecais de bezerros. *Rev. Bras. Parasitol. Vet.* 2003;12(2):135–7.
64. Lutz A. O *Schistosomum mansoni* e a schistosomatose segundo observações feitas no Brasil. *Mem Inst Oswaldo Cruz.* 1919;11(1):121–55. <https://doi.org/10.1590/S0074-02761919000100006>.
65. Hammer. Past version 3.25 Reference manual. Paleontological Statistics. New Jersey: Wiley; 2019.
66. Colwell RK, Coddington JA. Estimating terrestrial biodiversity through extrapolation. *Phil Trans R Soc Lond B.* 1994;345(1311):101–18. <https://doi.org/10.1098/rstb.1994.0091>.
67. Krebs CJ. *Ecological Methodology.* California: Benjamin Cummings; 1999.
68. Poole RW. *An introduction to quantitative ecology.* New York: McGraw-Hill; 1974.

## Publisher's Note

Springer Nature remains neutral with regard to jurisdictional claims in published maps and institutional affiliations.

**Ready to submit your research? Choose BMC and benefit from:**

- fast, convenient online submission
- thorough peer review by experienced researchers in your field
- rapid publication on acceptance
- support for research data, including large and complex data types
- gold Open Access which fosters wider collaboration and increased citations
- maximum visibility for your research: over 100M website views per year

**At BMC, research is always in progress.**

Learn more [biomedcentral.com/submissions](https://biomedcentral.com/submissions)

